FACTORS AFFECTING SITE RESPONSE ANALYSIS

by

Gökçe Tönük

B.S., Civil Engineering, Middle East Technical University, 1998

M.S., Geotechnical Engineering, Middle East Technical University, 2001

Submitted to the Kandilli Observatory and Earthquake Research Institute

in partial fulfillment of

the requirements for the degree of

Doctor of Philosophy

Graduate Program in Earthquake Engineering

Boğaziçi University

2009

To My Parents and My Husband, with all my love

ACKNOWLEDGEMENTS

I owe my deepest gratitude to my academic advisor, Prof. Dr. Atilla Ansal who has provided me with necessary assistance and encouragement through this study. I would also like to thank him for inspiring me to become an academician exactly like him: extremely enthusiastic, passionate, wise, insightful, patient, and renowned researcher. Although, I know it is not an easy dream to come true. Without his support and consultancy, this study would not have been possible and this much comprehensive.

The contributions of my dissertation defense committee members, Prof. Dr. Mustafa Erdik, Prof. Dr. Ayfer Erken, Prof. Dr. Kutay Özaydın and Prof. Dr. Erdal Şafak are gratefully appreciated, for reviewing this dissertation and valuable comments in such a limited time.

I am very pleased and feel lucky to have the chance to study in Kandilli, Department of Earthquake Engineering. The years here have broadened my knowledge and engineering skills. This is a great opportunity to thank all faculty members for their lectures. I was also very fortunate to have met wonderful persons such as Ebru Harmandar, Aslı Kurtuluş, Mine Demircioğlu, Karin Şeşetyan, Cüneyt Tüzün and Ufuk Hancılar. I appreciate their friendship. They all made Kandilli days enjoyable and complete.

I will never stop thanking my family: they have been and will always be important in every stage of my life. I am grateful to each member of Karaca and Tönük Families for their love and support. Especially, my dear sister, Gözde has reduced the distance and longing between us by calling and cheering me up every day.

My very special thanks go to my dear husband, Beltan Tönük, for being there with me and for me, whenever I needed him. He believed in me maybe more than myself at the times when I was frustrated and could do nothing. I will always appreciate his patience and support.

ABSTRACT

FACTORS AFFECTING SITE RESPONSE ANALYSIS

The objective of a site response analysis is to estimate free-field ground shaking characteristics during an earthquake for a specific hazard level and set of site conditions. The mandatory components for a site response analysis are: one or more design earthquake records with representative acceleration time histories, an idealization of the soil-rock system at the site of interest, and a scheme to generate response solutions to simplified assumed wave fields in other words appropriate modeling of the soil behavior. Normally, the free-field ground response is presented in terms of either response spectra or the variation of acceleration or velocity with time.

The study aims to review and improve different components of site response analyses in order to achieve a robust methodology for more comprehensive and realistic assessment. The effects of input acceleration time histories, the applied numerical methodology, stress and frequency dependence and nonlinear site response analysis were reviewed and methodologies were suggested based on case studies. Site response of layered soil deposits was analyzed using equivalent linear and modified equivalent linear schemes.

The developed methodology would be utilized to estimate earthquake characteristics on the ground for site specific investigations based on probabilistic earthquake hazard assessment.

Within this perspective, site response analysis was studied with respect to (a) the determination of different scaling parameters including derivation of attenuation relationships for these parameters, (b) the evaluation of scaling parameters with respect to magnitude and distance ranges, (c) the methodology of selection and scaling of input acceleration time histories for site response analyses, (d) the methodology for selection of ground motion parameters from site response analysis as design or damage parameters for

various earthquake engineering analysis such as liquefaction susceptibility, microzonation, vulnerability assessments for buildings and pipeline networks, (e) the methodology for confining stress and frequency dependence of modulus reduction and damping in equivalent linear site response analysis, (f) the review concerning the available equivalent linear site response analysis models and software, (g) formulation of modified version of Shake91 to account for stress and frequency dependency, (h) comparison of results with modified Shake91 based on selected borings, and (i) the review concerning nonlinear models for site response analysis.

ÖZET

SAHA DAVRANIŞ ANALİZLERİNE ETKİ EDEN FAKTÖRLER

Saha davranış analizlerinin amacı belli bir deprem tehlikesi ve zemin profiline yönelik olarak bir deprem esnasında zemin yüzeyinde oluşacak yer sarsıntısının özelliklerinin tahmin edilmesidir. Saha davranış analizi yapılabilmesi için: temsili ivme zaman kayıtlarından seçilmiş veya üretilmiş bir veya daha fazla tasarım deprem kaydına, analiz sahası zemin-kaya profilinin idealizasyonuna ve varsayılan basitleştirilmiş dalga yayılımında zemin profilinin davranış çözümlerinin üretilmesi için bir analiz yöntemine başka şekilde söylemek gerekirse saha davranışının uygun şekilde modellenmesine gerek vardır. Saha davranış analizlerinin sonuçları genellikle zemin yüzeyinde bulunan davranış spektrumu veya ivme veya hız zaman kayıtları şeklinde verilmektedir.

Bu çalışma, saha davranış analizi yapılabilmesi için gerekli unsurların, daha kapsamlı ve gerçekçi bir değerlendirmeye yönelik bir analiz methodu elde etmek için incelenmesini ve geliştirilmesini amaçlamaktadır. Çalışma kapsamında; girdi ivme zaman kayıtlarının, uygulanan numerik yöntemin, gerilme ve frekans bağımlı doğrusal olmayan zemin davranışının analiz üzerindeki etkileri incelenmiş, vaka analizlerine dayanarak yöntemler önerilmiştir. Tabakalı zemin profillerinin davranışları, eşdeğer doğrusal ve modifiye eşdeğer doğrusal analiz yöntemleri ile analiz edilmiştir.

Geliştirilen yöntem olasılıksal deprem tehlike analizine dayanan sahaya özel araştırmalara yönelik zemin yüzeyinde deprem özelliklerinin belirlenmesi için kullanılabilecektir.

Bu çerçevede, saha davranış analizleri (a) girdi ivme zaman kayıtları için farklı ölçeklendirme parametrelerinin elde edilmesi ve bu parametreler için azalım ilişkilerinin geliştirilmesi, (b) ölçeklendirme parametrelerinin deprem büyüklüğü ve uzaklığına göre etkilerinin incelenmesi, (c) saha davranış analizlerinde kullanılacak girdi deprem kayıtlarının seçimi ve ölçeklendirilmesi için yöntem geliştirilmesi, (d) saha davranış

analizlerinden elde edilecek parametrelerin sıvılaşma değerlendirmesi, mikrobölgeleme, bina ve altyapı elemanlarının hasar görebilirliğinin belirlenmesi gibi değişik deprem mühendisliği analizlerine yönelik tasarım veya hasar parametresi olarak seçilmesi için yöntem geliştirilmesi, (e) eşdeğer doğrusal analiz yönteminde dinamik kayma modülü ve sönüm oranı parametrelerinin frekans ve çevre basıncı bağımlılıklarını dikkate alan yöntemin geliştirilmesi, (f) mevcut eşdeğer lineer analiz yöntemlerinin ve bu yöntemleri kullanan saha davranış analizi programlarının incelenmesi, (g) Shake91 programının frekans ve çevre basıncı bağımlılığını dikkate alacak şekilde modifiye edilmesi, (h) seçilmiş zemin profilleri üzerinde sonuçların modifiye edilmiş Shake91 kullanılarak karşılaştırılması, (i) saha davranış analizlerinde doğrusal olmayan analiz modellerinin incelenmesi konuları dikkate alınarak çalışılmıştır.

TABLE OF CONTENTS

LIST OF FIGURES

LIST OF TABLES

LIST OF SYMBOLS / ABBREVIATIONS

a	Curvature coefficient
A	Zone in a microzonation map for most favorable 33 per cent
a(t)	Acceleration time history
AR	Amplification ratio
a_{rms}	Root-mean-square acceleration
ASI	Acceleration spectrum intensity
b	Scaling coefficient
B	Strain-displacement matrix
B	Zone in a microzonation map for the medium 34 per cent
b_1, b_2, b_3, b_4, b_5, b_6	Coefficients of the proposed predictive relationships
C	Zone in a microzonation map for most unsuitable 33 per cent
c_1, c_2, …, c_{10}	Coefficients of the predictive relationships
CAV	Cumulative absolute velocity
D or ξ	Material damping ratio
$D_{adjusted}$	Scaled and capped material damping
D_{Masing}	Damping estimated based on Masing behavior
D_{min}	Small strain material damping ratio
F	Faulting mechanism of the earthquake
f	Frequency
F(f)	Fourier amplitude of shear strain
F_a	Spectral amplification factor
f_e	Frequency above which nonlinear behaviour need not to be considered
F_{max}	Maximum value of F(f)
f_p	Inverse of the period when shear strain is maximum by the zero crossing method
f_p	The effects of body forces and prescribed boundary conditions for the fluid phase
frq	Loading frequency

f_s	The effects of body forces and prescribed boundary conditions for the solid-fluid mixture
G	Shear modulus
G*	Complex shear modulus
h	Fictitious depth measure
H	Permeability matrix
HW	Hanging wall term
I_a	Arias intensity
M or M_W	Moment magnitude
m	Adjusting parameter
M	Mass matrix
M_0	Seismic moment
m_b	Short-period body-wave magnitude
M_i	Magnitude of the i^{th} event (earthquake)
M_J	JMA magnitude
M_L	Local magnitude
m_{Lg} or m_N	Lg magnitude
M_S	Surface-wave magnitude
N	Number of loading cycles
OCR	Overconsolidation ratio
p	Pore-pressure vector
PGA	Peak ground acceleration
PGD	Peak ground displacement
PGV	Peak ground velocity
PI	Soil plasticity index
PSA or SA	Pseudo spectral acceleration
PSV or SV	Pseudo spectral velocity
Q	Discrete gradient operator
R	Distance term
r	Measure of the distance from the site to the source of the earthquake
r_{epi}	Epicentral distance
r_{hypo}	Hypocentral distance

r_{ij}	Distance for the j^{th} ground motion recording during the i^{th} event (earthquake)
r_{jb} or R_{JB}	Closest horizontal distance to the vertical projection of the rupture plane, Joyner and Boore distance
r_{rup}	Closest distance to the rupture plane
r_{seis}	Closest distance to the seismogenic part of the rupture plane
S	Compressibility matrix
S	Local site conditions term
S_a	Spectral acceleration at T=0.2s on the ground surface
SA_{max}	Maximum spectral acceleration
SD	Standard deviation
SI	Response spectrum intensity
S_S	Spectral acceleration at T=0.2s on the rock outcrop obtained from the seismic hazard analysis
T	Period
T_d	Total duration of the ground motion
U	Displacement vector
V_{s30}	Weighted average (equivalent) shear wave velocity
Y	Strong motion parameter of interest
Y_{ij}	Ground motion parameter for the j^{th} ground motion recording during the i^{th} event (earthquake)
$\bar{\theta}$	Model coefficient matrix
σ_0'	Mean effective confining pressure
η_i	The inter-event error term that represents between-group variability
ε_{ij}	The intra-event error term that represents within-group variability
τ^2	Variance of the inter-event error term, η_i
σ^2	Variance of the intra-event error term, ε_{ij}
σ'	Effective stress vector

α, β	Least-squares best-fit parameters
ω_0	Mean frequency of the strain spectrum
ϕ_1 through ϕ_{12}	Parameters that relate the normalized modulus reduction and material damping curves to soil type and loading conditions
γ_r	Reference strain
α	Ratio of equivalent uniform strain divided by maximum strain
γ	Shear strain
γ_{eff}	Effective shear strain
γ_{max}	Maximum shear strain
ε	Random error term
τ	Shear stress

AIC	Akaike's Information Criterion
CPT	Cone Penetration Test
DSHA	Deterministic seismic hazard analysis
EPRI	Electrical Power Research Institute
GMSM	Ground Motion Selection and Modification Program
HVSR	Horizontal to vertical spectral ratio method
NEHRP	National Earthquake Hazard Reduction Program
NGA	Next Generation Attenuation
nlme	Nonlinear mixed effects
PEER	Pacific Earthquake Engineering Research Center
PSHA	Probabilistic seismic hazard analysis
ReMi	Refraction Microtremor
SPT	Standard Penetration Test
UBC	Uniform Building Code

1. INTRODUCTION

Any structural or geotechnical earthquake analysis involves as the first step the estimation of earthquake characteristics on the ground surface at the selected site to be used for the engineering analysis. Earthquake ground motions are affected by source, path, and local site response effects. These effects are typically combined for implementation in engineering design practice using seismic hazard analyses.

The effects of local soil conditions are included in hazard analyses by using contemporary attenuation relationships derived from strong motion recordings to define the probability density function for a ground motion parameter conditioned on the occurrence of an earthquake with a particular magnitude at a particular distance from the site. These relations are derived from statistical regression of observed ground motion parameters, and include site effects through a site term. The site term, in turn, is derived using data from all sites within broadly defined categories (*e.g.*, rock and soil), and hence the site term represents a blended average site response effect from these sites. Because of the broad range of site conditions within the “rock” and “soil” site categories used in attenuation relations, it is possible that for a particular site condition the predictions from attenuation relations are inaccurate.

There are two common ways of accounting for local site effects to improve the accuracy of ground motion predictions: (1) adjustment of attenuation predictions through the use of empirical amplification factors like site parameters as suggested by Borcherdt (1994, 2002a and 2002b) and Crouse and McGuire (1996), (2) to adopt the comprehensive approach in estimating the site specific earthquake characteristics based on site response analysis using a more detailed site characterization.

Site effects has been incorporated in Uniform Building Code, UBC (1997) as site coefficients developed based on the study of National Earthquake Hazard Reduction Program, NEHRP (BSSC, 1997). The site coefficients were estimated using strong-motion recordings of the Loma Prieta Earthquake in 1989 for accelerations of up to 0.1 g, with supplementary numerical modeling using computer programs such as SHAKE (Schnabel *et* *al.*, 1972). Borcherdt (2002a) has shown the consistency of the current site coefficients and Northridge Earthquake recordings in 1994, which provides data of accelerations of up to 0.5 g. These sites are classified according to the weighted average (equivalent) 30m shear wave velocity (V_{s30}). A pair of amplification factors is given for short-period response near 0.2 second and for longer-period response above 1.0 second.

In regions of high seismicity where strong motion records are relatively abundant, site coefficients can be reliably developed by regression of recorded ground shaking parameters. In regions of low-to-moderate seismicity or of high seismicity but with rare recorded strong motion data, such empirical models cannot be obtained in the same way. On the other hand, the validity is questionable if the same set of coefficients is implemented directly in other regions of the world, due to the following reasons: (1) Site effects are interactive processes between the frequency content of the incoming seismic waves and the site condition. The frequency content of the incoming seismic waves varies significantly from high seismicity regions to low-to-moderate seismicity regions. (2) While using V_{s30} is a practical advantage as a parameter for site classification, the important effects of the site natural period should be recognized, particularly in conditions characterized by strong impedance contrasts. (3) The crustal structure underneath the soil sediments can significantly affect the site response, and particularly so for seismic wave components exceeding 1.0 second period. (4) The effects of multiple reflections within the soil medium (pertaining to resonance behavior) have typically not been parameterized in code provisions. The resonance phenomenon deserves special attention for soil sediments with the underlying bedrock of high impedance contrast.

Owing to the aforementioned limitations of using the developed site coefficients in other regions of the world and taking into consideration the possible differences in soil profiles even within relatively short distances and observations in previous earthquakes that site conditions are important (Field and Hough, 1997; Hartzell *et al.*, 1997), it may be more reliable to adopt the site response alternative for the assessment of site-specific ground motion characteristics.

The objective of a site response analysis is to estimate free-field ground shaking characteristics during an earthquake for a specific hazard level and set of site conditions.

The compulsory components for a site response analysis are: one or more design earthquake records with representative acceleration time histories, an idealization of the soil-rock system at the site of interest, and a scheme to generate response solutions to simplified assumed wave fields in other words appropriate modeling of the soil behavior. Normally, the free-field ground response is presented in terms of either response spectra or the variation of acceleration or velocity with time.

During earthquakes soil layers are subjected to multi-directional cyclic stresses with different amplitudes and frequencies that lead to cyclic deformations and to changes in stress-strain and strength properties of soil layers. A significant effort was spend by geotechnical earthquake engineers and researchers to find both practical and appropriate solution techniques for site response analysis under earthquake excitations. Within the scope of this thesis attempts were made to give critical overviews of the different components of site response analyses.

The effects of input acceleration time histories, the applied numerical methodology, stress and frequency dependence and nonlinearity of the site response analysis were reviewed and methodologies were suggested based on case studies. Site response of layered soil deposits were analyzed using equivalent-linear and modified equivalent linear schemes.

1.1. Objectives of the Study

The study aims to review and improve the different components of site response analyses in order to achieve a robust methodology for more comprehensive and realistic assessment. The developed methodology would be utilized to estimate earthquake characteristics on the ground surface for site specific investigations based on probabilistic earthquake hazard assessment.

Within this perspective, site response analysis was studied with respect to:

- the determination of different scaling parameters including derivation of attenuation relationships for these parameters,

- the evaluation of scaling parameters with respect to magnitude and distance ranges,
- the methodology of selection and scaling of input acceleration time histories for site response analyses,
- the methodology for selection of ground motion parameters from site response analysis as design or damage parameters for various earthquake engineering analysis such as liquefaction susceptibility, microzonation, vulnerability assessments for buildings and pipeline networks, and *etc*.
- the methodology for confining stress and frequency dependence of modulus reduction and damping in equivalent linear site response analysis,
- the review concerning the available equivalent linear site response analysis models and software,
- the formulation of modified version of Shake91 (Idriss and Sun, 1992) to account for stress and frequency dependence,
- the comparison of results with modified Shake91 based on selected borings, and
- the review concerning nonlinear models for site response analysis.

1.2. Methodology and Approach

The study is composed of the following parts:

1.2.1. Input Motion: Selection and Scaling

Seismic design practice, that used to be based on a strength based approach, entered a rapidly transforming era in the 1990's. Performance based design philosophy that is taking over, involves designing engineering structures taking into account the expected regional seismic action that may take place during the economic life-time of the structure and is based on design according to limit levels of physical damage due to seismic actions. From the design point of view, this requires a detailed understanding of the factors and parameters that describe and quantify damage in a most efficient way for an engineering structure and identification and estimation of earthquake ground motion parameters that correlate with these damage parameters (Priestley, 2000).

From the perspective of performance based earthquake engineering, there are three issues that are either being or need to be addressed by the geotechnical earthquake engineering community. The first concerns the setting and estimation of performance and damage criteria for different geotechnical structures. This is often about the estimation of damaging ground deformation levels for a natural site or for a geotechnical structure. The second is related to the estimation and modeling of the uncertainty in the material properties of soils and of ground response. The third is about selection, scaling and modification (*i.e.,* due to soil-structure interaction) of earthquake ground motion to be used as input in the analyses (Stewart *et al.*, 2001, 2002). In this first part of the thesis study, first and third issues of the performance based design concept were studied.

Using 1D equivalent-linear and nonlinear soil models at a site with pre-determined levels of earthquake hazard, first the resulting response variability was investigated when analyzed under a series of ground motion records selected as compatible with the site-specific earthquake hazard. Then using the same family of records, this time scaled with respect to intensity measures such as peak ground acceleration (PGA), peak ground velocity (PGV), and Arias intensity (I_a), *etc.* the analysis were repeated and the variability introduced by scaling and the effectiveness of scaling methods was evaluated including the selection of records from different distance ranges. This investigation is considered as a step towards understanding how ground motion scaling affects the site response.

At this point, two problems may arise: First, the selection of ground motion parameters as damage parameters in various geotechnical earthquake engineering analysis; second, determining the values of these selected ground motion parameters. Attenuation relationships are limited to only few of the ground motion parameters, such as peak ground acceleration, peak ground velocity and spectral accelerations. New empirical attenuation relationships for the prediction of the engineering ground motion parameters other than the traditional ones are developed and site response analyses are conducted using scaling parameters determined from proposed empirical attenuation relationships for the selected ground motion parameters.

Scaling of input time histories can be carried out in time-domain and in frequency domain. In time-domain, scaling involves only the amplitude of the time series (*i.e.*, PGA, PGV, Arias Intensity, I_a; root mean square acceleration, a_{rms}), whereas in frequency domain scaling, the frequency content is changed within a pre-determined frequency window (*i.e.,* spectral intensity, SI).

1.2.2. Site Response Analysis: Equivalent Linear Approach

One of the important issues in specifying site specific input design motion is to account for nonlinearity in site response which is dependent on expected earthquake source and existing site characteristics. Soils behave nonlinearly when subjected to strong levels of ground shaking. The effect of nonlinearity is to reduce the amount of amplification as the input ground motion level is increased. This phenomenon is due to the increase in hysteretic damping and degradation and softening in soils with strain level and accumulation. At low strain levels, the relationship is essentially elastic.

In the field of geotechnical engineering, it is well established by laboratory and field tests that stress – strain relationships of soils are strain dependent, nonlinear and hysteretic, especially for large shear strain levels. And recently, with increasing number of good quality strong motion data, evidence of nonlinear site response in acceleration records has become more visible.

The actual nonlinear stress-strain behavior of cyclically loaded soils can be approximated by equivalent linear soil properties. The equivalent linear approach to one-dimensional ground response analysis of layered sites has been coded into a widely used computer program called SHAKE (Schnabel *et al.*, 1972). However, although the equivalent linear approach is computationally convenient and provides reasonable results for many practical problems, it remains an approximation to the actual nonlinear process of seismic ground response.

In the second part of the thesis, efforts were spent to study the modifications that can be implemented to improve the effectiveness of Shake91 code for practical applications. The modifications introduced are the use of confining pressure dependent modulus degradation and damping curves and frequency dependence of the iteration scheme in the code.

1.2.3. Site Response Analysis Method: Nonlinear Approach

An alternative approach is to analyze the actual nonlinear response of a soil deposit using direct numerical integration in the time domain. Most currently available nonlinear one-dimensional site response computer programs characterize the stress-strain behavior of the soil by cyclic stress – strain models such as the hyperbolic model. Others have been based on advanced constitutive models such as the nested yield surface.

In order to study the nonlinearity in site response, vertical array records and profiles where nonlinearity has been evidenced were investigated; the comparison of literally available nonlinear site response models was reviewed.

1.2.4. Microzonation Methodology and Site Response Analysis

Microzonation is identification of areas having different earthquake hazard potentials. The seismic microzonation maps would indicate the distribution of these potentials thus providing an input for urban planning and earthquake mitigation priorities at an urban scale.

Site specific free field earthquake characteristics on the ground surface are the essential components for microzonation with respect to ground shaking intensity, liquefaction susceptibility and for the assessment of the seismic vulnerability of the urban environment. The adopted microzonation methodology is based on a grid (cell) system and is composed of three stages: In the first stage, regional seismic hazard analyses need to be conducted to estimate earthquake characteristics on the rock outcrop for each cell. In the second stage, the representative site profiles should be modeled based on the available borings and in-situ tests. The third stage involves site response analyses for estimating the earthquake characteristics on the ground surface and the interpretation of the results for microzonation (Ansal *et al.*, 2004a, 2004b, 2005b, 2005c, 2007b and 2007c). In addition to the generation of base maps for urban planning, microzonation with respect to spectral accelerations, peak acceleration and peak velocity on the ground surface can be used to assess the vulnerability of the building stock (Ansal and Tönük, 2007a; Ansal *et al.,* 2004c, 2005a, 2006a, 2007a, 2009) and lifeline systems (Ansal *et al.*, 2008). The spectral accelerations on the ground surface to be used in the vulnerability assessment of the building stock are determined based on elastic acceleration response spectra obtained from site response analyses.

1.3. Organization of the Study

Throughout this study, factors affecting site response analysis have been reviewed and the effects of site response analysis methodology on the microzonation and site specific assessment of earthquake ground motion characteristics have been evaluated.

In first two chapters, the input motion component of site response analysis methodology is evaluated. Chapter 2 presents derivation of empirical attenuation relations to predict strong ground motion parameters on rock sites based on Next Generation Attenuation (NGA) database (PEER). The predictive relations are proposed for eight strong motion parameters and are used to determine the effects of different scaling parameters in Chapter 3.

In Chapter 3, the methodology of selection and scaling of input acceleration time histories for site response analyses is reviewed. A parametric study is performed based on large number of site response analyses with input motions scaled with respect to selected set of intensity measures. The results are evaluated with respect to the scaling options used for site response analysis for different engineering applications.

In Chapter 4 and 5, different site response analysis methods (equivalent linear and nonlinear, respectively) have been reviewed, and the merits and disadvantages of each are explained. In Chapter 4, the methods to improve the accuracy of equivalent linear method are considered, and the modifications that are implemented in Shake91 are presented.

Beside the review concerning nonlinear models for site response analysis, studies concerning identification of nonlinear behavior based on ground motion records and vertical array data are given in Chapter 5.

The comparison of site response based on equivalent linear model with and without stress and frequency dependence is given in Chapter 6 with respect to selected set of borings.

The conclusions and limitations of this research, along with some recommendations for future studies are presented in Chapter 7.

2. EMPIRICAL PREDICTIVE RELATIONS FOR ENGINEERING GROUND MOTION PARAMETERS

2.1. Attenuation Relations

2.1.1. Introduction

Two basic methods used to estimate strong ground motion in engineering practice, are known as deterministic seismic hazard analysis, DSHA and probabilistic seismic hazard analysis, PSHA. Both methods require a procedure for estimating strong ground motion from the specified seismological parameters. This estimation is usually based on predictive relationships, also known as attenuation relations for a particular ground motion parameter formulated in terms of quantities that affect the process most strongly. These relations are based on available earthquake records and are either fully empirical, or rely on empirical data to calibrate theoretical models.

Attenuation relationships relate ground motion parameters to the magnitude of an earthquake and the distance away from the fault rupture. They are developed by statistical evaluation of a large set of ground motion data. The greater the size of the data set, the more robust is the relationship. It is important to remember that these relationships are only as good as the data set upon which they are based.

Attenuation relationships have been established for ground motion parameters including peak ground acceleration, peak ground velocity, peak ground displacement, and spectral quantities and developed for different regions and fault types (strike-slip versus subduction and interplate versus intraplate). These relations have been reviewed and their use in engineering has been discussed in the literature (Ambraseys and Bommer, 1995; Abrahamson and Shedlock, 1997; Campbell, 2003; Douglas, 2003; Abrahamson *et al.*, 2008).

2.1.2. Functional Form of the Attenuation Relations

The functional form of the predictive relationships is usually selected to reflect the mechanics of the ground motion process as closely as possible. The relations generally have a form similar to (Campbell, 2003; Kramer, 1996):

$$\underbrace{\ln Y}_{1} = \underbrace{c_1 + c_2 M + c_3 M^{c_4}}_{2} - \underbrace{c_5 \ln R}_{3} + \underbrace{c_6 R}_{5} + \underbrace{c_7 F + c_8 HW + c_9 S}_{6} + \varepsilon \qquad (2.1)$$

where the distance term R is given by one of the alternative expressions:

$$R = \begin{cases} r + \overbrace{c_{10} \exp(c_{11} M)}^{4} \\ \text{or} \\ \sqrt{r^2 + [c_{10} + \exp(c_{11} M)]^2} \end{cases} \qquad (2.2)$$

In the above equations, Y is the strong motion parameter of interest, M is magnitude, F is the faulting mechanism of the earthquake, HW is the hanging wall term, S is a description of the local site conditions beneath the site, ε is a random error term with a mean of zero and a standard deviation of $\sigma_{\ln Y}$ (the standard error of estimate of ln Y), and r is a measure of the distance from the site to the source of the earthquake. In the more complicated forms of the equations, the coefficients c_5, c_9 , and c_{10} are defined in terms of M and R.

Explanations for the numbered terms in the common form of predictive relationship in Equation (2.1) and (2.2) are as follows:

1: Peak values of strong motion parameters are generally log-normally distributed; consequently regressions are performed on the natural logarithm of the data, which is normally distributed.

2: ln $Y \alpha c_2 M$ term is consistent with the original definition of earthquake magnitude. Several magnitude scales are derived from the logarithm of various peak ground motion parameters. As a result, ln Y is approximately proportional to M.

3: The expression ln $Y \alpha -c_5$ ln R is consistent with the geometric attenuation of the seismic wave front as it propagates away from the earthquake source. The assumption of $c_5=1$ in some attenuation relations comes from the theoretical value for spherical spreading of the wave front from a point source in a homogeneous whole space.

4: Strong motion at a site is produced sometimes by waves arriving from a distance R and sometimes by waves arriving from greater distances due to the fact that the area over which fault rupture occurs increases with increasing magnitude. The effective distance is therefore greater than R by an amount that increases with increasing magnitude.

5: The expression ln $Y \alpha -c_6 R$ is consistent with the anelastic attenuation that results from material damping (absorption of the energy carried by stress waves by the materials they travel through) and scattering as the seismic waves propagate through the crust.

6: The relation between Y and the remaining parameters have been established over the years from both empirical and theoretical ground-motion modeling. Fault rupture mechanism (F), the location of a site on or off the hanging wall of dip-slip faults (HW), and local site conditions (S) are observed to affect ground motion parameter.

2.1.3. Model Parameters and Factors Affecting Attenuation

A complete description of ground motion requires defining its amplitude as a function of time by means of a time history or equivalently in the frequency domain by means of a Fourier spectrum. However, for most engineering applications such a complex description of ground motion is not necessary. Instead, simple time-domain and frequency-domain parameters are used to define strong ground motion. Peak ground acceleration and peak ground velocity have been the most common time-domain parameters used in engineering. They represent the maximum absolute amplitude of ground motion measured from a recorded or synthetic acceleration or velocity time history. In the design of a structure, natural period and natural frequency are incorporated through the use of a response spectrum. The most common response spectral parameters are pseudoacceleration (PSA or SA) and pseudovelocity (PSV or SV).

Earthquake magnitude is used to define the "size" of an earthquake. There are many different scales that can be used to define magnitude. The magnitude scales that have commonly been used in the development of attenuation relations throughout the world are moment magnitude (denoted M or M_W), surface-wave magnitude M_S, short-period body-wave magnitude m_b, local magnitude M_L, Lg magnitude (denoted m_{Lg} or m_N), and JMA magnitude M_J. These magnitude scales are compared in Figure 2.1. Since its strong physical and seismological basis that M_W is by definition related to seismic moment M_0, a measure of the seismic energy radiated by an earthquake, M_W is increasingly preferred as the worldwide standard for quantifying magnitude.

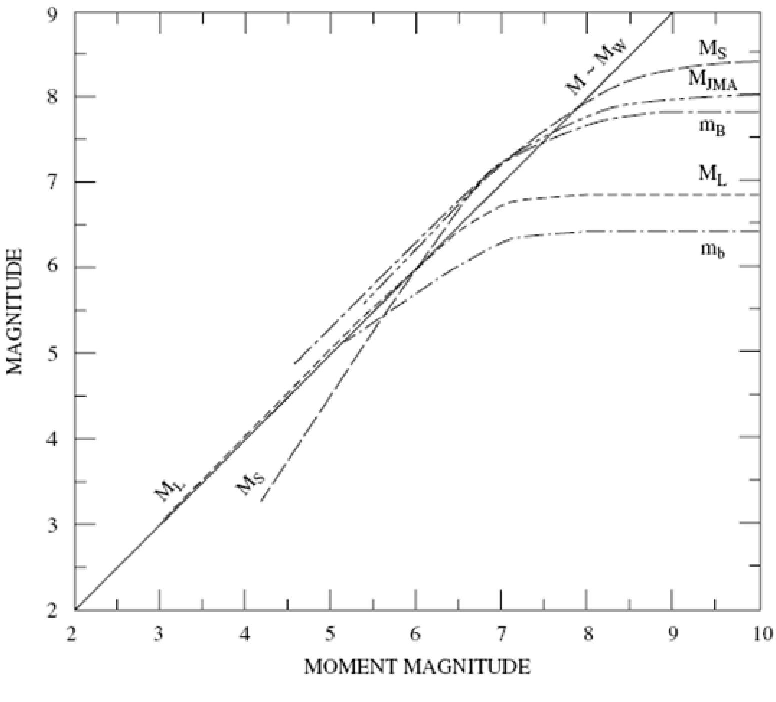

Figure 2.1. Comparison of magnitude measures (Heaton *et al.*, 1986)

Site to source distance is used to characterize the decrease in ground motion as it propagates away from the earthquake source and measured differently by different researchers. Common definitions of R are shown in Figure 2.2 with the researchers using them.

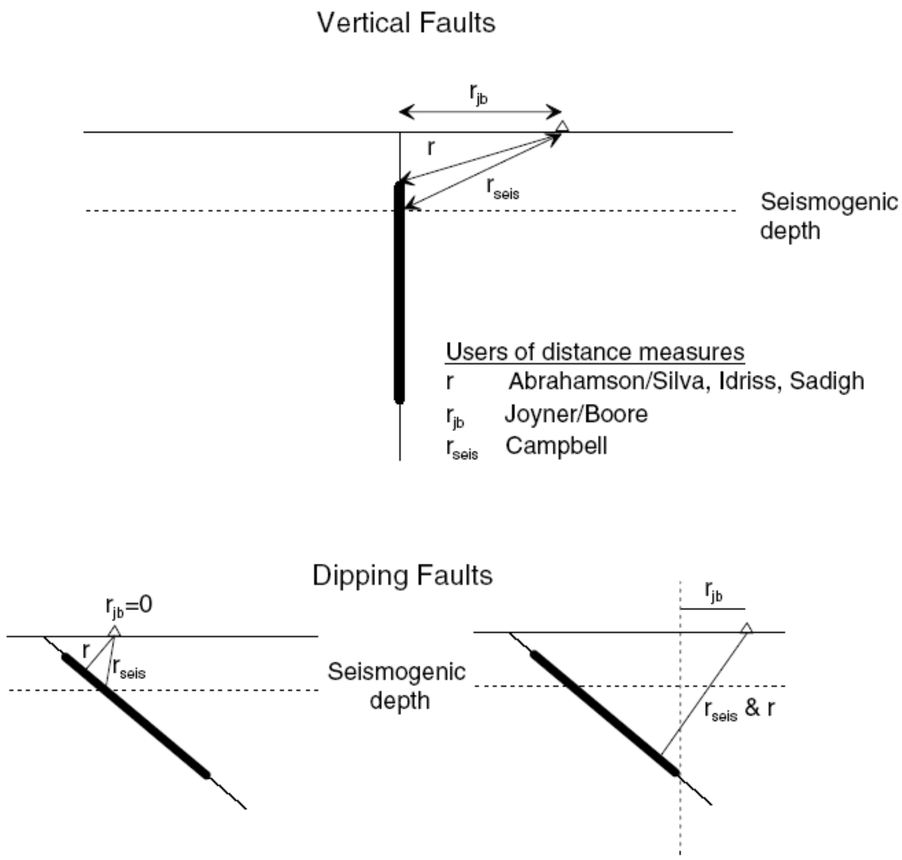

Figure 2.2. Comparison of distance measures (Abrahamson and Shedlock, 1997)

Distance measures can be grouped into two broad classes depending on whether they treat the earthquake source as a single point or as a finite fault rupture. Point-source distance measures include epicentral distance r_{epi} and hypocentral distance r_{hypo}. Hypocentral distance is defined as the point within the Earth where the earthquake rupture begins. Epicentral distance is the point on the Earth's surface directly above the hypocenter. r_{epi} and r_{hypo} are poor measures of distance for earthquakes with large rupture areas. They are primarily used for characterizing distances for small earthquakes that can be reasonably represented by a point source. There are three finite-source distance measures that are commonly used in practice: r_{jb} or the closest horizontal distance to the vertical projection of the rupture plane, r_{rup} or the closest distance to the rupture plane, and r_{seis} or the closest distance to the seismogenic part of the rupture plane. Although r_{jb} is reasonably easy to estimate for a future (design) earthquake, r_{rup} and r_{seis} are not as easily determined, particularly when the earthquake is not expected to rupture the entire seismogenic width of the crust.

The faulting mechanism, also referred to as the type or style of faulting, characterizes the direction of slip on the fault plane, seismologically known as the rake angle. Rake angle is a continuous variable representing the angle between the direction of slip on the fault plane and the strike or the orientation of the fault on the Earth's surface. Rake angle has not been used directly in an attenuation relation to define faulting mechanism. Instead, the faulting mechanism has been classified in terms of two or more categories. Most earthquakes in active tectonic regions have one of four focal mechanisms: strike-slip, reverse, oblique, and normal (Figure 2.3). The values of rake angle corresponding to these faulting mechanisms are 0° for left-lateral strike-slip faulting, 180° for right-lateral strike-slip faulting, 90° for reverse faulting, and 270° for normal faulting (Lay and Wallace, 1995). Thrust faulting is a special case of reverse faulting in which the dip angle of the rupture plane is less than 45°. A combination of strike-slip with either reverse-slip or normal-slip is known as oblique faulting and will have a rake angle that falls between given values.

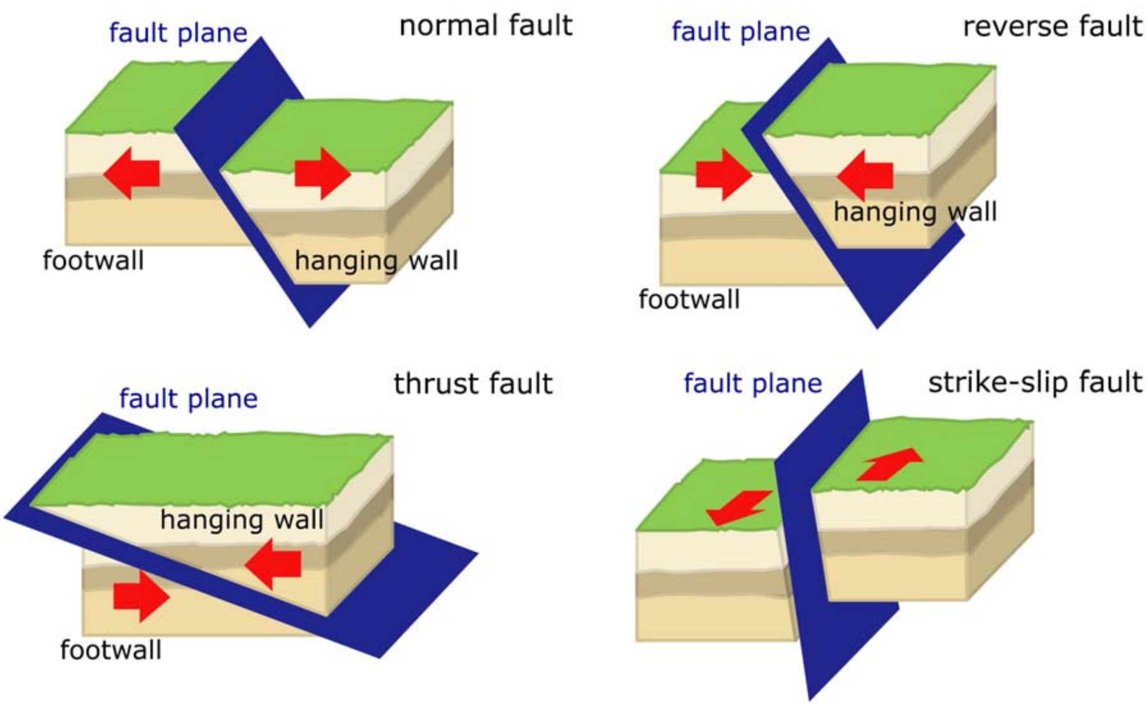

Figure 2.3. Main types of fault motion

The bias that results solely from rupture mechanism is represented in each of the major attenuation relationships for active regions through use of an f(F) term in the regression equation. Researchers have taken this term as constant, period-dependent, distance-dependent, and/or magnitude-dependent. Factor f(F) generally increases median ground motion estimates, with the exception of long-period spectral components at large magnitudes, which are decreased. The strike-slip mechanism is generally taken as a "reference" mechanism with no correction (*i.e.*, F=0). Significant differences are observed between reverse earthquake motions and strike-slip and Campbell (1981) empirically demonstrated that reverse and thrust faulting causes higher ground motion than strike-slip or normal faulting. No corrections are generally made for normal-slip earthquakes. Relatively little data are available for oblique-slip earthquakes, and the f(F) correction for oblique-slip is often taken as half of f(F) for reverse earthquakes.

The hanging wall is that portion of the crust that lies above the rupture plane of a dipping fault and the footwall is that portion of the crust that lies below this plane. Researches reveal that sites located on the hanging wall of a reverse or thrust fault generally exhibit higher-than-average ground motion and that sites located on the footwall generally have lower-than average ground motion. Figure 2.4 defines the geometric limits of the hanging wall for dip-slip faults.

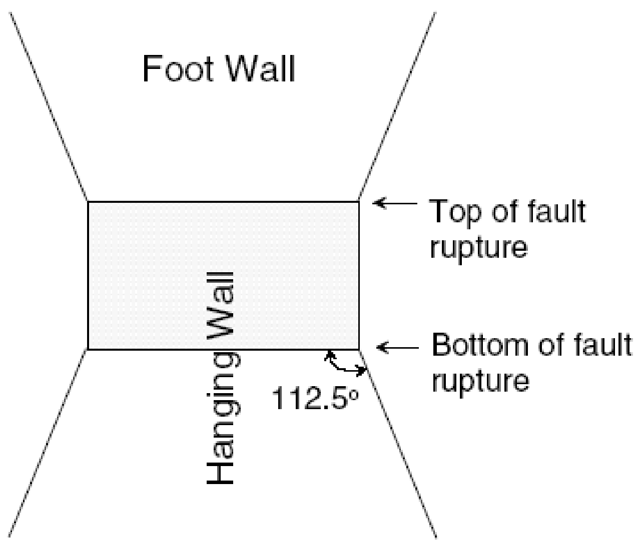

Figure 2.4. Definition of footwall and hanging wall where the separation point is the vertical projection of the top of the fault rupture (Abrahamson and Somerville, 1996)

The effect of geologic and local soil conditions underlying seismographs can significantly influence the characteristics of recorded ground motion. To partially account for this effect, a site term, f(S), is generally included in regression equations for median ground motion parameters. Local site conditions describe the materials that lie directly beneath the site from the surface to basement rock. They are usually defined in terms of surface or near-surface geology, shear wave velocity, and the depth of sediments beneath the site. The value of the site term decreases as the rock acceleration increases, which incorporates nonlinearity.

The tectonic regime in which earthquakes occur is a fundamental factor affecting ground motion characteristics. Most earthquakes occur in one of four basic regimes: (1) shallow-crustal earthquakes in active tectonic regions, (2) shallow-crustal earthquakes in stable tectonic regions, (3) intermediate-depth earthquakes (also known as Wadati-Benioff or intraslab earthquakes) within subducting plates, and (4) earthquakes along the interface of two subducting plates. The shallow-crustal environment can be further divided into compressional and extensional stress regimes.

2.1.4. Regression Analysis

Whether developed from empirical observations or theoretical data, all attenuation relations are derived from a statistical fitting procedure known as regression analysis (Draper and Smith, 1981). A regression analysis is used to determine the best estimate of the coefficients in Equations (2.1) and (2.2) using statistical fitting procedures such as minimum least squares or maximum likelihood (Campbell, 2003).

There are different methods used by the researchers for performing a regression analysis for the purpose of developing an attenuation relation (Stewart *et al.*, 2001):

- <u>Two-step regression:</u> Joyner and Boore (1981) proposed a two-step regression procedure where in the first step all data points are weighted equally to derive the shape of the function describing the variation of spectral acceleration with distance and in the second step all events are weighted equally to derive the magnitude dependence of spectral quantities.

- Weighted nonlinear least-squares regression: Campbell (1981) uses a weighted least squares regression that is performed as follows: [1] The ground motion inventory is first "binned" according to M and R (*i.e.*, all data within a limited range of M and R is placed into a "bin"), [2] each bin of data is given equal weight in the regression, and [3] within a bin, the collective data from each event are weighted equally.

- Random effects regression: Brillinger and Priesler (1984) developed a random effects model that is typically applied as described by Abrahamson and Youngs (1992). As part of the regression procedure, estimates of inter- and intra-event error are produced, as are "event terms" that represent the event-specific mean residuals in the data. Regression coefficients are estimated from a data set in which ground motion parameters are modified by subtraction of event terms. With the data set "corrected" in this manner, all data points are weighted equally. The standard error is the sum of the inter- and intra-event error. Joyner and Boore (1993, 1994) have also proposed a one-step regression procedure that is similar in concept to the Brillinger and Preisler (1984) method and produces regression results similar to the two-step procedure.

- Free regression: Idriss (1991b) does not perform formal regression analysis, but has developed relations that are judgment based. The relations are formed by postulating a model, studying the residuals, and revising the model as necessary.

Each of these methods has its strengths and weaknesses but they all have the same intended purpose that is to mitigate the bias introduced by the uneven distribution of recordings with respect to magnitude, distance, and other seismological parameters. The advantage of two-step and random effect regression methods is that they provide a direct estimate of the intra- and inter-earthquake components of randomness.

2.2. Objective and Motivation of the Study

Attenuation relationships are limited only to few ground motion parameters, such as peak ground acceleration, peak ground velocity and spectral accelerations. In this Chapter, new empirical attenuation relationships other than the traditional ones, for the prediction of the engineering ground motion parameters on rock outcrop are proposed based on Next Generation Attenuation (NGA) database.

The motivation was to determine the values of selected ground motion parameters that are essential to estimate the significance of the factors affecting site response analysis. The intention is to evaluate site response in a comprehensive way concerning the influence of selection and scaling of input ground motion on the calculated ground motion parameters selected as ground motion intensity measures or in other words damage parameters in various geotechnical earthquake engineering analysis. Using scaling parameters determined from proposed empirical attenuation relationships for the selected ground motion parameters, site response analyses are conducted to assess how ground motion scaling affects the calculated ground motion characteristics on the ground surface.

Methods for estimating ground motion parameters are essential since level of ground shaking for earthquake resistant design and thus damage potential of an earthquake are defined based on different ground motion parameters. The better damage indicators are the parameters that can reflect nearly all of the amplitude, frequency content and duration characteristics of an earthquake ground motion. Empirical attenuation relationships proposed in this study are for the prediction of various engineering ground motion parameters that incorporate in their definition previously mentioned characteristics. For this study, peak ground acceleration (PGA), peak ground velocity (PGV), root-mean-square acceleration (a_{rms}), Arias intensity (I_a), cumulative absolute velocity (CAV), maximum spectral acceleration (SA_{max}), response spectrum intensity (SI) and acceleration spectrum intensity (ASI) are selected as representative ground motion parameters. These selected ground-motion parameters are defined through Equations (2.3) to (2.8) and are evaluated for sites with average shear wave velocity at the upper 30 m, $V_{s30} \geq 500$ m/s representing soft rock-rock site condition.

The intended use of these engineering strong-motion parameters primarily is to determine their effectiveness. Some of the parameters correlate well with several damage parameters of structural performance, liquefaction, seismic slope stability, vulnerability assessments, microzonation studies *etc.* For example, for earthquake-resistant design, the earthquake ground motion defined based on the elastic acceleration response spectrum.

However, using the acceleration response spectrum in current seismic design practice does not directly account for the influence of the duration of strong motion or for the hysteretic behavior of the structure. Instead, a design approach based on input energy has the potential to address the effects of the duration and hysteretic behavior directly. Some examples on the use of engineering ground-motion parameters are; generation of shake maps for rapid visualization of the extent of the expected damages to be used for emergency response, loss estimation, and public information (Wald *et al.,* 1999); the development of early warning systems for the reduction of the seismic risk of vital facilities, such as nuclear power plants (EPRI, 1988), pipelines, high-speed trains; and estimation of damage potential due to liquefaction (Kramer and Mitchell, 2005).

2.3. Strong Motion Database

The strong motion records used in this study are obtained from the NGA database maintained at the Pacific Earthquake Engineering Research Center (PEER) website because of its high quality and availability for the supplied information required and homogeneity due to the same processing procedures used. The overall database available consists of 3551 multi-component records from 173 shallow crustal earthquakes ranging in magnitude from 4.2 to 7.9. In addition to the ground motion parameters, a large and comprehensive list of metadata characterizing the recording conditions of each record is also available.

Proposed relations are derived using a subset (Table 2.1) of NGA data comprising 547 pairs of horizontal records obtained during 72 shallow crustal earthquakes with magnitudes $4.5 < M < 8$ and hypocentral distances in the range of $1\text{km} < r_{hypo} < 325\text{km}$ for the sites with average shear wave velocity at the upper 30 m, $V_{s30} \geq 500$ m/s. A representation of the distribution of the strong motion data as a function of moment magnitude and distance is shown in Figure 2.5 and in Figure 2.6 with respect to style of faulting.

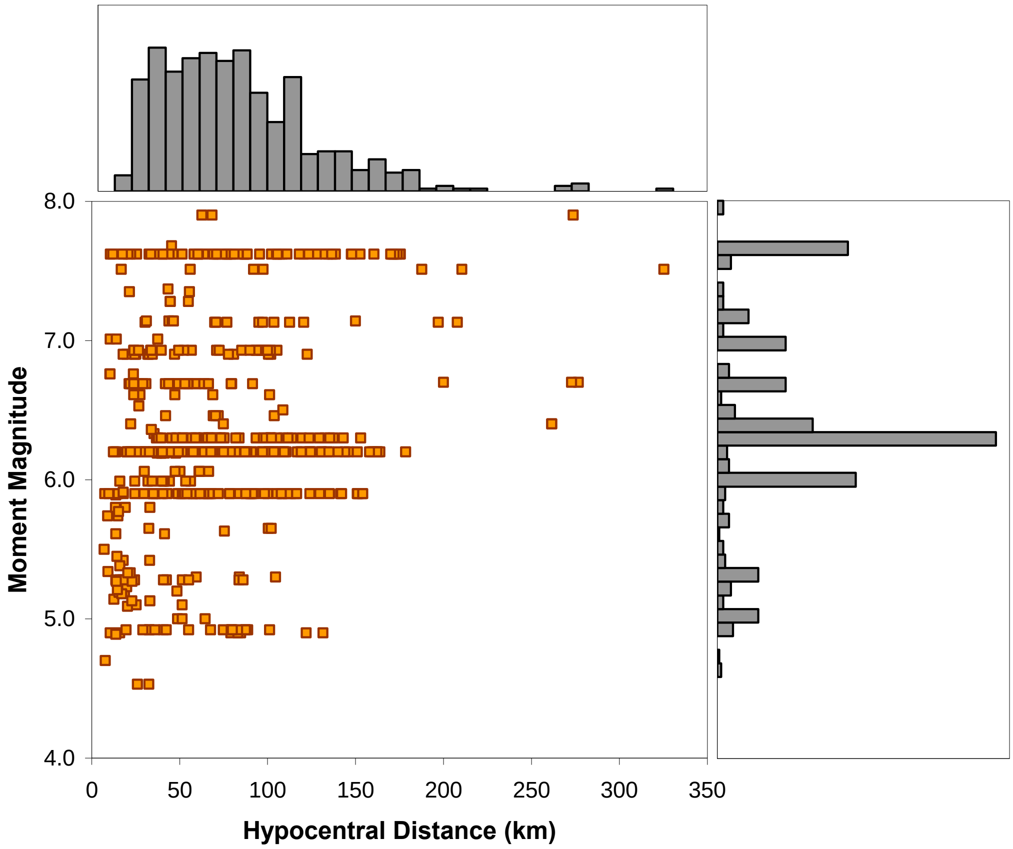

Figure 2.5. Distribution of the selected datasets in magnitude and hypocentral distance

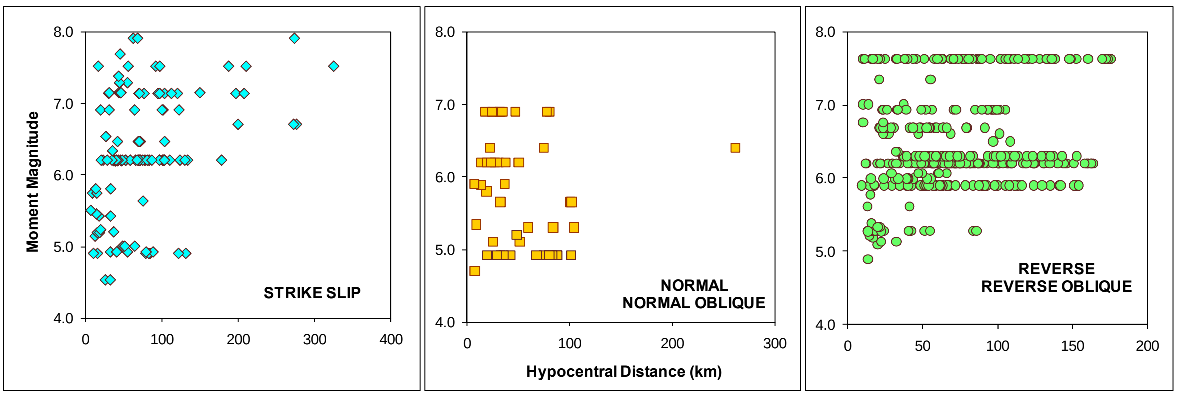

Figure 2.6. Distribution of the selected datasets in magnitude and hypocentral distance with respect to style of faulting

Table 2.1. Database of strong motion records used in the regression analysis

No.	Earthquake Name	YEAR MODY HRMN	Hypocenter Latitude (deg)	Hypocenter Longitude (deg)	Hypocenter Depth (km)	Earthquake Magnitude	Mechanism Based on Rake Angle	Number of Stations
1	San Francisco	1957 0322 1944	37.6700	-122.4800	8.0	5.28	Reverse	1
2	Parkfield	1966 0628 0426	35.9550	-120.4983	10.0	6.19	Strike Slip	1
3	Lytle Creek	1970 0912 1430	34.2698	-117.5400	8.0	5.33	Reverse Oblique	2
4	San Fernando	1971 0209 1400	34.4400	-118.4100	13.0	6.61	Reverse	6
5	Hollister-03	1974 1128 2301	36.9202	-121.4663	6.1	5.14	Strike Slip	1
6	Oroville-01	1975 0801 2020	39.4390	-121.5280	5.5	5.89	Normal	1
7	Oroville-03	1975 0808 0700	39.5020	-121.5120	7.6	4.70	Normal	1
8	Friuli, Italy-01	1976 0506 2000	46.3450	13.2400	5.1	6.50	Reverse	1
9	Friuli, Italy-02	1976 0915 0315	46.3750	13.0670	3.7	5.91	Reverse	1
10	Tabas, Iran	1978 0916	33.2150	57.3230	5.8	7.35	Reverse	2
11	Dursunbey, Turkey	1979 0718 1312	39.6600	28.6500	7.0	5.34	Normal	1
12	Coyote Lake	1979 0806 1705	37.0845	-121.5054	9.6	5.74	Strike Slip	2
13	Norcia, Italy	1979 0919 2136	42.7300	12.9600	6.0	5.90	Normal	2
14	Imperial Valley-06	1979 1015 2316	32.6435	-115.3088	10.0	6.53	Strike Slip	1
15	Livermore-01	1980 0124 1900	37.8550	-121.8160	12.0	5.80	Strike Slip	1
16	Livermore-02	1980 0127 0233	37.7370	-121.7400	14.5	5.42	Strike Slip	2
17	Anza (Horse Canyon)-01	1980 0225 1047	33.5050	-116.5140	13.6	5.19	Strike Slip	2
18	Victoria, Mexico	1980 0609 0328	32.1850	-115.0760	11.0	6.33	Strike Slip	1
19	Irpinia, Italy-01	1980 1123 1934	40.8059	15.3372	9.5	6.90	Normal	9
20	Irpinia, Italy-02	1980 1123 1935	40.8464	15.3316	7.0	6.20	Normal	7
21	Coalinga-01	1983 0502 2342	36.2330	-120.3100	4.6	6.36	Reverse	1
22	Coalinga-02	1983 0509 0249	36.2460	-120.2990	12.0	5.09	Reverse	1
23	Coalinga-03	1983 0611 0309	36.2560	-120.4500	2.4	5.38	Reverse	1
24	Coalinga-04	1983 0709 0740	36.2510	-120.4000	9.0	5.18	Reverse	1
25	Coalinga-05	1983 0722 0239	36.2410	-120.4090	7.4	5.77	Reverse	1
26	Coalinga-06	1983 0722 0343	36.2220	-120.4070	7.9	4.89	Reverse	1
27	Coalinga-07	1983 0725 2231	36.2290	-120.3980	8.4	5.21	Reverse	1
28	Coalinga-08	1983 0909 0916	36.2240	-120.2320	6.7	5.23	Strike Slip	1
29	Borah Peak, ID-02	1983 1029 2329	44.2390	-114.0700	10.0	5.10	Normal	2
30	Morgan Hill	1984 0424 2115	37.3060	-121.6950	8.5	6.19	Strike Slip	4
31	Lazio-Abruzzo, Italy	1984 0507 1750	41.7100	13.9020	14.0	5.80	Normal	1
32	Drama, Greece	1985 1109 2330	41.2253	23.9951	10.8	5.20	Normal Oblique	1
33	Nahanni, Canada	1985 1223	62.1870	-124.2430	8.0	6.76	Reverse	3
34	Hollister-04	1986 0126 1920	36.8040	-121.2847	8.7	5.45	Strike Slip	1
35	N. Palm Springs	1986 0708 0920	34.0000	-116.6117	11.0	6.06	Reverse Oblique	6
36	San Salvador	1986 1010 1749	13.6330	-89.2000	10.9	5.80	Strike Slip	1
37	Baja California	1987 0207 0345	32.3880	-115.3050	6.0	5.50	Strike Slip	1
38	Whittier Narrows-01	1987 1001 1442	34.0493	-118.0810	14.6	5.99	Reverse Oblique	10
39	Whittier Narrows-02	1987 1004 1059	34.0600	-118.1035	13.3	5.27	Reverse Oblique	2
40	Loma Prieta	1989 1018 0005	37.0407	-121.8829	17.5	6.93	Reverse Oblique	22
41	Roermond, Netherlands	1992 0413 0120	51.1700	5.9250	14.6	5.30	Normal	3
42	Cape Mendocino	1992 0425 1806	40.3338	-124.2294	9.6	7.01	Reverse	3
43	Landers	1992 0628 1158	34.2000	-116.4300	7.0	7.28	Strike Slip	3
44	Big Bear-01	1992 0628 1506	34.2100	-116.8300	13.0	6.46	Strike Slip	5
45	Northridge-01	1994 0117 1231	34.2057	-118.5539	17.5	6.69	Reverse	28
46	Kobe, Japan	1995 0116 2046	34.5948	135.0121	17.9	6.90	Strike Slip	4
47	Kozani, Greece-01	1995 0513 0847	40.1569	21.6746	12.6	6.40	Normal	2
48	Dinar, Turkey	1995 1001 1557	38.0600	30.1500	5.0	6.40	Normal	2
49	Kocaeli, Turkey	1999 0817	40.7270	29.9900	15.0	7.51	Strike Slip	7
50	Chi-Chi, Taiwan	1999 0920	23.8603	120.7995	6.8	7.62	Reverse Oblique	66
51	Duzce, Turkey	1999 1112	40.7746	31.1870	10.0	7.14	Strike Slip	5
52	Sitka, Alaska	1972 0730	56.7700	-135.7840	29.0	7.68	Strike Slip	1
53	Upland	1990 0228	34.1437	-117.6973	4.5	5.63	Strike Slip	1
54	Manjil, Iran	1990 0620	36.8101	49.3530	19.0	7.37	Strike Slip	1
55	Sierra Madre	1991 0628	34.2591	-118.0010	12.0	5.61	Reverse	2
56	Northridge-05	1994 0117 0043	34.3765	-118.6982	11.3	5.13	Reverse Oblique	2
57	Northridge-06	1994 0320 2120	34.2313	-118.4750	13.1	5.28	Reverse	13
58	Little Skull Mtn,NV	1992 0629	36.7200	-116.2860	12.0	5.65	Normal	3
59	Hector Mine	1999 1016	34.5740	-116.2910	5.0	7.13	Strike Slip	11
60	Yountville	2000 0903	38.3788	-122.4127	10.1	5.00	Strike Slip	3
61	Big Bear-02	2001 0210	34.2895	-116.9458	9.1	4.53	Strike Slip	2
62	Anza-02	2001 1031	33.5083	-116.5143	15.2	4.92	Normal Oblique	13
63	Gilroy	2002 0514	36.9667	-121.5987	10.1	4.90	Strike Slip	7
64	Nenana Mountain, Alaska	2002 1023	63.5144	-148.1100	4.2	6.70	Strike Slip	3
65	Denali, Alaska	2002 1103	63.5375	-147.4440	4.9	7.90	Strike Slip	3
66	Big Bear City	2003 0222	34.3100	-116.8480	6.3	4.92	Strike Slip	5
67	Chi-Chi, Taiwan-02	1999 0920 1757	23.9400	121.0100	8.0	5.90	Reverse	58
68	Chi-Chi, Taiwan-03	1999 0920 1803	23.8100	120.8500	8.0	6.20	Reverse	46
69	Chi-Chi, Taiwan-04	1999 0920 2146	23.6000	120.8200	18.0	6.20	Strike Slip	38
70	Chi-Chi, Taiwan-05	1999 0922 0014	23.8100	121.0800	10.0	6.20	Reverse	52
71	Chi-Chi, Taiwan-06	1999 0925 2352	23.8700	121.0100	16.0	6.30	Reverse	47
72	Northridge-01	1994 0117 1231	34.2057	-118.5539	17.5	6.69	Reverse	1

Only free-field records were used excluding records obtained in the basements of buildings, records in the first floor of buildings with three stories or higher, records at the dam toes, crests and abutments in order to minimize the possible bias associated with the effects of such buildings in the recorded ground motion.

The records obtained from any earthquake with missing information such as stations without two horizontal components, stations without V_{s30} definition or earthquakes without fault mechanism information were also excluded from the analysis.

2.4. Model Parameters

A brief description of the dependent and independent variables used to develop the regression analysis is given subsequently. The independent variables consist of those parameters that describe the source, travel path, and site conditions that determine the character and the strength of the ground motion.

Geometric mean of horizontal components are used to derive the new attenuation relations for ground motion parameters previously stated as a function of the moment magnitude (M, to avoid saturation effects for magnitudes greater than 6) and closest distance to the vertical projection of the fault plane (Joyner and Boore distance, r_{jb}).

Differences between the various definitions of distance measures tend to be more significant in the near field, but less in the far field. For earthquakes where the location of the causative fault has not been reported, mainly earthquakes with $M_w \leq 6$, epicentral distance, r_e is used instead. For small earthquakes r_e and r_{jb} are similar because of the small rupture planes of such earthquakes. The style of faulting parameter is included in the predictive relations to distinguish between different source types and is classified into three categories: Strike – slip, Normal / Normal Oblique and Reverse / Reverse Oblique.

Engineering ground-motion parameters are the dependent variables that are being estimated in the regression analysis and a short description of these parameters is presented next.

Peak ground velocity is, simply, the largest absolute value of velocity in the time series. PGV is less sensitive to the higher-frequency components of ground motion and is more likely than PGA to characterize ground-motion amplitude accurately at intermediate frequencies.

Root-mean-square acceleration (a_{rms}) is a measure of the average rate of energy imparted by the ground motion and is defined as:

$$a_{rms} = \sqrt{\frac{1}{T_d} \int_0^{T_d} [a(t)]^2 \, dt} \tag{2.3}$$

where a(t) is the acceleration time history, and T_d is the total duration of the ground motion. This parameter is often useful for engineering purposes because it incorporates the effect of duration and it is not strongly influenced by large, high-frequency accelerations, which typically occur only over a very short period. However, a_{rms} does not provide any information about the frequency content because it is the sum of the input energy at all frequencies. Obviously, a_{rms} depends on the method used to define strong-motion duration. In this study, the definition of duration is based on the time interval between the points at which five per cent and 95 per cent of the total energy has been recorded.

Arias intensity (I_a), as defined by Arias (1970), is the total energy per unit weight stored by a set of undamped simple oscillators at the end of the ground motion. The Arias intensity for ground motion is calculated as follows:

$$I_a = \frac{\pi}{2g} \int_0^{\infty} [a(t)]^2 \, dt \tag{2.4}$$

Cumulative absolute velocity (CAV) is defined as the integral of the absolute value of ground acceleration over the seismic time-history record:

$$CAV = \int_0^{T_d} |a(t)| \, dt \tag{2.5}$$

where |a (t)| is the absolute value of the acceleration, and T_d is the total duration of the ground motion.

Spectrum acceleration (S_a) is the most common response spectral parameter and is related to spectrum velocity (S_v) and spectrum displacement (S_d) by the expression:

$$S_a = \frac{2\pi}{T} S_v = \omega S_v = \left(\frac{2\pi}{T}\right)^2 S_d = \omega^2 S_d \tag{2.6}$$

where T is the undamped natural period of a single-degree of- freedom (SDOF) oscillator. Although S_a provides a convenient tool for specifying an earthquake input, it does not provide information about the duration of strong ground shaking.

Spectrum intensity (SI) as originally proposed by Housner (1952) may be expressed as the area under the pseudovelocity response spectrum within the period range [0.1, 2.5], namely,

$$SI = \int_{0.1}^{2.5} S_v(T, \xi)\, dT \tag{2.7}$$

The justification given to the integration limits was that they cover a range of typical periods of vibration of urban buildings. Therefore, Housner spectrum intensity may be considered as an overall measure of the capability of an earthquake to excite a population of buildings with a fundamental period between 0.1 and 2.5 sec. The integer interval recommended by Housner gives good correlation with damage to long period structures, but poorer correlation with damage of short period structures.

To characterize strong ground motion for analysis of concrete dams, which generally have fundamental periods of less than 0.5 sec, Von Thun *et al.* (1988) introduced the acceleration spectrum intensity, defined as,

$$ASI = \int_{0.1}^{0.5} S_a(T, \xi = 0.05)dT \quad (2.8)$$

i.e., the area under the acceleration response spectrum between periods of 0.1 sec and 0.5 sec.

2.5. Regression Method and Functional Form

Ten different functional forms of the empirical equation are selected based on theoretical model and each functional form was evaluated to achieve the best fit to the dataset of each ground motion parameter. A nonlinear mixed effect model was used to derive the equations and to determine the coefficients of the independent variables because it accounts for the correlation between ground motions from the same earthquake whereas the ordinary one-stage method does not. The two-stage maximum-likelihood method was not used because it underestimates σ for sets with many singly-recorded earthquakes (Spudich *et al.*, 1999). The dataset used has 28 singly-recorded earthquakes out of 72.

The mixed effects model takes the form

$$\log Y_{ij} = f\left(M_i, r_{ij}, \overline{\theta}\right) + \eta_i + \varepsilon_{ij} \quad (2.9)$$

where Y_{ij} and r_{ij} are the ground motion parameter and distance, respectively, for the j^{th} ground motion recording during the i^{th} event (earthquake). Also, M_i is the magnitude of the i^{th} event, $\overline{\theta}$ is the model coefficient matrix.

The error associated with residuals between predicted and observed values of Y_{ij} in this model is comprised of two terms, η_i and ε_{ij}: The inter-event term, η_i; represents between-group variability resulting from differences in the data recorded from different earthquakes, while the intra-event term, ε_{ij}; represents within-group variability resulting from differences in the data recorded among the different stations for the same earthquake. These two error terms, η_i and ε_{ij} are assumed to be independent and normally distributed with variances, τ^2 and σ^2 ; respectively. The total standard error for this mixed effects model is then $\sqrt{\sigma^2 + \tau^2}$.

A maximum likelihood approach is used to estimate the model coefficients, $\overline{\theta}$; and the variances, τ^2 and σ^2. A commercial software (S-Plus Software) was employed for the estimation of the model coefficients for the mixed effects model.

The Akaike's Information Criterion (AIC) is employed (Akaike, 1974) to compare the models of different functional forms. AIC is a penalized likelihood criterion, and is defined as follows:

$$AIC = -2\log likelihood + k(npar) \tag{2.10}$$

where n_{par} is the number of the random coefficients in the fitted model, and k is 2 for classical AIC. The value of AIC itself, for a given dataset has no meaning. It becomes remarkable when it is compared with the AIC of a series of models, the model with the lowest AIC being the "best" model among all models specified for the data at hand.

Two different functional forms among 10 different ones were selected, $f\left(M, R_{JB}, \overline{\theta}\right)$; for the attenuation model concerning eight ground motion parameters that includes the model coefficient matrix, $\overline{\theta}$; as follows:

$$\ln\left(Y_{ij}\right) = b_1 + b_2 M - b_3 * \ln\left(\sqrt{R_{JB}^2 + h^2}\right) + b_4 * \sqrt{R_{JB}^2 + h^2} + b_5 F_{ij} \tag{2.11}$$

$$\ln\left(Y_{ij}\right) = b_1 + b_2 M - \left(b_3 + b_4 M\right) * \ln\left(R_{JB} + 10\right) + b_5 * R_{JB} + b_6 F_{ij} \tag{2.12}$$

where Y_{ij} is the geometric mean of the two horizontal components of the ground motion parameter from the j^{th} recording of the i^{th} event, M_i is the moment magnitude of the i^{th} event, and R_{ij} is the closest horizontal distance to the vertical projection of the rupture from the i^{th} event to the location of the j^{th} recording.

The style of faulting parameter, F takes on values as follows: F=0 for Strike – slip, F=0.5 for Normal / Normal Oblique and F=1.0 for Reverse / Reverse Oblique. The coefficients to be estimated are b_1; b_2; b_3; b_4; b_5; b_6 and h. Logarithmic standard deviations are also of interest—smaller values indicate better model fits to data. The coefficient, h; is sometimes referred to as a 'fictitious' depth measure implying that interpretation of h is not clear and its value is estimated as part of the regression.

The model coefficient matrix, $\overline{\theta}$; is made up of the coefficients, b_1; b_2; b_3; b_4; b_5; b_6 and h. In the mixed effects model, these coefficients may be treated as either fixed or random based on physical reasoning. To decide which of the coefficients in the model need random effects to account for their between-earthquake variation and which can be treated as purely fixed effects is a crucial step in the model-building. The procedure starts with random effects for all parameters and then examines the fitted model to decide which, if any, of the random effects can be eliminated from the model. The near-zero estimate for the standard estimation of one random effect suggests that this term could be dropped from the model and treated as a fixed effect. The Akaike's Information Criterion (AIC) is also employed to compare the models treating the parameters either fixed or random.

As separate values of the magnitude-dependent term in Equation (2.11) and (2.12) associated with the coefficient b_2 cannot be estimated with a single M_i value per earthquake, this coefficient should be treated as fixed. Doing otherwise can lead to computational difficulties (*e.g.,* convergence problems). Similarly, according to Davidian and Giltinan (1995), treating the model coefficient, b_1; as fixed is reasonable. In estimating the model coefficients, where the coefficients, $b_1$and b_2 are always considered as fixed while b_3; b_4; b_5 and h are modeled as either fixed or random.

2.6. Regression Analysis Results

The *nlme* toolbox available with the S-Plus software is employed for estimation of the model coefficients for the mixed effects model. Based on the mixed effects model, Table 2.2 presents attenuation coefficients, b_1; b_2; b_3; b_4; b_5; b_6 and h and the logarithmic standard deviation for proposed strong ground motion parameters.

Table 2.2. Empirical attenuation coefficients and logarithmic standard deviation values for the geometric mean of the parameter calculated based on the mixed effects model

$$\ln\left(Y_{ij}\right) = b_1 + b_2 M - b_3 * \ln\left(\sqrt{R_{JB}^2 + h^2}\right) + b_4 * \sqrt{R_{JB}^2 + h^2} + b_5 F + \varepsilon_{ij}$$

Y	**b1**	**b2**	**b3**	**b4**	**b5**	**h**	ε_{ij}
PGA	-1.3162	0.6086	1.5237	0.0040	0.0863	11.5547	0.537
RMSacc	-2.8283	0.6280	1.5653	0.0052	0.0829	10.9722	0.539
AI	-5.3938	1.6673	2.3296	0.0031	0.0295	10.1132	0.951
CAV	-6.1027	1.1047	0.7728	-0.0020	-0.0661	8.7406	0.461
SAmax	0.4803	0.5671	1.5016	0.0022	-0.0138	14.0440	0.560
ASI	-2.9416	0.7765	1.3941	0.0019	0.1138	11.8311	0.522

$$\ln\left(Y_{ij}\right) = b_1 + b_2 M - \left(b_3 + b_4 M\right) * \ln\left(R_{JB} + 10\right) + b_5 * R_{JB} + b_6 F_{ij}$$

Y	**b1**	**b2**	**b3**	**b4**	**b5**	**b6**	ε_{ij}
PGV	6.8377	-0.0453	3.2451	-0.2950	0.0021	0.1115	0.648
SI	5.3856	0.2965	2.7515	-0.2343	0.0015	0.1831	0.710

The predicted empirical attenuation relationships for eight engineering ground-motion parameters for three magnitude bins (M=4.5-5.5, M=5.5-6.5 and M=6.5-7.5) are plotted with respect to calculated values from records in Figure 2.7, Figure 2.9, Figure 2.11, Figure 2.13, Figure 2.15, Figure 2.17, Figure 2.19 and Figure 2.21 for comparison purposes.

The proposed regression models for the engineering ground-motion parameters were validated by means of residual analysis. For the model to be unbiased, both the inter- and intraevent residuals should have zero mean and be uncorrelated with respect to the parameters in the regression model (Campbell and Bozorgnia, 2003). The correlation analysis has confirmed that the residuals were uncorrelated with magnitude, distance, and predicted engineering ground-motion parameters at greater than 99 per cent level of confidence. These figures (Figure 2.8, Figure 2.10, Figure 2.12, Figure 2.14, Figure 2.16, Figure 2.18, Figure 2.20 and Figure 2.22) show that the regression models are unbiased with respect to magnitude and distance.

The effectiveness of the proposed relations can also be evaluated by comparing predicted mean values from proposed relations with the observed (as in the case of PGA) or calculated parameters from recorded acceleration time histories (Figure 2.23). The mean and mean ± one standard deviation curves of proposed equations are given in Figure 2.24.

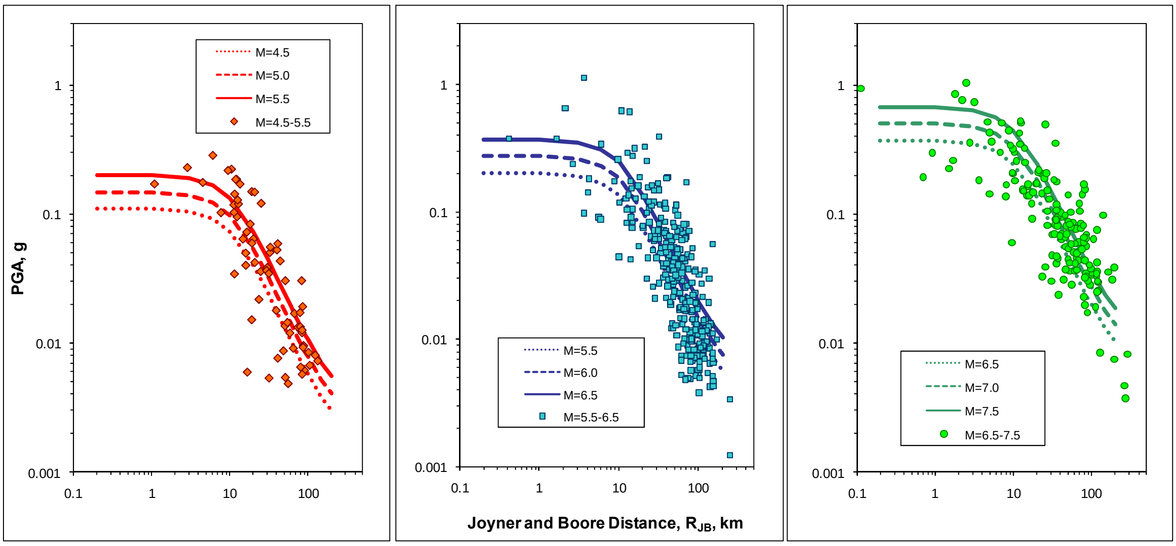

Figure 2.7. Comparison of model predictions of PGA at mean with observed data for three bins of magnitude ranges

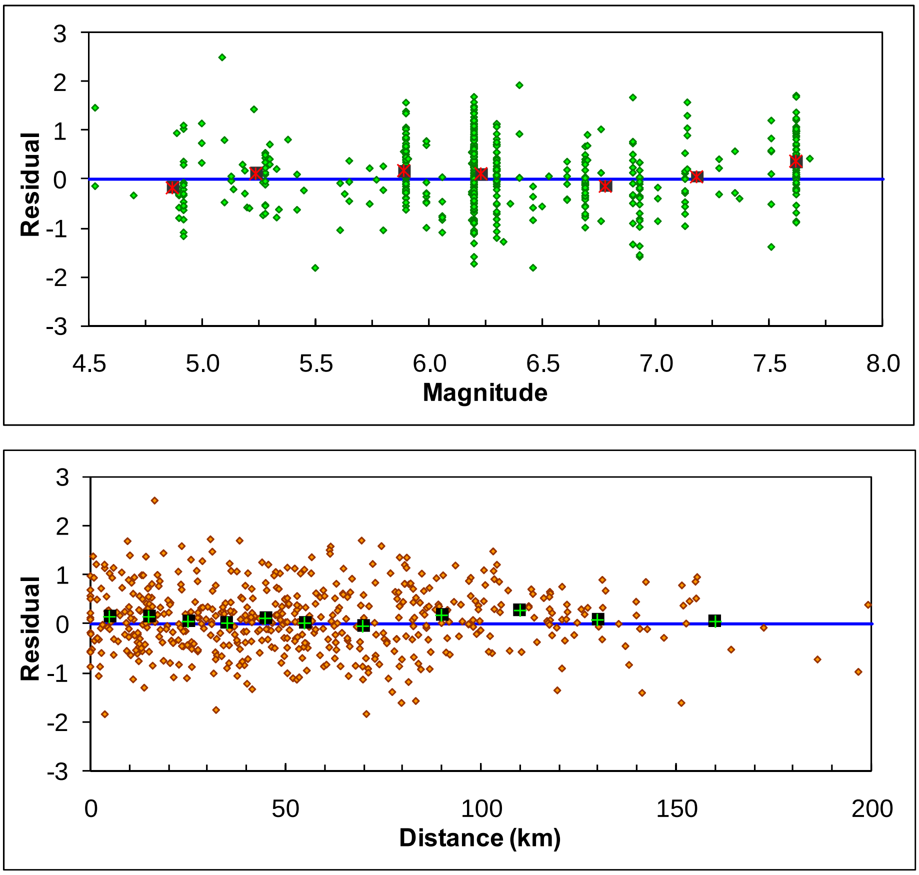

Figure 2.8. Residuals versus magnitude and distance using the derived equation for estimating PGA (Black solid points indicate values averaged over magnitude or distance bins)

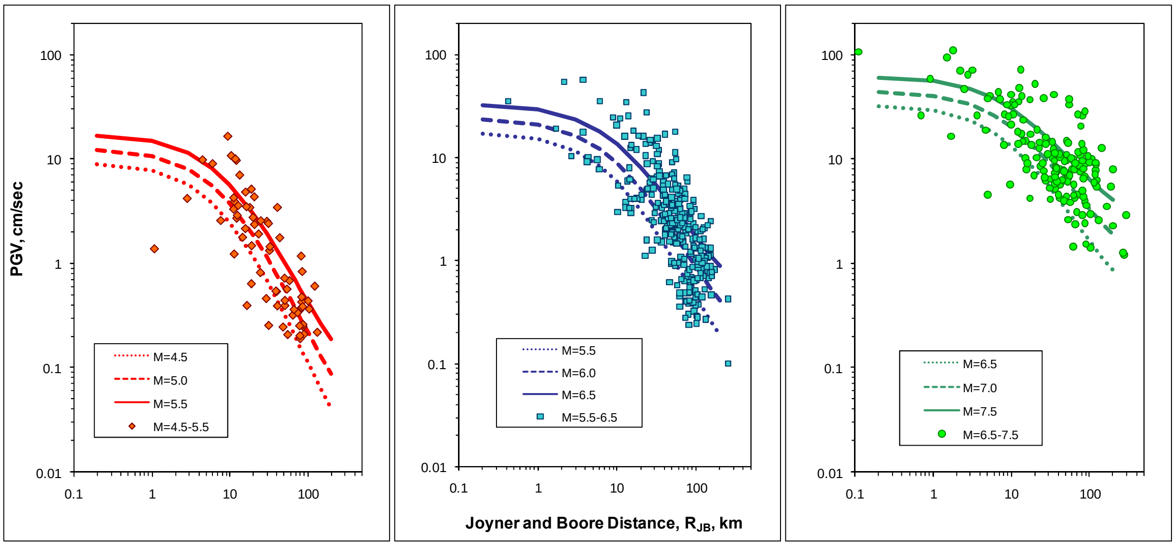

Figure 2.9. Comparison of model predictions of PGV at mean with observed data for three bins of magnitude ranges

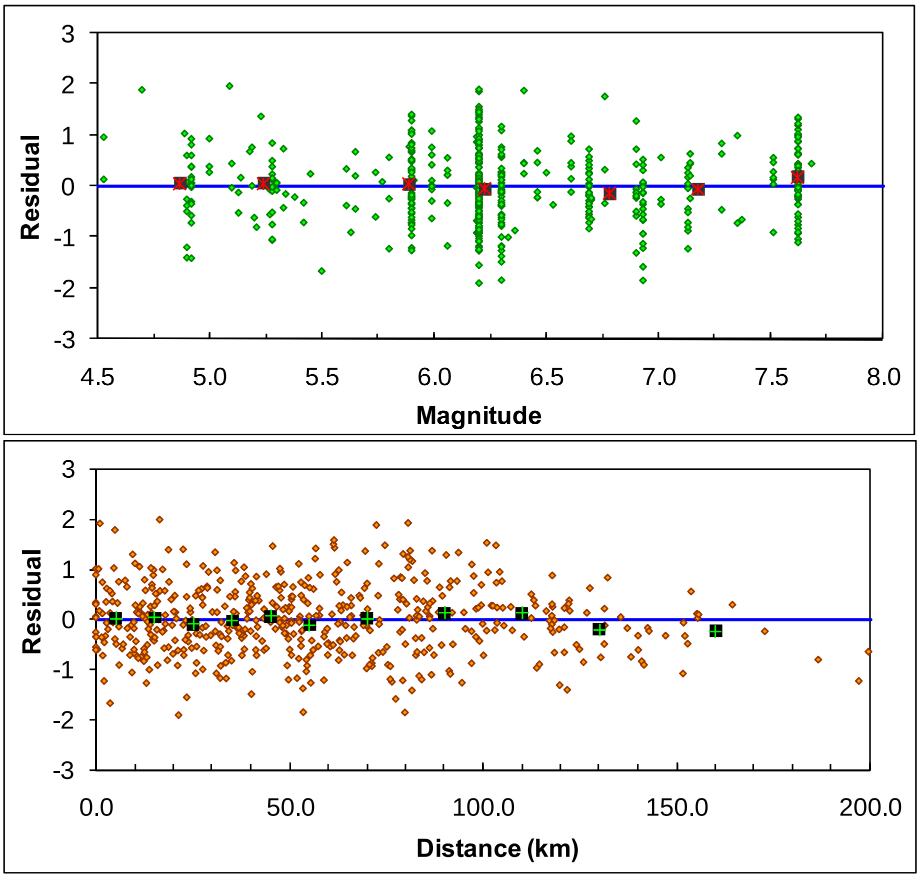

Figure 2.10. Residuals versus magnitude and distance using the derived equation for estimating PGV (Black solid points indicate values averaged over magnitude or distance bins)

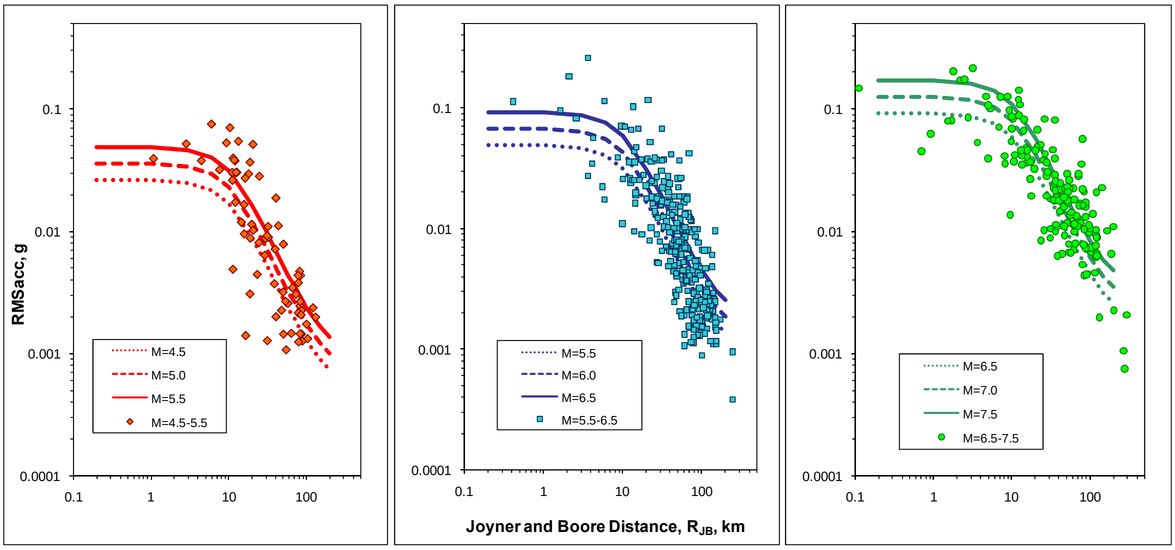

Figure 2.11. Comparison of model predictions of a_{rms} at mean with observed data for three bins of magnitude ranges

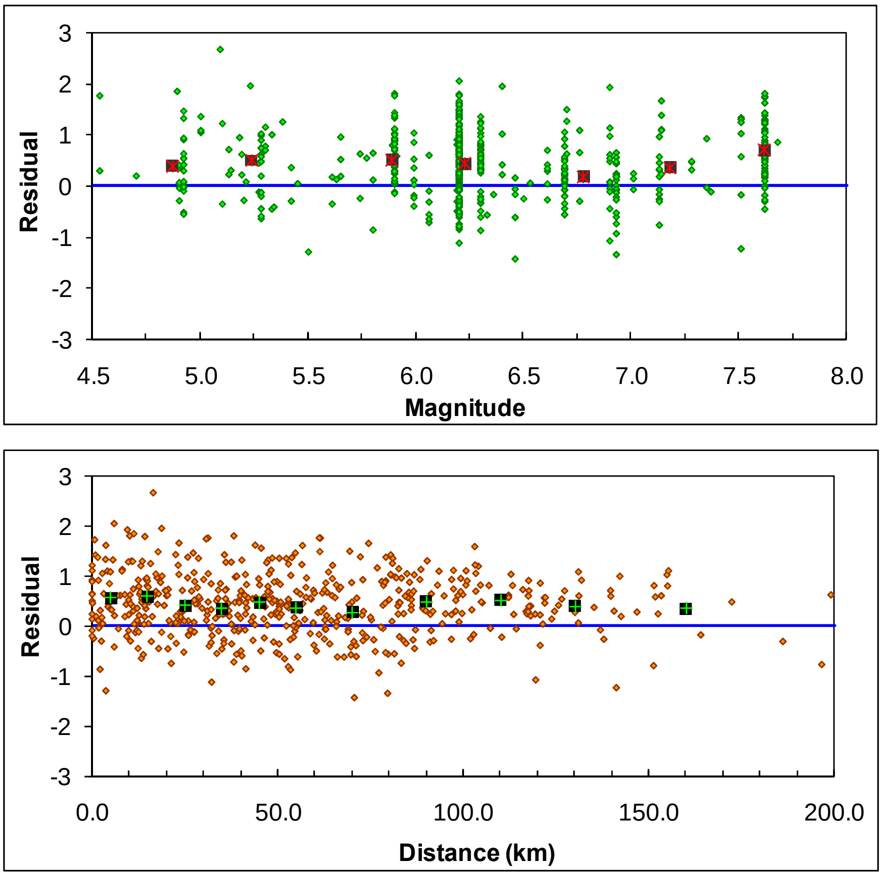

Figure 2.12. Residuals versus magnitude and distance using the derived equation for estimating a_{rms} (Black solid points indicate values averaged over magnitude or distance bins)

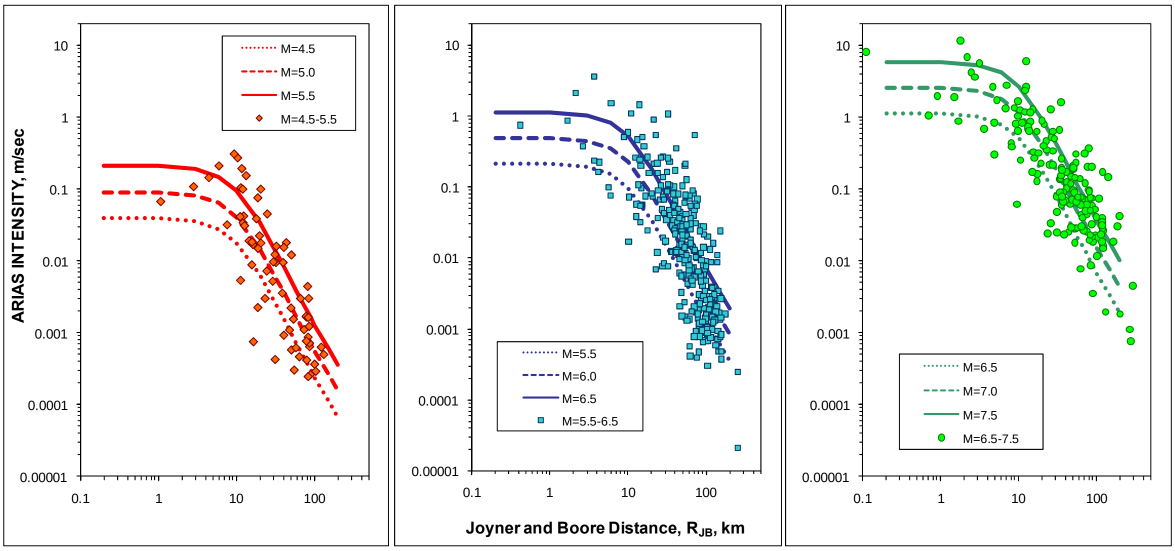

Figure 2.13. Comparison of model predictions of AI at mean with observed data for three bins of magnitude ranges

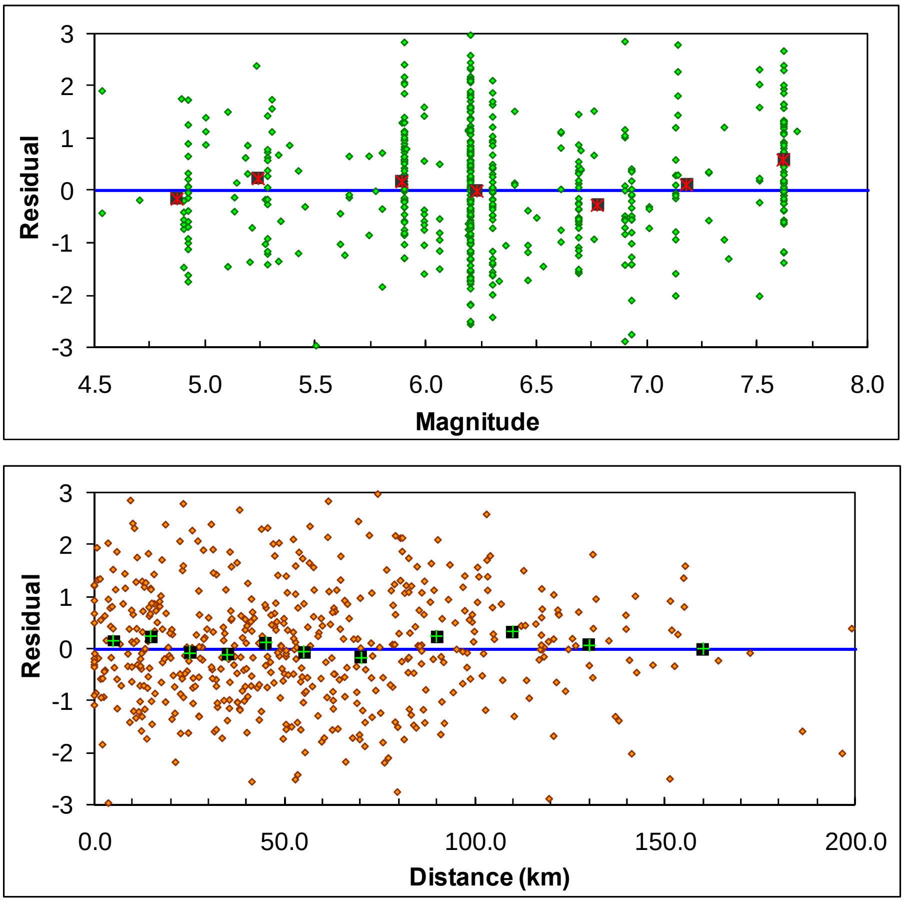

Figure 2.14. Residuals versus magnitude and distance using the derived equation for estimating AI (Black solid points indicate values averaged over magnitude or distance bins)

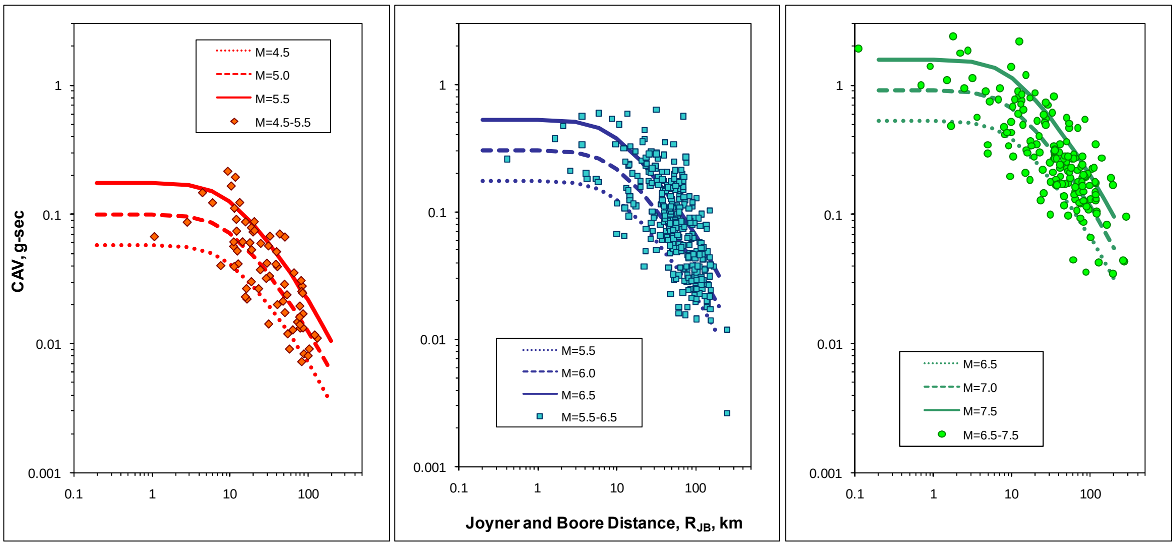

Figure 2.15. Comparison of model predictions of CAV at mean with observed data for three bins of magnitude ranges

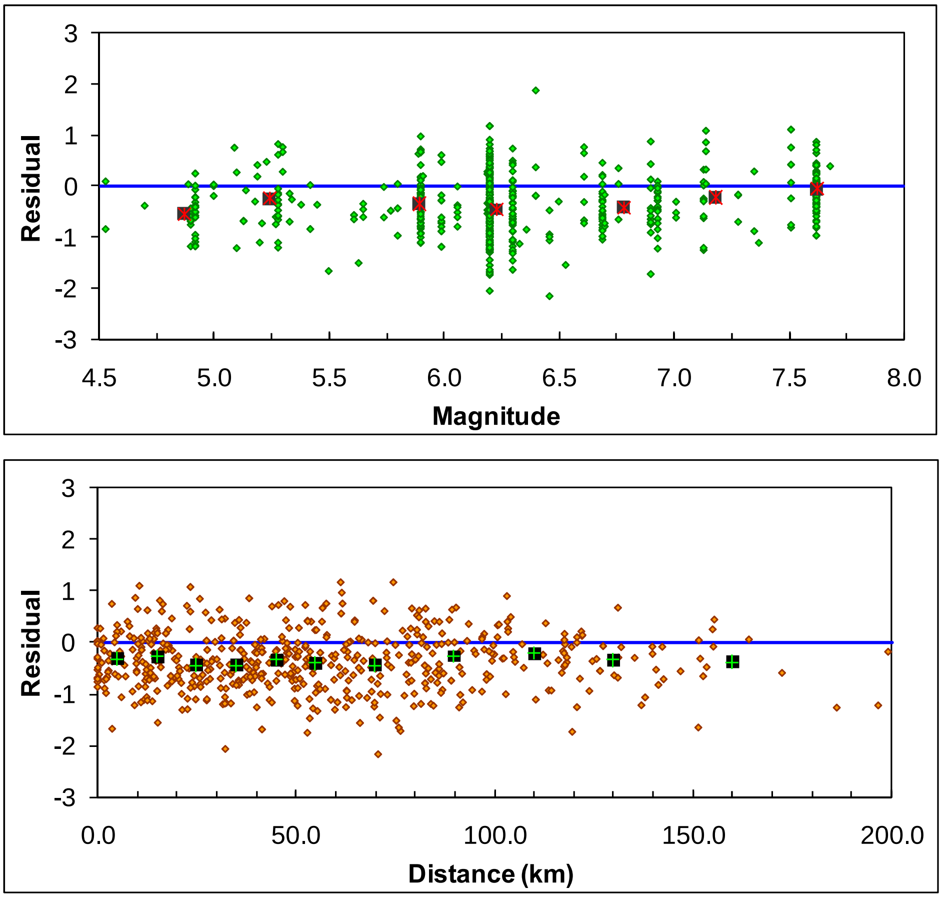

Figure 2.16. Residuals versus magnitude and distance using the derived equation for estimating CAV (Black solid points indicate values averaged over magnitude or distance bins)

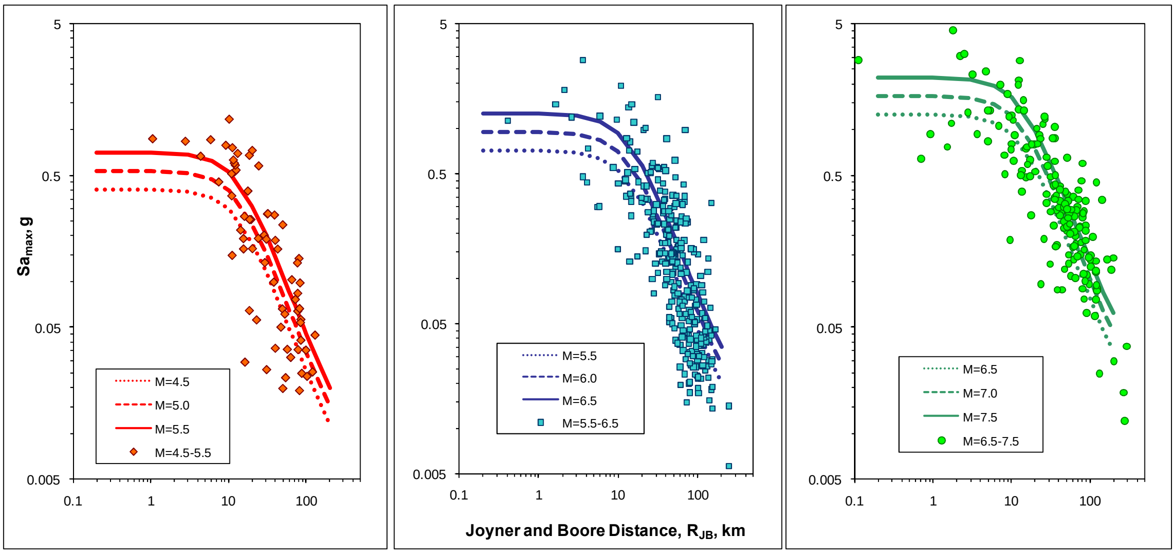

Figure 2.17. Comparison of model predictions of SA_{max} at mean with observed data for three bins of magnitude ranges

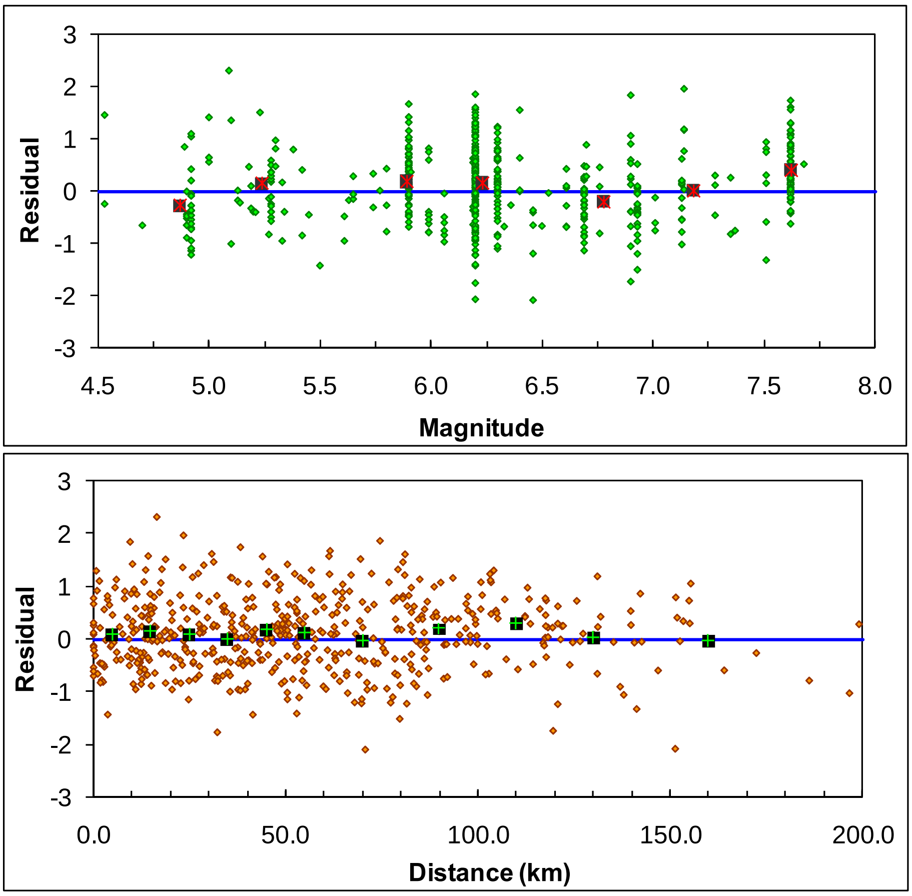

Figure 2.18. Residuals versus magnitude and distance using the derived equation for estimating SA_{max} (Black solid points indicate values averaged over magnitude or distance bins)

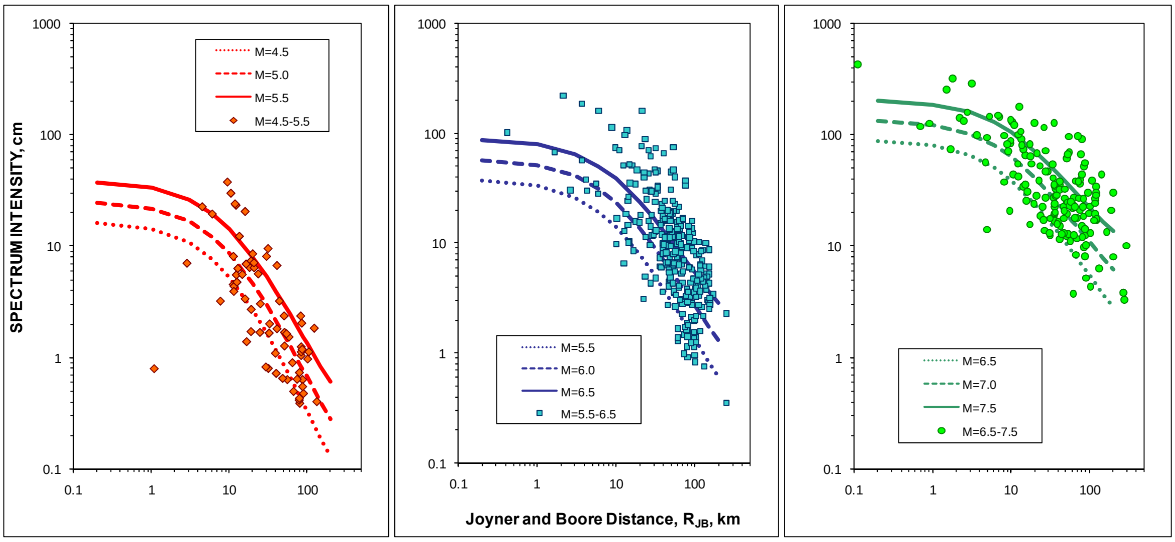

Figure 2.19. Comparison of model predictions of SI at mean with observed data for three bins of magnitude ranges

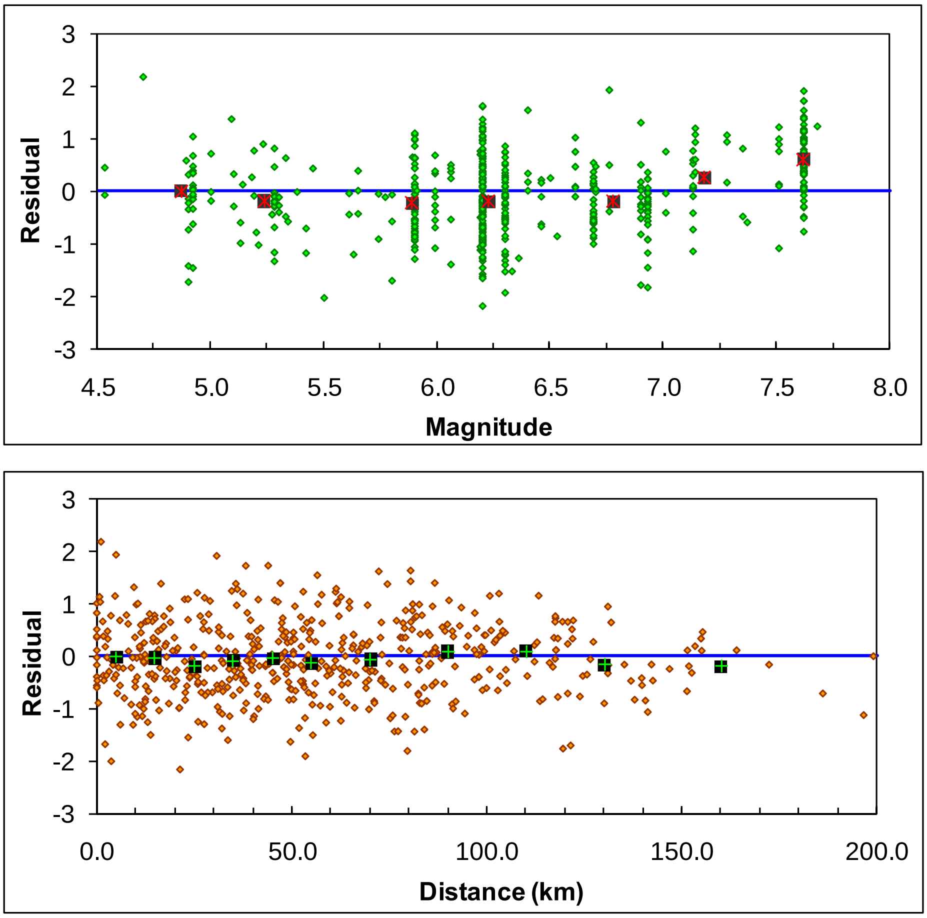

Figure 2.20. Residuals versus magnitude and distance using the derived equation for estimating SI (Black solid points indicate values averaged over magnitude or distance bins)

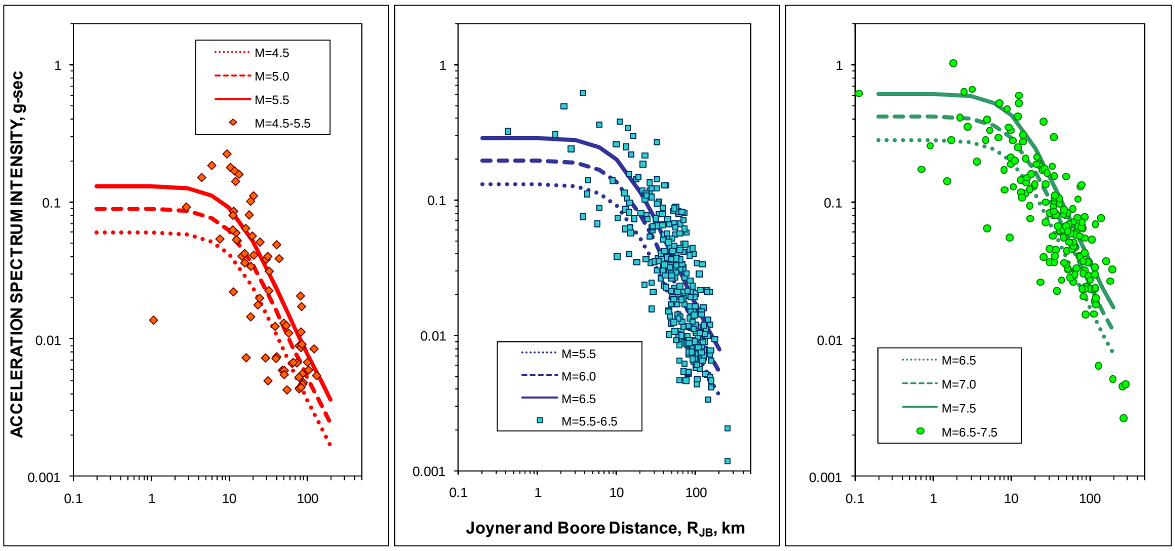

Figure 2.21. Comparison of model predictions of ASI at mean with observed data for three bins of magnitude ranges

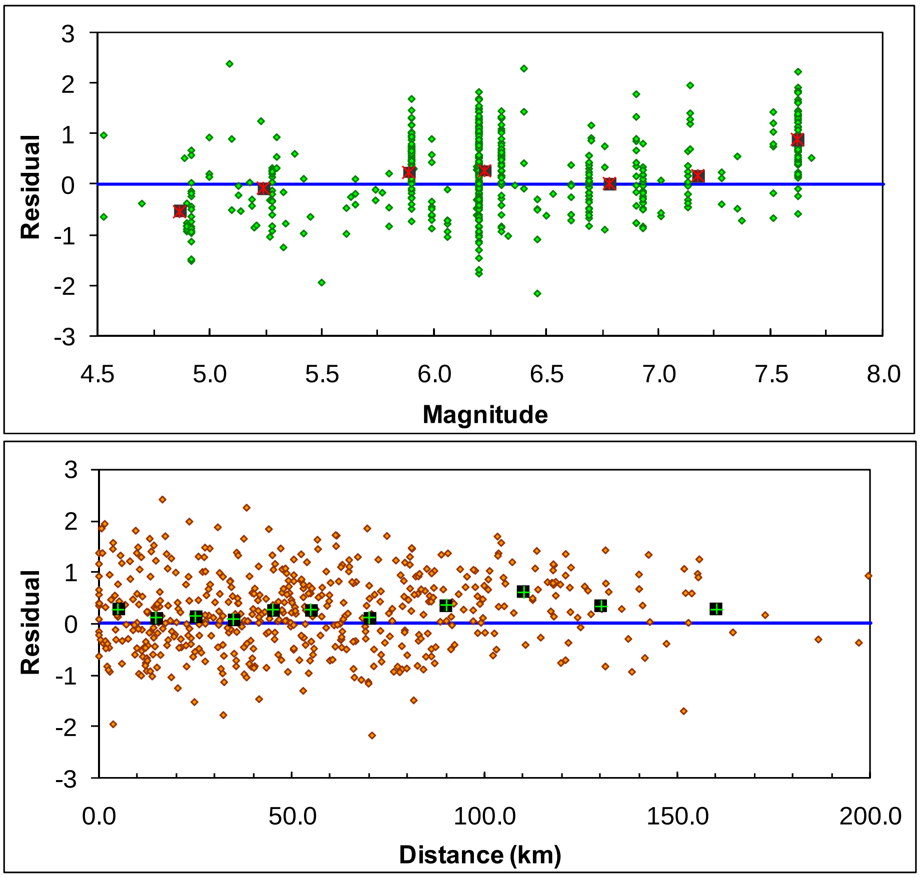

Figure 2.22. Residuals versus magnitude and distance using the derived equation for estimating ASI (Black solid points indicate values averaged over magnitude or distance bins)

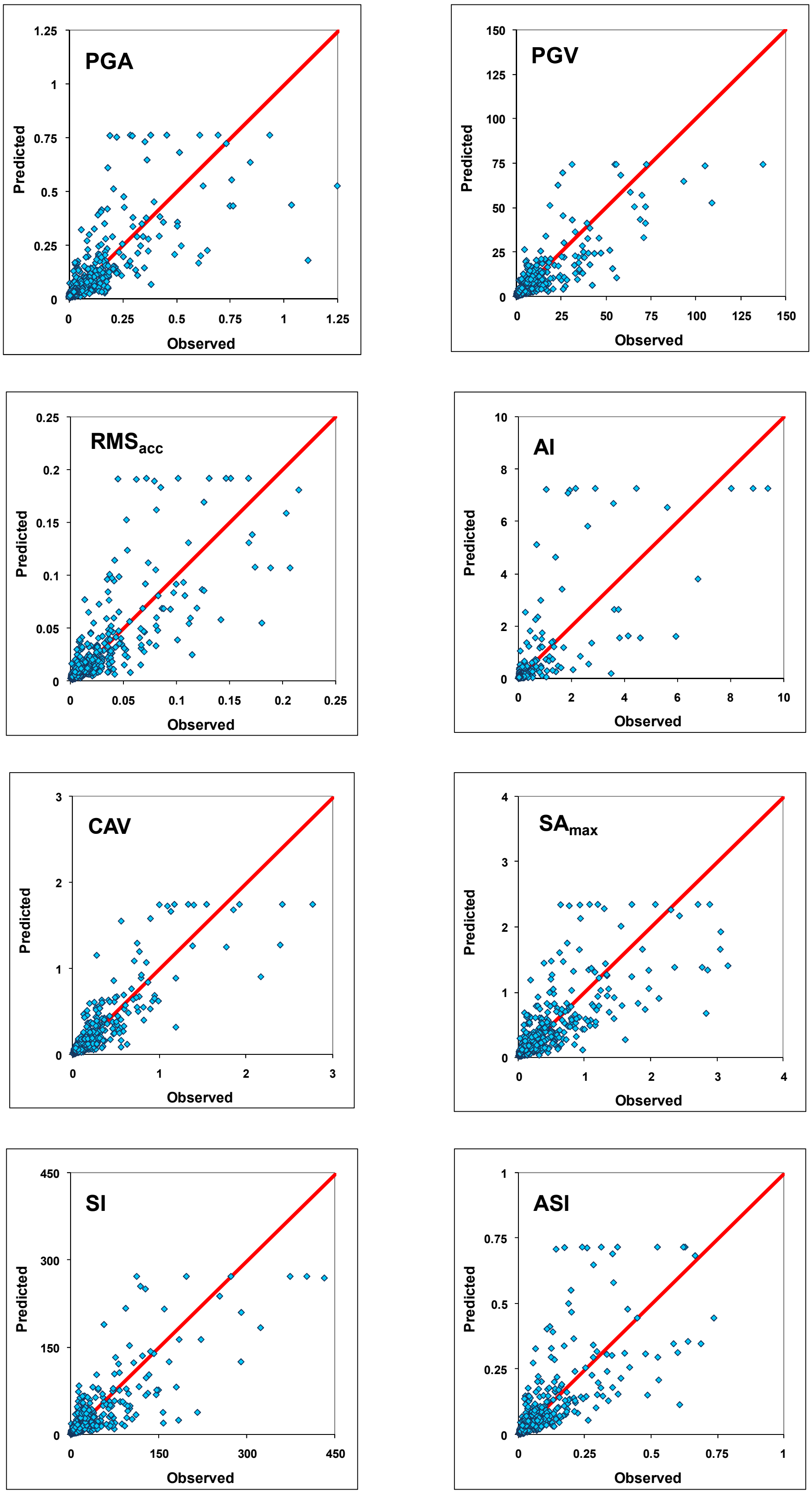

Figure 2.23. Comparison of predicted ground motion parameters with observed parameters (PGA) or calculated (except PGA) parameters from acceleration time histories

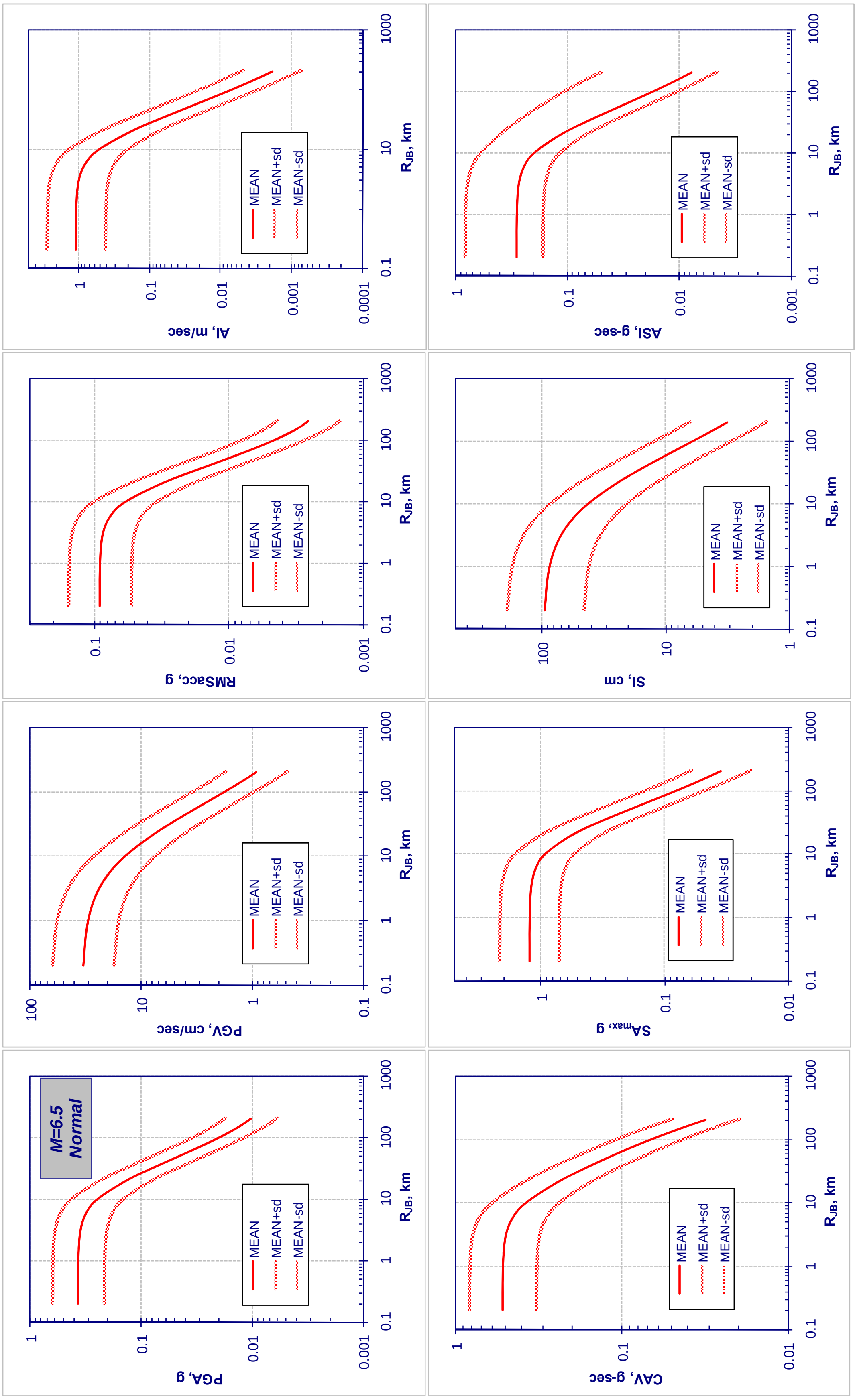

Figure 2.24. Mean and mean ± 1sd curves of predicted ground motion parameters

2.7. Comparison of Proposed Relations with Previous Studies

2.7.1. Next Generation Attenuation Model, NGA and Comparison of Predicted PGA with NGA Models

"Next Generation of Ground Motion Attenuation Models", NGA project is a series of closely coordinated research projects coordinated by the Lifelines Program of the Pacific Earthquake Engineering Research Center (PEER) in partnership with the U.S. Geological Survey and Southern California Earthquake Center. The main topic areas are earthquake ground motion and site response. The objective of the program is to develop new ground motion prediction relations through a comprehensive research that will satisfy the needs of current practice in earthquake engineering by merging views of experienced attenuation model developers with current research results.

Five sets of ground motion models were developed by five teams (Abrahamson and Silva, 2008; Boore and Atkinson, 2008; Campbell and Bozorgnia, 2008; Chiou and Youngs, 2008; Idriss, 2008) for shallow crustal earthquakes in the western United States and similar active tectonic regions. As a final product, all NGA models were required to be applicable to the following requirements (Power *et al.*, 2008):

- Ground motion parameters of peak ground acceleration (PGA), peak ground velocity (PGV), and 5 per cent damped elastic pseudo-response spectral acceleration in the period range of 0 to 10 seconds;
- Average horizontal component of ground motion, as well as ground motion in the fault – strike- normal (FN) and fault – strike – parallel (FP) directions;
- Shallow crustal earthquakes (strike-slip, reverse normal earthquakes) in the western United States;
- Moment magnitude range of 5 to 8.5 (strike-slip earthquakes) and 5 to 8 (reverse and normal earthquakes;
- Distance range of 0 to 200 km;
- Commonly used site classification schemes, including the NEHRP classification scheme.

The NGA program was scheduled and supported by a series of research projects to perform the following tasks:

- Database development: to have an enhanced strong motion database using recent earthquakes and metadata which will be current, consistent and verified;
- 1-D rock simulation: to satisfy the need for extrapolation beyond data;
- Evaluation of predictors (distance and magnitude scaling, footwall / hanging wall, style of faulting, directivity, *etc.*);
- Site classification and site effects: to provide an improved basis for decisions to define site classes and account for site effects using tools like site response analysis and simulation of 3-D basin response;
- Statistical methods: to consider measurement error of predictor, missing values in predictor variable and correlation in residuals;
- Development of NGA models and evaluations

Although started with the same objectives and same data set, new ground motion models developed by five groups as part of NGA project have differences by means of data sets used, model parameterizations, use of analytical models and the resulting ground motions (median and variability). The main features of the functional forms of the five NGA models are summarized in Table 2.3.

The proposed equations for PGA in this Thesis are compared with NGA predictive relations and generally agree with the newest researches of NGA except for the near field range especially for small or large earthquakes.

Table 2.3. Comparison of functional forms of NGA models developed by five groups

$\ln Y =$	**Magnitude and distance scaling**	**Style of faulting factor**	**Aftershock factor**	**Rupture depth factor**	**Hanging-wall factor**	**Site factor (Nonlinear site amplification)**	**Large distance factor**	**Soil / sediment depth factor**
Abrahamson & Silva	$f_1(M, R_{rup})$	$+ a_{12}F_{RV} + a_{13}F_{NM}$	$+ a_{15}F_{AS}$	$+ f_6(Z_{TOR})$	$+ F_{HW} f_4(R_{jb}, R_{rup}, R_x, W, \delta, Z_{TOR}, M)$	$+ f_5(PGA_{1100}, V_{S30})$	$+ f_8(R_{rup}, M)$	$+ f_{10}(Z_{1.0}, V_{S30})$
	$f_1(M, R_{rup}) = \begin{cases} a_1 + a_4(M - c_1) + a_8(8.5 - M)^2 + [a_2 + a_3(M - c_1)]\ln(R) & \text{for } M \le c_1 \\ a_1 + a_5(M - c_1) + a_8(8.5 - M)^2 + [a_2 + a_3(M - c_1)]\ln(R) & \text{for } M > c_1 \end{cases}$ where $R = \sqrt{R_{rup}^2 + c_4^2}$							
Boore & Atkinson	$F_M(M, U, SS, NS, RS) + F_D(R_{JB}, M)$			(Implicit through R_{JB})	(Implicit through R_{JB})	$+ F_S(V_{S30}, R_{JB}, pga4nl)$		
	$F_D(R_{JB}, M) = [c_1 + c_2(M - M_{ref})]\ln(R/R_{ref}) + c_3(R - R_{ref})$ $F_M(M) = \begin{cases} e_1U + e_2SS + e_3NS + e_4RS + e_5(M - M_h) + e_6(M - M_h)^2 & \text{for } M \le M_h \\ e_1U + e_2SS + e_3NS + e_4RS + e_7(M - M_h) & \text{for } M > M_h \end{cases}$ where $R = \sqrt{R_{JB}^2 + h^2}$							
Campbell & Bozorgnia	$f_{mag}(M) + f_{dis}(M, R_{RUP})$	$+ c_7F_{RV} f_{flt,Z}(Z_{TOR}) + c_8F_{NM}$			$+ c_9 f_{hng,R}(R_{RUP}, R_{JB}) f_{hng,M}(M)$ $f_{hng,Z}(Z_{TOR}) f_{hng,\delta}(\delta)$	$+ f_{site}(V_{S30}, A_{1100})$		$+ f_{sed}(Z_{2.5})$
	$f_{mag} = \begin{cases} c_0 + c_1M & M \le 5.5 \\ c_0 + c_1M + c_2(M - 5.5) & 5.5 < M \le 6.5 \\ c_0 + c_1M + c_2(M - 5.5) + c_3(M - 6.5) & M > 6.5 \end{cases}$ $f_{dis} = (c_4 + c_5M)\ln\left(\sqrt{R_{RUP}^2 + c_6^2}\right)$							
Chiou & Youngs	$f_{mag}(M) + f_{dis}(M, R_{RUP})$	$c_1 + [c_{1a}F_{RV} + c_{1b}F_{NM} + c_7(Z_{TOR} - 4)](1 - AS) + [c_{10} + c_{7a}(Z_{TOR} - 4)]AS$			$+ c_9 F_{HW} f(R_X, R_{JB}, R_{RUP}, Z_{TOR}, \delta)$	$+ f_{site}(V_{S30}, y_{ref}(T))$	$+ f(R_{RUP}, M)$	$+ f_{sed}(Z_{1.0})$
	$f_{mag}(M) = c_2(M - 6) + \frac{c_2 - c_3}{c_n}\ln\left(1 + e^{c_n(c_M - M)}\right)$ $f_{dis}(M, R_{RUP}) = c_4\ln[R_{RUP} + c_5\cosh\{c_6\max(M - c_{HM}, 0)\}] + (c_{4a} - c_4)\ln\left(\sqrt{R_{RUP}^2 + c_{RB}^2}\right)$							
Idriss	$\alpha_1(T) + \alpha_2(T)M - [\beta_1(T) + \alpha_2(T)M]\ln(R_{rup} + 10) + \gamma(T)R_{rup} + \varphi(T)F$			Not applicable				Not applicable

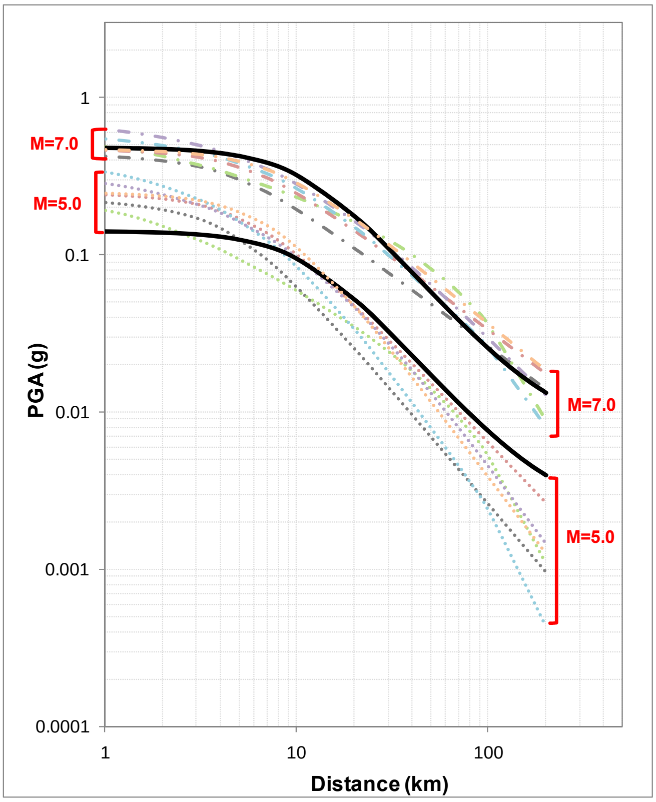

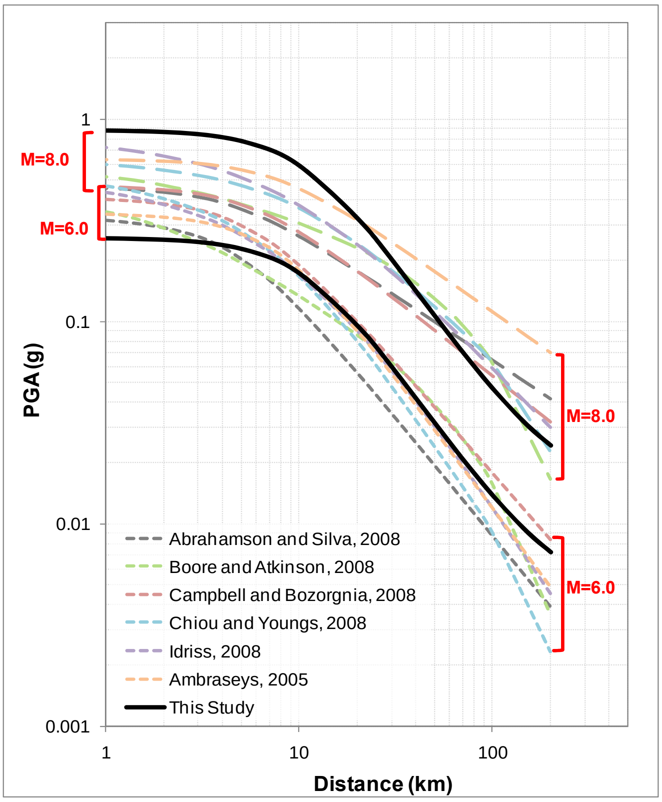

Figure 2.25. Comparison of the derived PGA attenuation relationship with those proposed by NGA researchers (2008) and Ambraseys (2005). The relationships are evaluated for M5, M6, M7 and M8, strike-slip fault mechanism, and rock soil category.

2.7.2. Comparison of Predicted PGV

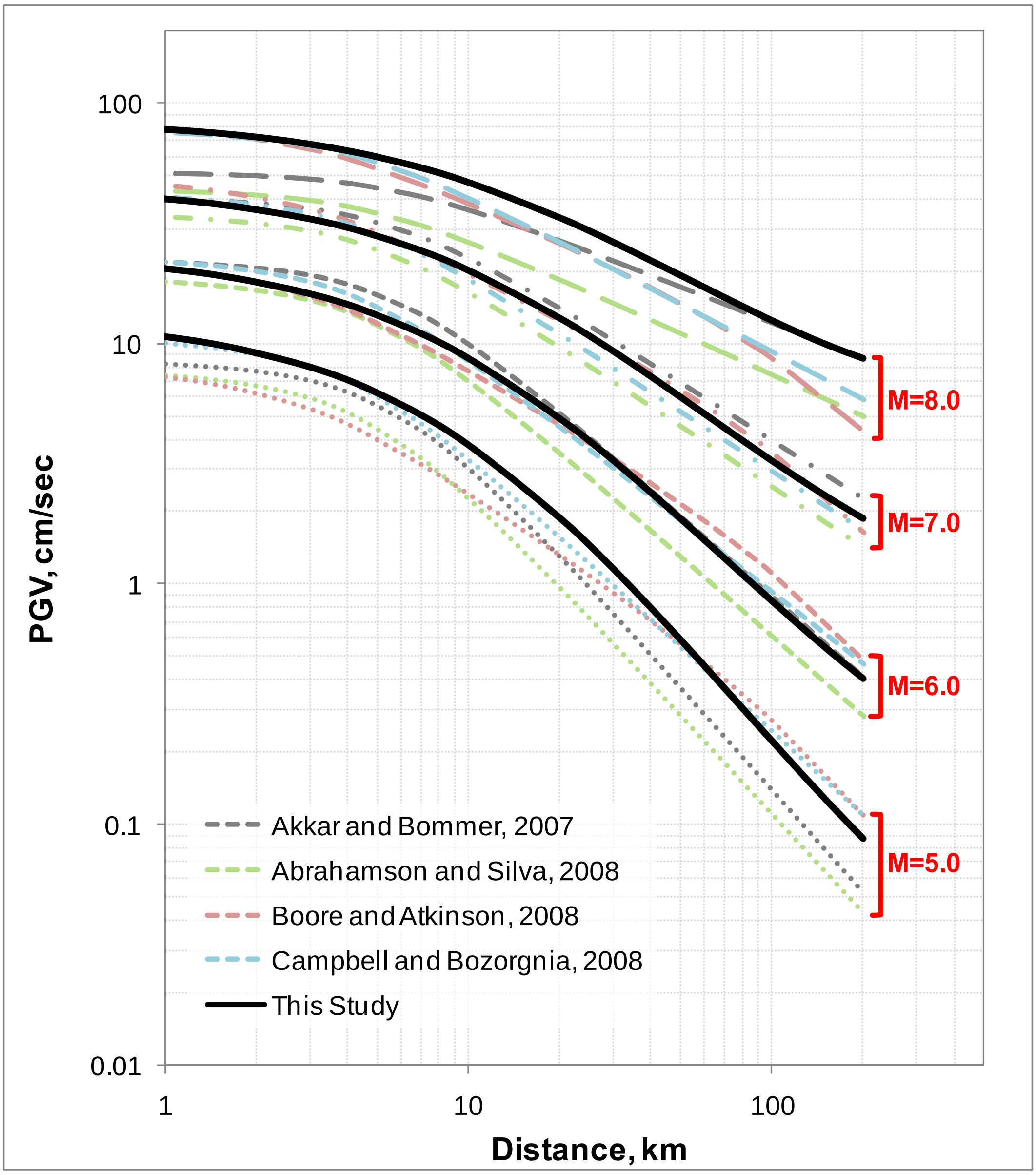

Figure 2.26. Comparison of the derived PGV attenuation relationship with those proposed by NGA researchers (2008) and Akkar and Bommer (2007). The relationships are evaluated for M5, M6, M7 and M8, strike-slip fault mechanism, and rock soil category.

2.7.3. Comparison of Predicted Arias Intensity

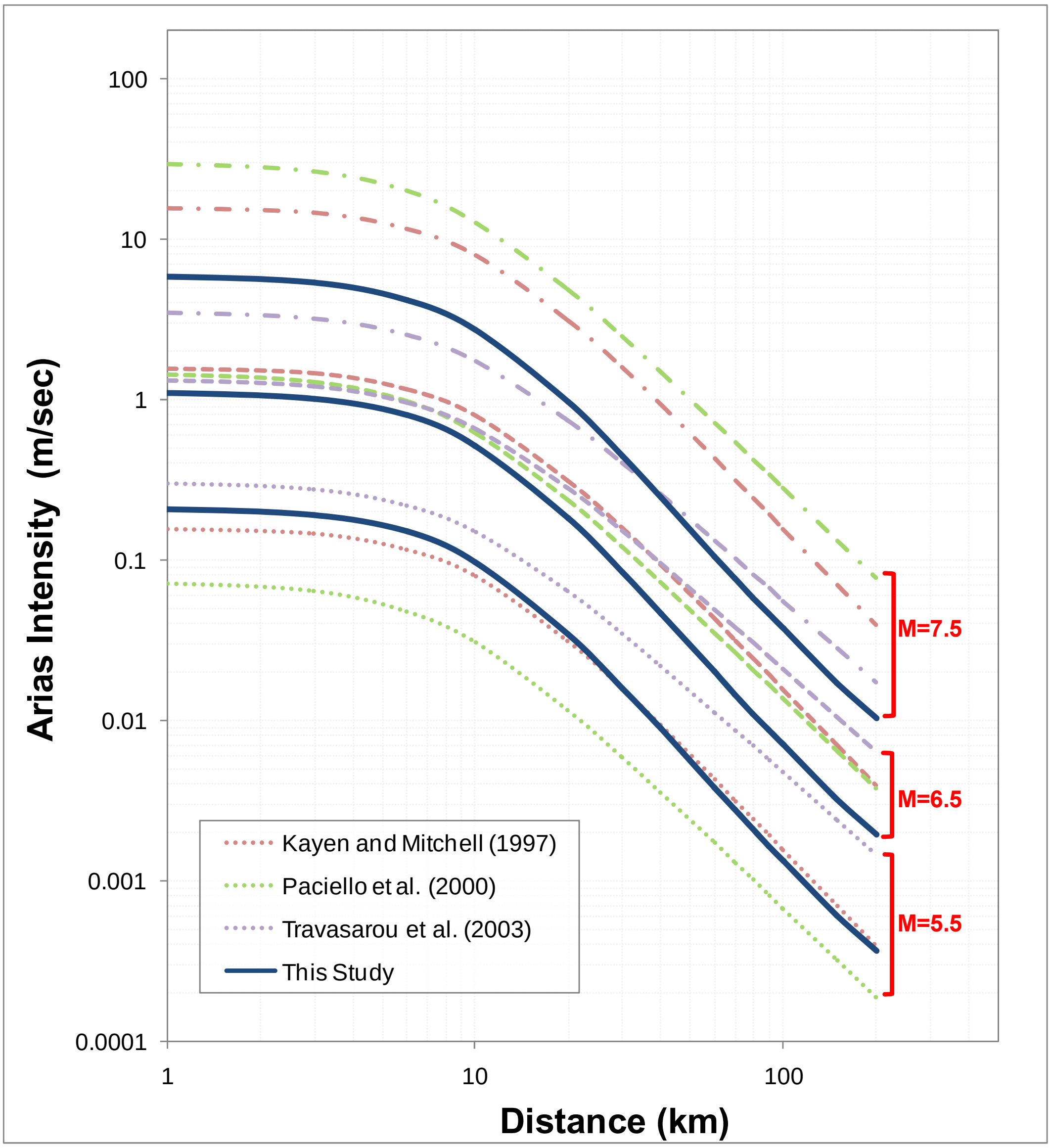

Figure 2.27. Comparison of proposed attenuation relationship for Arias Intensity with three existing relationships for three different magnitude earthquakes on a reverse fault at a 'rock' site

2.7.4. Comparison of Predicted Root Mean Square Acceleration, a_{RMS}; Cumulative Absolute Velocity, CAV; Spectrum Intensity, SI

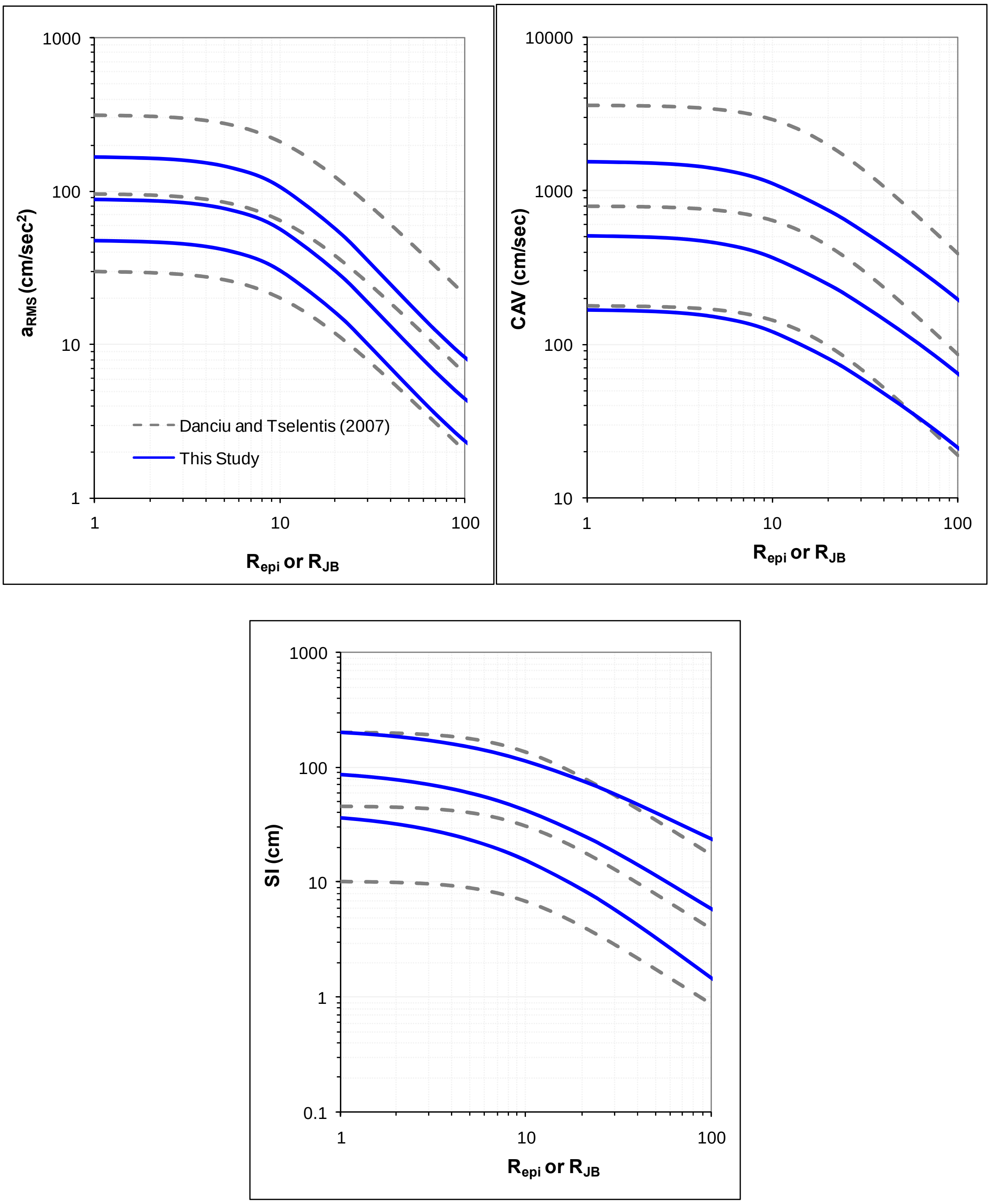

Figure 2.28. Comparison of proposed attenuation relationship for root mean square Acceleration, a_{RMS}; cumulative absolute velocity, CAV; spectrum intensity, SI with Danciu and Tselentis (2007) relationships for three different magnitude earthquakes (M5.5, M6.5 and M7.5) on a normal fault at a 'rock' site

2.8. Summary and Results

New empirical attenuation relations have been developed for eight ground motion parameters which are PGA, PGV, root mean square of acceleration, Arias intensity, cumulative absolute velocity, maximum spectral acceleration, spectrum intensity and acceleration spectrum intensity. These engineering ground motion parameters have the advantage of describing ground-motion damage potential. They capture the effects of amplitude, frequency content, duration, and / or energy of a ground-motion record. These parameters were selected to be used as scaling parameters in the proceeding Chapter. The need for developing new predictive relations was due to the lack of existing relation for some of the parameters selected.

The proposed attenuation model was derived adopting nonlinear fixed effect regression model based on the NGA, PEER dataset. The proposed relations are valid for magnitudes in the range of M=5.0 – 8.0 and Joyner and Boore distance with the range R_{JB}= 1 – 150 km.

The validity of the model is demonstrated by comparison with previous studies. However, existing relationships are limited to some of the selected parameters. In general, for the parameters compared, the proposed relationships are in good agreement with previously proposed attenuation relationships. The shapes of the present equations follow a trend similar to the proposed equations. While comparing the proposed relations, not only NGA relations were used but also, some other relations developed for other regions of the world like Europe and Middle East were also checked.

The differences observed in the comparison of the proposed relations with other studies can be attributed to the different amounts of data that these relationships have been based on, various options to take the horizontal components, different distance definitions, soil categories, and fault-type definitions. Also in some studies alternative definitions of ground motion parameters are used as in the case of Arias intensity such as largest of the two horizontal peaks, arithmetic average, or their geometric mean which can also explain the observed discrepancies.

There is a higher proportion of data from large distances, where regional differences in crustal structure and attenuation become important, used in this study and therefore the large variability in these far-field records contribute to the scatter. Although extra coefficients were included in the equation to model the differences between ground motions from earthquakes with different styles of faulting, many of the derived coefficients are not significant for faulting types.

3. INPUT MOTION: SELECTION AND SCALING

3.1. Introduction

The uncertainty in site response analysis can be considered as a result of the uncertainties related to stratification and properties of the soil layers, definition of the bedrock depth, analysis method, and due to the variability introduced by the selected input acceleration time histories. This chapter describes the procedures used to select and scale time histories to be used as input for ground response analyses and discusses variability associated with performing ground response calculations at the selected sites concerning these procedures.

Studies carried out on the nonlinear response of structures under input ground motion records selected and scaled to different criteria such as peak ground acceleration, peak ground velocity, Arias intensity, effective peak velocity *etc.* have shown that for the same structural model there exists a significant response variability (Martinez-Rueda, 1998), stressing the necessity for better assessment of the effects of the input motion characteristics to achieve more realistic evaluation of structural performance and implying the need for identification of better ground motion intensity measures for nonlinear structural response (Naeim *et al*., 2004). Similar response patterns are also observed for natural and man-made geotechnical structures and similar need also exists for evaluating site response analysis.

There are two kinds of scaling used in earthquake engineering: source spectral scaling and ground motion scaling. Source spectral scaling is concerned with the interdependence of parameters related to the earthquake source, such as earthquake magnitude, fault slip, corner frequency, stress drop, fault size (*i.e.,* length and width) *etc.* How these parameters scale with each other, is ultimately used for the determination of the correct values in ground motion simulation studies in earthquake engineering and in understanding the underlying physics of the rupture processes in geophysics and seismology.

Ground motion scaling, on the other hand, is basically emerging as a need following recent developments in the earthquake resistant design philosophy (Kappos and Kyriakakis, 2000) as a need for using the most appropriate set of strong ground motion time series (Bommer and Acevedo, 2004) recorded or simulated in dynamic analysis of structures.

Ground Motion Selection and Modification (GMSM) Program maintained at the Pacific Earthquake Engineering Research Center (PEER) has a mission to provide guidance and tools to the engineering community on appropriate GMSM methods for nonlinear dynamic analyses. Geotechnical projects are example of a nonlinear system that can be highly sensitive to the selection of input ground motion. It is possible to select time series such that their seismological and geotechnical conditions are consistent with the design earthquake and whose acceleration response spectra match the design spectrum but whose nonlinear response are very different. Selection based on seismological principles leads to large variability results. The GMSM program proposes two solutions to this problem:

(1) Perform a high end analysis that uses more records:

- Large number of ground motions
- Regression on the results of the nonlinear dynamic analysis (Figure 3.1)
- Coupling the regression with ground motion prediction equations that gives best estimate of structural response

(2) Be smarter about picking records:

- PEER GMSM Working Group concluded that selecting time series based on record properties that affect nonlinear response leads to a decrease in variability and better estimates of response.

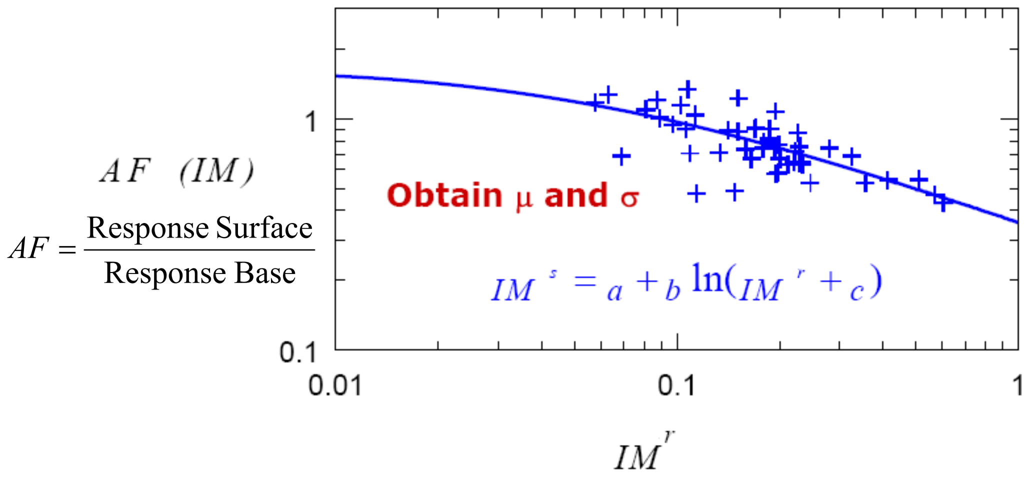

Figure 3.1. Schematic presentation of regression on the results of the nonlinear dynamic analysis (Goulet, 2008)

Studies on microzonation with respect to peak spectral accelerations using two different sets of three real (compatible with the time dependent earthquake hazard assessed for Zeytinburnu and scaled with respect to the peak accelerations) and one set of three simulated (compatible with the time dependent earthquake hazard spectra) acceleration time histories reveal that independent than the scenario selected, acceleration time histories used in site response analysis, in other words source characteristics are very important (Ansal and Tönük, 2007b). Acceleration time histories recorded during same or different earthquakes on different soil conditions may be very unlike which introduces a significant uncertainty in engineering applications and unrealistic estimations of earthquake characteristics.

As can be observed from Figure 3.2, even though there is a general agreement among all three options, there are also differences that produce difficulties to select one option and estimate the building stock vulnerability based on that selection. Using synthetic acceleration time histories generally yielded higher amplitudes indicating more conservative solution. However, the degree of conservatism cannot be defined and the generated acceleration records may be considered unrealistically demanding. Thus for that case, the use of scaled regional earthquake hazard compatible real acceleration records appears more suitable for microzonation studies.

In the case of using real acceleration records, it could be preferable to conduct site response analyses using large sets of data. One approach that can be followed is the probabilistic interpretation of the calculated elastic acceleration response spectra from all site response analyses using as much as possible number of real input acceleration records obtained on compatible tectonic, seismic and site conditions (Ansal and Tönük, 2007b). This approach has the advantage of defining the hazard level in accordance with the purpose of the microzonation and for vulnerability assessment.

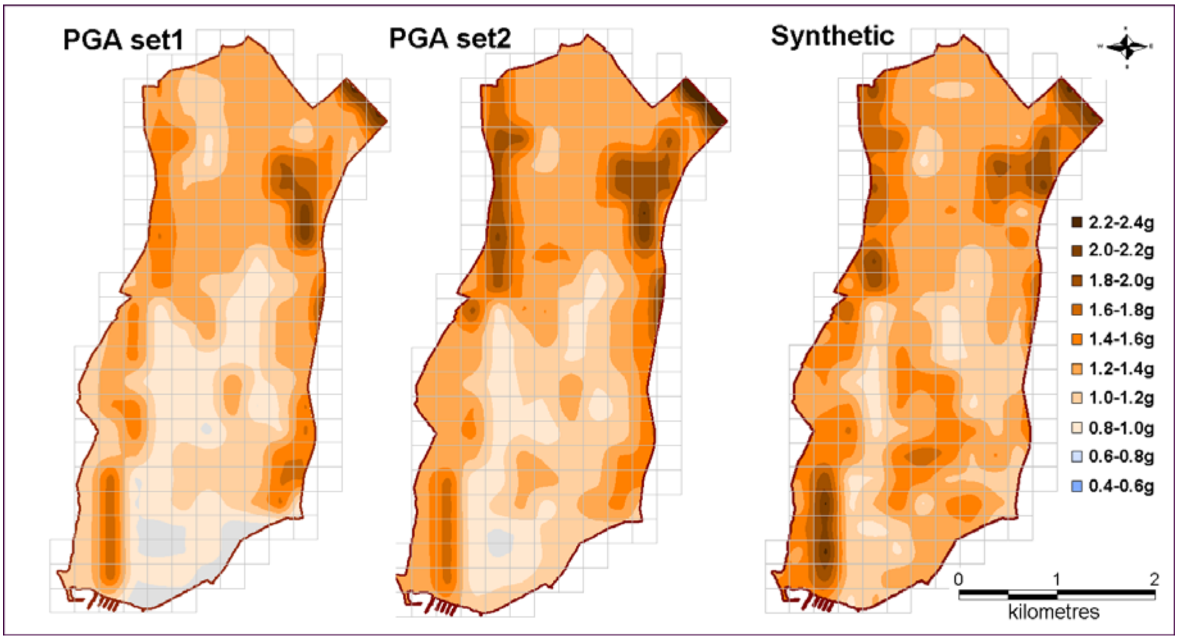

Figure 3.2. Microzonation of Zeytinburnu with respect short period (T=0.2s) spectral accelerations using two sets of PGA scaled real and one set of synthetic acceleration input motion

3.2. Methodology

1D equivalent linear soil model Shake91 by Idriss and Sun (1992) was used to conduct site response analyses at selected sites with pre-determined level of earthquake hazard. First, the resulting response variability is investigated when analyzed under a series of ground motion records selected compatible with the site-specific earthquake hazard. Site specific earthquake hazard is considered as dependent on the fault type, magnitude range, and epicenter distance. Then using the same set of input strong ground motion records this time scaled to different intensity measures such as peak ground acceleration, peak ground velocity and Arias intensity, the analysis is repeated and the uncertainty introduced by scaling and the effectiveness of different scaling parameters were evaluated.

PEER database was used to select specific time histories representing possible realizations of the motion that would have been expected at the selected sites. The selected time histories were scaled as described later, and then used as input for ground response analyses for the sites selected. The seismological criteria by which these rock time histories were selected are as follows, where the term "target" refers to a characteristic of the causative earthquake for the subject site:

- Magnitude: Selected recordings must have been triggered by an event with a magnitude within ± 0.5 of the target.
- Distance: For specific cases, records are selected within 10 km range of the expected source distance to the site.
- Amplitude: Time histories were sought that had a PGA within a factor of two to three of the target PGA on rock (evaluation of target PGA on rock is based on the hazard studies for that specific site).
- Site Condition: Time histories were selected from sites underlain by geologic rock or with a thin (< 20 m) layer of soil overlying rock. The site condition corresponds to soft, weathered rock – rock having an average shear wave velocity that has been estimated as $V_{s30} \geq 500$ m/s.

Scaling of input time histories can be carried out in time-domain and in frequency domain. In time-domain scaling involves only the amplitude of the time series (*i.e.*, PGA, PGV, AI, root mean square acceleration, a_{rms}), whereas in frequency domain scaling the frequency content is changed within a pre-determined frequency window (*i.e.,* spectral intensity, SI).

Scaling of input time histories was carried out in time-domain that involves only the amplitude of the time series. Linear scaling is preferred in this study since the main concern was to search the effectiveness of different scaling parameters on the damage parameter predicted at the ground surface. Using a frequency scaling method by means of design spectrum matching was not chosen because the additional variability due to the change in the frequency content of time histories may not so easily compared for different scaling parameters. Individual time histories are scaled up or down by factor so that their maximum acceleration values matches the target value in an average sense. The scaling factor was determined as the ratio of PGA of time history giving the target scaling parameter value over the PGA of the unscaled time history.

The distance compatibility criteria is also evaluated by conducting site response analysis using different sets of earthquake time histories recorded for the same fault type and magnitude range at different fault distances scaled in a similar manner.

3.3. Case Studies

3.3.1. Izmir Case Study

The first case study selected for evaluating the effects of scaling on site response is near the city of Izmir. The site response analyses were conducted using Shake91 for the four soil profiles where in-hole shear wave measurements were performed previously. Even though these four borings are at the same site with spacing around 100m, the measured shear velocity profiles given in Figure 3.3 indicates the variability in the site conditions at one large construction site where for all practical purposes only one site specific design spectra is needed. This situation was normally encountered in many cases where site specific design parameters are needed for the design purpose. Thus the effects of scaling for each soil profile were evaluated together to observe the effects of site variability in relation with the scaling of input ground motion.

The scaled records were applied as outcrop motion where the engineering bedrock (V_s=750m/s) was taken at 45m depth. The regional earthquake hazard analysis yielded an earthquake magnitude of 6.5-7 with an epicenter distance of 10-20km. The hazard compatible input earthquake data, composed of 20 acceleration time histories recorded between 10-20km epicenter distances, are listed in Table 3.1. Site response analyses were conducted using scaling parameters determined from related empirical attenuation relationships as (Ambraseys *et al.*, 2005; Akkar and Bommer, 2007; Travasarou, *et al.*, 2003) PGA=0.25g, PGV=30cm/s, and AI=55cm/s.

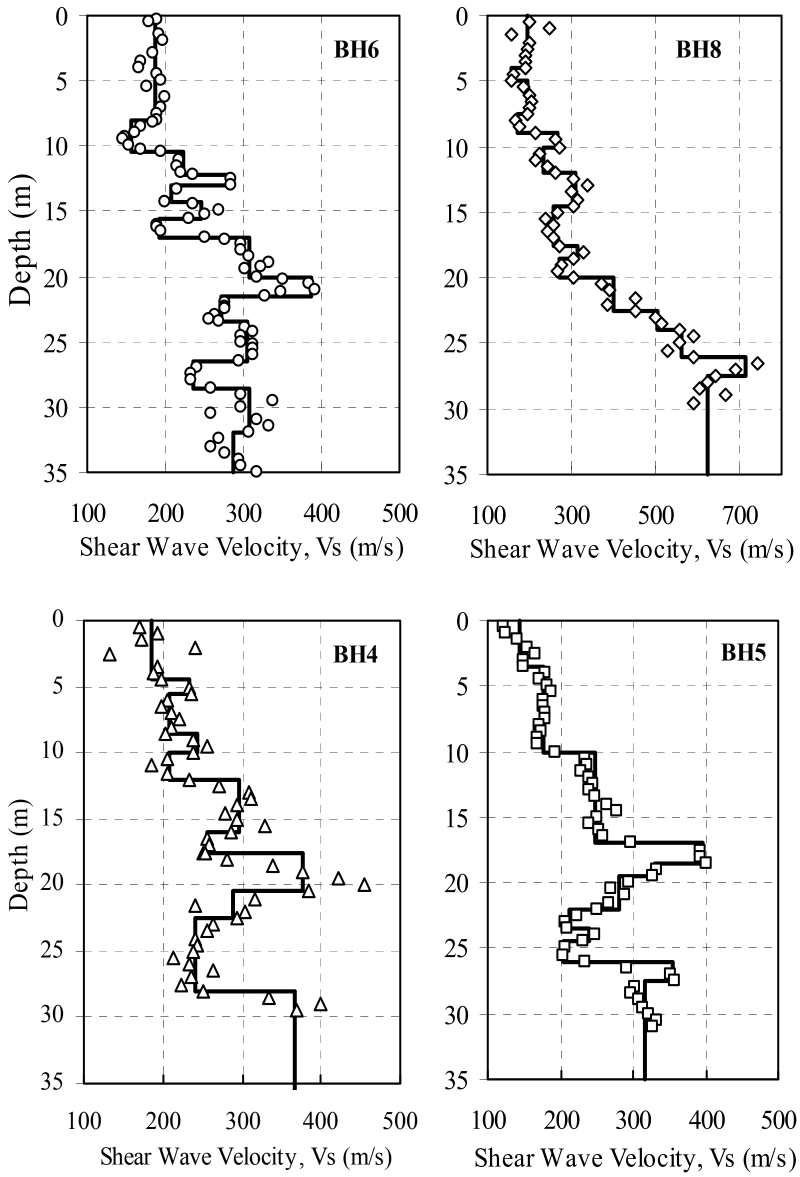

Figure 3.3. Four soil profiles used in site response analyses for the first case study

The results are presented in terms of histograms of peak accelerations and spectral accelerations at 0.2s obtained by fitting an envelope NEHRP design spectra. The peak ground acceleration histograms calculated for four soil profiles, shown separately in Figure 3.4, indicates the importance of the variations in the soil profiles. Thus one option to account for these differences in the soil profile at the site is to consider the site response results obtained for four soil profiles together and determine the variation of peak ground acceleration with respect different scaling procedures adopted.

Table 3.1. Earthquake records used for Izmir case study

Earthquake	Station	Year	M	Joyner-Boore Dist. (km)	PGA (g)	PGV (cm/s)	PGD (cm)	V_{s30} (m/s)
San Fernando	Pacoima Dam (upper left abut)	1971	6.6	9.52	1.16	76	18	2016
Irpinia, Italy	Auletta	1980	6.9	8.14	0.06	6	4	1000
Irpinia, Italy	Bagnoli Irpinio	1980	6.9	6.78	0.16	26	10	1000
Irpinia, Italy	Sturno	1980	6.9	9.19	0.29	47	22	1000
Loma Prieta	Gilroy - Gavilan Coll.	1989	6.9	8.84	0.33	27	5	730
Loma Prieta	Gilroy Array #1	1989	6.9	9.87	0.44	35	7	1428
Northridge	LA - Chalon Rd	1994	6.7	9.87	0.21	23	4	740
Northridge-	LA 00	1994	6.7	4.92	0.32	32	5	706
Northridge	Pacoima Dam (downstr)	1994	6.7	4.92	0.41	37	5	2016
Northridge	Pacoima Dam (upper left)	1994	6.7	1.69	1.43	75	12	2016
Northridge	Santa Susana Ground	1994	6.7	3.22	0.25	16	6	715

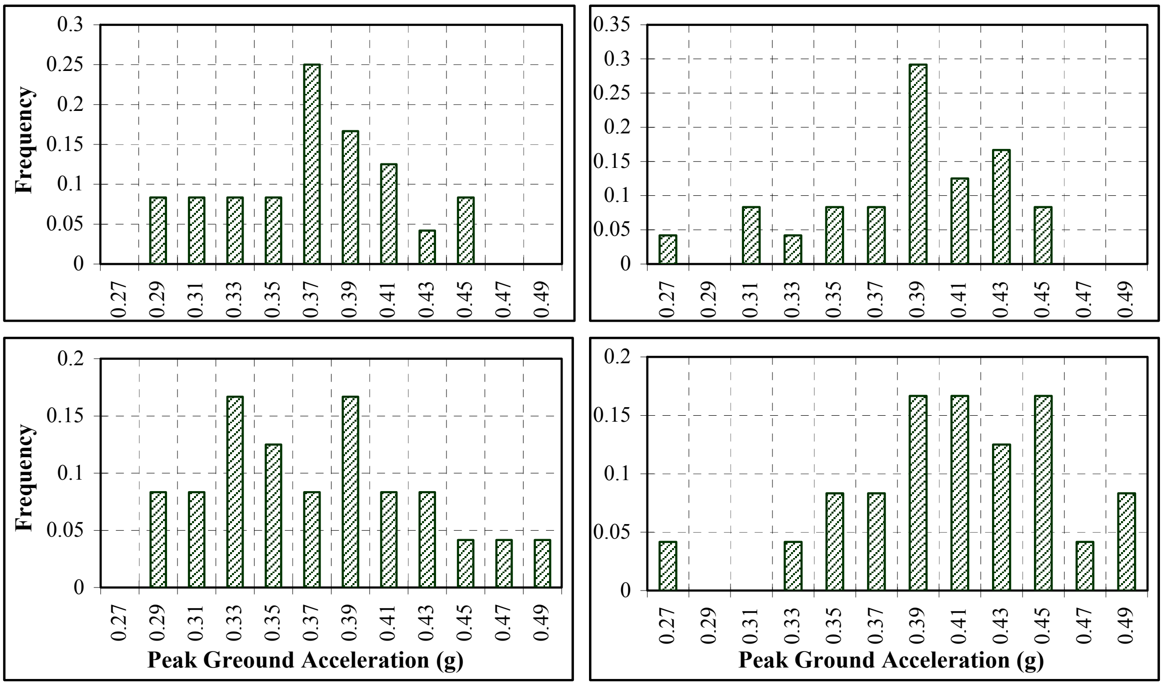

Figure 3.4. Histograms of PGA on the ground surface for PGA scaled acceleration records for four soil profiles

If each PGA distribution is assumed as possible variations concerning the input motion and if each PGA distribution is modeled by probability distribution models, it would be possible to estimate, with certain level of exceedance probability, the peak ground acceleration on the ground surface that can be used for the design of the engineering structures. Thus assuming that the exceedance level can be taken as 10 per cent, the peak ground accelerations were determined based on the best fit by Beta or Weibull statistical distribution models. The calculated PGAs for three scaling method used are shown in Figure 3.5. Based on the histograms for the calculated PGAs for all four borings for the three scaling option using the considered input motions, it seems that among three scaling procedures, taking into consideration all three parameters calculated to determine the variability in each set (kurtosis and normalized standard deviation being minimum, and range being the smallest), the PGA scaling appears to be the most suitable scaling parameter in terms of calculated peak ground accelerations on the ground surface if they happen to be the a suitable damage parameter (*i.e.,* liquefaction susceptibility analysis). It is interesting to note that PGV scaled records gave the largest PGA value while Arias intensity scaled records gave the lowest PGA value.

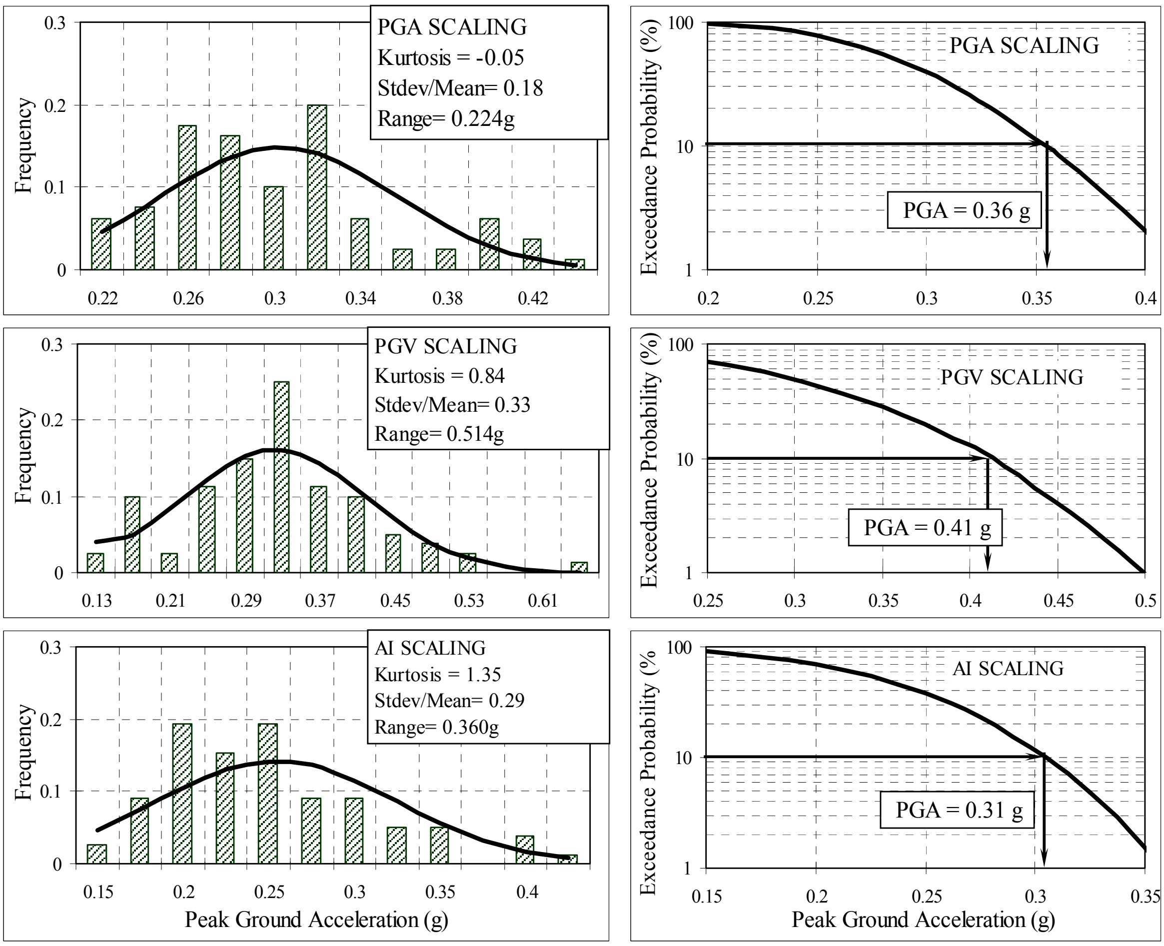

Figure 3.5. Histograms of PGA on the ground surface for PGA, PGV, and AI scaled records

In the case of spectral accelerations at 0.2s the characteristics of the statistical distributions have changed significantly as shown in Figure 3.6. Arias intensity (AI) scaling yielded the smallest range and Kurtosis while PGA scaling yielded the largest range and Kurtosis. Thus with respect to spectral accelerations at 0.2s, AI scaling gave the most suitable solution with the smallest variability. In addition, the lowest value of the spectral acceleration at 0.2s is also obtained from the AI scaling results.

If we consider spectral acceleration at 0.2s as the main damage parameter for the geotechnical engineering structures, than it is possible to suggest the use of AI scaling as the first option when conducting site response at a site to determine the design ground motions for geotechnical engineering structure.

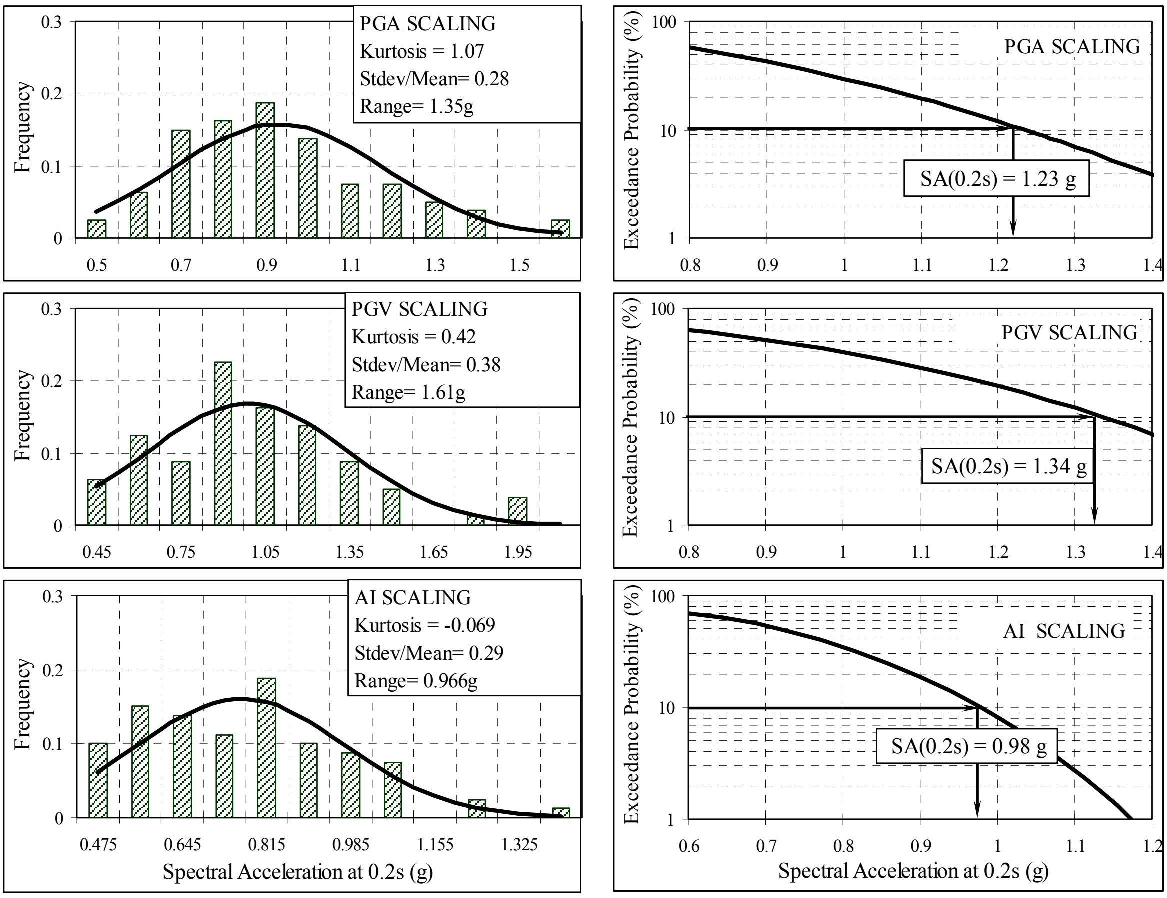

Figure 3.6. Histograms of $S_a(0.2s)$ on the ground surface for PGA, PGV, and AI scaled records

3.3.2. Gölcük Case Study

The second site is located in Gölcük; a town in the epicenter area of the 1999 Kocaeli, Turkey Earthquake. Detailed site investigations were carried out in the town as a part of the post earthquake studies. The regional earthquake hazard is dominated by strike slip faulting, that generates earthquakes in the magnitude range of 7.0-7. 5.

The ground motion data are obtained from PEER. The selection criteria were earthquake mechanism as strike slip, magnitude range as 7.0-7.5; and distance range was taken as 10-40km that was grouped in 10km intervals, site conditions B or C according to NEHRP classification. The regional earthquake hazard is can be characterized by PGA=0.35g, PGV=30cm/sec, SA (0.2s) =0.33g, SA (1.0s) =0.75g (Erdik *et al.*, 2004). AI is estimated as 2m/s for the magnitude and distance range considered based on the empirical attenuation relationship proposed (Travasaro *et al.,* 2003; Siyahi *et al.,* 2001). In the resulting data set there are records from three major events: Kocaeli, Turkey; Duzce, Turkey and Landers, USA Earthquakes. The data, summarized in Table 3.2, are scaled to PGA=0.35g, PGV=30cm/s and AI=2m/s for site response analysis.

The main purpose of this case was to study the effects of releasing the distance requirement in selecting the previously recorded site specific hazard compatible earthquake time histories. The results are presented in terms of peak ground accelerations and response spectral accelerations at the ground surface. Ground motions scaled with respect to PGA, PGV and AI are used as input for the three sets of input motion for the site response analyses.

The results obtained from the parametric study are shown in Figure 3.7 with respect to the calculated elastic acceleration response spectra at the ground surface. Each column of spectrum in Figure 3.7 shows the acceleration response spectrum calculated using the previously recorded time histories at a distance in order of 10-20km, 20-30km and 30-40 km from the ruptured fault with no scaling, with PGA, PGV and Arias Intensity scaling. The last graph in the column shows the comparison among different scaling procedures in terms of average spectrum. It is interesting to observe that PGA scaling always gave the highest spectral accelerations concerning other scaling procedures adopted in this study.

When the results are compared with respect to average spectral accelerations calculated using different time histories recorded at different distances as given in Figure 3.8, there is a minor difference in PGA scaled input motions, in PGV or AI scaled records there is almost no difference. However, if one looks at the scatter and the change in the range of the calculated acceleration spectrum shown in Figure 3.7, the distance to the faults appears to be an effective parameter. Even though the actual recorded time histories show the opposite trend, the scatter and range increases with the distance of the recorded time histories for the PGA, PGV and AI scaled input motions. This could lead to different spectral accelerations if the scatter is evaluated by statistical procedure in a probabilistic way. Therefore it would be recommendable to select the real time histories for site response analysis at compatible distance range as determined by the site specific hazard study.

Table 3.2. Ground motion data set used in analyses - earthquake mechanism: strike-slip, distance range: 0-40 km, magnitude range: 7.0-7.5

Station	Earthquake	Date	M_w	r_{epi} (km)	PGA (g)	
					EW	NS
0-10 km						
375	Düzce	11/12/99	7.1	8.2	0.514	0.970
1058	Düzce	11/12/99	7.1	0.9	0.111	0.073
1059	Düzce	11/12/99	7.1	8.5	0.133	0.147
Izmit	Kocaeli	08/17/99	7.4	4.8	0.22	0.152
Sakarya	Kocaeli	08/17/99	7.4	3.1	0.376	
24 Lucerne	Landers	28/06/92	7.3	1.1	0.785	0.721
10-20 km						
531	Düzce	11/12/99	7.1	11.4	0.118	0.159
1061	Düzce	11/12/99	7.1	15.6	0.134	0.107
1062	Düzce	11/12/99	7.1	13.3	0.257	0.114
Arcelik	Kocaeli	08/17/99	7.4	17.0	0.218	0.149
Gebze	Kocaeli	08/17/99	7.4	17.0	0.244	0.137
Joshua Tree	Landers	06/28/92	7.3	11.3	0.274	0.284
Morongo	Landers	06/28/92	7.3	17.7	0.188	0.140
20-30 km						
362	Düzce	11/12/99	7.1	27.4	0.026	0.042
12149 Desert	Landers	06/28/92	7.3	23.2	0.171	0.154
5070 NPS	Landers	06/28/92	7.3	24.2	0.136	0.134
23 Coolwater	Landers	06/28/92	7.3	21.2	0.283	0.417
100 MCF	Landers	06/28/92	7.3	21.2	0.126	0.125
30-40 km						
Lamont 1060	Düzce	11/12/99	7.1	30.2	0.053	0.028
Barstow	Landers	06/28/92	7.3	36.1	0.132	0.135
Göynük	Kocaeli	17/8/99	7.4	35.5	0.132	0.119
Iznik	Kocaeli	17/8/99	7.4	31.8	0.136	0.098
Palm Springs	Landers	06/28/92	7.3	37.5	0.076	0.089
Mudurnu	Düzce	11/12/99	7.1	33.6	0.12	0.056

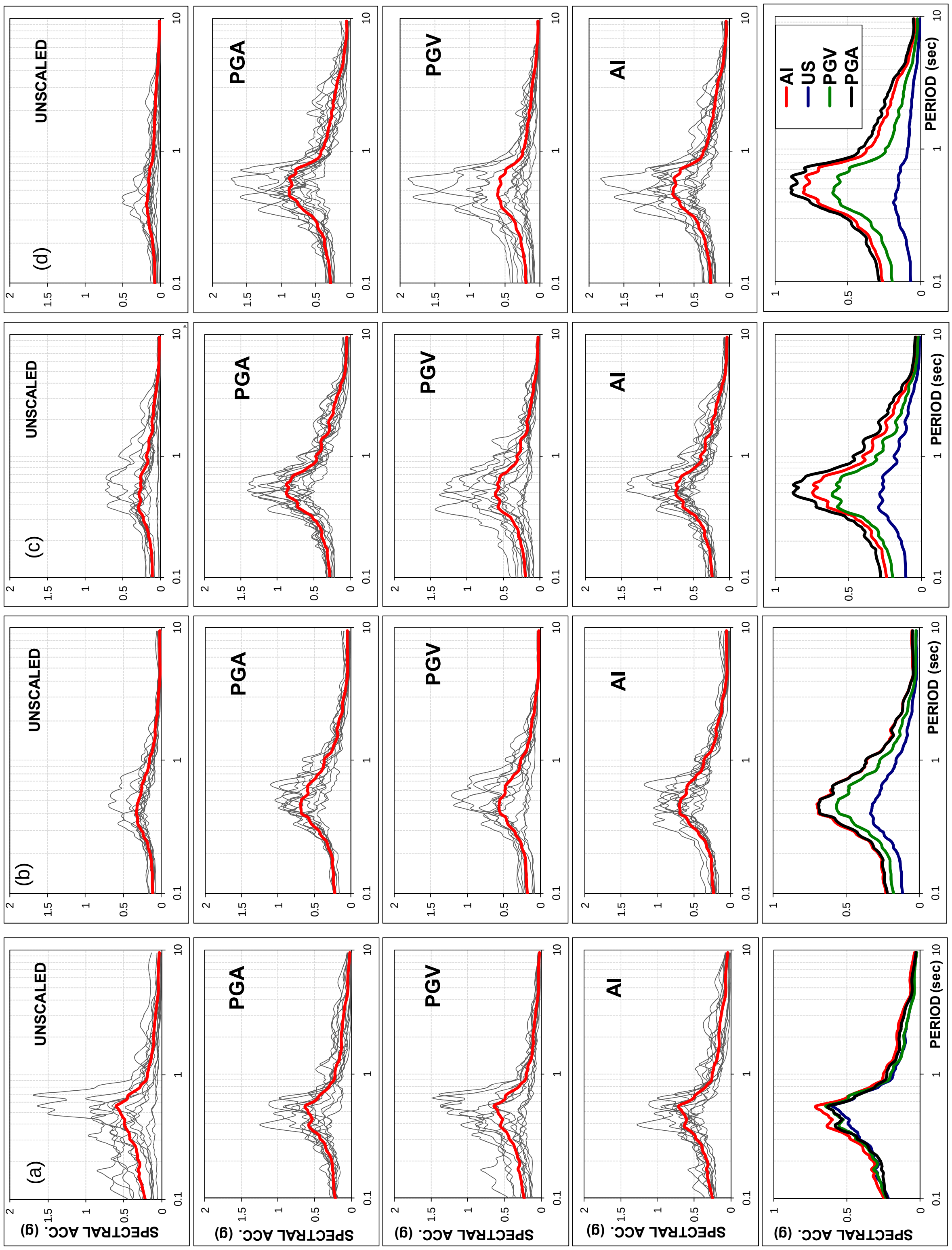

Figure 3.7. Calculated elastic acceleration response spectrum for three distance ranges (a) 0-10 km; (b) 10-20 km; (c) 20-30 km; (d) 30-40 km using unscaled, PGA, PGV, and Arias Intensity scaled time histories; last row: average spectral accelerations with respect to scaling procedure

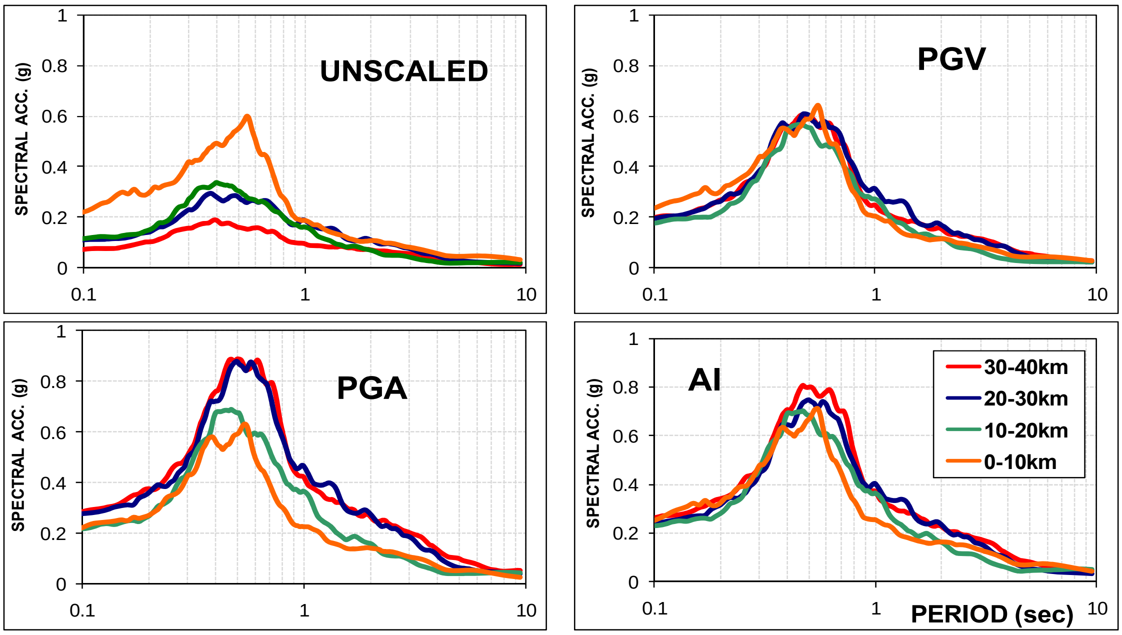

Figure 3.8. Average spectral accelerations from site response analyses conducted using real time histories recorded at different distances with respect to scaling procedure

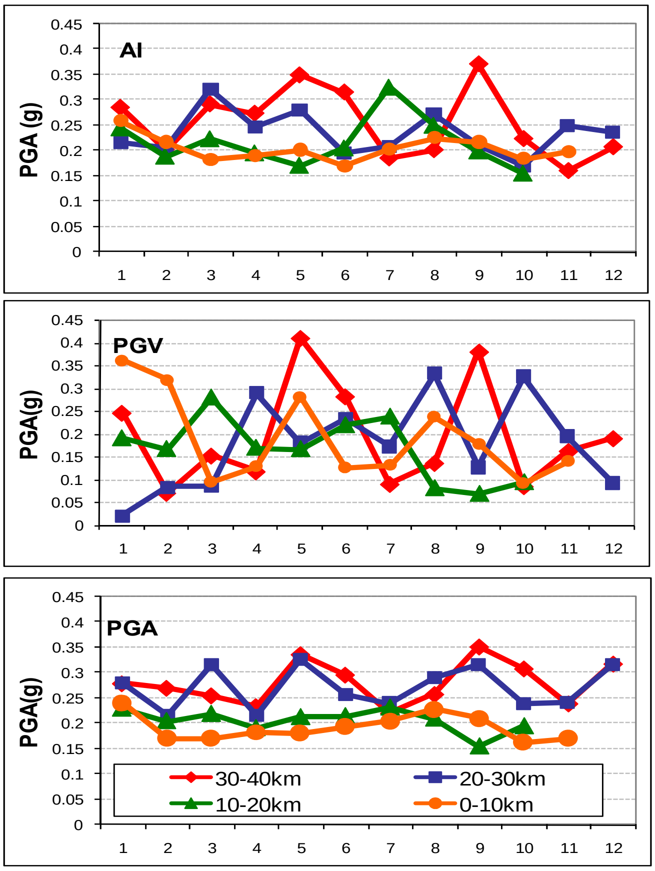

Figure 3.9. Variation of peak ground accelerations from site response analyses using real time histories recorded at different distances with respect to scaling procedure

The situation is similar in terms of the calculated peak ground accelerations as shown in Figure 3.9. The scatter is much less for PGA scaled input motions as well as the scatter is less for all the scaled time histories recorded within 10-20km range.

3.4. General Scaling Study

A detailed parametric study was conducted to evaluate the effects of input motion scaling by considering eight scaling parameters (PGA; PGV; Arias Intensity, I_a; Root Mean Square Acceleration, a_{rms}; Cumulative Absolute Velocity, CAV; Spectrum Intensity, SI and Acceleration Spectrum Intensity, ASI) for three different real soil profiles with different depths (182m, 100m and 45m) but similar average shear wave velocities (V_{s30}=267 m/s, 294 m/s, 304 m/s) for three earthquake hazard levels (M=6-6.5, M=6.5-7, and M=7-7.5). Input acceleration time histories were selected from data set used to estimate the attenuation relationships in Chapter 2.

3.4.1. Soil Profiles

A very comprehensive site investigation study was carried out on the European side of Istanbul as part of the large-scale microzonation project for the Istanbul Metropolitan Municipality (OYO, 2007). 2912 borings (mostly down to 30m depth with approximately 250m spacing) were conducted within an area of about 182 km^2 to investigate local soil conditions. Standard Penetration Test (SPT), Cone Penetration Test (CPT), PS-Logging, Refraction Microtremor (ReMi), seismic reflection and refraction measurements were carried out at each borehole location. Samples collected in the field were tested in the laboratory to determine index and engineering properties of local soils within the investigated area.

The selected three soil profiles are from Istanbul Microzonation Study conducted (Figure 3.10). Shear wave velocity profiles are based on in-situ measurements conducted using PS Logging in-hole seismic wave velocity measurements as well as in-situ geophysical seismic wave velocity measurements and based on empirical correlation with respect to SPT blow counts.

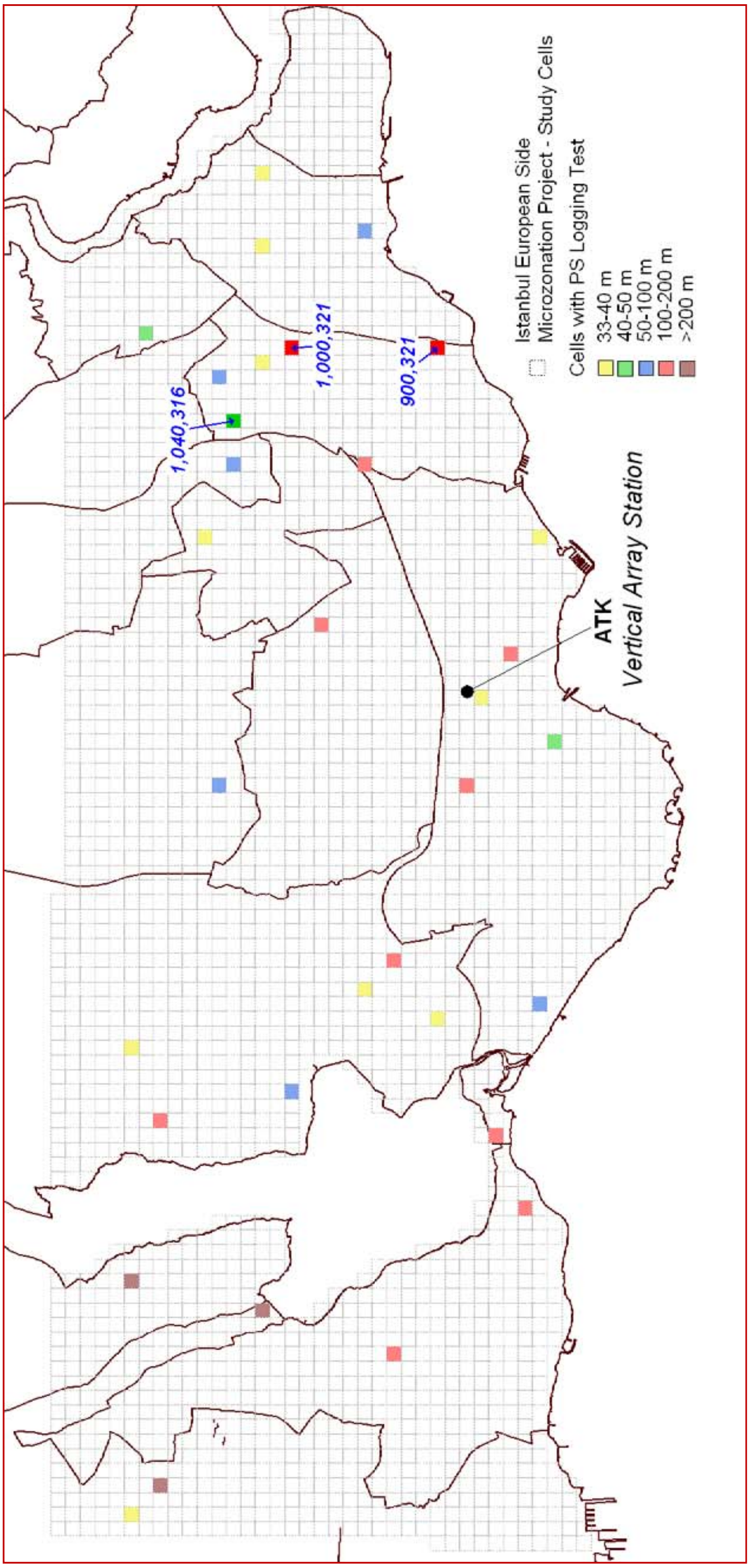

Figure 3.10. Location map for selected soil profiles on the Istanbul European side microzonation project study cells

In addition to the shear wave velocity measurements in these soil profiles, the types of soil layers are determined based on laboratory index tests and thus site characterization was reliable and sufficiently detailed in assigning modulus reduction and damping curves.

In order to evaluate the effect of soil profile depth on scaling analysis, three soil profiles (Figure 3.11, Figure 3.12, Figure 3.13) with similar equivalent shear wave velocity (V_{s30}=267 m/s, 294 m/s, 304 m/s) but with different thicknesses were selected to conduct the parametric study.

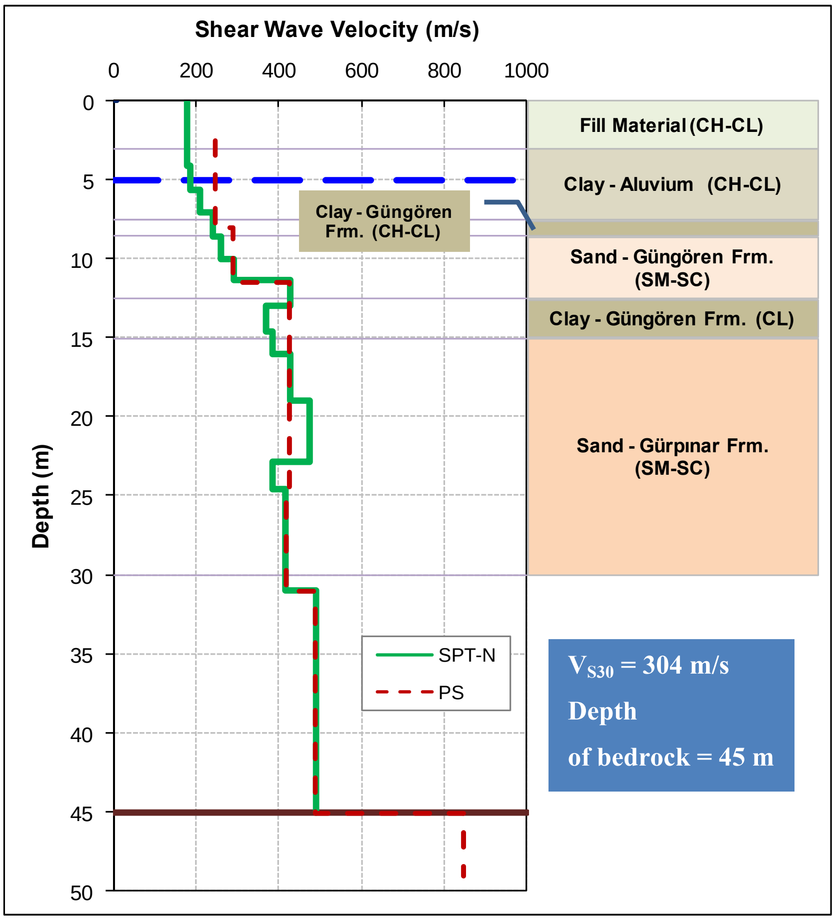

Figure 3.11. Soil profile 3 (1040316) used in site response analyses for the general scaling study

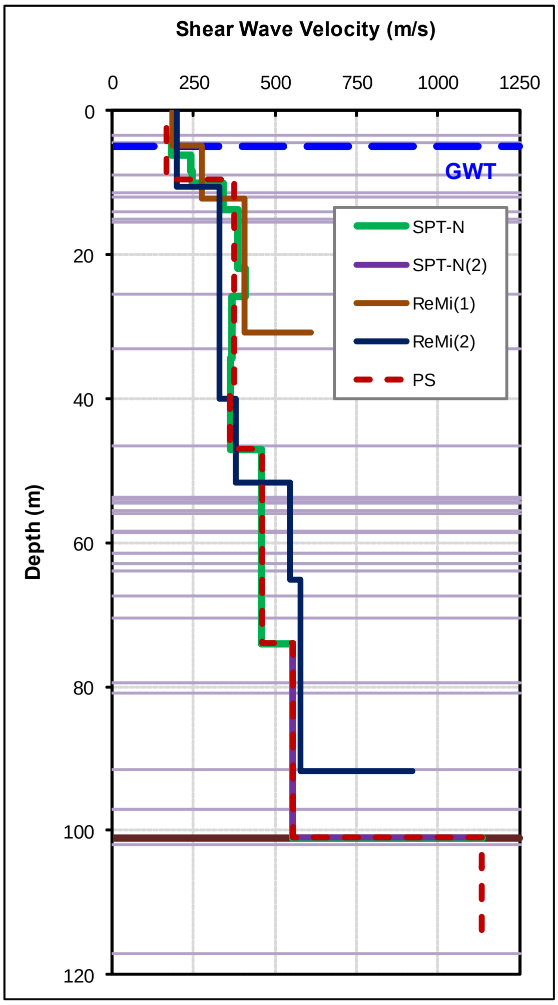

Formation	Top Depth of Layer (m)	Bottom Depth of Layer (m)	Lithology
Fill Material	0	3.5	Fill
Bakırköy	3.5	4.5	Clay (ML)
Güngören	4.5	9	Clay (CL-CH)
Güngören	9	11.5	Sand (CH)
Güngören	11.5	12	Clay
Güngören	12	12.1	Marn
Güngören	12.1	14	Clay
Güngören	14	15	Clay
Güngören	15	15.5	Sand
Güngören	15.5	25.5	Clay (CL, CL-CH, SM-SC)
Güngören	25.5	33	Clay (CL-CH)
Güngören	33	46.5	Clay
Gürpınar	46.5	53.8	Claystone
Gürpınar	53.8	54	Marn
Gürpınar	54	54.3	Claystone
Gürpınar	54.3	54.5	Marn
Gürpınar	54.5	55.5	Claystone
Gürpınar	55.5	56	Clay
Gürpınar	56	58.5	Sand
Gürpınar	58.5	58.7	Siltstone
Gürpınar	58.7	61.4	Sand
Gürpınar	61.4	61.5	Marn
Gürpınar	61.5	63	Sand
Gürpınar	63	64	Claystone
Gürpınar	64	67.5	Clay
Gürpınar	67.5	70.5	Sand
Gürpınar	70.5	79.5	Claystone
Gürpınar	79.5	81	Sand
Gürpınar	81	91.5	Sand
Gürpınar	91.5	97	Sand
Gürpınar	97	102	Clay
Trakya	102	117	Graywacke

Figure 3.12. Soil profile 2 (1000321) used in site response analyses for the general scaling study

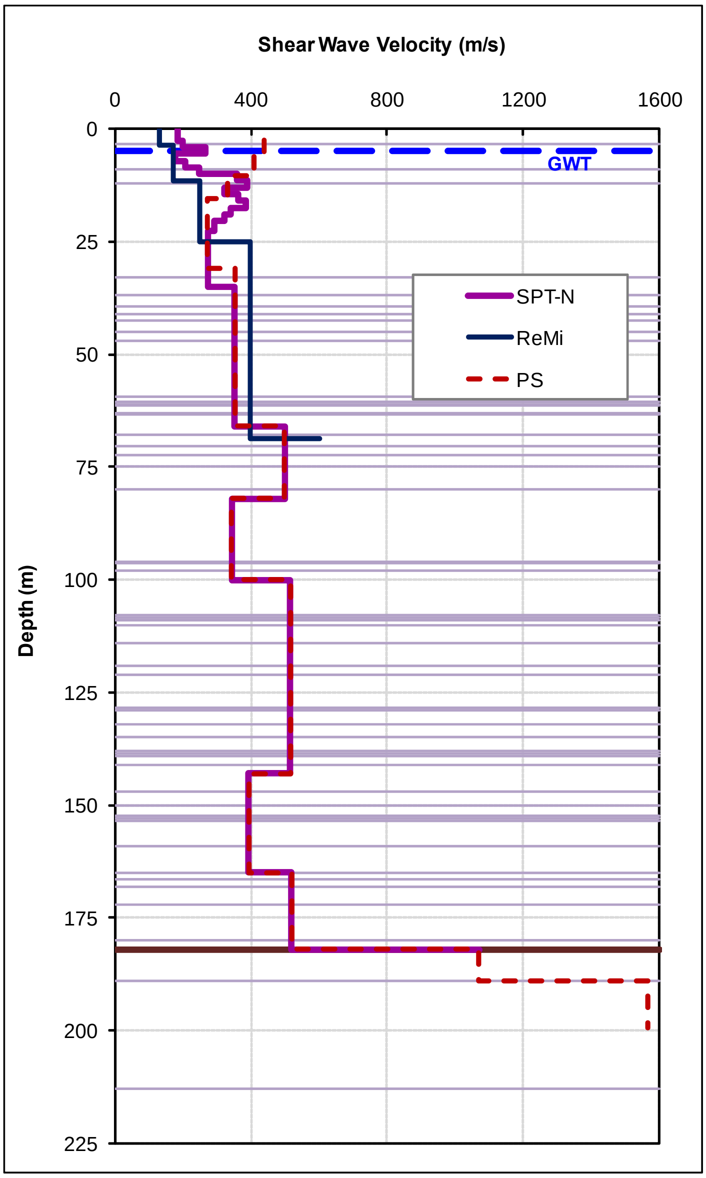

Formation	Top Depth of Layer (m)	Bottom Depth of Layer (m)	Lithology
Fill Material	0	3.5	Fill (GM-GC)
Alluvium	3.5	9	Clay (CH, CL)
Alluvium	9	12	Sand (ML)
Güngören	12	33	Clay (CH, CL)
Gürpınar	33	37	Claystone
Gürpınar	37	39.5	Sandstone
Gürpınar	39.5	41	Clay
Gürpınar	41	42.5	Claystone
Gürpınar	42.5	45	Sand
Gürpınar	45	47	Clay
Gürpınar	47	59.5	Claystone
Gürpınar	59.5	60.5	Sandstone
Gürpınar	60.5	61	Siltstone
Gürpınar	61	61.5	Sandstone
Gürpınar	61.5	63	Sand
Gürpınar	63	63.5	Claystone
Gürpınar	63.5	68	Sand
Gürpınar	68	70.5	Claystone
Gürpınar	70.5	72.5	Sand
Gürpınar	72.5	75	Siltstone
Gürpınar	75	80	Claystone
Gürpınar	80	96	Sand
Gürpınar	96	96.4	Claystone
Gürpınar	96.4	98	Sandstone
Gürpınar	98	108	Claystone
Gürpınar	108	108.5	Sandstone
Gürpınar	108.5	109	Claystone
Gürpınar	109	110	Sandstone
Gürpınar	110	114	Siltstone
Gürpınar	114	119	Sandstone
Gürpınar	119	121	Claystone
Gürpınar	121	128.5	Sand
Gürpınar	128.5	129	Claystone
Gürpınar	129	132	Sand
Gürpınar	132	135	Claystone
Gürpınar	135	138	Sandstone
Gürpınar	138	138.5	Siltstone
Gürpınar	138.5	139	Claystone
Gürpınar	139	141	Sandstone
Gürpınar	141	147	Sand
Gürpınar	147	150	Gravel
Gürpınar	150	152.5	Sand
Gürpınar	152.5	153	Siltstone
Gürpınar	153	153.5	Gravel
Gürpınar	153.5	159	Siltstone
Gürpınar	159	165	Sand
Gürpınar	165	166.5	Gravel
Gürpınar	166.5	168	Sandstone
Gürpınar	168	172	Sand
Gürpınar	172	180	Sand
Gürpınar	180	189	Sandstone
Trakya	189	213	Graywacke

Figure 3.13. Soil profile 1 (900321) used in site response analyses for the general scaling study

3.4.2. Time History Database

Time histories used for site response analysis are grouped based on magnitude and distance ranges. Site response analysis for eight scaling parameters were conducted for nine sets corresponding to three magnitude ranges (6.0-6.5, 6.5-7.0, 7.0-7.5) and three distance ranges (0-30km, 30-60km, 60-90km). Numbers of input motion in each bin are given in Table 3.3.

Table 3.3. Scaling study magnitude and distance bins and number of input motions

MAGNITUDE	DISTANCE	NO of INPUT MOTIONS	BIN NAME
6.0 – 6.5	0-30 km	45	1A
	30-60 km	92	1B
	60-90 km	64	1C
6.5 – 7.0	0-30 km	34	2A
	30-60 km	31	2B
	60-90 km	26	2C
7.0 – 7.7	0-30 km	49	3A
	30-60 km	49	3B
	60-90 km	31	3C

3.4.3. Scaling Parameters

The variation PGA for the three sub bins of first bin (1A: M= 6.0-6.5 and R= 0-30 km, 1B: M= 6.0-6.5 and R= 30-60 km, 1C: M= 6.0-6.5 and R= 60-90 km) of the input motions scaled with respect to eight different scaling parameters are given in the Figure 3.14. Although the target PGA was selected as 0.25 g, input motion PGAs show variation in the range of 0.1 – 0.55 g.

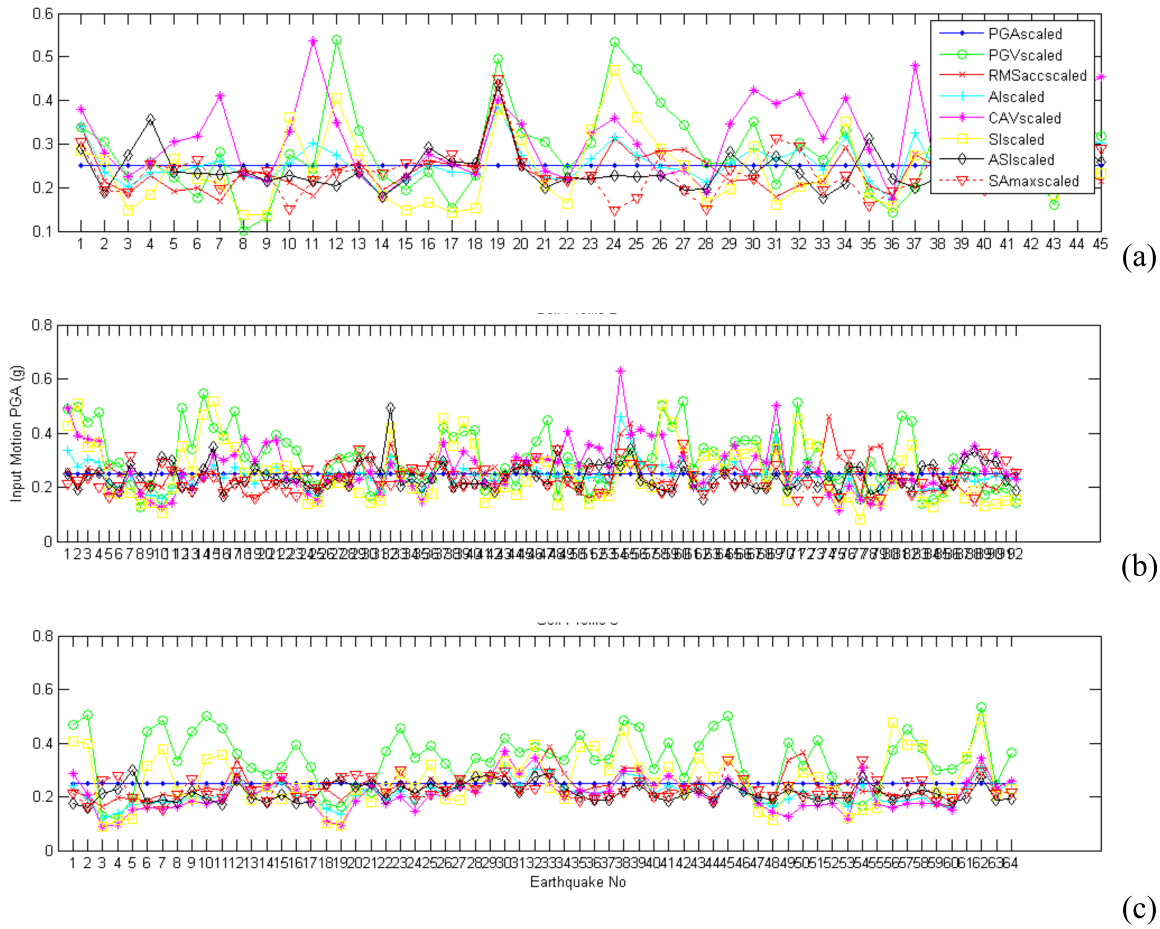

Figure 3.14. The variation of PGA for the (a) 1A bin (M= 6.0-6.5 and R= 0-30 km), (b) 1B bin (M= 6.0-6.5 and R= 30-60 km) and (c) 1C bin (M= 6.0-6.5 and R= 60-90 km) of the input motions scaled with respect to eight different scaling parameters

3.4.4. Scaling Results

All the results are given in the Appendix A, for the parametric study on scaling. Histograms of (a) peak ground acceleration, PGA; (b) peak ground velocity, PGV; (c) maximum spectral accelerations, SA_{max} for three soil profiles calculated on the ground surface from the site response analysis that used input time histories scaled with respect to eight scaling parameters are the first three figures for each bin of magnitude and distance. Variation of mean, mean±sd and range of PGA, PGV and SA_{max} and variation of kurtosis, variance and SD/mean for three soil profiles with respect to scaling parameters are the following two figures in the Appendix A.

The results for the three soil profiles are given through the following figures:

In Figure 3.15, Figure 3.16 and Figure 3.17, the response spectra for PGA scaling case are given for nine bins of magnitude and distance pairs to compare the average spectrum of each bin.

The following bar charts (Figure 3.18, Figure 3.19 and Figure 3.20) visualize all the results of this parametric study based on the variation of PGA SD/Mean again given for each soil profile.

The variations of SD/Mean for three damage parameters (PGA, PGV and SA_{max}) with magnitude for three soil profiles with respect to scaling parameters are shown in the Figure 3.21, Figure 3.22 and Figure 3.23.

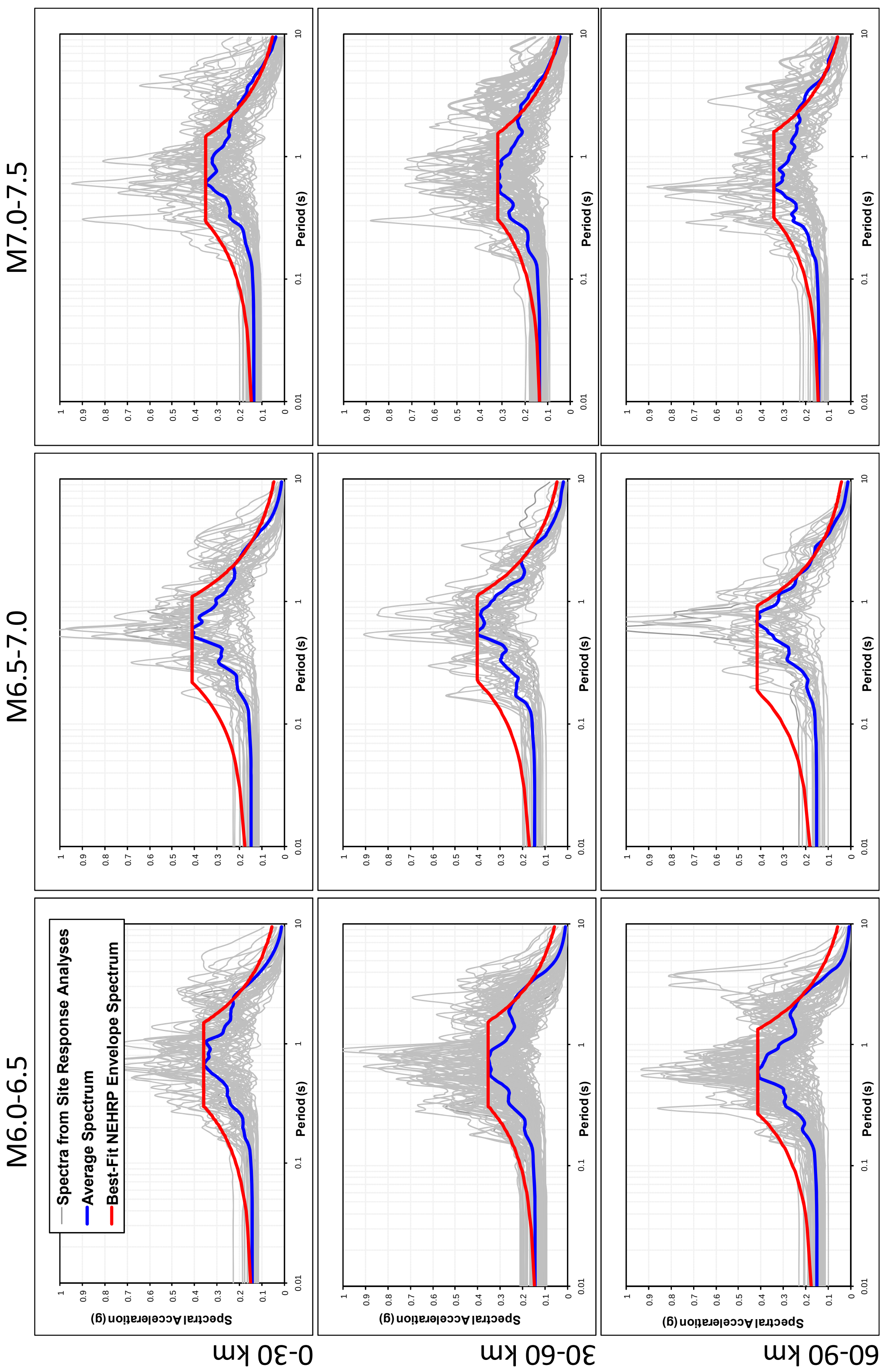

Figure 3.15. Soil profile 1 – response spectra for PGA scaling case for nine bins of magnitude and distance pairs

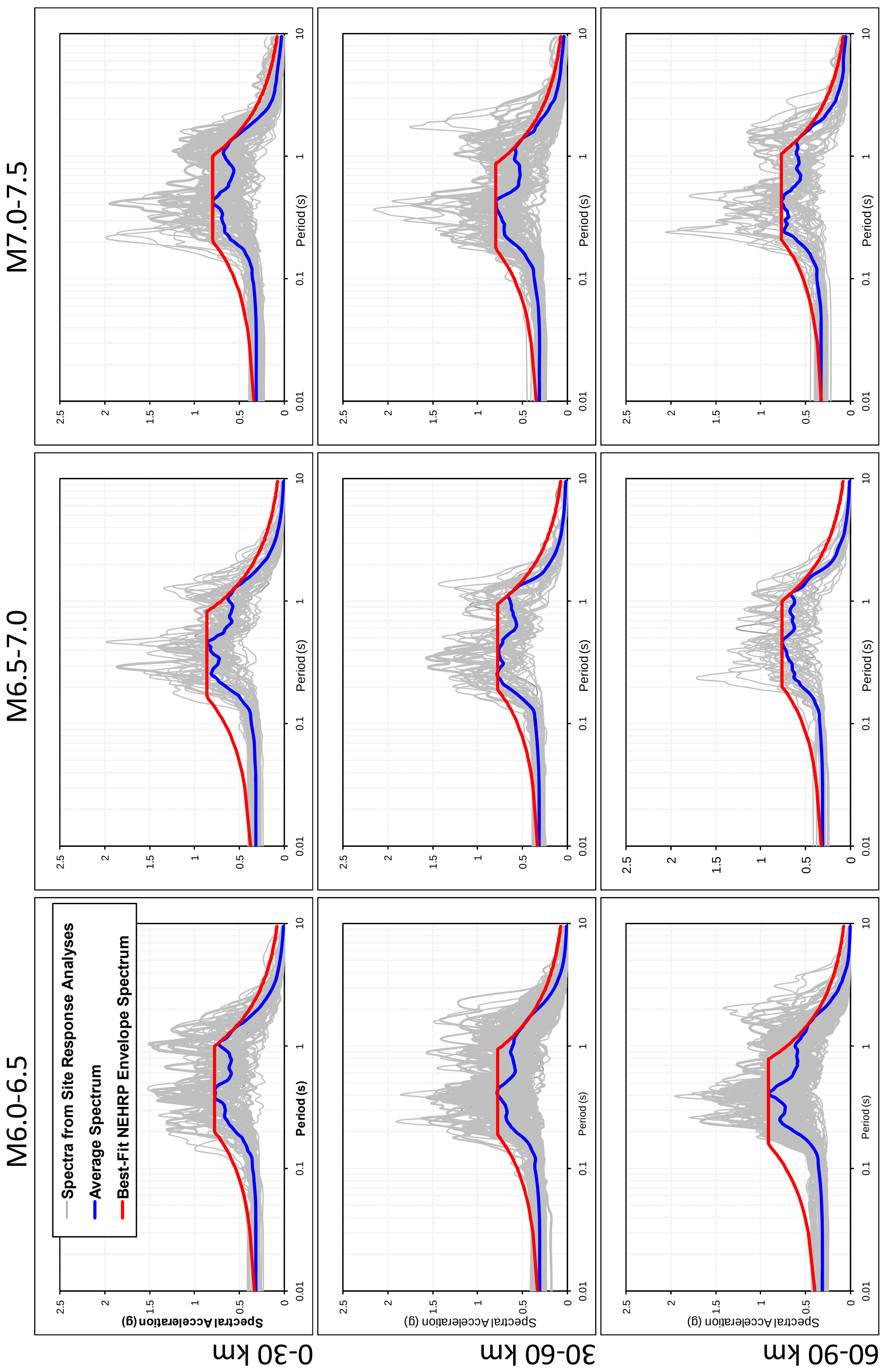

Figure 3.16. Soil profile 2 – response spectra for PGA scaling case for nine bins of magnitude and distance pairs

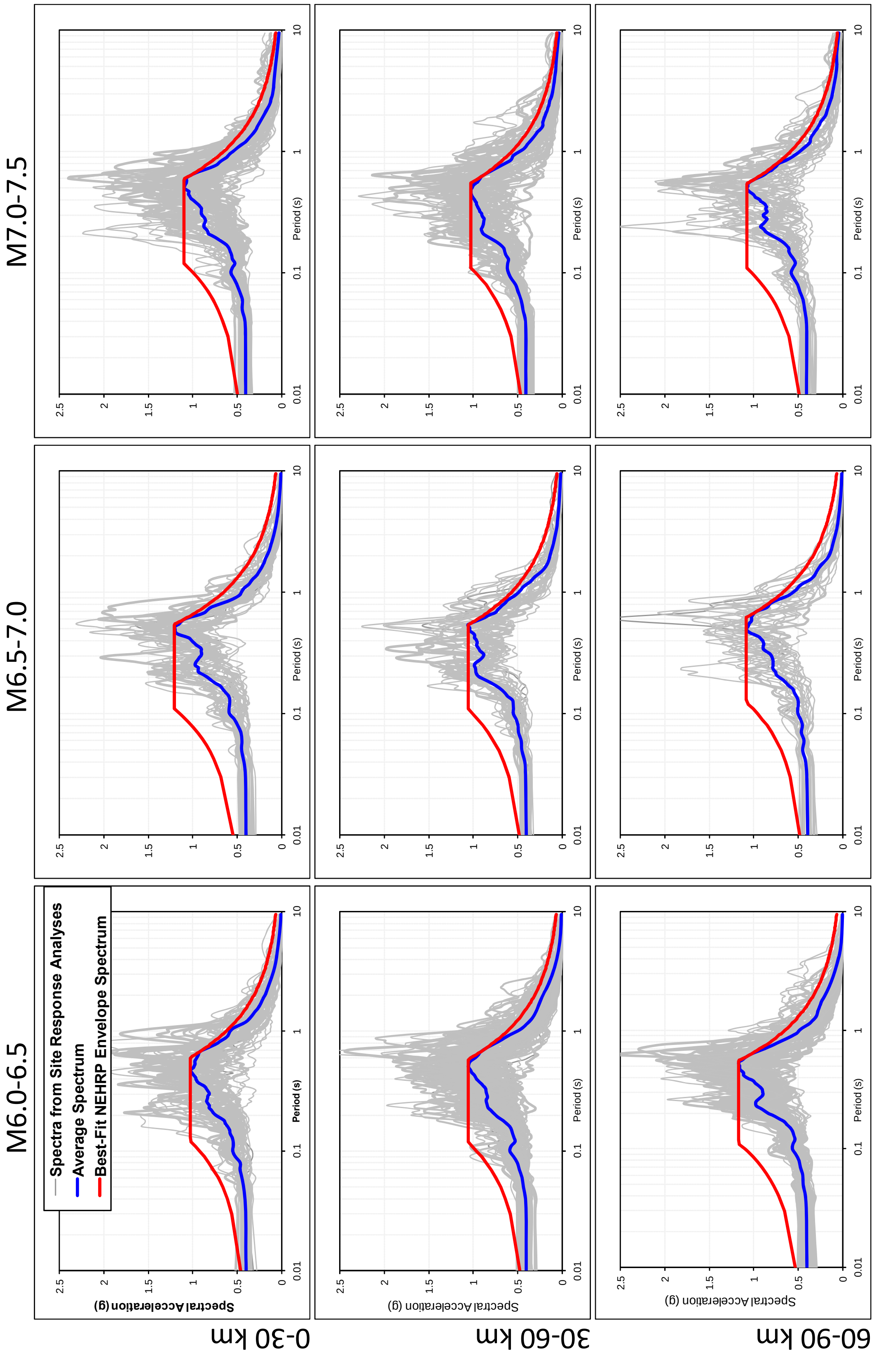

Figure 3.17. Soil profile 3 – response spectra for PGA scaling case for nine bins of magnitude and distance pairs

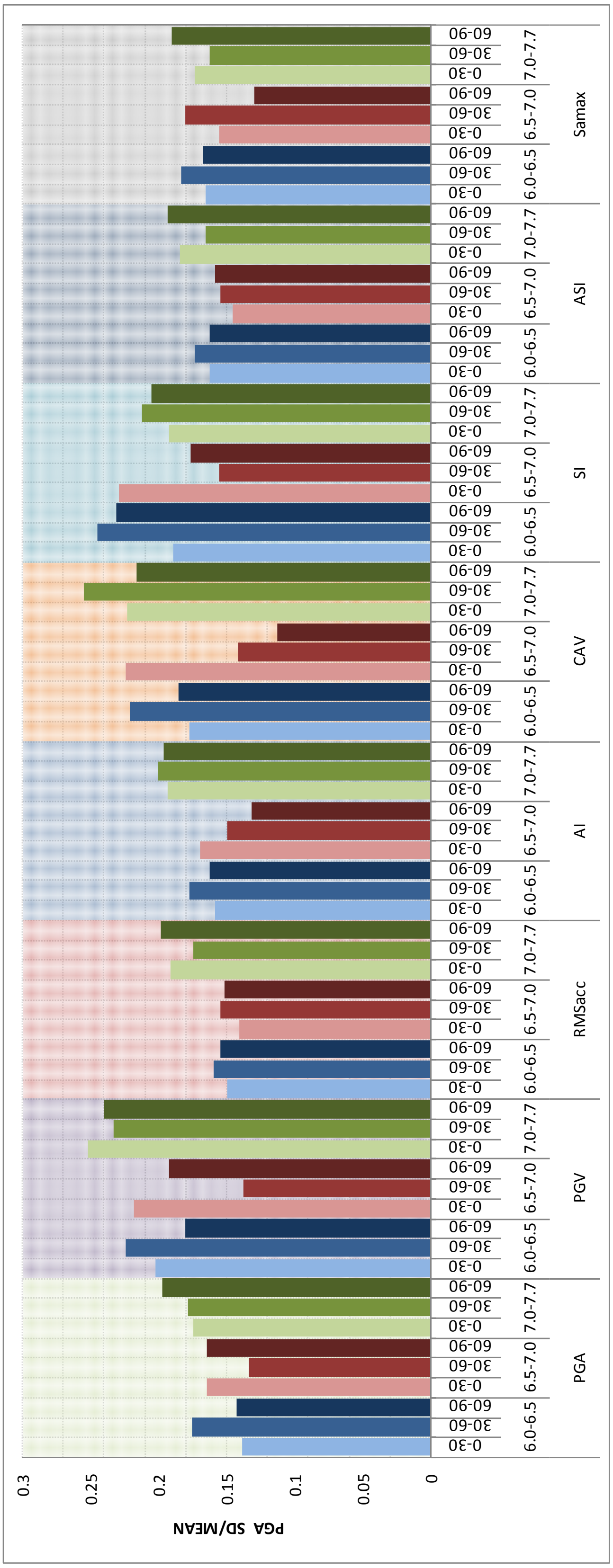

Figure 3.18. Soil profile 1 – all the results of the parametric study based on the variation of PGA SD/Mean

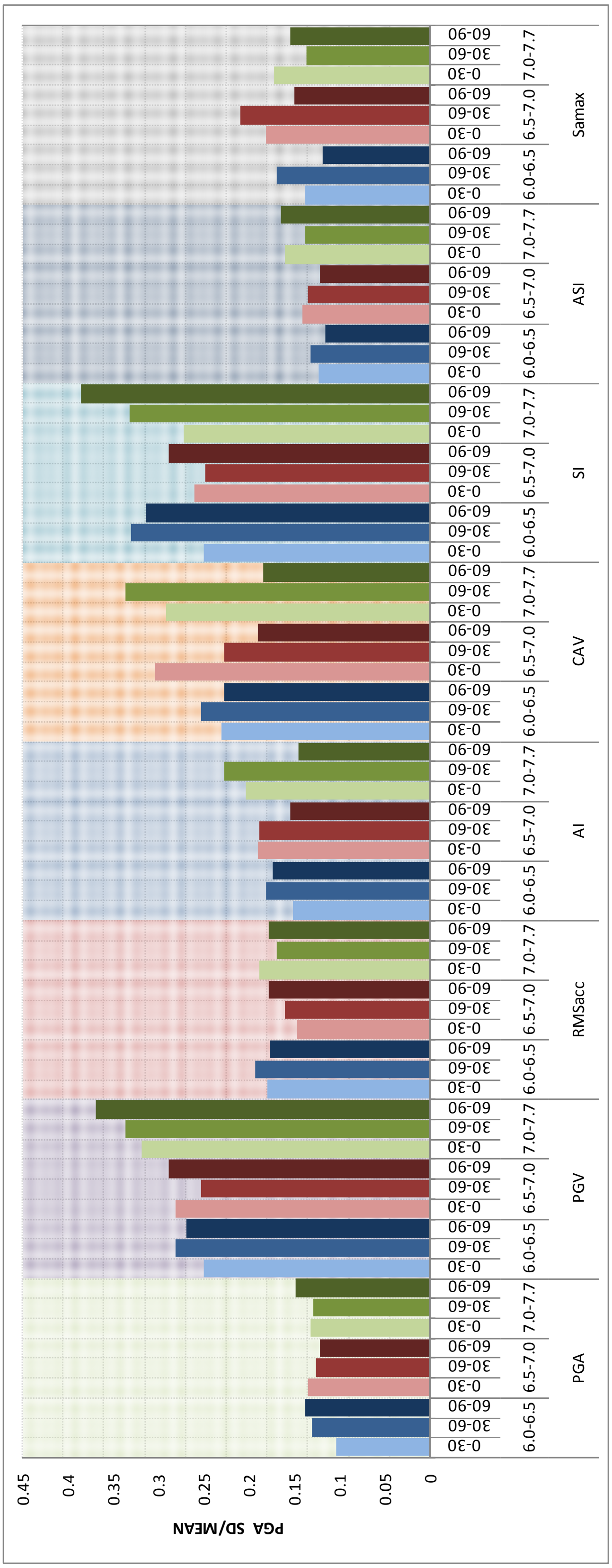

Figure 3.19. Soil profile 2 – all the results of the parametric study based on the variation of PGA SD/Mean

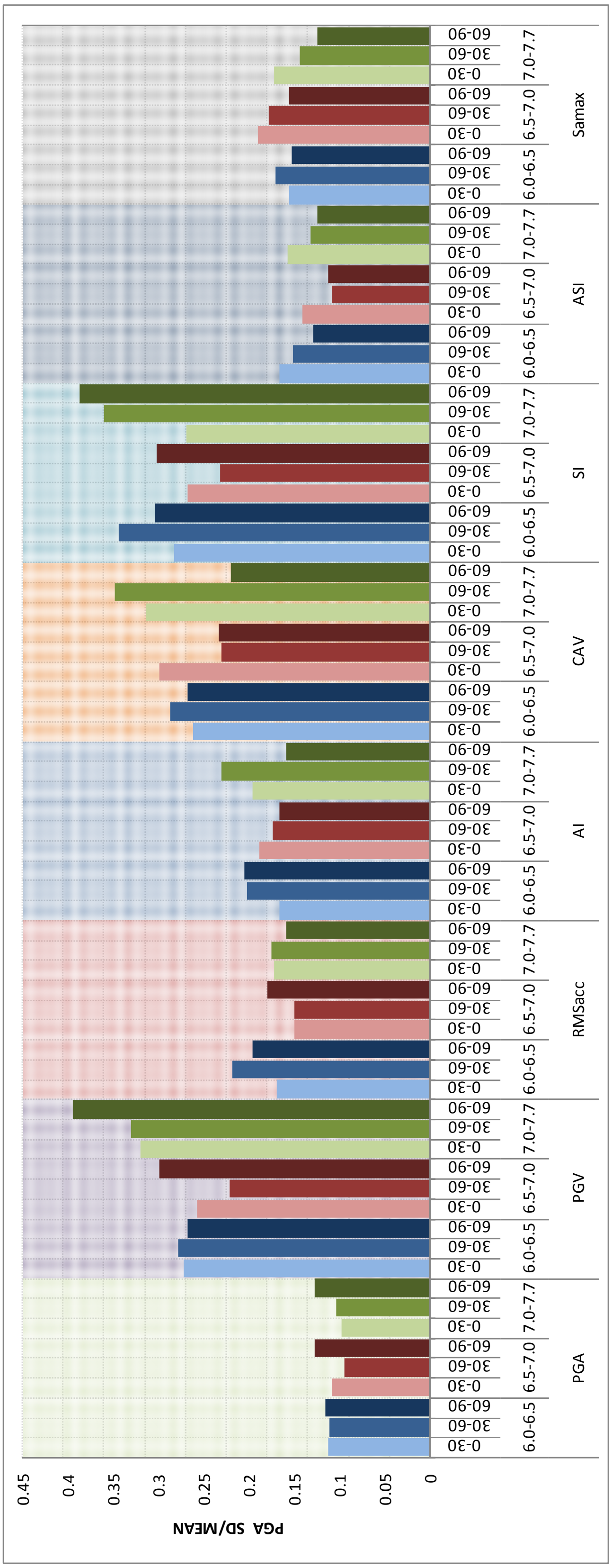

Figure 3.20. Soil profile 3 – all the results of the parametric study based on the variation of PGA SD/Mean

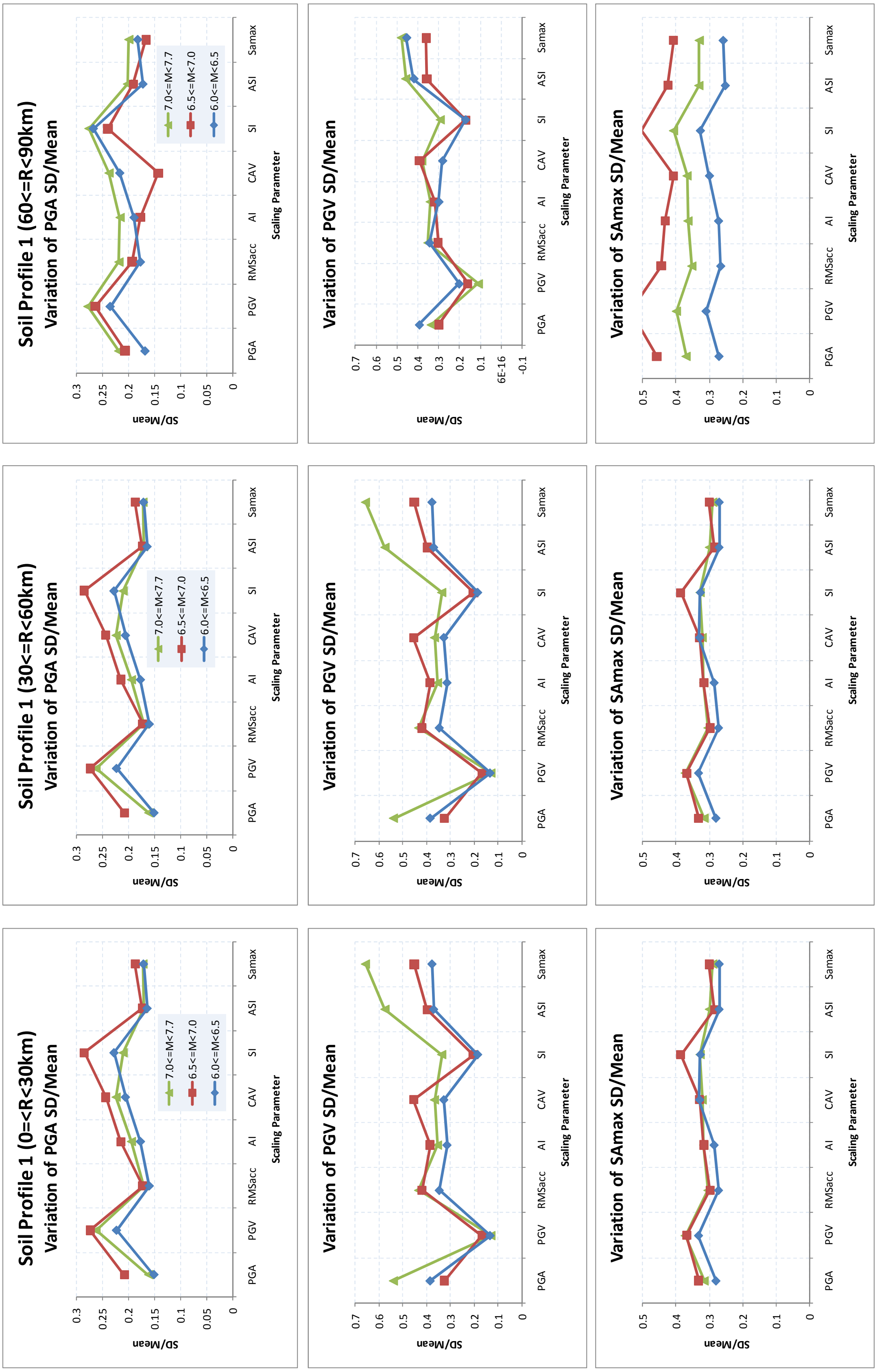

Figure 3.21. Soil profile 1 – variation of SD/Mean for three damage parameters (PGA, PGV and SA $_{max}$) with magnitude with respect to scaling parameters

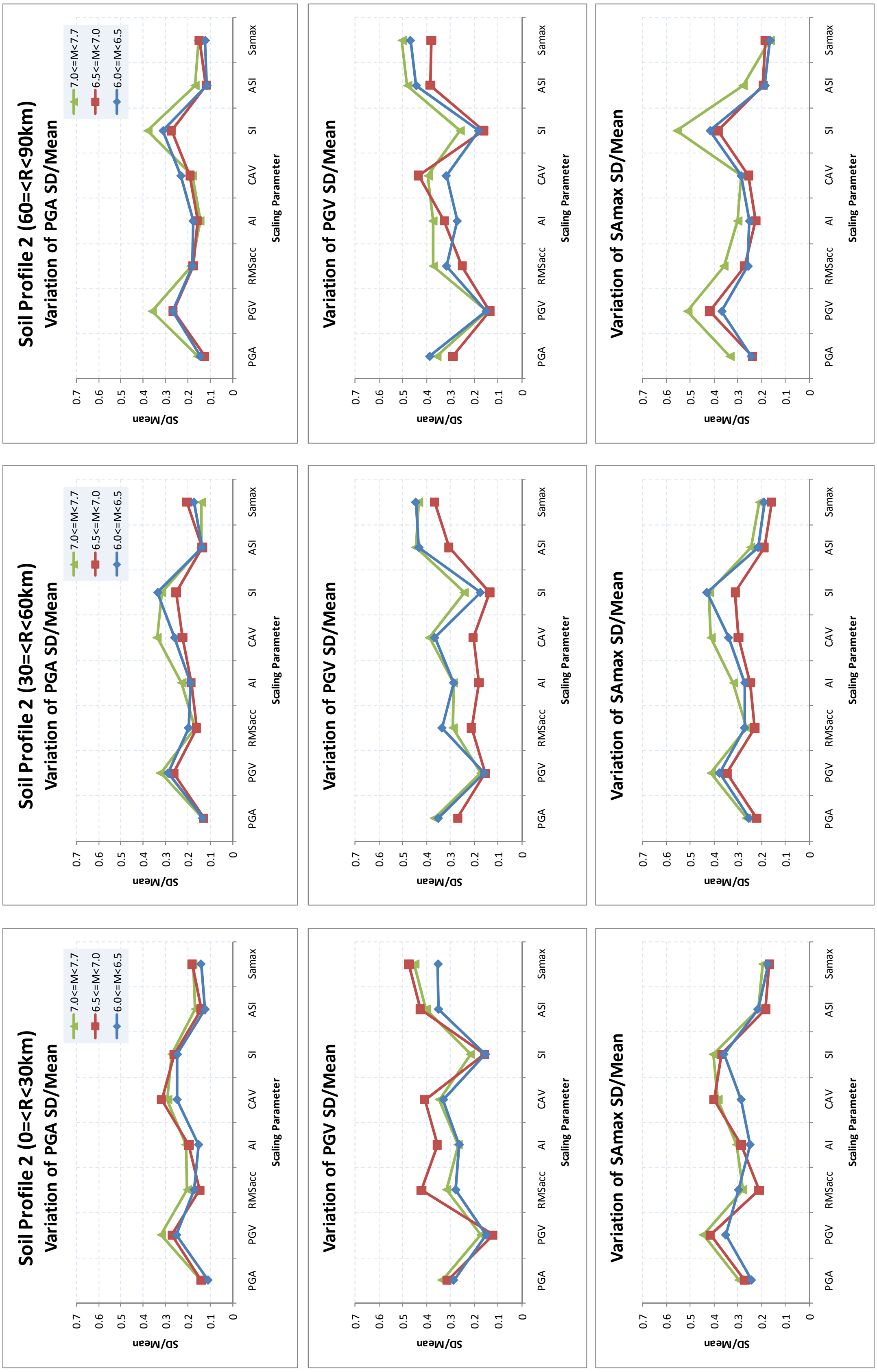

Figure 3.22. Soil profile 2 – variation of SD/Mean for three damage parameters (PGA, PGV and SA $_{max}$) with magnitude with respect to scaling parameters

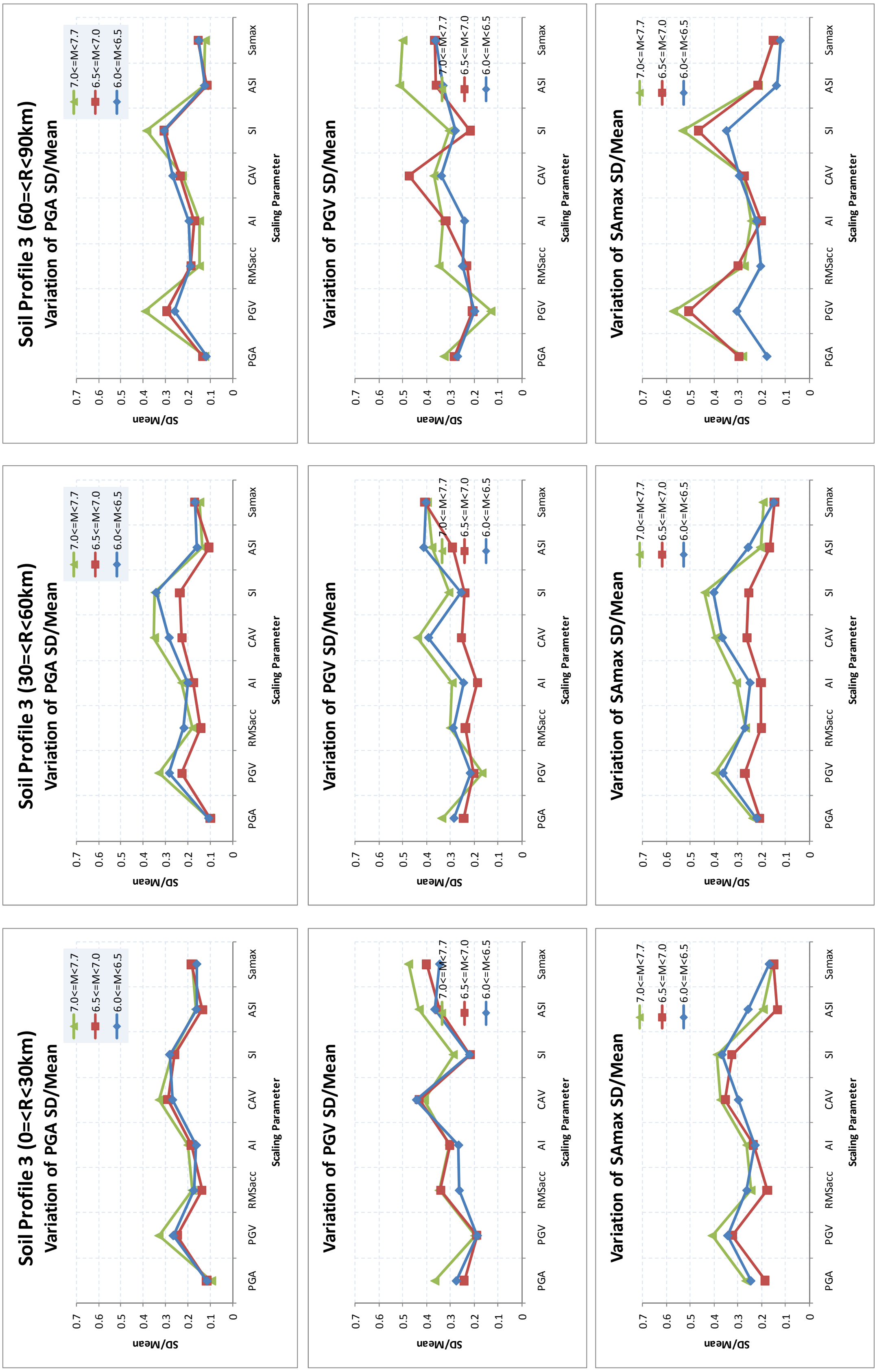

Figure 3.23. Soil profile 3 – variation of SD/Mean for three damage parameters (PGA, PGV and SA $_{max}$) with magnitude with respect to scaling parameters

3.5. Summary and Results

Although selected in accordance with the site-specific hazard parameters the ground motions may have different characteristics in time and frequency domain and thus play an important role in model behavior by introducing a significant scatter in non-linear dynamic response. Scaling the records for time-domain analysis to values chosen consistent with site-specific hazard parameters is a way to handle this situation. Scaling the input motion according to the most appropriate parameters so that the scatter of the model response is reduced is also important when design is required for different performance levels such as limit, serviceability *etc.* and also for displacement and acceleration sensitive structures and components (Heuze *et al.,* 2004).

Site response analyses should be performed using a bin of input motions. The number of time histories in the bin should be large enough to provide a stable estimate of the median and to provide a smaller variation.

Using scaling parameters determined from proposed empirical attenuation relationships, it is investigated to understand how ground motion selection and scaling affects the site response.

Presented results for two case studies are for the 10-40km distance and 6.5-7.5 magnitude range. The analyses were carried out using Shake91 computer code thus the obtained results directly depend on the formulation adopted in this code.

In the first case study conducted it was observed that scaling with respect to Arias intensity especially in the case of spectral accelerations at 0.2s, yielded the most suitable scaling option among the three scaling procedures studied for conducting site response analyses if the damage parameter is selected as spectral accelerations. However, in the cases where damage parameter can be taken as peak ground accelerations (*i.e.,* liquefaction susceptibility or landslide hazard) than scaling with respect to peak acceleration should be preferred as suggested in EC8 (CEN, 2006).

In the second case study, it appears that distance to the fault is one of the earthquake hazard parameters that may affect the outcome both with respect to peak ground or spectral accelerations, thus in selecting real time histories, the records need to be selected compatible with the regional hazard in terms of fault type, magnitude and fault distance.

The general parametric study on scaling with eight different scaling parameters on three damage parameters (PGA, PGV, SA_{max}) based on nine bins of magnitude and distance pairs for three soil profiles reveal that: (1) when there are enough large number of input motions, the variation of average damage parameter is not sensitive to selected magnitude – distance bin, (2) the soil profile depth is a dominating factor on the results, as the profile gets deeper the selection of scaling parameter is not important, (3) the selection of scaling parameter is closely related with the damage parameter, the variance in the PGA and SA_{max} is smaller when the input motions are scaled with respect to acceleration based parameters like PGA, Arias intensity, acceleration spectrum intensity, and the variance in the PGV is smaller when the input motions are scaled with respect to velocity based parameters like PGV, cumulative absolute velocity, (4) SD/mean is a preferable comparison parameter, for which the minimum value may indicate the best scaling parameter.

4. SITE RESPONSE ANALYSIS: EQUIVALENT LINEAR APPROACH

4.1. Introduction

Site response analysis refers to the modification of vertically propagating body waves as they pass through shallow sediments. The analysis consists of numerical modeling of one-dimensional shear wave propagation through horizontal sediment layers. The analysis requires knowledge of ground motions at the base of the sediments. There are two crucial elements for ground response modeling: (1) the dynamic behavior of soil subject to cyclic excitation in shear, and (2) computational models for the nonlinear response of sediment layers to vertical wave propagation.

Site response analysis models solve wave propagation problem for a layered, nonlinear medium. The principal characteristic distinguishing various analysis routines is the manner in which nonlinear soil properties are modeled in the analysis. In other words, the methods differ in the simplifying assumptions that are made, in the representation of stress–strain relations of soil and in the methods used to integrate the equation of motion. There are two general categories of models for representing nonlinear soil behavior in site response analyses: equivalent-linear and fully-nonlinear models.

For site response analysis, the nonlinear soil properties need to be characterized. Seed and Idriss (1970) and Hardin and Drnevich (1972) expressed nonlinear characteristics of soil subjected to cyclic load as shear modulus and damping ratio as a function with respect to shear strain. Figure 4.1 schematically shows dynamic deformation characteristics test to compute them by triaxial and torsional shear test apparatus (Yoshida and Iai, 1998). Shear modulus, G is the slope of the relationship between shear stress and shearing strain representing the shear stiffness of the soil. Material damping ratio, ξ (h in Figure 4.1), is a measure of the proportion of dissipated energy to the maximum retained strain energy during each cycle at a given strain amplitude.

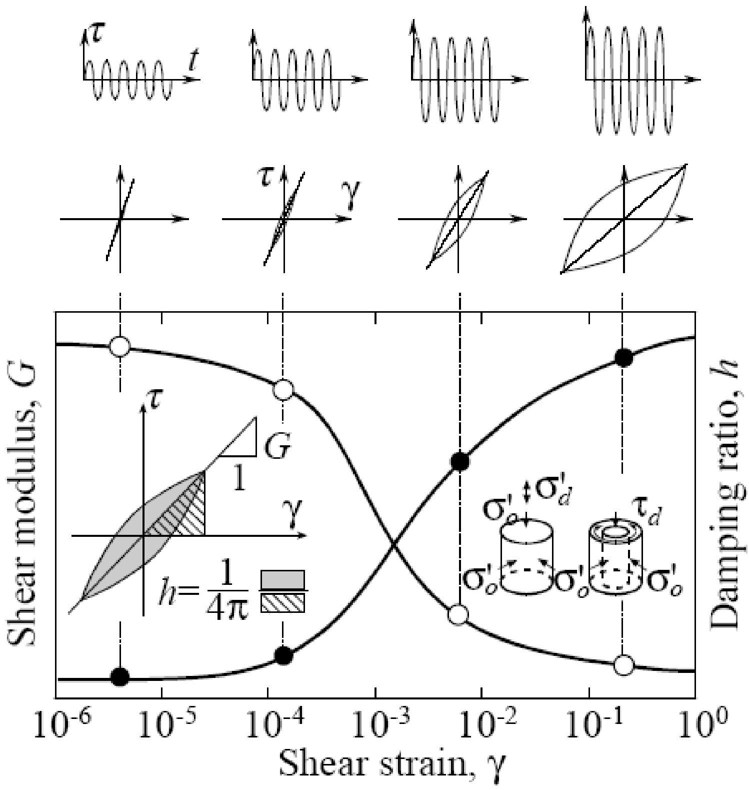

Figure 4.1. Schematic figure showing the data processing in dynamic deformation characteristics test (Yoshida and Iai, 1998).

The nonlinear behavior of soil can be modeled by an equivalent-linear characterization of dynamic soil properties (Seed and Idriss, 1970). The equivalent-linear method models the nonlinear variation of soil shear moduli and damping ratio as a function of shear strain. The hysteretic stress-strain behavior of soils under symmetrical loading is represented by an equivalent modulus, G, and an equivalent damping ratio, ξ, as shown in Figure 4.1. An iterative procedure, based on linear dynamic analysis, is performed to find the G and ξ corresponding to the computed shear strains. Initial estimates of the shear strains and corresponding estimates of G and ξ are provided for the first iteration. For the second and subsequent iterations, G and ξ values are determined corresponding to an "effective" strain, γ_{eff} that is computed as a fraction (α) of the maximum shear strain from the previous iteration:

$$\gamma_{eff} = \alpha \gamma_{\max} \tag{4.1}$$

Idriss and Sun (1992) recommended that α can be taken as a function of earthquake magnitude (M) as follows:

$$\alpha = \frac{M-1}{10} \tag{4.2}$$

The nonlinearity can be controlled by the coefficient α, but the value of 0.65 is frequently used as if it were a constant. Iterations are repeated until estimated and computed values of G and ξ match within a specified level of tolerance.

The most widely used computer program currently utilizing equivalent linear model is Shake91 (Idriss and Sun, 1992), which is a modified version of the program SHAKE (Schnabel *et al.*, 1972). The program uses an equivalent-linear, total stress analysis procedure to compute the response of a one-dimensional, horizontally layered viscoelastic system subjected to vertically propagating shear waves.

4.2. Advantages and Limitations of Equivalent Linear Method

The advantages of the equivalent-linear approach are that parameterization of complex nonlinear soil models is avoided and the mathematical simplicity of a linear analysis is preserved. A truly nonlinear approach requires the specification of the shapes of hysteresis curves and their cyclic dependencies through an increased number of material parameters. In the equivalent-linear methodology the soil data are utilized directly and, because the problem is linear at each iteration and the material properties are frequency independent, the damping is rate independent and hysteresis loops close.

There are a few limitations of using the equivalent linear model. Because the model is linear, it cannot be used to calculate permanent displacements since the shear strain returns to zero after loading is complete. The inherent linearity of the soil can also lead to spurious resonances that would not occur in the field. Moreover, the equivalent linear model is not capable of modeling pore pressures because a total stress approach is used in the analysis. Proper selection of an effective shear strain is required to prevent over- or under-softening of the response (Kramer and Paulsen, 2004).

4.3. Equivalent Linear Site Response Analysis Codes

4.3.1. Shake91

Program SHAKE computes the response in a system of homogeneous, visco-elastic layers of infinite horizontal extent subjected to vertically travelling shear waves (Figure 4.2).

The program is based on the exact continuum solution to the wave equation (Kanai, 1951) adapted for use with transient motions through the Fast Fourier Transform algorithm (Cooley and Tukey, 1965). The nonlinearity of the shear modulus and damping is accounted for by the use of equivalent linear soil properties (Idriss and Seed, 1968; Seed and Idriss, 1970) using an iterative procedure to obtain values for modulus and damping compatible with the effective strains in each layer. The program is able to handle systems with variation in both moduli and damping and takes into account the effect of the elastic base. The object motion can be given in any one layer in the system and new motions can be computed in any other layer (Figure 4.3).

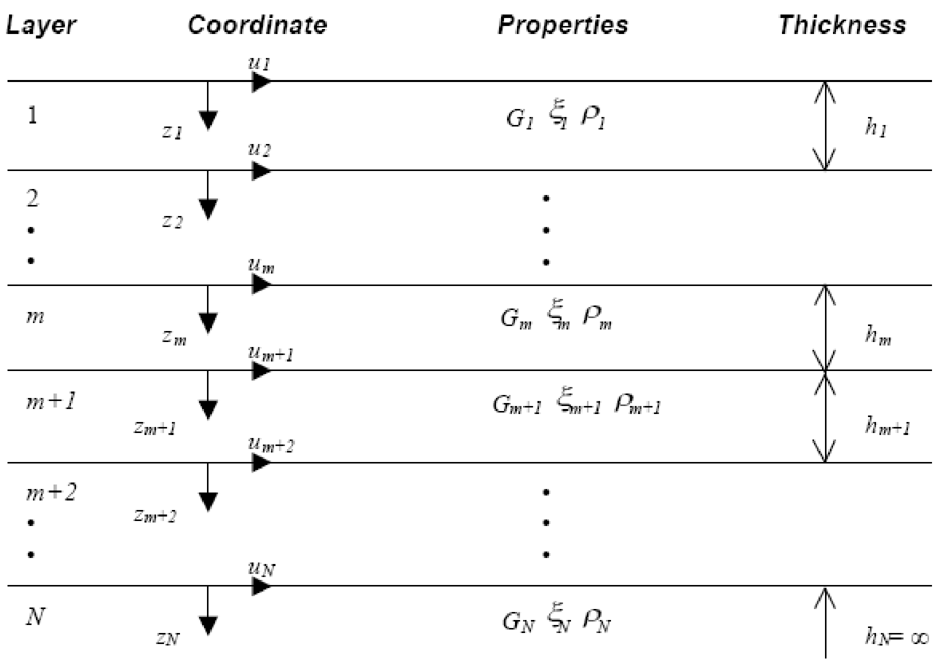

Figure 4.2. One-dimensional layered soil deposit system (after Schnabel *et al.*, 1972)

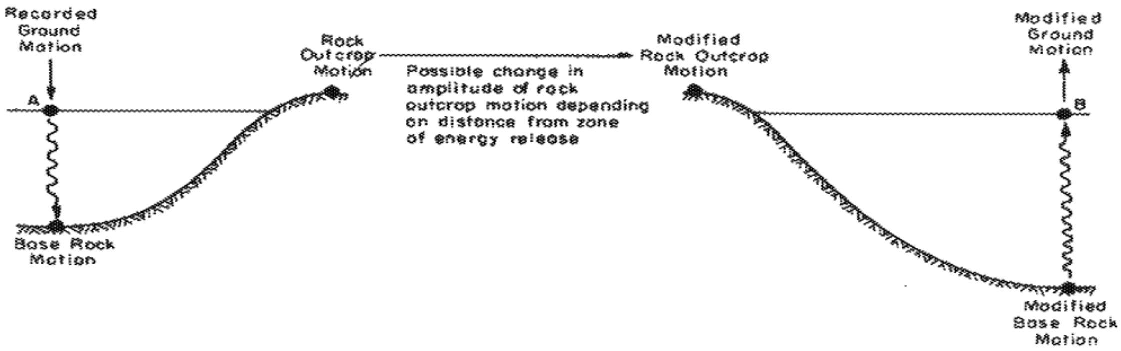

Figure 4.3. Schematic representation of the procedure for computing effects of local soil conditions on ground motions (after Schnabel *et al.*, 1972)

The following set of operations can be performed by the program:

- Read the input motion, find the maximum acceleration, scale the values up or down, and compute the predominant period.
- Read data for the soil deposit and compute the fundamental period of the deposit.
- Compute the maximum stresses and strains in the middle of each sublayer and obtain new values for modulus and damping compatible with a specified percentage of the maximum strain.
- Compute new motions at the top of any sublayer inside the system or outcropping from the system.
- Compute Fourier Spectra for the motions.
- Compute response spectra for motions.
- Compute amplification function between two sublayers.
- Compute stress or strain – time history in the middle of any sublayer.

SHAKE is a FORTRAN computer program which is based upon a batch-file format, *i.e.,* a sequential series of options saved in an ASCII input file control the operation of the program. The options incorporated into Shake91 are as given in Table 4.1.

Table 4.1. The options incorporated into Shake91

<table>
<tr><th colspan="2">Option</th><th>Description</th></tr>
<tr><td rowspan="5">INPUT</td><td>1</td><td>Dynamic soil properties</td></tr>
<tr><td>2</td><td>Data for soil profile</td></tr>
<tr><td>3</td><td>Input (object) motion</td></tr>
<tr><td>4</td><td>Assignment of object motion to the top of the specified sublayer or to the corresponding outcrop</td></tr>
<tr><td>5</td><td>Number of iterations specified and ratio of uniform strain to maximum strain</td></tr>
<tr><td rowspan="6">OUTPUT</td><td>6</td><td>Sublayers at top of which peak accelerations and time histories are computed and saved</td></tr>
<tr><td>7</td><td>Sublayers at top of which time history of shear stress or strain is computed and saved</td></tr>
<tr><td>8</td><td>Time history of object motion</td></tr>
<tr><td>9</td><td>Response spectrum</td></tr>
<tr><td>10</td><td>Amplification spectrum</td></tr>
<tr><td>11</td><td>Fourier amplitudes</td></tr>
</table>

In SHAKE, the values of shear modulus and damping ratio are determined by iterations so that they become consistent with the level of strain induced in each layer. As shown in Figure 4.4, the values of G_0 and ξ_0 are initialized at their small strain values, and the maximum shear strain $\gamma_{\max}$ and effective shear strain γ_{eff1} are calculated. Then the compatible values G_1 and ξ_1 corresponding to γ_{eff1} are found for the next iteration. The equivalent linear analysis is repeated with new values of G and ξ until the values of G and ξ are compatible with the strain induced in all layers.

The iteration procedure for equivalent linear approach in each layer is as follows:

1. Initialize the values of G^i and ξ^i at their small strain values.

2. Compute the ground response, and get the amplitudes of maximum shear strain $\gamma_{\max}$ from the time histories of shear strain in each layer.

3. Determine the effective shear strain γ_{eff} from $\gamma_{\max}$:

$$\gamma_{eff}^{i} = R_{\gamma}\gamma_{\max}^{i} \tag{4.3}$$

where R_{γ} is the ratio of the effective shear strain to maximum shear strain, which depends on the earthquake magnitude. R_{γ} is specified in input; it accounts for the number of cycles during earthquakes. R_{γ} is the same for all layers.

4. Calculate the new equivalent linear values G^{i+1} and ξ^{i+1} corresponding to the effective shear strain γ_{eff} .

5. Repeat steps 2 to 4 until the differences between the computed values of shear modulus and damping ratio in two successive iterations fall below some predetermined value in all layers. Generally 8 iterations are sufficient to achieve convergence.

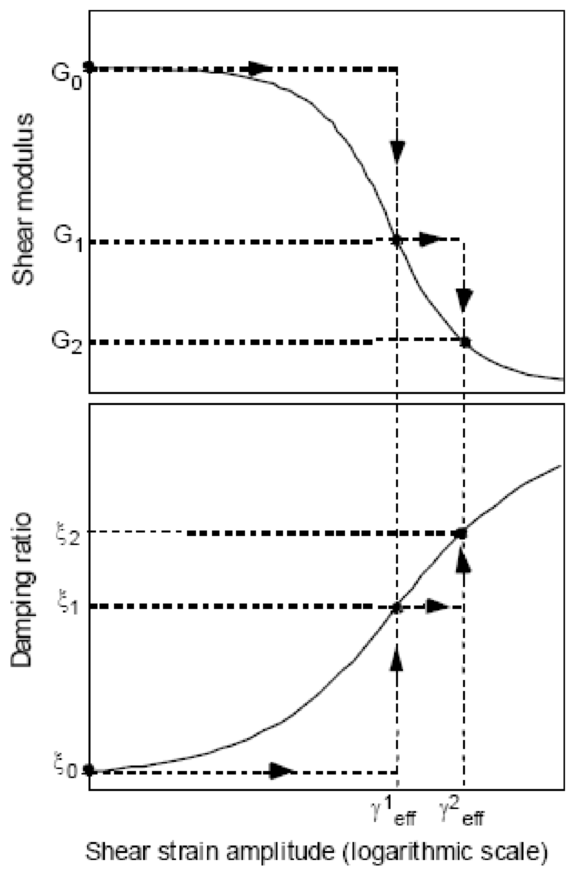

Figure 4.4. Iteration of shear modulus and damping ratio with shear strain in equivalent linear analysis

There are several advantages in SHAKE in the practical use. Source list is open, which enable to use any computer and to modify depending on users request. Data preparation is easy. It requires G- γ and ξ- γ relationships for soil data; therefore no engineering judgment is required. Moreover, the most important advantage is that it can compute incident wave at arbitrary depth from the earthquake data at the ground surface or any other depth.

4.3.2. DEEPSOIL – Equivalent Linear

DEEPSOIL (Hashash *et al.*, 2009) is a one-dimensional site response analysis program that can perform both a) 1-D nonlinear and b) 1-D equivalent linear analyses and features an intuitive graphical user interface. DEEPSOIL was developed by Youssef Hashash and Duhee Park at University of Illinois at Urbana-Champaign.

DEEPSOIL graphical user interface is composed of five stages/windows for equivalent linear and intuitively guides the user from the beginning to the end of the site response analysis.

- *Analysis type selection:* First step is selection of analysis type. The user selects either Frequency or Time domain analysis. Analysis type is further divided into Linear/Equivalent for frequency domain. User should also choose the bedrock type and how the stiffness of soil layers will be defined (either in shear wave velocity or as shear modulus).
- *Define soil profile/properties:* This stage defines the soil profile and soil properties. In addition, the units of the input data will be selected. Another input is the water table location.
- *Analysis control:* Analysis control stage allows selection of Fourier transform type, iteration number, and complex shear modulus type.
- *Motion control:* Input motion and layers for output display will be selected. For frequency domain analysis, the motion can be imposed as either rock outcrop or within soil profile. Also for frequency domain analysis, the number of calculation points should be selected for Fast Fourier Transform (power of 2). Deconvolution can also be performed.

- *Output:* Various outputs can be visually displayed / printed / exported to a text file. The outputs of DEEPSOIL are acceleration / strain / stress time histories, response spectrum, Fourier amplitude spectrum, Fourier amplification ratio spectrum. In addition, PGA profile can be displayed. Convergence check windows allow checking whether the equivalent linear analysis has reached converged (or whether the selected iteration number is sufficient).

DEEPSOIL equivalent linear model employs an iterative procedure in the selection of the shear modulus and damping ratio soil properties as in the case of SHAKE. These properties can be defined by discrete points for which the G/Gmax and damping ratio (%) are defined as functions of strain (%) or by defining the soil parameters to be used in the hyperbolic model.

The main features of DEEPSOIL when compared with SHAKE are unlimited number of layers, material properties and number of acceleration data points of input motion. Additionally, DEEPSOIL allows a choice among three types of complex shear modulus formula which are:

- Frequency Independent Complex Shear Modulus (Kramer, 1996)
  The frequency independent shear modulus results in frequency independent damping and is recommended to be used in the analysis.

$$G^* = G(1 + i2\xi) \tag{4.4}$$

- Frequency Dependent Complex Shear Modulus (Udaka, 1975)
  The frequency dependent shear modulus results in frequency dependent damping, and should be used with caution. This is the same modulus used in Shake91.

$$G^* = G\left(1 - 2\xi^2 + i2\sqrt{1-\xi^2}\right) \tag{4.5}$$

- Simplified Complex Shear Modulus (Kramer, 1996)
  This is a simplified form of frequency independent shear modulus defined as:

$$G^* = G\left(1 - \xi^2 + i2\xi\right) \tag{4.6}$$

The program has the same advantage as SHAKE that in a Batch Mode analysis, the user can select many input motions to perform the response analysis of each soil profile.

4.3.3. EERA

In 1998, the computer program EERA was developed in FORTRAN 90 starting from the same basic concepts as SHAKE (Bardet *et al.*, 1998). EERA stands for Equivalent-linear Earthquake Response Analysis. EERA is a modern implementation of the well-known concepts of equivalent linear earthquake site response analysis.

There are four basic commands in the EERA pull-down menu:

1. *Process Earthquake Data* - Read and process earthquake input motion (input/output in worksheet *Earthquake*)
2. *Calculate Compatible Strain* (EERA) - Read profile, material curves, and execute the main iterative calculation (input/output in worksheet *Iteration*)
3. *Calculate Output*
   - *Acceleration/Velocity/Displacement* - Calculate time history of acceleration, relative velocity and displacement at the top of selected sub-layers (input/output in worksheet *Acceleration*)
   - *Stress/Strain* - Calculate stress and strain at the middle of selected sublayers (input/output in worksheets *Strain*)
   - *Amplification* - Calculate amplification factors between two sub-layers (input/output in worksheets *Ampli*)
   - *Fourier Spectrum* - Calculate Fourier amplitude spectrum of acceleration at the top of selected sub-layer. (input/output in worksheet *Fourier*)
   - *Response Spectrum* - Calculate all response spectra at the top of selected sub-layers (input/output in worksheet *Spectra*)
   - *All of the above* - Calculate all the output

4. *Duplicate Worksheet* - Duplicate selected worksheet for defining new material curves, and adding new output (*e.g.*, response spectra for several sub-layers)

An EERA workbook is made of nine types of worksheets, which have predefined names that should not be changed. As indicated in Table 4.2, six of nine types of worksheet can be duplicated and modified using *Duplicate Worksheet* in the EERA pull-down menu. This feature is useful for obtaining output at several sub-layers and defining additional material curves. Table 4.2 also indicates the number of input required in each worksheet.

Table 4.2. Types of worksheets in EERA and their contents

Worksheet	Contents	Duplication	Number of input
Earthquake	Earthquake input time history	No	7
Mat I	Material curves (G/G_{max} and Damping versus strain for material type i)	Yes	Dependent on number of soil layers
Profile	Vertical profile of layers	No	Dependent on number of data points per material curve
Iteration	Results of main calculation	No	3
Acceleration	Time history of acceleration / velocity / displacement	Yes	2
Strain	Time history of stress and strain	Yes	1
Ampli	Amplification between two sub-layers	Yes	4
Fourier	Fourier amplitude spectrum of acceleration	Yes	3
Spectra	Response spectra	Yes	3

In general, an EERA site response analysis is performed in three successive steps.

Step 1

- Define all earthquake data in worksheet *Earthquake*
- Use *Process Earthquake Data*

Step 2

- Define the soil profile in worksheet *Profile*
- Define all the material stress-strain response curves in worksheets *Mat...*
- Define the main calculation parameters in worksheet *Iteration*
- Use *Calculate Compatible Strain*

Step 3

- Define the input parameters in worksheets *Acceleration*
- Use *Calculate Output* and *Acceleration/...*
- Define the input parameters in worksheets *Strain*
- Use *Calculate Output* and *Stress-Strain*
- Repeat the same process for *Ampli*, *Fourier*, and *Spectra*

4.3.4. Comparison of Equivalent Linear Site Response Codes

Two equivalent linear site response analysis programs, SHAKE and DEEPSOIL were compared to search the impact of different schemes on the predicted ground motion parameters. Both programs have the same advantage of allowing selection of many input motions simultaneously to perform the response analysis of each soil profile.

Both programs were run using the M=6.0 – 6.5 and R=0 – 30 km (2A) bin of general scaling case. Although, unlimited number of layers, material properties and acceleration data points can be used as input in DEEPSOIL, in order to provide the harmonization, number of layers, material properties and number of acceleration data points were limited (51 number of layers with sublayers, 13 material properties, 4096 number of input motion data points) and exactly same values were input to DEEPSOIL. Unlike SHAKE, DEEPSOIL has three options for complex shear modulus formula selection. This property was also compared. The comparison is presented in Figure 4.5 through Figure 4.7 where acceleration spectrums were given for three soil profiles.

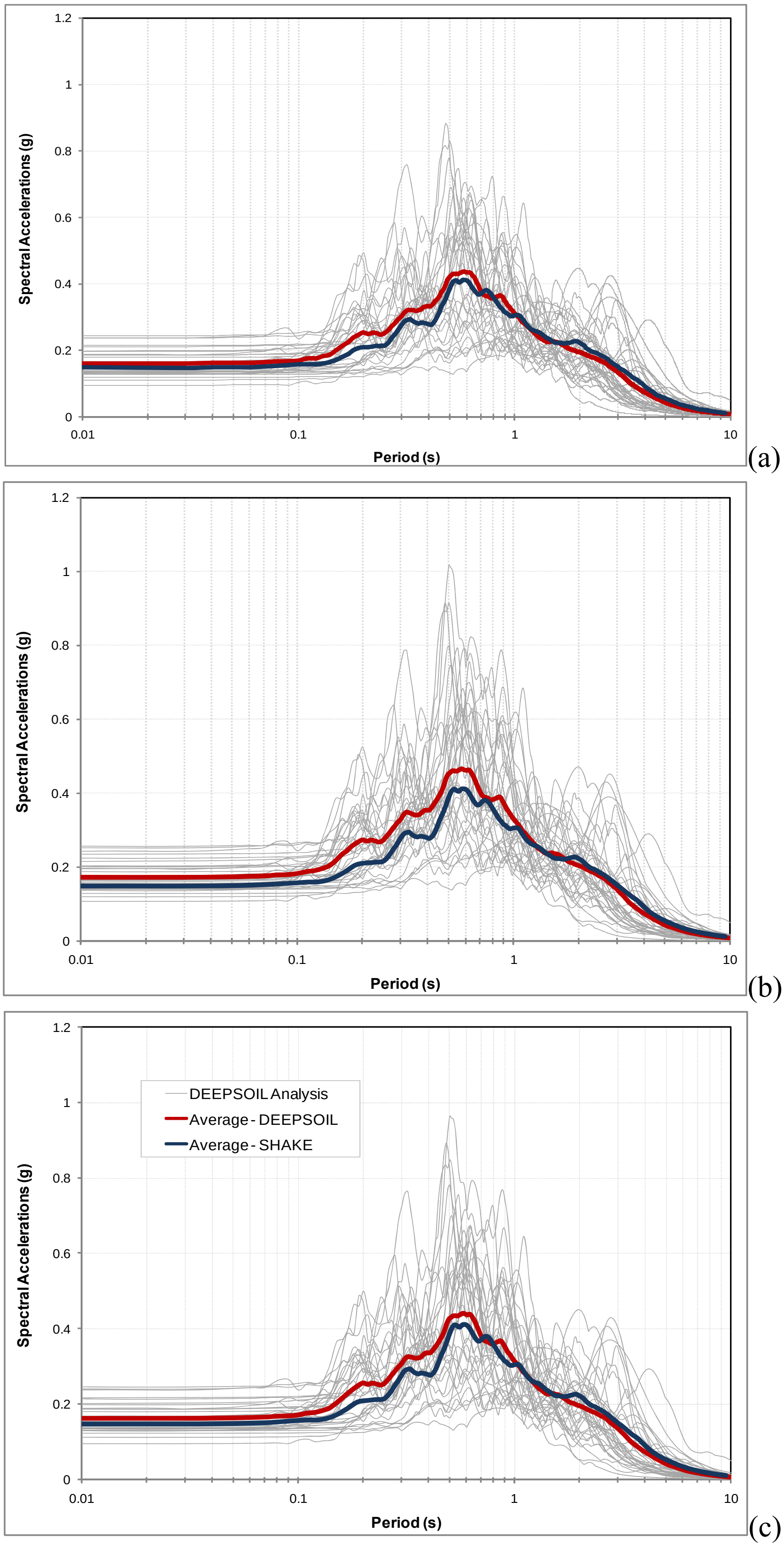

Figure 4.5. Comparison of SHAKE and DEEPSOIL equivalent linear schemes for soil profile 1 and M=6.0-6.5 and R=0-30 km bin input motions using (a) frequency independent, (b) frequency dependent (c) simplified complex shear modulus

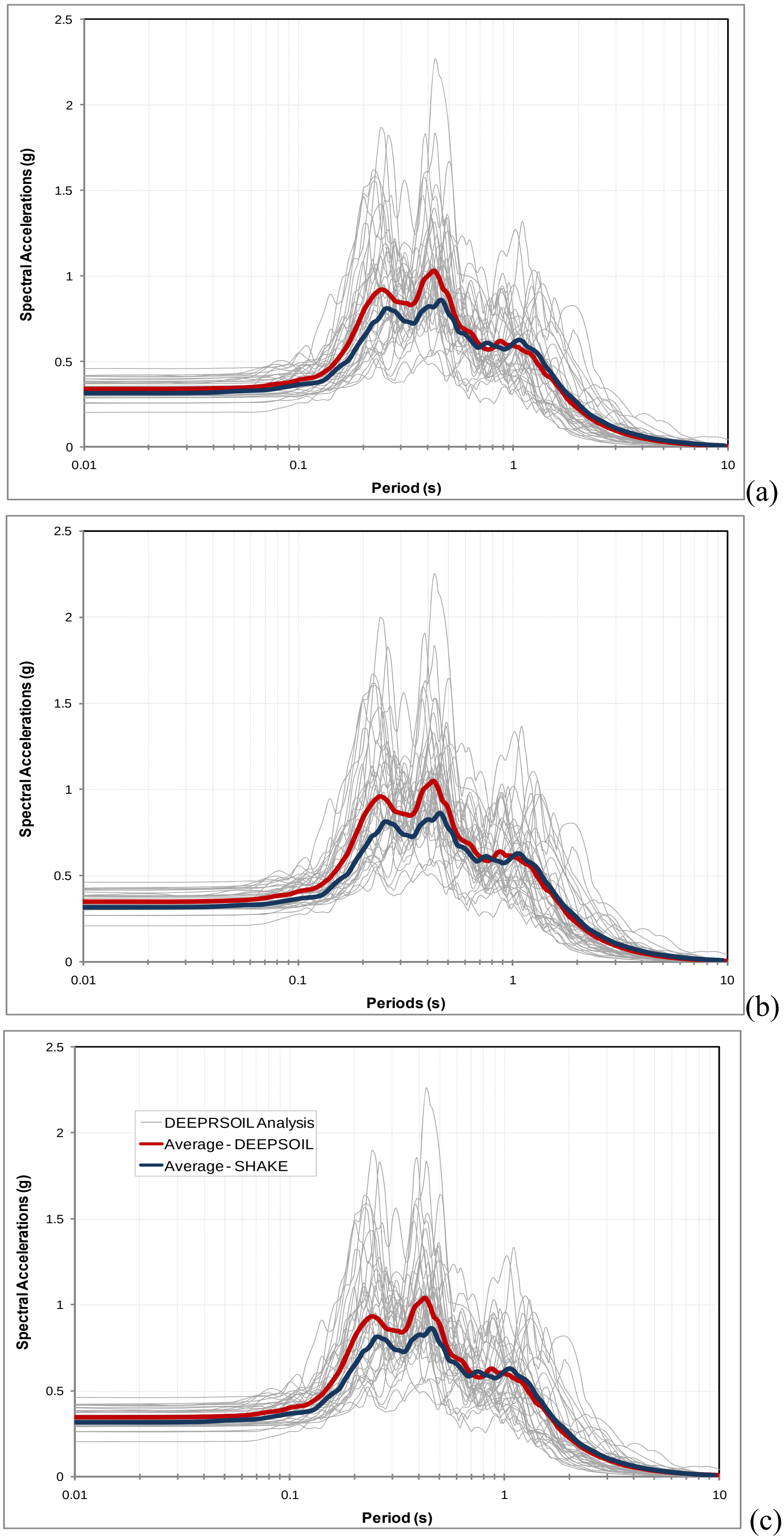

Figure 4.6. Comparison of SHAKE and DEEPSOIL equivalent linear schemes for soil profile 2 and M=6.0-6.5 and R=0-30 km bin input motions using (a) frequency independent, (b) frequency dependent (c) simplified complex shear modulus

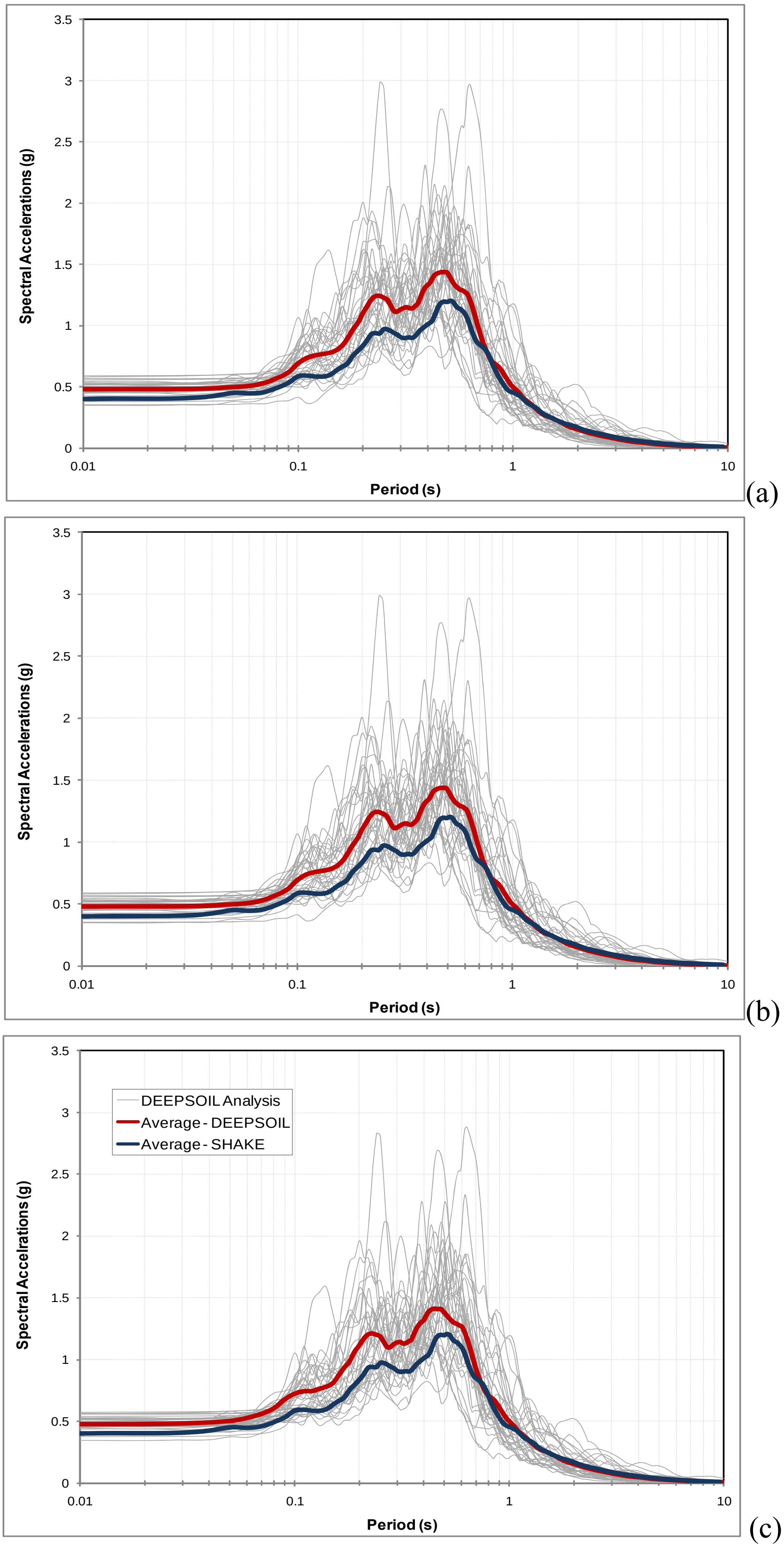

Figure 4.7. Comparison of SHAKE and DEEPSOIL equivalent linear schemes for soil profile 3 and M=6.0-6.5 and R=0-30 km bin input motions using (a) frequency independent, (b) frequency dependent (c) simplified complex shear modulus

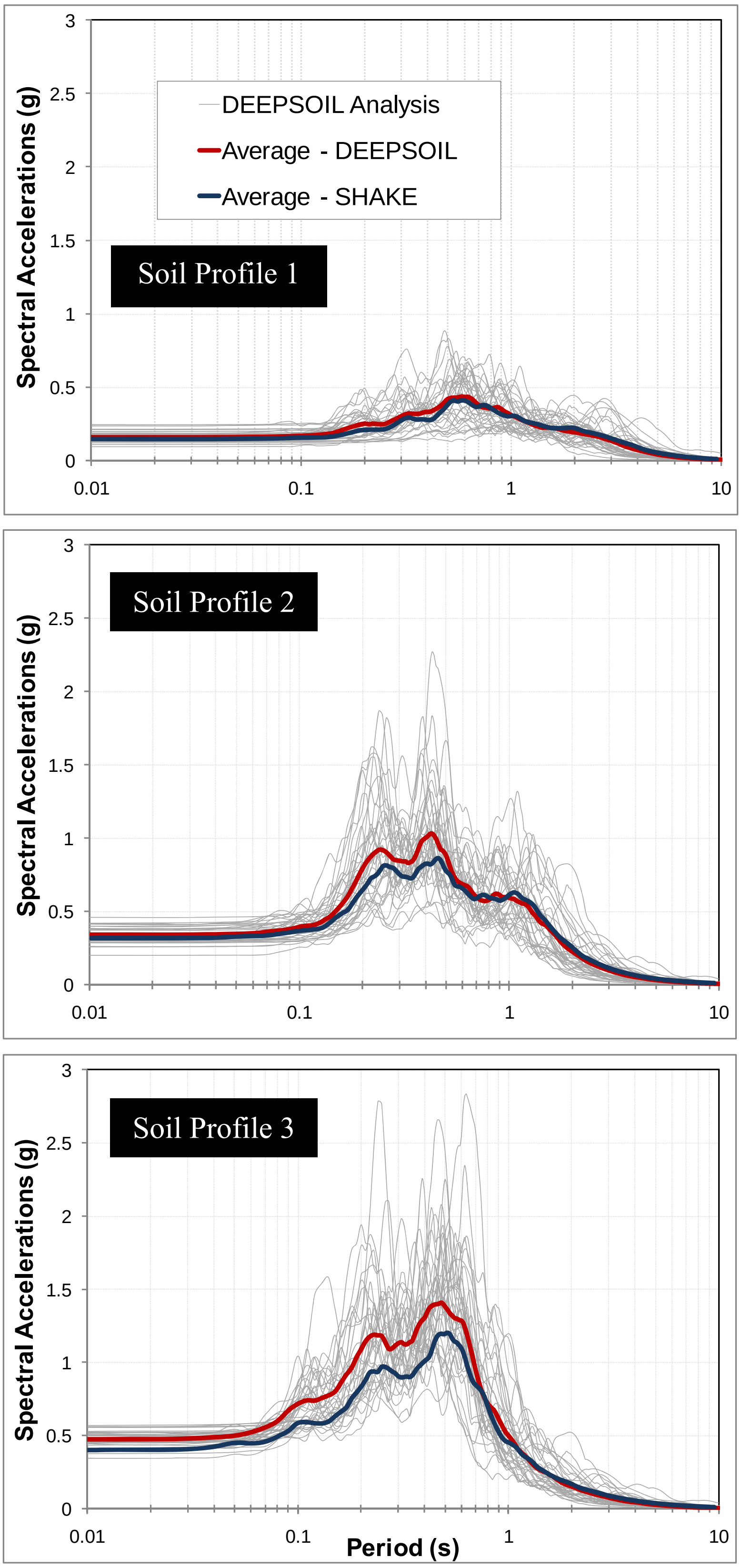

Figure 4.8. Comparison of SHAKE and DEEPSOIL equivalent linear schemes for three soil profiles and M=6.0-6.5 and R=0-30 km bin input motions using frequency independent simplified complex shear modulus

As it is seen in the figures, average of DEEPSOIL analysis gives slightly higher values as compared with the average spectrum obtained from SHAKE analysis for all of three soil profiles and three complex shear modulus options of DEEPSOIL. Although, both programs use frequency dependent complex shear modulus (second option of DEEPSOIL) as the common way of treating shear modulus, the difference between two programs is smaller for the first option (frequency independent) of treating shear modulus for first soil profile, which is the deepest profile among three. The divergence is not recognizably different for three options in the other two soil profiles. The difference is observed to increase as the profile gets shallower (Figure 4.8).

4.4. Effect of Effective Confining Pressure Dependency of Nonlinear Dynamic Soil Properties on Site Response Analysis

Nonlinear dynamic soil properties are affected by a number of parameters which have varying levels of importance. These factors have been studied by researchers over the past decades. Some of the investigators proposed nonlinear generic curves for use in site response analysis (Seed *et al.*,1986; Vucetic and Dobry, 1991). Proposed curves were derived from dynamic tests at effective confining pressures around one atmosphere.

Research on determining modulus degradation and material damping curves at different effective confining pressures indicate that modulus degradation and material damping curves become increasingly linear as confining pressure increases. The normalized modulus degradation and material damping curves are observed to shift to higher strains and minimum material damping is observed to decrease with increasing confining pressure.

The effect of mean effective confining pressure on normalized modulus reduction and material damping curves is presented in Figure 4.9 based on results of cyclic triaxial tests on specimens of Toyoura Sand (Kokusho, 1980). The graph indicates that the rate of reduction in shear modulus with strain becomes greater as the confining stress decreases and it may be seen that the damping ratio tends to increase with decreasing confining stress.

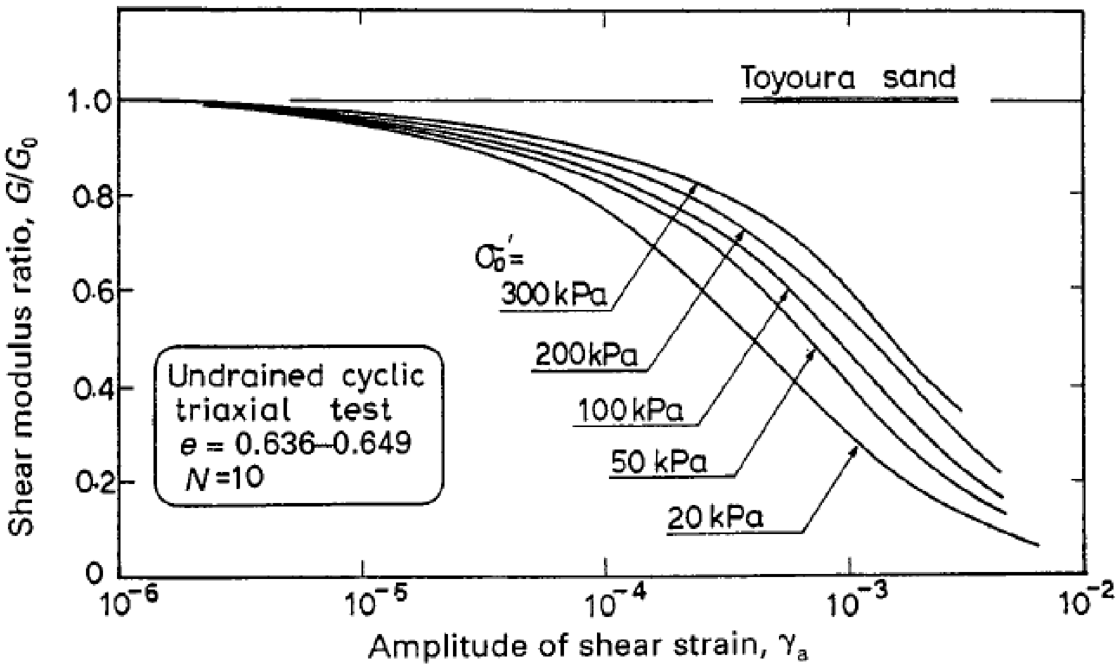

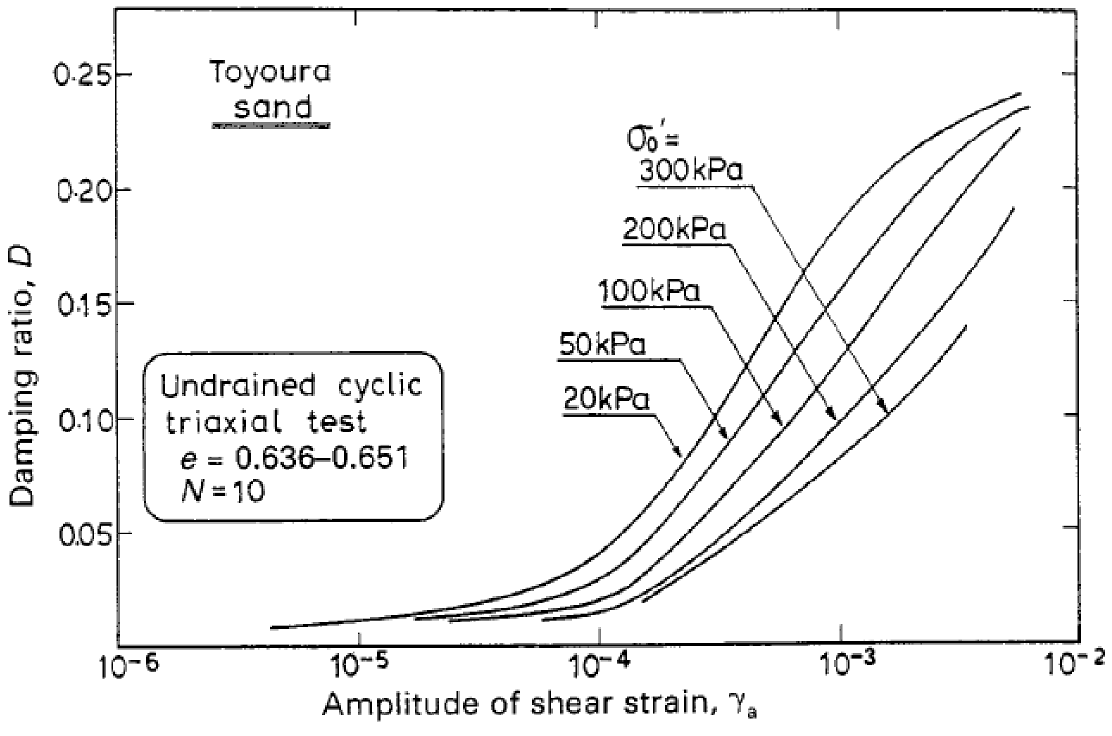

Figure 4.9. Effect of confining stress on the strain-dependent shear modulus and damping ratio (Kokusho, 1980)

4.5. Effect of Frequency Dependent Behavior on Site Response Analysis

Comparisons between the equivalent linear and nonlinear analyses were also made by several researchers. When compared with earthquake observation, the nonlinear analysis is shown to agree with the observed record better than the equivalent linear analysis. Generally, equivalent linear analysis has a tendency to give larger peak acceleration and shear stress under large earthquakes, and lower amplification in high frequency range. The reason of the latter phenomena is clear; damping ratio evaluated from the effective strain γ_{eff} is too large for small amplitude (high cycle) vibration. This effect becomes predominant under the small to medium earthquake, resulting in smaller acceleration. The use of smaller α value in Equation (4.2) can improve it.

On the other hand, there are two opinions on the reason of the former phenomena. Finn *et al.* (1978) compared dynamic response of a model ground by three computer codes SHAKE, DESRA and CHARSOIL. DESRA uses hyperbolic model, and CHARSOIL uses Ramberg-Osgood mode. Results by two nonlinear analyses are almost the same but SHAKE gives larger shear stress. He explained that large amplification comes from the resonance because equivalent linear analysis is a linear analysis.

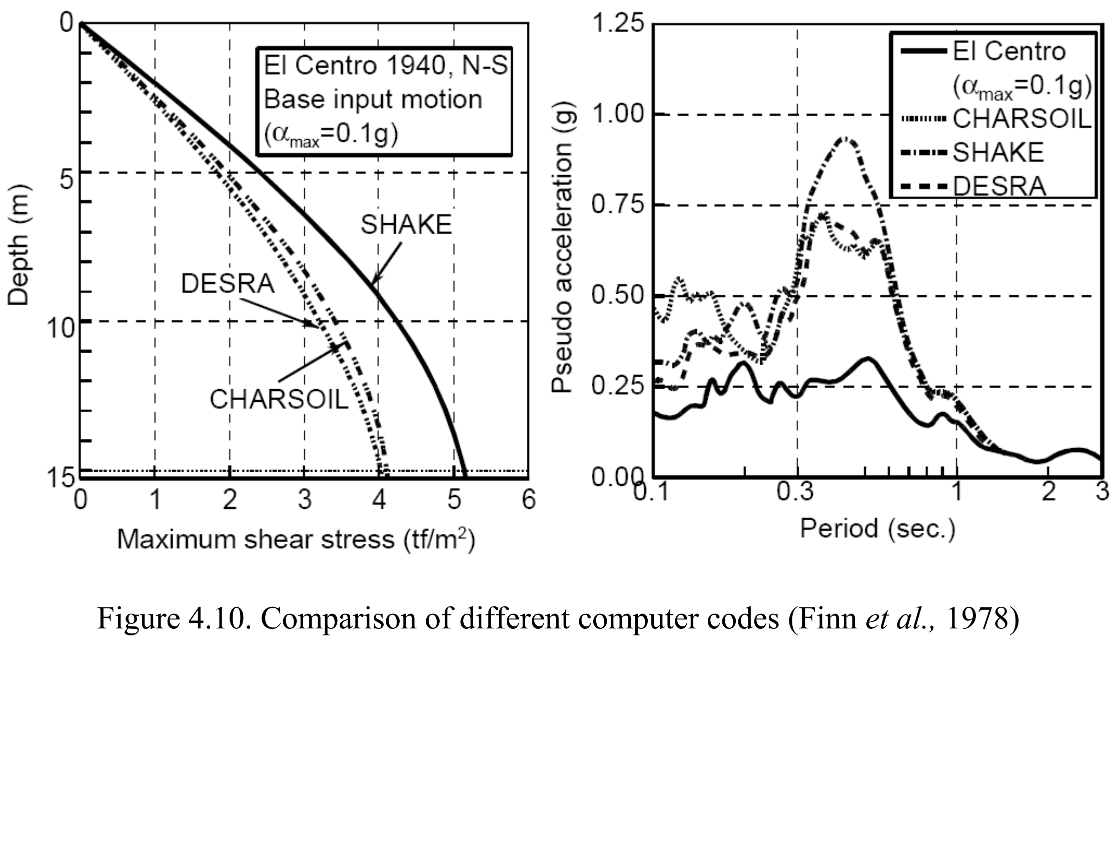

Figure 4.10. Comparison of different computer codes (Finn *et al.,* 1978)

Yoshida (1994) showed another opinion. If solid line in Figure 4.11 is a stress-strain curve specified for the analysis and γ_{max} is a maximum strain, then linear relation used in the equivalent linear analysis is a line OAC. Therefore peak shear stress is not τ_2 at point B that lies on the specified stress-strain curve, but τ_1. In the same manner, when specified stress-strain curve is a solid line Figure 4.11, then the peak stress-peak strain relationship is expressed to be a dashed line; the shear stress is always overestimated. This is the reason why equivalent linear analysis gives larger shear stress than the nonlinear analysis. If the former opinion is true, SHAKE always gives larger acceleration regardless of the magnitude of the ground motion. If the latter opinion is true, larger acceleration begin to appear as nonlinear behavior becomes predominant.

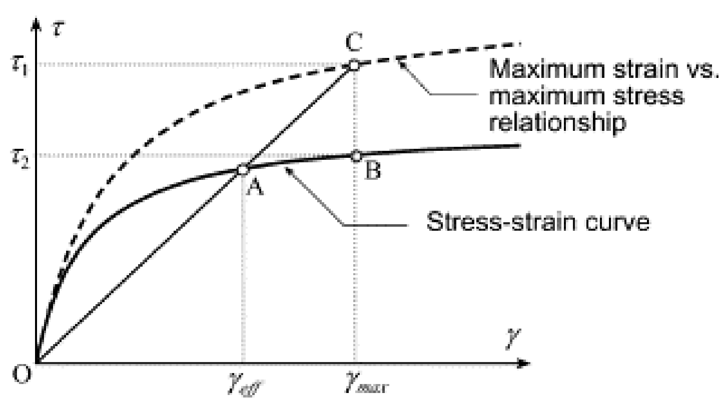

Figure 4.11. The mechanism of the overestimation of the shear stress by the equivalent linear method (Yoshida *et al.*, 2002)

4.5.1. FDEL Model

Sugito *et al.* (1994) improved lower amplification in high frequency range disadvantage of the equivalent linear analysis by taking frequency dependent characteristics into account. They put effective strain in each frequency component as

$$\gamma_{eff} = \alpha \frac{F(f)}{F_{\max}} \gamma_{\max} \tag{4.7}$$

where F(f) denotes Fourier amplitude of shear strain emphasizing it a function with respect to frequency f, and F_{max} denotes maximum value of F(f). They suggested $\alpha = 0.65$ is a relevant value, which is the same as in most SHAKE analysis. This method is called FDEL.

Although physical meaning of Equation (4.7) is not clear, this modification sometimes improves equivalent linear analysis significantly. Ueshima and Nakazono (1996) reported that the deconvolution of the vertical array record at Lotung site, Taiwan is well simulated by FDEL as shown in Figure 4.12. However, since FDEL gives larger acceleration than SHAKE, applicability to strong ground shaking becomes less accurate than SHAKE because SHAKE already overestimates maximum stress and peak acceleration in many cases. FDEL analysis sometimes does not converge when the actual Fourier amplitude of strain is used in evaluating the effective strain by means of Equation (4.7). In the actual calculation, therefore, Fourier spectrum is smoothed and the result depends on the method to smooth it.

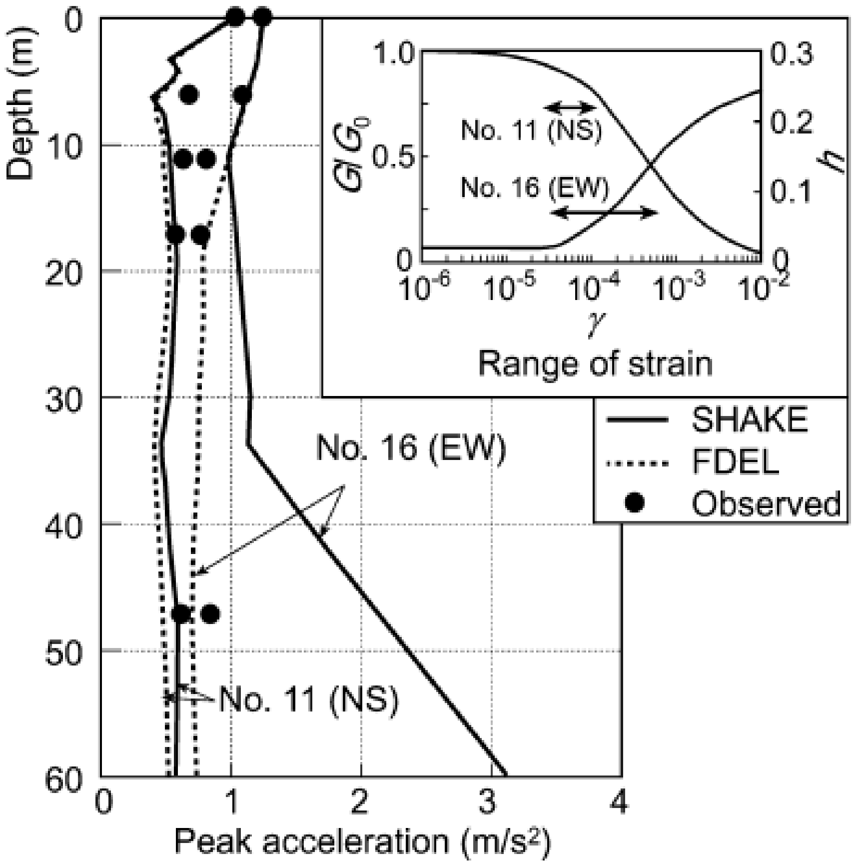

Figure 4.12. Deconvolution by SHAKE and FDEL (Ueshima and Nakazono, 1996)

4.5.2. DYNEQ Algorithm

Yoshida *et al.* (2002) proposed Equation (4.8) to evaluate an effective strain from which shear modulus and damping ratio is computed among various functions.

$$\begin{cases} \gamma_{eff} = \gamma_{\max} & f_p > f \\ \gamma_{eff} = \gamma_{\max}\left\{1-\left(\dfrac{\log f - \log f_p}{\log f_e - \log f_p}\right)^m\right\} & f_p \le f \le f_e \\ \gamma_{eff} = 0 & f > f_e \end{cases} \tag{4.8}$$

where f_p is inverse of the period T when shear strain is maximum by the zero crossing method, f_e is the frequency above which nonlinear behavior need not to be considered, and m is a parameter. Effective strain is expressed by *m*th order polynomial equation of $\log f$ between f_p and f_e, and is constant outside this frequency range. Two parameters f_e and m are adjusting parameters to obtain good prediction, and it is proposed to use $m = 2$ and $f_e = 15$ Hz based on the researchers' experience (Yoshida *et al.*, 2002). A computer code, DYNEQ was developed based on the proposed method by Yoshida and Suetomi (1996).

Applicability of DYNEQ equivalent linear method was examined from the simulation of vertical array record at the Shin-Fuji transformer station during the Kanagawaken-Yamanashiken -Kenkyo Earthquake of 1983 by Yoshida and Suetomi (1996). Although the magnitude of the earthquake is not large to be 6.0, record with large acceleration was obtained because epicentral distance is only about 18km. Soil profile at this site is shown in Figure 4.13(a). Earthquake records are obtained at the ground surface and GL-28m. The peak acceleration, maximum stress and maximum strain are compared in Figure 4.13(b) for the convolution analysis in which the record at GL-28m is used as input.

FDEL overestimates acceleration at the ground surface very much and DYNEQ shows the closest to the observed record. Figure 4.14 shows acceleration time histories, and Figure 4.15 shows stress-strain relationships at the third layer (GL-5m~GL-7m) where maximum strain is the largest. Overestimation of the peak acceleration occurs in SHAKE and FDEL at the predominant maximal points, and this overestimation is clear to come from the overestimation of the shear stress. All three methods show similar waveforms except maximal point. It is noted that the acceleration before the main shaking (before three seconds) is well simulated by FDEL and DYNEQ whereas SHAKE underestimate it. This is a typical effect of the small amplification in high frequency region by SHAKE because waves with small amplitude are predominant before the main shaking.

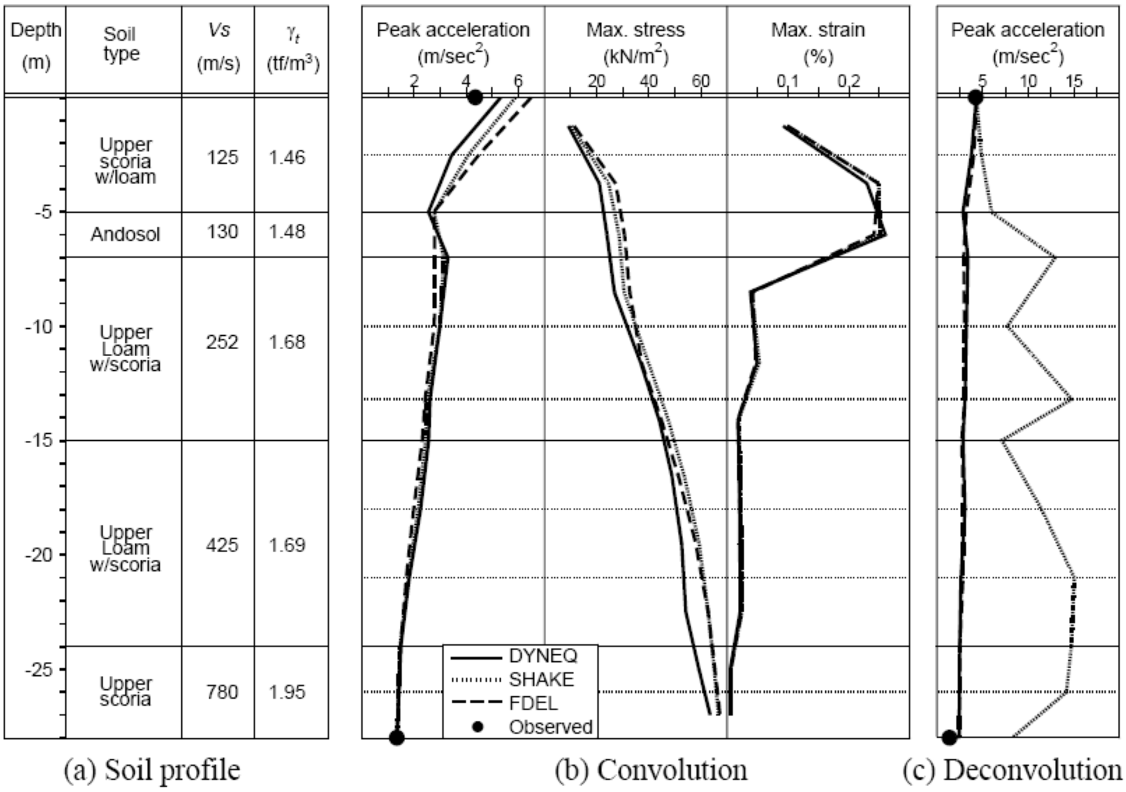

Figure 4.13. Soil profile at the Shin-Fuji transformer vertical array station during the Kanagawaken-Yamanashiken - Kenkyo Earthquake of 1983 (Yoshida and Suetomi, 1996)

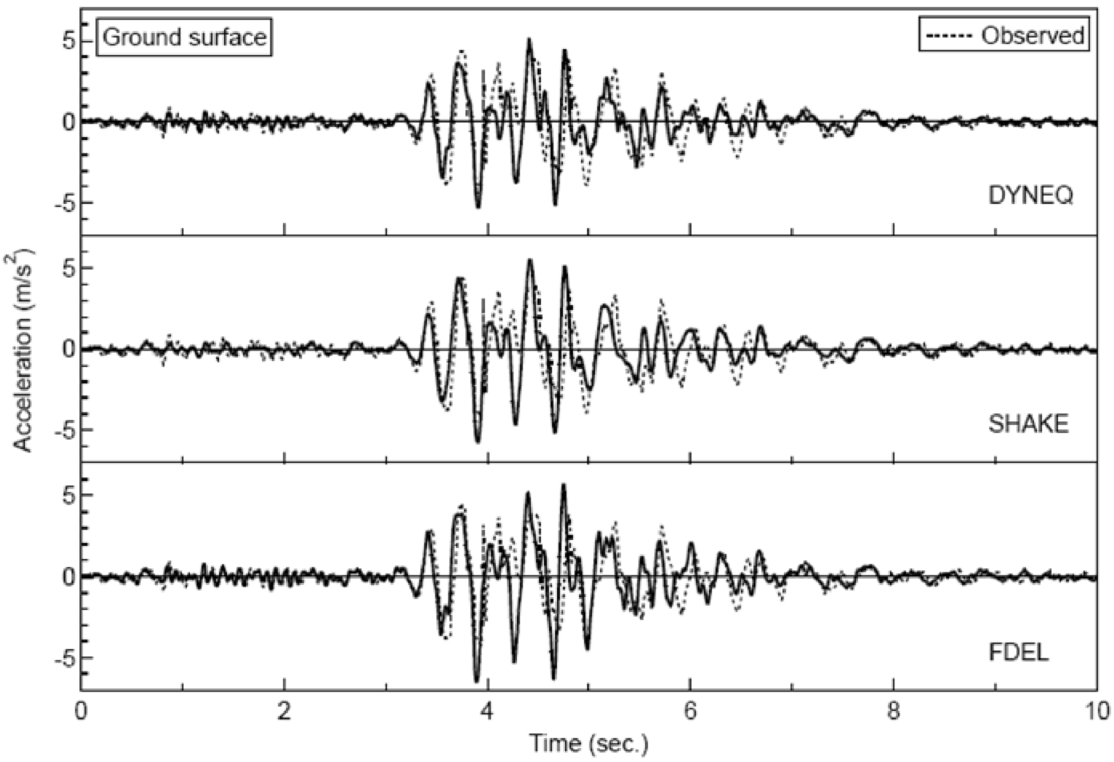

Figure 4.14. Comparison of acceleration time histories at the ground surface (Yoshida and Suetomi, 1996)

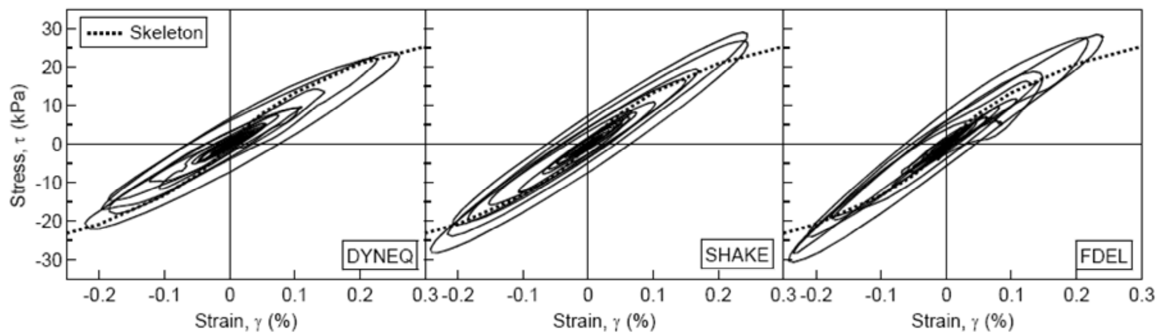

Figure 4.15. Stress-strain curves at the third layer (GL-5m~GL-7m) where maximum strain is the largest (Yoshida and Suetomi, 1996)

Yoshida and Suetomi, 1996 examined the accuracy and applicability of DYNEQ from the simulation of the vertical array records from medium to large strain more than one per cent. The comparison with the equivalent linear methods SHAKE and FDEL was also conducted. The main conclusions they arrived are as follows:

1. SHAKE overestimates peak acceleration under large ground shaking and underestimates amplification in high frequency region, which are two significant shortages and come from the same cause to evaluate the effective strain from the maximum strain. The effect of these shortages appears even when the maximum strain is less than 0.1 per cent. The latter shortage makes the waveform of the acceleration smooth in the convolution analysis, and becomes the cause of the unrealistic large base motion and divergence of the analysis in the deconvolution analysis under large ground shaking.

2. FDEL overestimates acceleration always larger than SHAKE, therefore, its applicability is the worst among three methods under large ground shaking because SHAKE already overestimates the peak acceleration. The frequency region to consider nonlinear behavior is narrow, which becomes the cause of the appearance of the large amplitude waves with several Hz. under large ground motion. Therefore, even if FDEL has advantage more than SHAKE, it is limited to small ground shaking behavior as Sugito *et al.* (1994) examined.

3. DYNEQ is applicable to large strains more than 1per cent. It always shows the most accurate simulation than other two equivalent linear methods. Applicability of DYNEQ to very large strain more than two per cent was not examined because of the lack of the relevant vertical array record. A more downhole observation of the strong earthquake is desired to confirm it.

4. All equivalent linear methods are not applicable on the liquefaction phenomena. It is reasonable conclusion because specified material property does not consider the behavior after liquefaction. The examination on the applicability of the effective stress method on the liquefaction phenomena is remained in the future.

5. Deconvolution analysis is easy under small ground shaking because all three methods show nearly the same results. It, however, becomes to be more difficult than convolution analysis under large ground shaking. DYNEQ showed nearly the same response for both analyses; reproductively by other methods is worse than DYNEQ. SHAKE is not applicable for deconvolution analysis under large

ground shaking with shear strain is about 0.1 per cent at maximum unless high frequency component is neglected or effective strain is reduced, which makes the error large.

4.5.3. FDM Method

Assimaki and Kausel (2002) proposed an improved version of the Seed–Idriss iterative linear model. This model takes into account the frequency- and amplitude-dependent nature of the strains, which in turn requires the model's material parameters to be frequency dependent, even if the material itself is rate independent when loaded cyclically. The proposed scheme not only provides results that match more closely the inelastic behavior of soils undergoing seismic deformations in shear, but it does so without substantially adding complexity to the iterative algorithm.

The following iterative procedure has been tested and found to give satisfactory results by Assimaki and Kausel (2002):

1. Preliminary steps
   - Choose a baseline-corrected earthquake record as input excitation, compute the ground velocity record by numerical integration, and obtain the Fourier transform for both of these.
   - Subdivide the layered profile into a sufficient number of thin sub-layers to characterize properly the spatial variation of inelastic effects.
   - Assign to each layer an initial modulus and damping consistent with a peak strain that is roughly estimated as the ratio of the peak ground velocity and the (small strain) shear wave velocity of that layer.

2. Iterative algorithm
   - Using a standard wave amplification model (*i.e.*, Haskell– Thompson), determine the transfer functions for the strains at the center of each layer for a unit input velocity (not input acceleration) specified at bedrock or rock outcrop. (This circumvents the problem of having to divide the acceleration

transfer functions by the frequency, which produces uncertain results at low frequencies.)

- Multiply each transfer function by the input velocity spectrum, Fourier invert the result to obtain strain time histories, and find the true peak strains γ_{max}.
- In each layer, determine the mean frequency ω_0 of the strain spectrum, and the least-squares best-fit parameters α, β needed in Equation (4.9). Multiply this normalized equation by γ_{max} to obtain the smooth frequency-dependent strain spectrum for that layer.

$$\left|\frac{\gamma(\omega)}{\gamma_0}\right| = \begin{cases} 1, & \omega \le \omega_0 \\ \dfrac{\exp\left(-\alpha \dfrac{\omega}{\omega_0}\right)}{\left(\dfrac{\omega}{\omega_0}\right)^{\beta}}, & \omega > \omega_0 \end{cases} \tag{4.9}$$

- Use the smooth spectrum curve thus obtained to extract the frequency-dependent soil parameters, *i.e.*, the shear modulus reduction factor and the fraction of damping, see Figure 4.16. Modify the soil constants accordingly.
- Compare the peak strains with their values in the previous iteration. Iterate as necessary.
- After the convergence criterion is satisfied, compute the acceleration (or other) response time histories wherever desired.

Figure 4.17 presents the results of the simulation for this very deep site. As can be seen, the time histories of acceleration at the free surface computed with both the frequency-dependent model and the true inelastic model are very similar indeed. By comparison, an analysis using the conventional Seed–Idriss iterative method (Figure 4.18) predicts a motion of lesser intensity and lacking the high frequencies components.

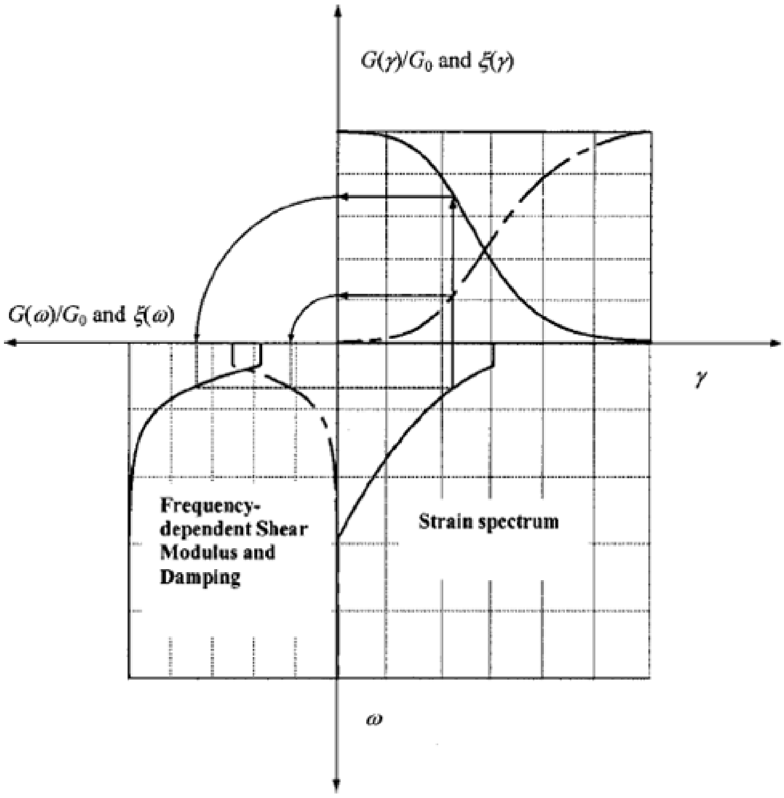

Figure 4.16. Composite sketch of three figures summarizing the choice of frequency-dependent material parameters (Assimaki and Kausel, 2002)

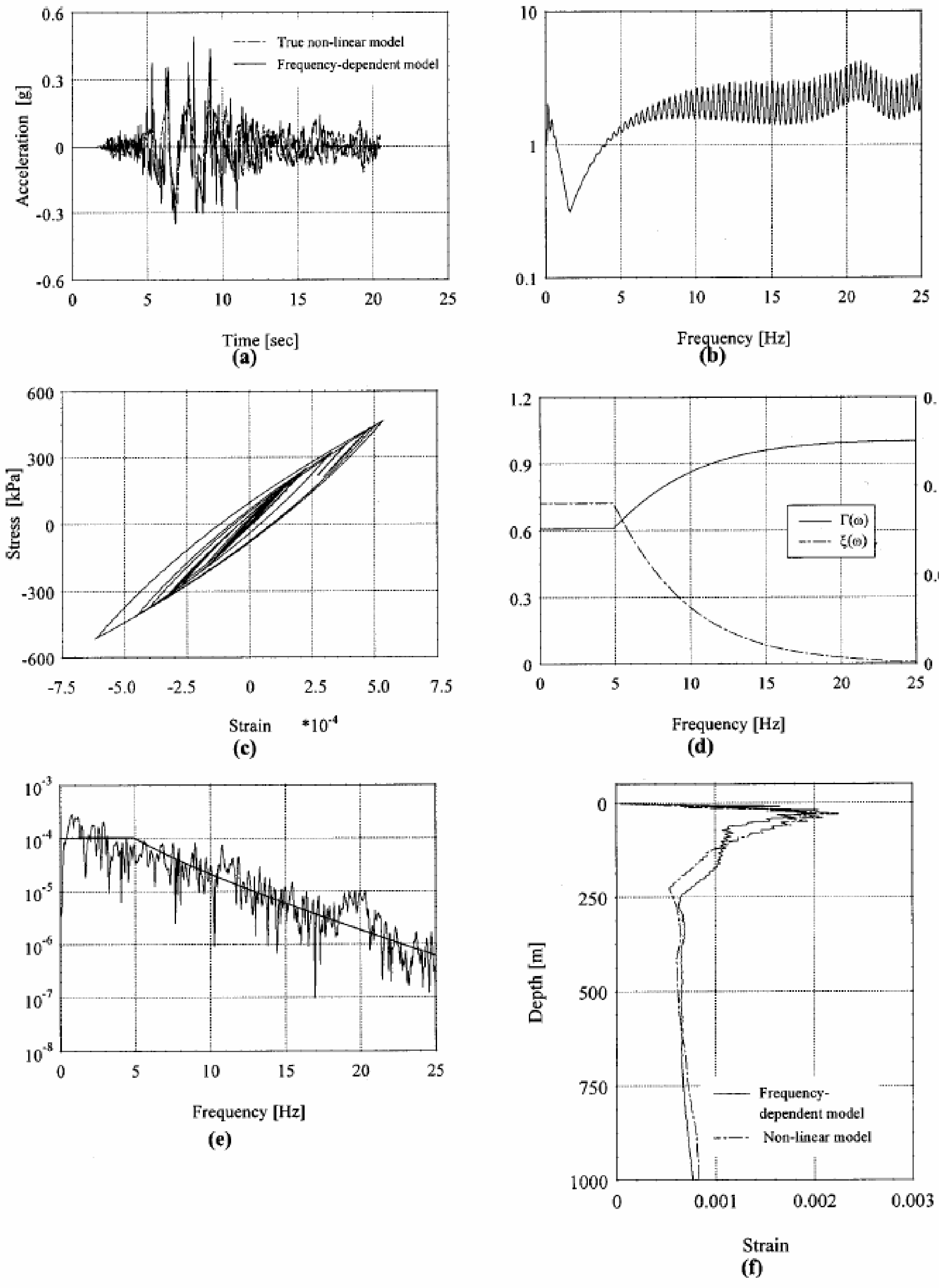

Figure 4.17. (a) Response at top caused by Kobe Earthquake at rock; (b) transfer function from rock to surface; (c) hysteresis loop, middle layer; (d) soil degradation parameters, top layer; (e) smooth strain spectrum, top layer; and (f) variation of maximum strain with depth (Assimaki and Kausel, 2002)

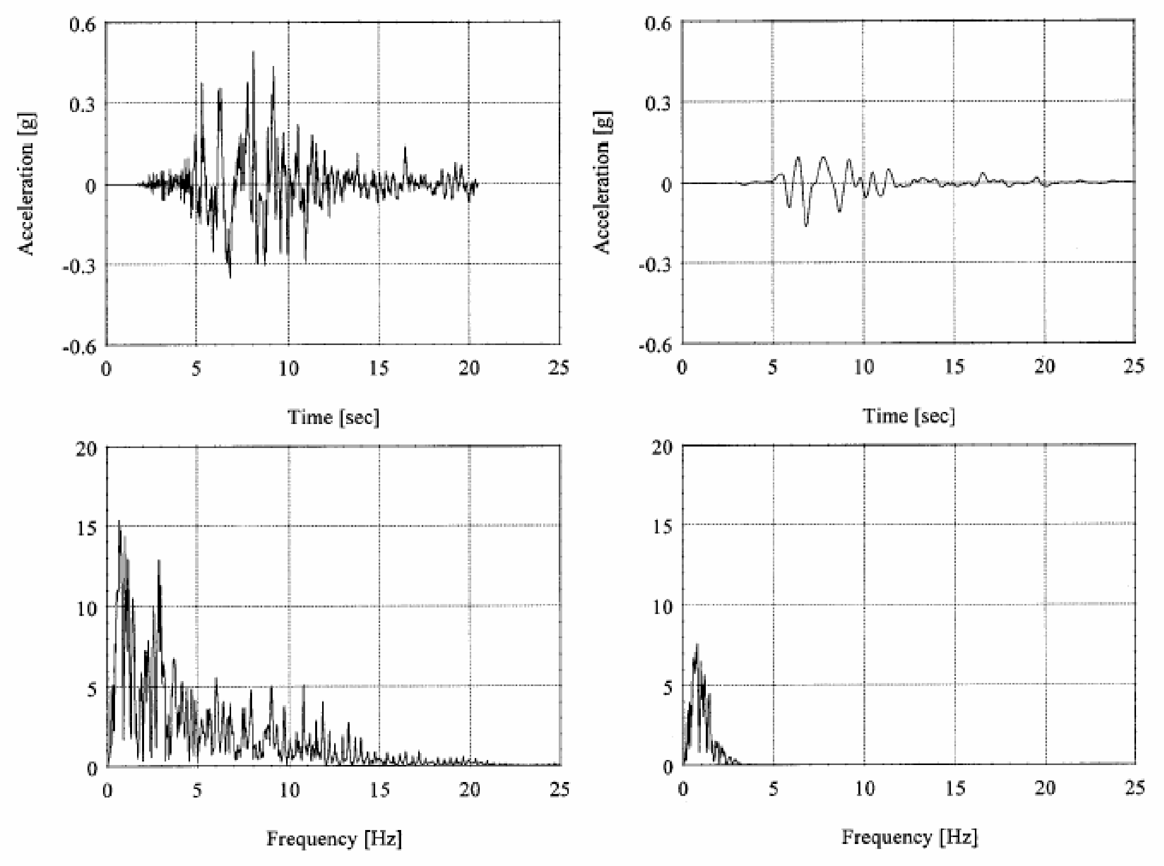

Figure 4.18. Frequency model (left) versus standard iterative algorithm (right); response at free surface: time history (top) and Fourier spectra (bottom) (Assimaki and Kausel, 2002)

4.6. Modifications to Shake91 to Improve Accuracy of Equivalent Linear Method

4.6.1. Adopting Family of Effective Stress Dependent Modulus Degradation and Material Damping Ratio Curves

The problem of site response for deep profiles is that for large depths, even small damping values affect motion significantly. If a site response analysis is needed for large depths, the damping must be modified such that it reduces with increasing depth, reaching very small values at large depths. Ideally, the damping used has to be calibrated with seismological models of the near-crust (these models account for damping in a different fashion and are calibrated for long-period motions).

Site response analysis carried out to evaluate the effect of confining pressure dependency on predicted ground motions show that using confining pressure dependent curves results in larger intensity ground motions than those predicted with average generic curves (Darendeli *et al.*, 2001) as shown in Figure 4.19.

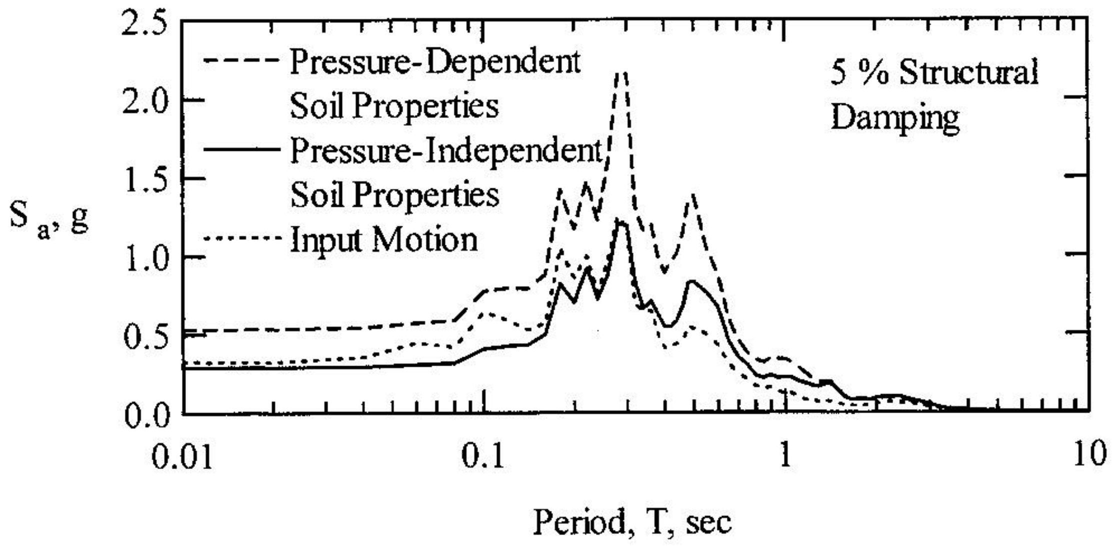

Figure 4.19. Impact on nonlinear site response of accounting for the effect of confining pressure on dynamic soil properties (Darendeli *et al.*, 2001)

SHAKE analysis were repeated for the three soil profiles adopting family of effective stress depending modulus degradation and material damping curves. The curves are developed from the proposed soil model by Darendeli (2001) for each sublayer of the soil profiles. Darendeli (2001) proposed a four – parameter model that can be used to characterize normalized modulus reduction and material damping curves. The model is based on the hyperbolic soil model originally developed by Hardin and Drnevic (1972).

After the four model parameters (reference strain, curvature coefficient, small strain material damping and scaling coefficient) are calculated for the soil plasticity and loading conditions, the (4.10) through (4.15) are utilized to estimate the modulus degradation and material damping curves as follows:

Normalized modulus reduction curve:

$$\frac{G}{G_{max}} = \frac{1}{1+\left(\frac{\gamma}{\gamma_r}\right)^a} \tag{4.10}$$

where;

G/G_{max} = normalized modulus

γ = shearing strain

γ_r = reference strain (parameter of the model)

a = curvature coefficient (parameter of the model)

$$\gamma_r = \left(\phi_1 + \phi_2 * PI * OCR^{\phi_3}\right) * \sigma_0'^{\phi_4} \tag{4.11}$$

$$a = \phi_5 \tag{4.12}$$

where;

σ_0' = mean effective confining pressure (atm)

PI = soil plasticity index (%)

OCR = overconsolidation ratio

ϕ_1 through ϕ_5 = parameters that relate the curve to soil type and loading conditions

Material damping curve:

$$D_{Adjusted} = b * \left(\frac{G}{G_{max}}\right)^{0.1} * D_{Masing} + D_{min} \tag{4.13}$$

where;

$$D_{Masing} = c_1 D_{Masing,a=1} + c_2 D_{Masing,a=1}{}^2 + c_3 D_{Masing,a=1}{}^3$$

$$D_{Masing,a=1} = \frac{1}{\pi}\left[4\frac{\gamma - \gamma_r \ln\left(\frac{\gamma+\gamma_r}{\gamma_r}\right)}{\frac{\gamma^2}{\gamma+\gamma_r}} - 2\right]$$

$$c_1 = -1.1143a^2 + 1.8618a + 0.2523$$

$$c_2 = 0.0805a^2 - 0.0710a - 0.0095$$

$$c_3 = -0.0005a^2 + 0.0002a + 0.0003$$

b	=	scaling coefficient (parameter of the model)
D_{Masing}	=	damping estimated based on Masing behavior
D_{min}	=	small strain material damping ratio (parameter of the model)
$D_{adjusted}$	=	Scaled and capped material damping

$$D_{min} = \left(\phi_6 + \phi_7 * PI * OCR^{\phi_8}\right) * \sigma_0'^{\phi_9} * \left[1 + \phi_{10} * \ln\left(frq\right)\right] \tag{4.14}$$

$$b = \phi_{11} + \phi_{12} * \ln(N) \tag{4.15}$$

where;

σ_0'	=	mean effective confining pressure (atm)
PI	=	soil plasticity index (%)
OCR	=	overconsolidation ratio
frq	=	Loading frequency
N	=	Number of loading cycles
ϕ_6 through ϕ_{12}	=	parameters that relate the curve to soil type and loading conditions

Figure 4.20 through Figure 4.23 shows the normalized modulus reduction and material damping curves for different soil types; clean sand, sand with high fines content, silt and clay; with PI=0 %, PI=0 %, PI=15 % and PI=15 %, respectively subjected to 0.25, 1, 4 and 16 atm in-situ mean effective stresses and ten cycles of loading at 1 Hz to visualize effective stress dependency of dynamic soil properties.

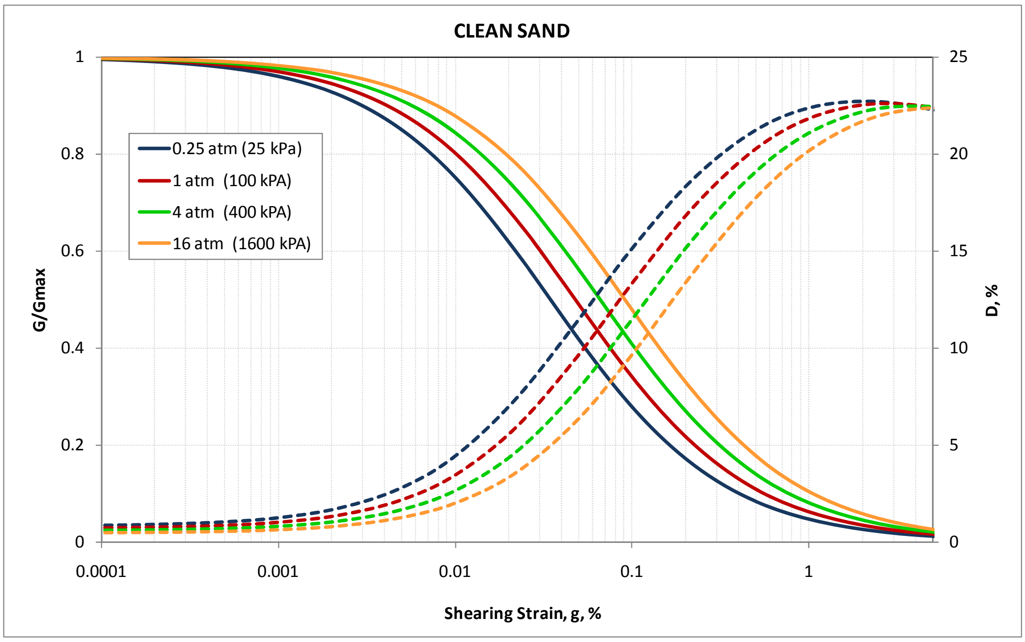

Figure 4.20. Modulus degradation and material damping curves for clean sands subjected to four levels of effective confining pressure utilized from the proposed model by Darendeli (2001)

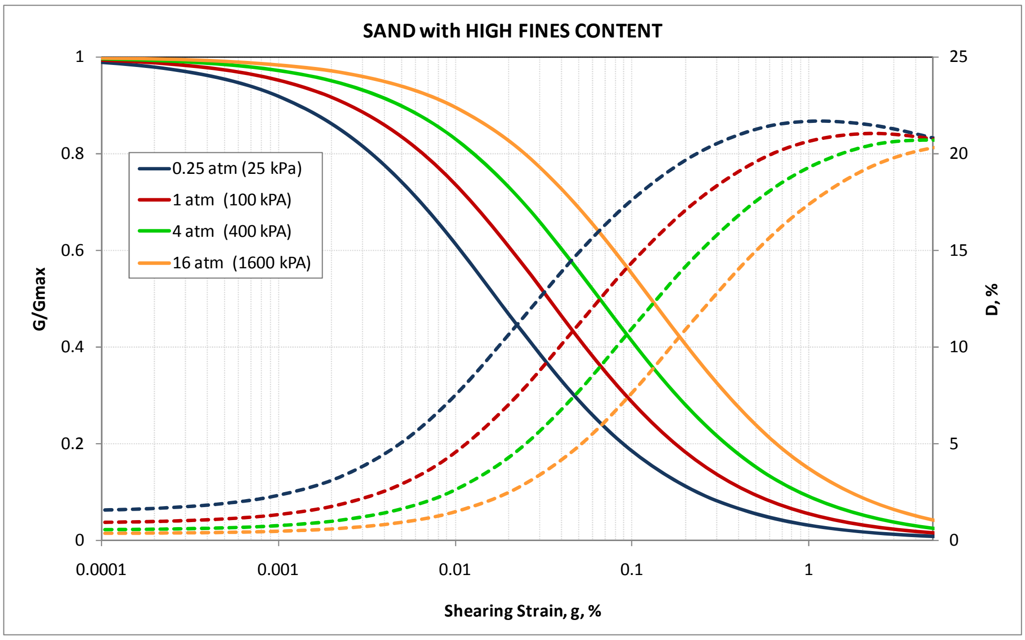

Figure 4.21. Modulus degradation and material damping curves for sands with high fines content subjected to four levels of effective confining pressure utilized from the proposed model by Darendeli (2001)

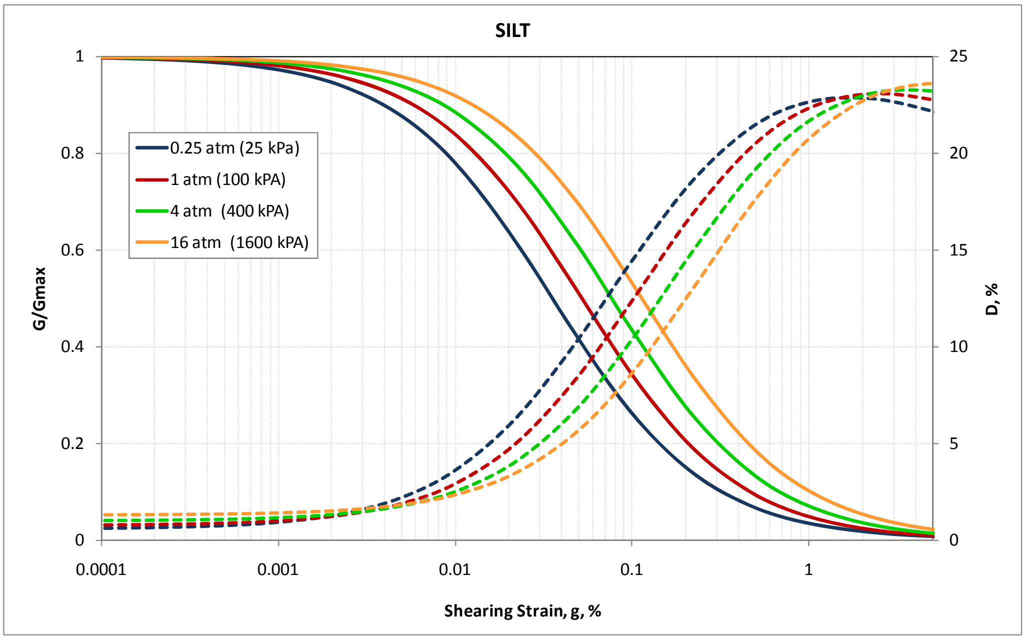

Figure 4.22. Modulus degradation and material damping curves for silts subjected to four levels of effective confining pressure utilized from the proposed model by Darendeli (2001)

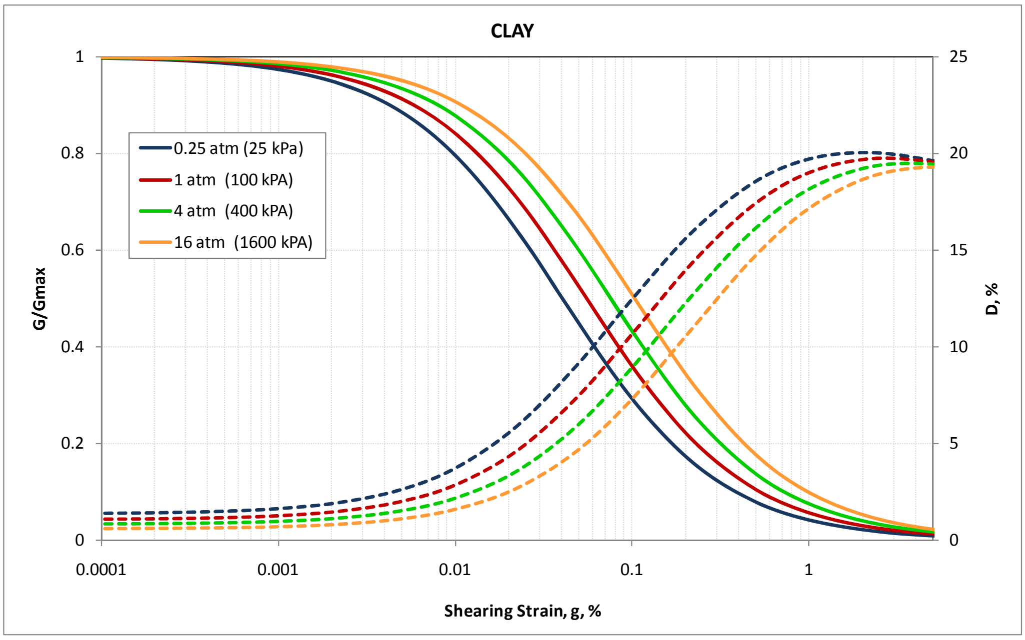

Figure 4.23. Modulus degradation and material damping curves for clays subjected to four levels of effective confining pressure utilized from the proposed model by Darendeli (2001)

Modulus degradation and material damping curves were developed for all sublayers of each soil profile and SHAKE analysis were repeated to see the difference when the confining effective stress dependency is taken into account in the analysis.

The results of site response analysis run with modified Shake91 by adopting family of effective stress dependent modulus degradation and damping curves are given in Figure 4.24 through Figure 4.31 for eight different scaling methods and three soil profiles.

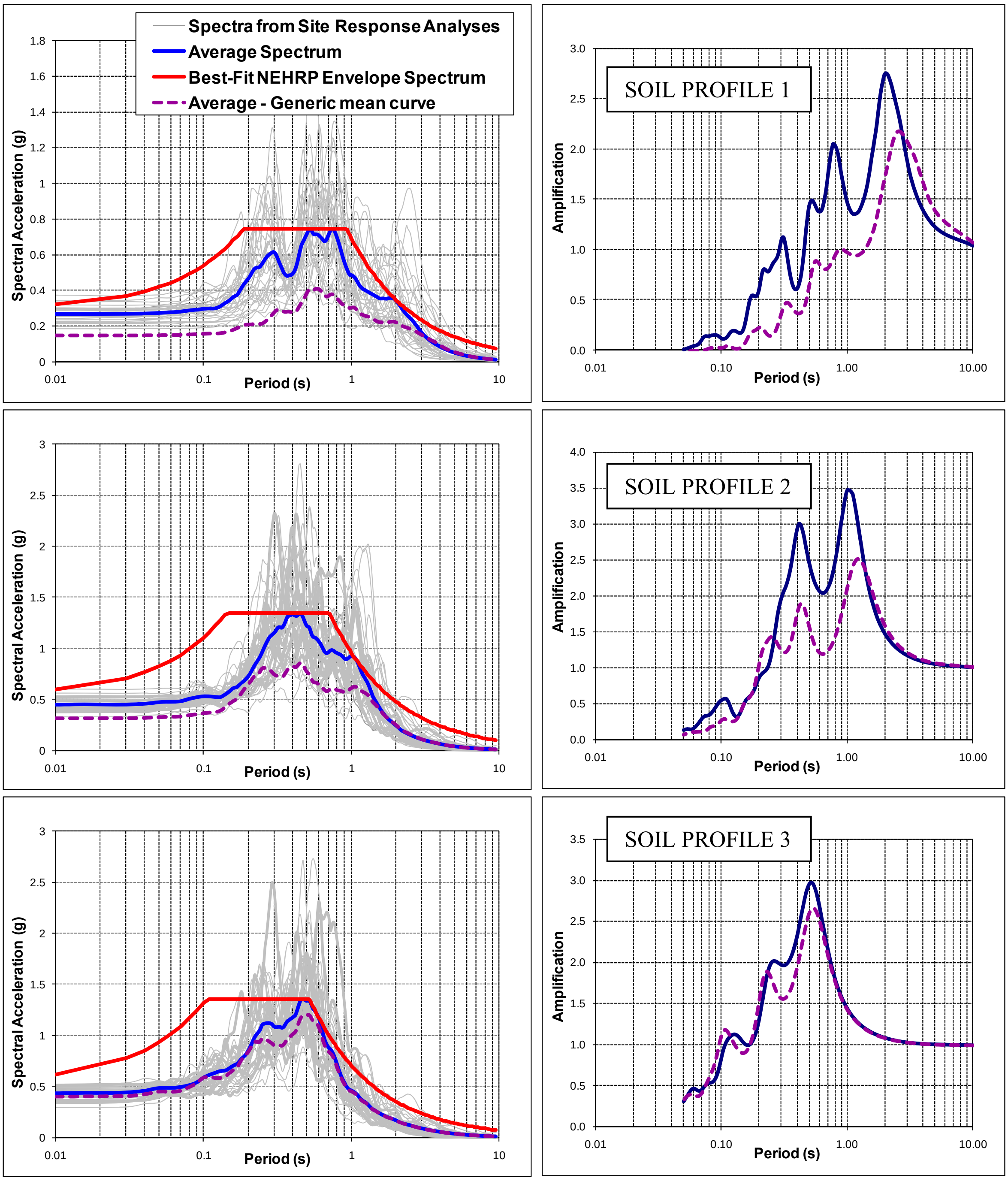

Figure 4.24. Comparison of average acceleration response spectra and amplification spectra of site response analysis with effective stress dependent curves (solid lines) and with generic curves (dash line) for three soil profiles – PGA scaling case

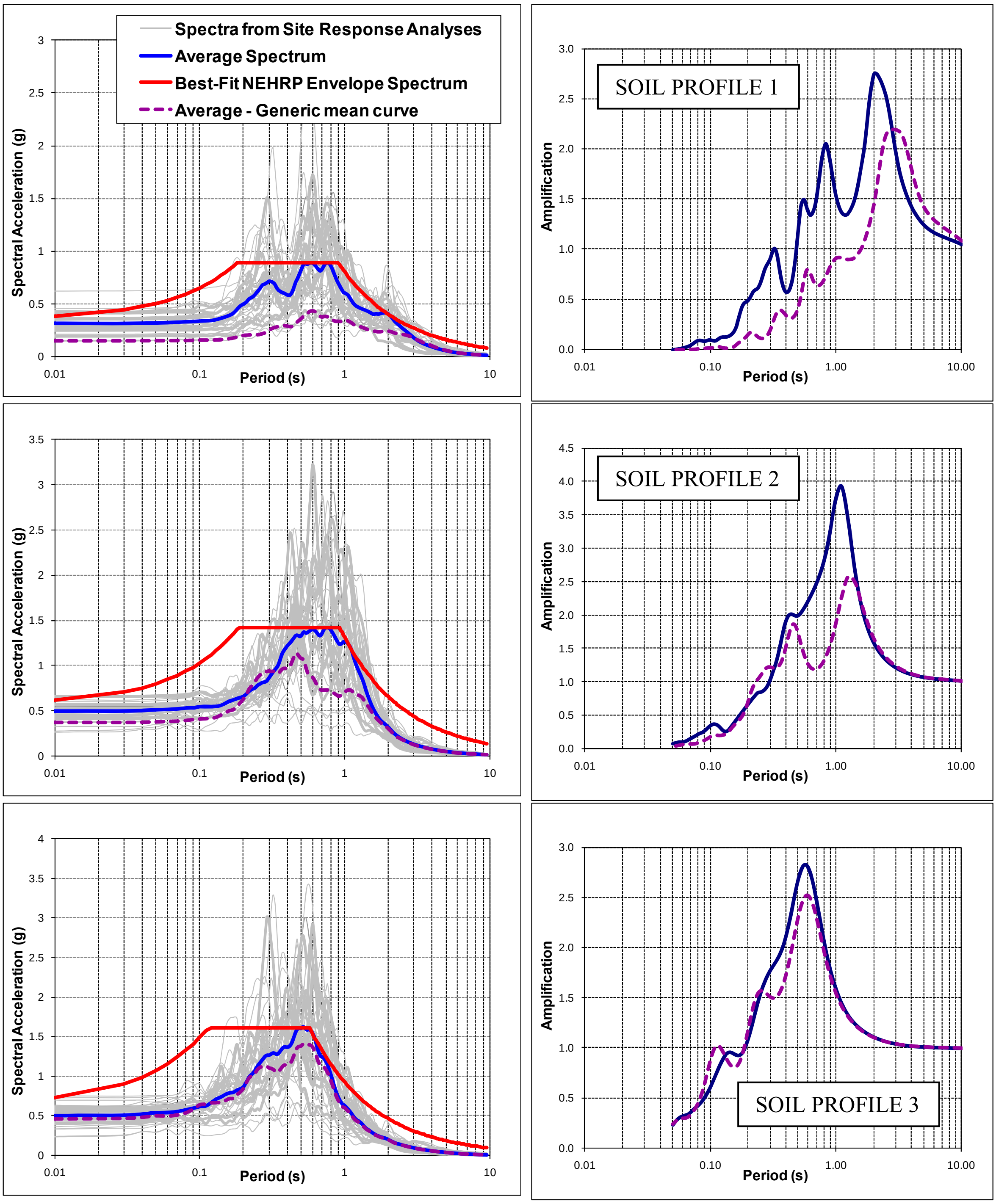

Figure 4.25. Comparison of average acceleration response spectra and amplification spectra of site response analysis with effective stress dependent curves (solid lines) and with generic curves (dash line) for three soil profiles – PGV scaling case

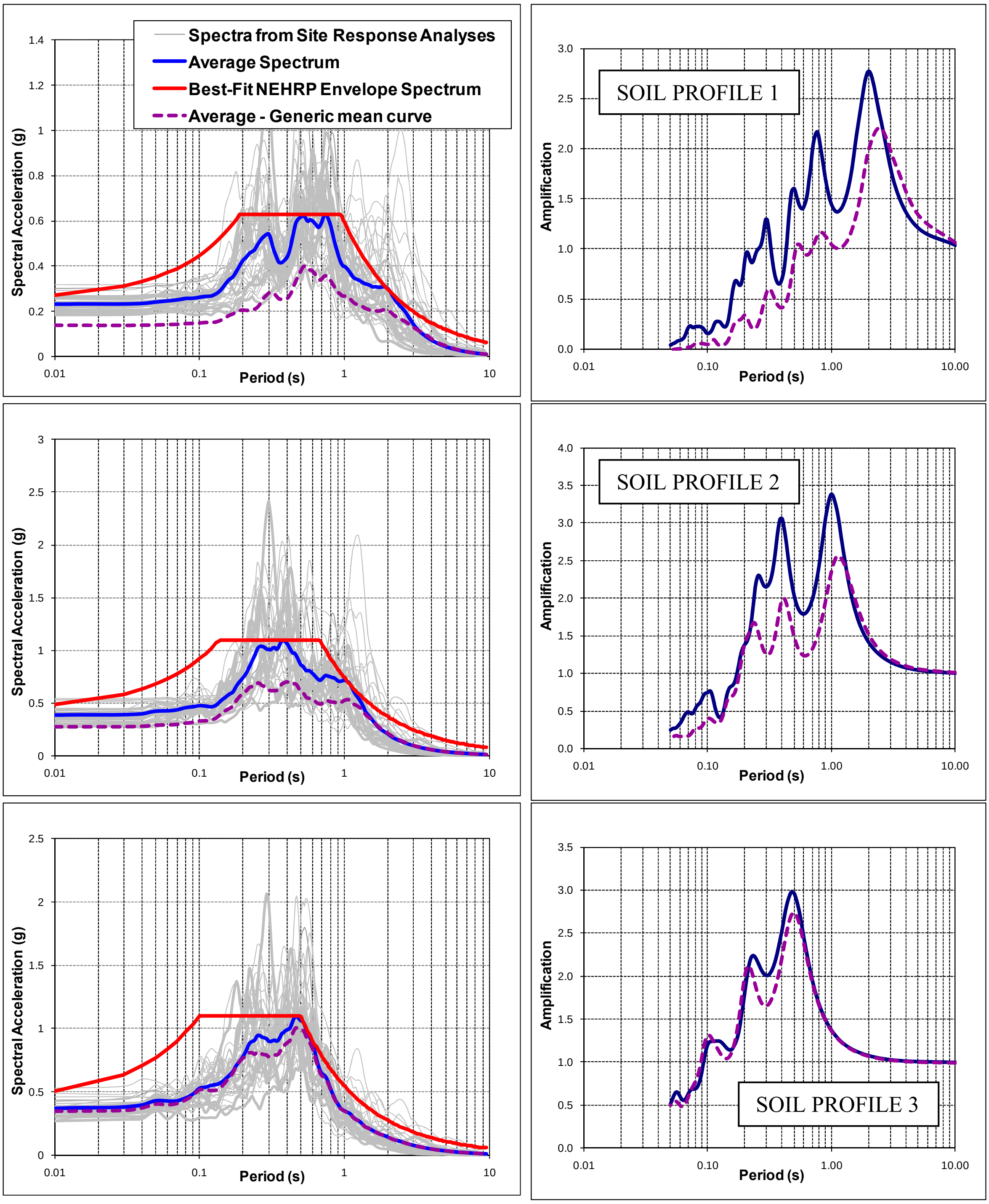

Figure 4.26. Comparison of average acceleration response spectra and amplification spectra of site response analysis with effective stress dependent curves (solid lines) and with generic curves (dash line) for three soil profiles – a_{RMS} scaling case

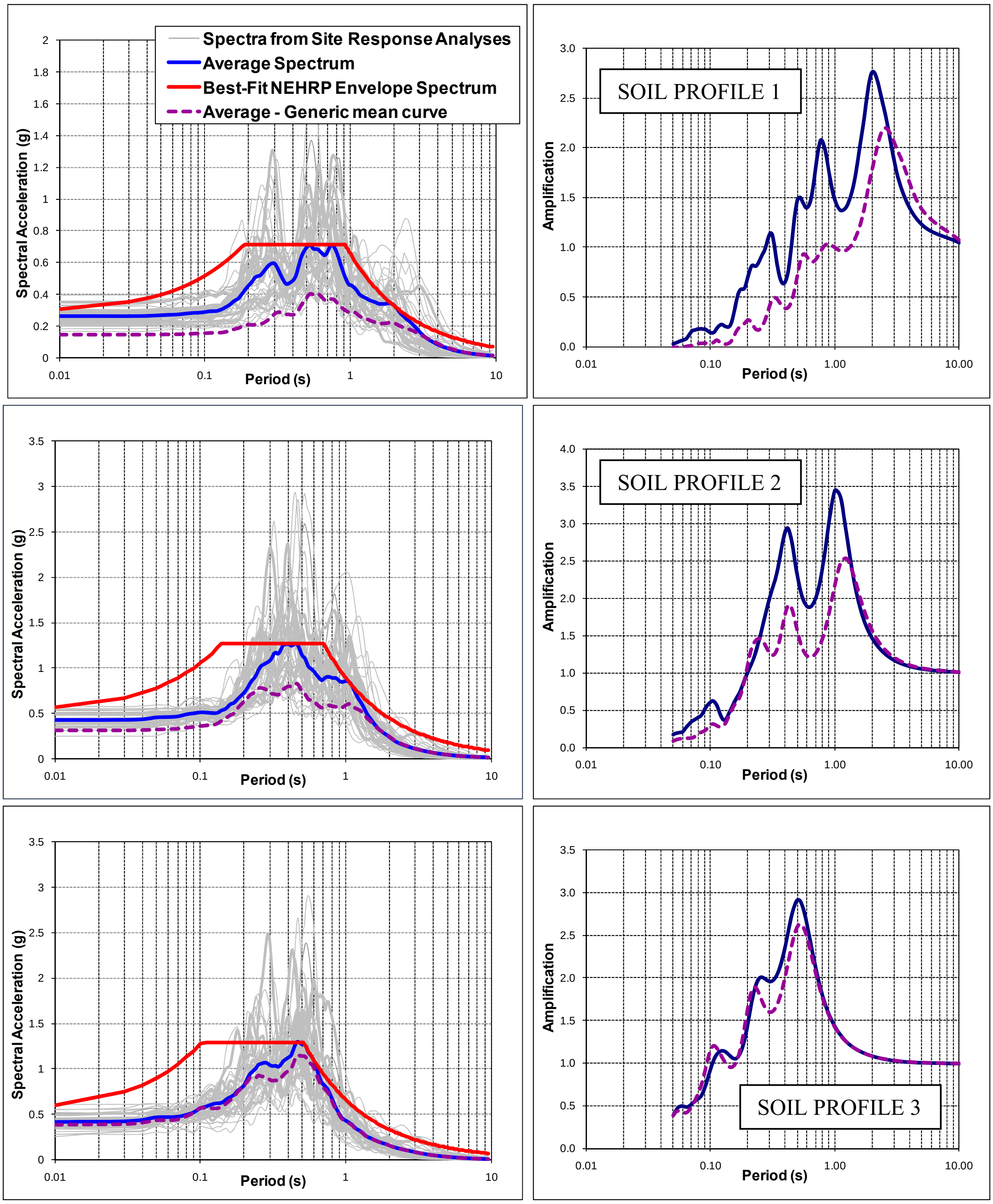

Figure 4.27. Comparison of average acceleration response spectra and amplification spectra of site response analysis with effective stress dependent curves (solid lines) and with generic curves (dash line) for three soil profiles – AI scaling case

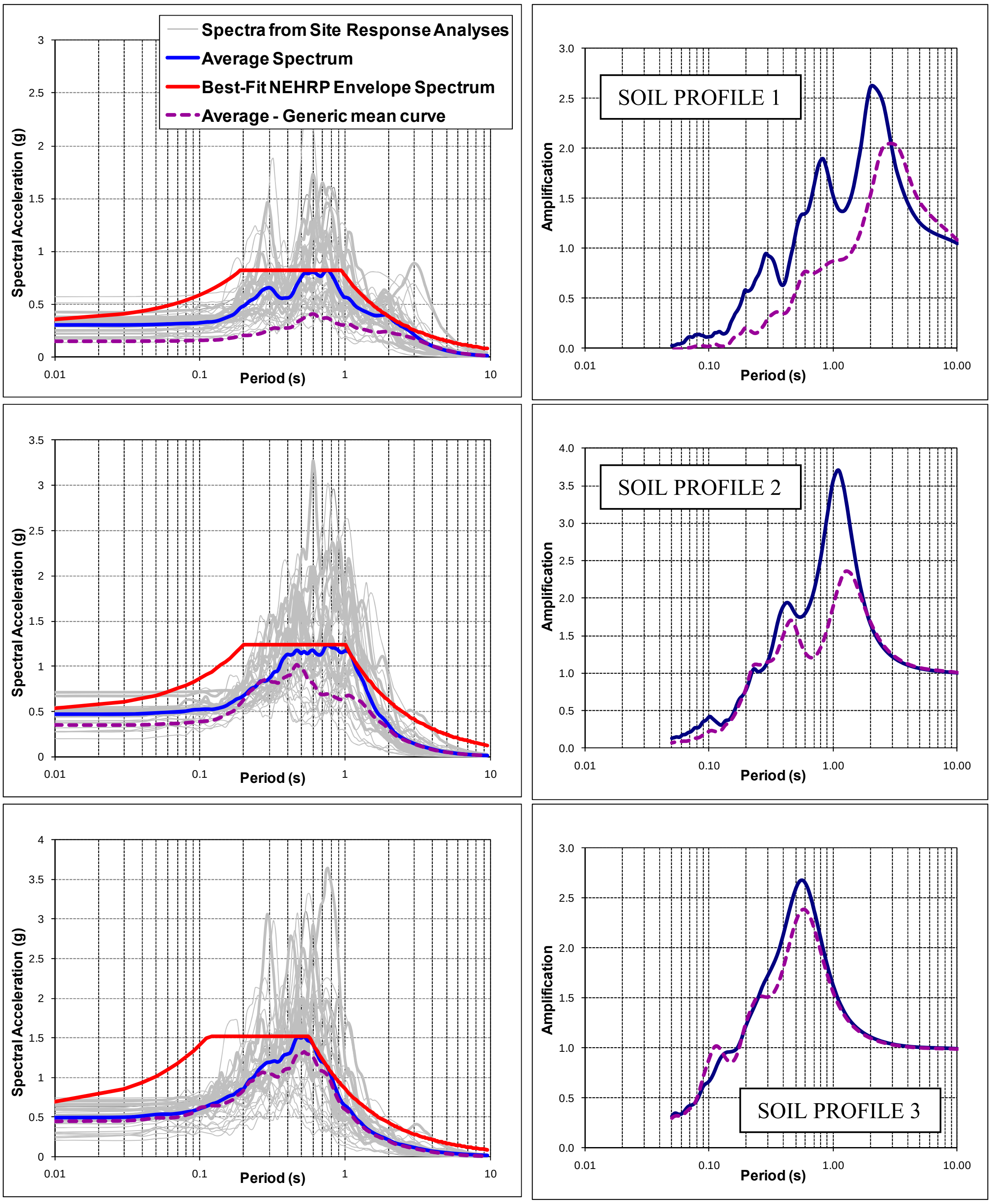

Figure 4.28. Comparison of average acceleration response spectra and amplification spectra of site response analysis with effective stress dependent curves (solid lines) and with generic curves (dash line) for three soil profiles – CAV scaling case

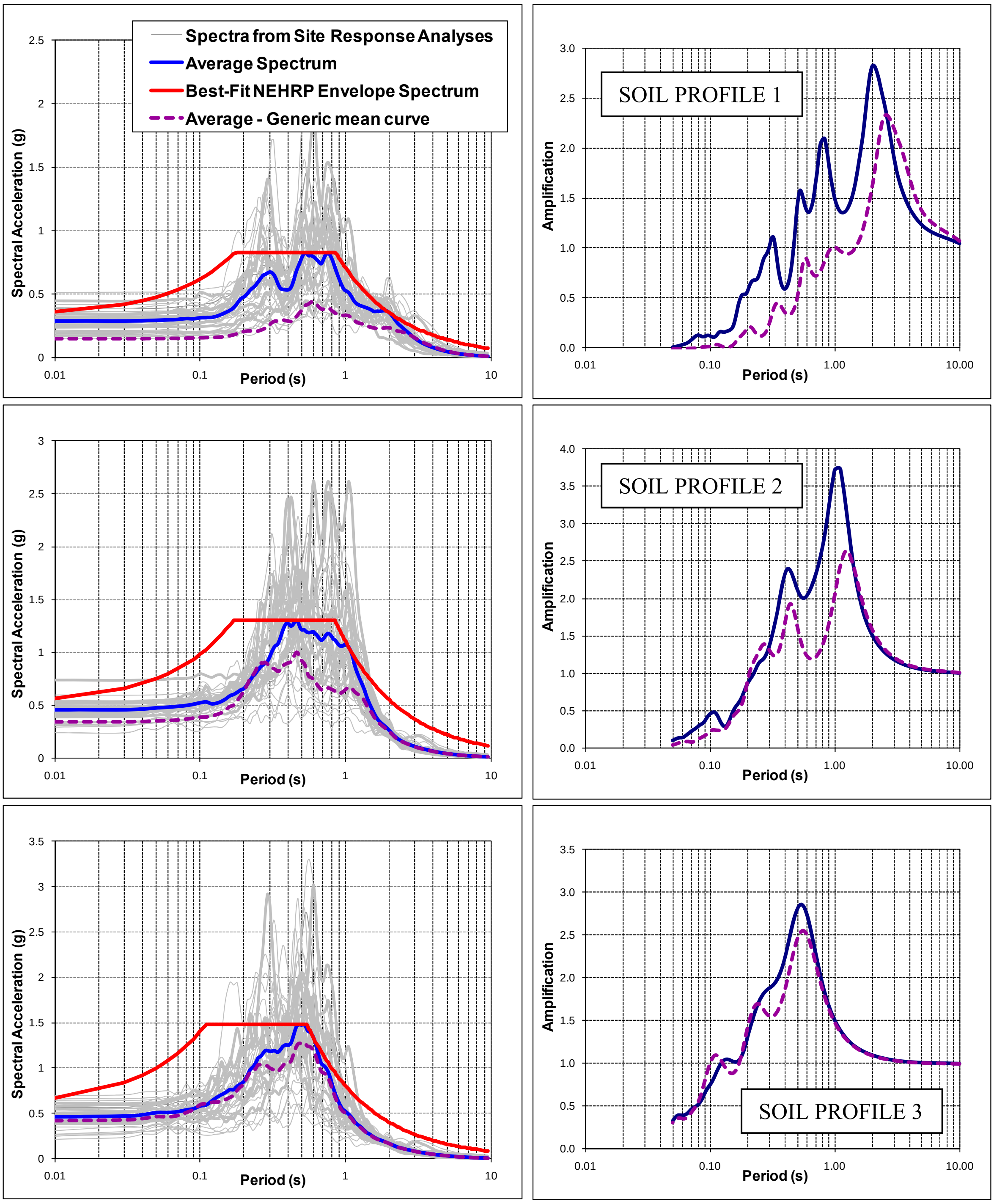

Figure 4.29. Comparison of average acceleration response spectra and amplification spectra of site response analysis with effective stress dependent curves (solid lines) and with generic curves (dash line) for three soil profiles – SA_{max} scaling case

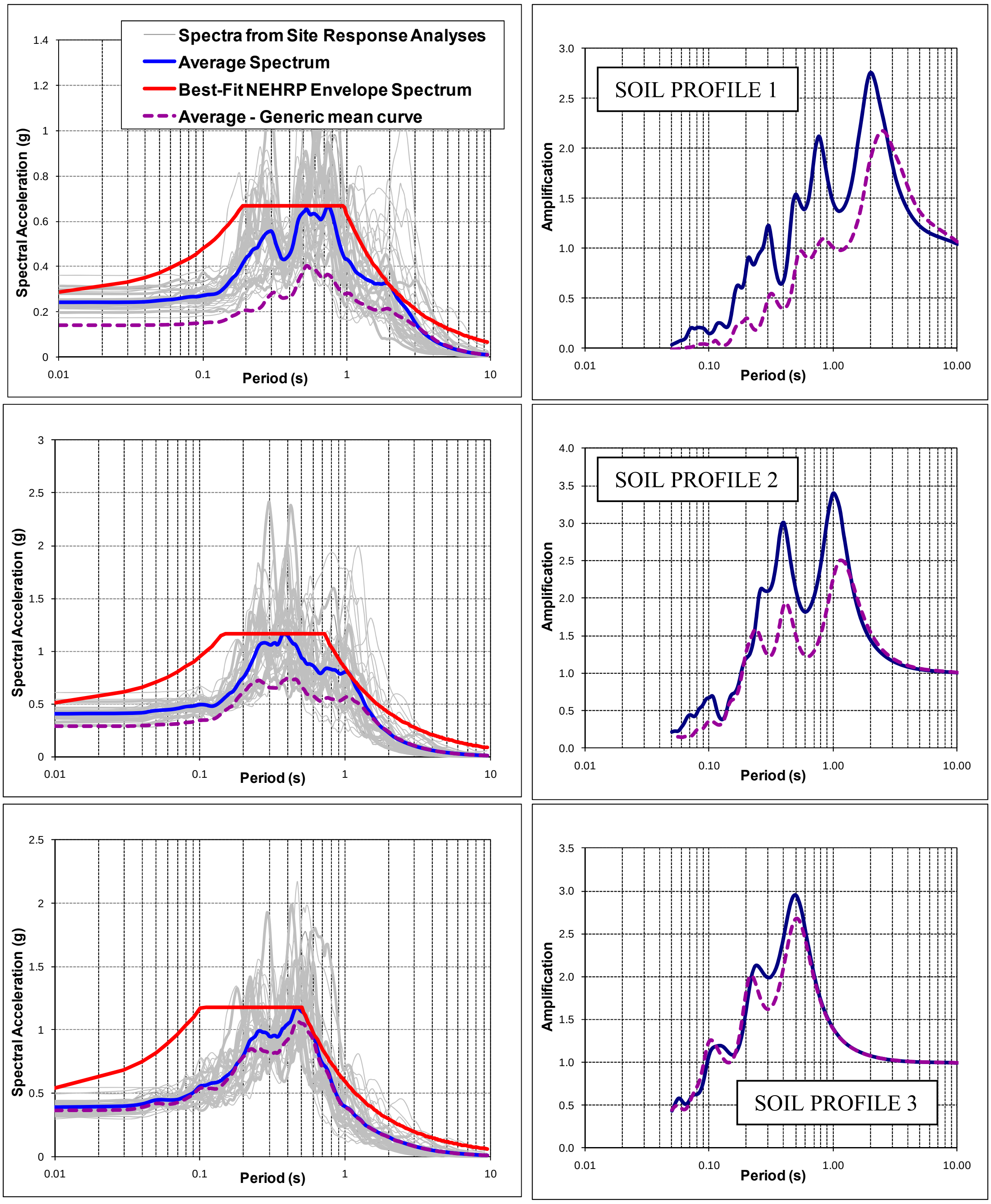

Figure 4.30. Comparison of average acceleration response spectra and amplification spectra of site response analysis with effective stress dependent curves (solid lines) and with generic curves (dash line) for three soil profiles – SI scaling case

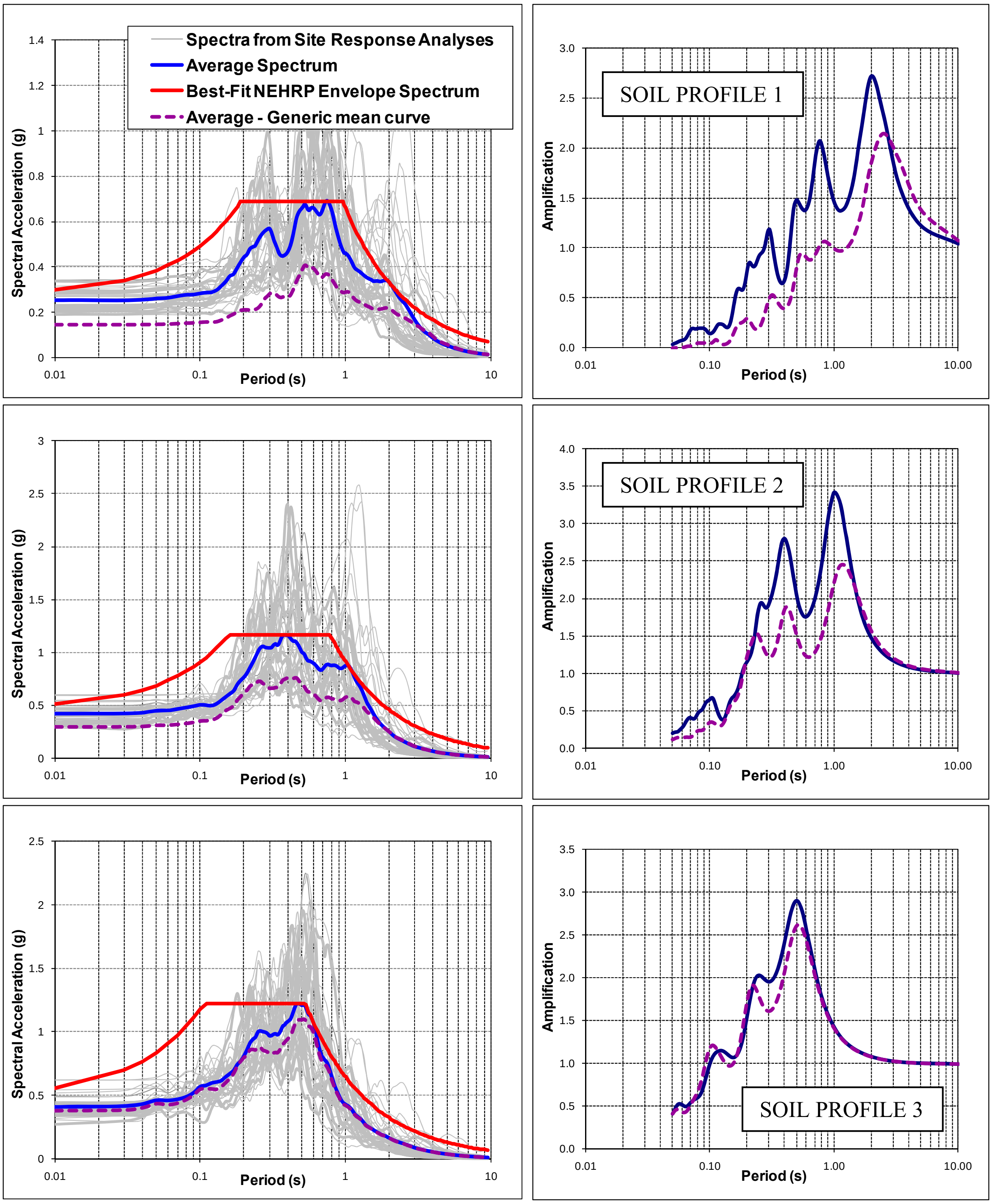

Figure 4.31. Comparison of average acceleration response spectra and amplification spectra of site response analysis with effective stress dependent curves (solid lines) and with generic curves (dash line) for three soil profiles – ASI scaling case

4.6.2. Adopting FDEL Method to Account for Frequency Dependent Behavior on Site Response Analysis

Site response analysis were repeated taking frequency dependent characteristics into account on predicted ground motions adopting FDEL methodology suggested by Sugito *et al.* (1994).

This modification improved lower amplification in high frequency range disadvantage of the equivalent linear analysis. The modification is to put effective strain in each frequency component as given in Equation (4.7). The modification is applied to the actual Fourier amplitude of strain in evaluating the effective strain not to the smoothed Fourier spectrum since the result depends on the method of smoothing, although smoothing is recommended for convergence problems.

The results of site response analysis run with modified Shake91 by adopting effective stress dependency and by adopting FDEL methodology are given in Figure 4.32 for PGA scaling method and three soil profiles.

4.7. Summary and Results

Site response analysis models solve wave propagation problem for a layered, nonlinear medium. The principal characteristic distinguishing various analysis routines is that the methods differ in the simplifying assumptions that are made, in the representation of stress–strain relations of soil and in the methods used to integrate the equation of motion. There are two general categories of models for representing nonlinear soil behavior in site response analyses: equivalent-linear and fully-nonlinear models.

The equivalent-linear method models the nonlinear variation of soil shear moduli and damping ratio as a function of shear strain. The hysteretic stress-strain behavior of soils under symmetrical loading is represented by an equivalent modulus, G, and an equivalent damping ratio, ξ. An iterative procedure, based on linear dynamic analysis, is performed to find the G and ξ corresponding to the computed shear strains.

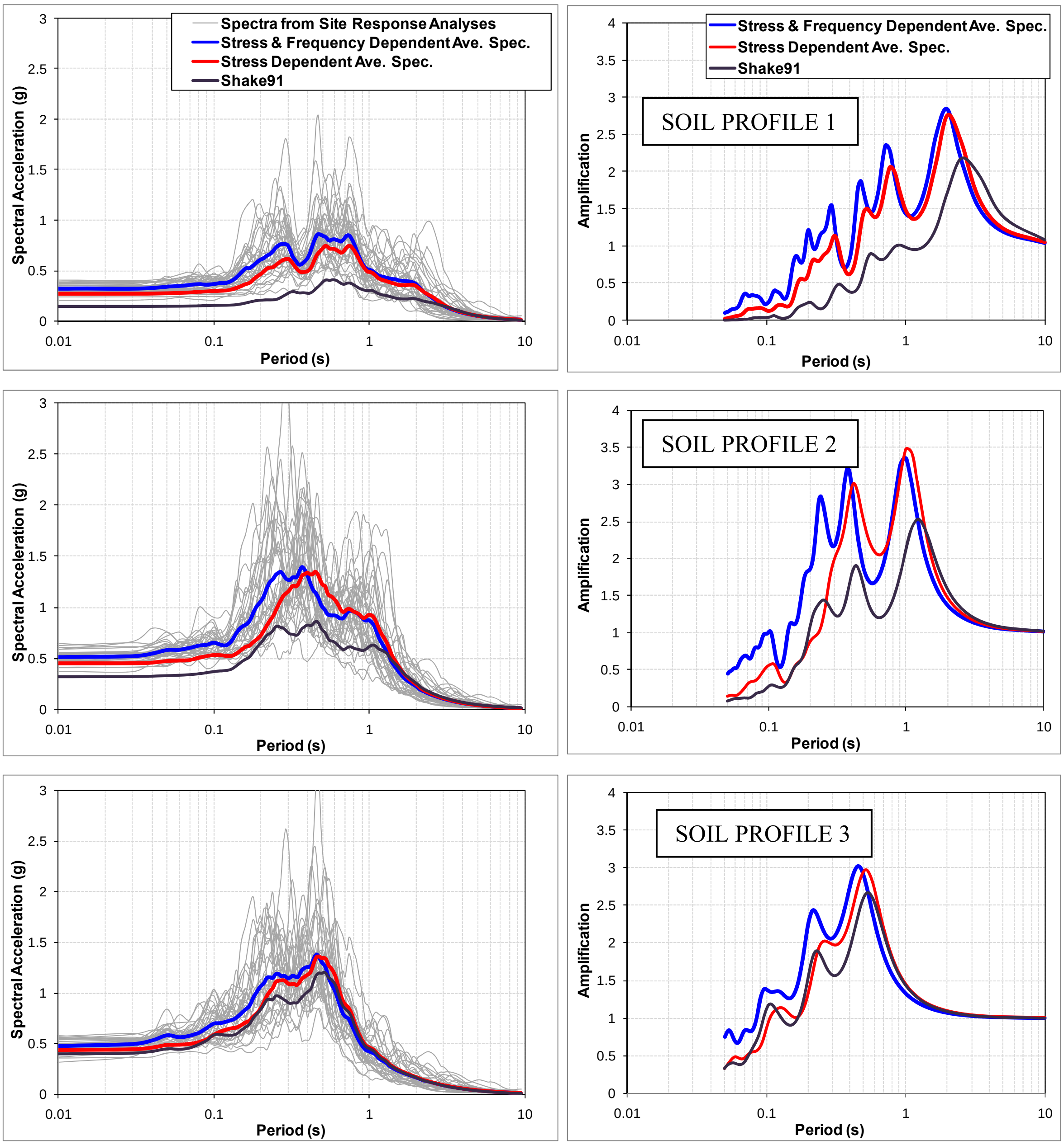

Figure 4.32. Comparison of average acceleration response spectra and amplification spectra of site response analysis taking into account frequency dependency (solid lines) and with generic curves (dash line) for three soil profiles – PGA scaling case

Two equivalent linear site response analysis programs, SHAKE and DEEPSOIL were compared to search the impact of different schemes on the predicted ground motion parameters. Average of DEEPSOIL analysis gives slightly higher values as compared with the average spectrum obtained from SHAKE analysis for all of three soil profiles and three complex shear modulus options of DEEPSOIL. The difference is observed to increase as the profile gets shallower.

SHAKE analysis were repeated for the three soil profiles adopting family of effective stress depending modulus degradation and material damping curves to modify SHAKE to take into account effective stress dependency of dynamic properties. The curves are developed from the proposed soil model by Darendeli (2001) for each sublayer of the soil profiles. Site response analysis carried out to evaluate the effect of confining pressure dependency on predicted ground motions show that using confining pressure dependent curves results in larger intensity ground motions than those predicted with average generic curves because of the fact that modulus degradation and material damping curves become increasingly linear as confining pressure increases.

Analyses based on stress dependent dynamic properties were rerun adopting frequency dependent characteristics into Shake91. This modification by taking frequency dependent behavior into account improved lower amplification in high frequency range disadvantage of the equivalent linear analysis. The improvement was more pronounced as the soil profile gets deeper.

5. SITE RESPONSE ANALYSIS: NONLINEAR APPROACH

5.1. Introduction

Nonlinearity of the sites has significant importance on the ground motion characteristics. Local site effects on the nonlinear response have been recognized for many years (Seed and Idriss, 1982). Particularly, the combined effect of the dynamic stiffness and the depth of the soil are very influential (Marek *et al.*, 1999). The deep sediments affect surface motions in two opposite ways. Younger and less consolidated sediments may amplify seismic waves several times more than hard rocks do because of different impedance and resonance effects. But, at the same time, because of a reduction in high frequency content due to intrinsic attenuation and wave scattering, this amplification is damped (Boore and Joyner, 1991). According to Cultrera *et al.* (1999), nonlinear effects on seismic waves would be an increase in damping and a decrease in propagation velocity, with consequent reduction in high-frequency amplitudes and shifts to lower frequencies of the spectral resonant peaks of the soil deposit. Nonlinear soil response may be typically defined as the decrease in near-surface amplification of seismic waves as the amplitude of the input wave increases. It is believed that as strain increases, an increasingly hysteretic character of the stress-strain relationship in soils causes this phenomenon. At low strains, that is for the weak ground motion accompanying small earthquakes, the relationship is essentially linear and the amplification due to sediments is well understood in terms of linear elasticity, but for strong ground motions such as large earthquakes there has been always a debate on the associated amplification (Idriss, 1991a; Aki, 1993; Yu *et al.*, 1993; Wen, *et al.*, 1994; Elgamal *et al.*, 1995; Kazama, 1996; Chin and Aki, 1991; Beresnev and Wen, 1996; Aguirre and Irikura, 1997; Su *et al.*, 1998, Beresnev *et al.*, 1998; Higashi and Sasatani, 2000; Bonilla *et al.*, 2005).

5.2. Nonlinear Soil Behaviors

Observations indicate that properties of soil layers could be modified due to cyclic stresses induced by earthquake ground motion. Cyclic tests conducted on undisturbed samples as well as the field evidence have shown degradation of soil stiffness and shear strength characteristics of local soil layers with shear strain accumulation. In evaluating the behavior of soils under cyclic stresses, one alternative is to consider stress-strain and shear strength properties separately. Dynamic shear modulus, damping ratio, and their variation with shear strain may be regarded as the dynamic stress-strain properties of soils. Cyclic stress amplitudes and number of cycles leading to failure or excessive deformations may be defined as dynamic shear strength characteristics. The results obtained from cyclic laboratory tests conducted on undisturbed samples subjected to different shear stress amplitudes and different loading patterns indicate the presence of threshold cyclic shear stress amplitudes with respect to elastic, elasto-plastic and plastic behavior. In addition, the degradation of soil stiffness and accumulation of excess pore pressures may cause significant reduction in shear strength and may induce bearing capacity and slope failures as well as additional settlements as observed in many locations after the 1999 Kocaeli Earthquake.

An important interpretation of the observed cyclic soil behavior was the suggestion of two shear strain threshold levels, the first one as the beginning point of nonlinear behavior and the second one as the beginning point of inelastic behavior (Vucetic, 1994). Another important observation was the effect of soil plasticity expressed in terms of plasticity index on the degradation of dynamic shear modulus and damping ratio with respect to shear strain amplitude (Vucetic and Dobry, 1991).

A series of stress controlled multistage triaxial tests were conducted on normally consolidated undisturbed clay samples obtained from a boring in Izmit after the 1999 Kocaeli Earthquake (Okur and Ansal, 2007, 2004). The maximum shear modulus, G_{max}, as well as the modulus reduction and increase of damping ratio for each sample were determined to evaluate the threshold cyclic shear stress levels as shown in Figure 5.1.

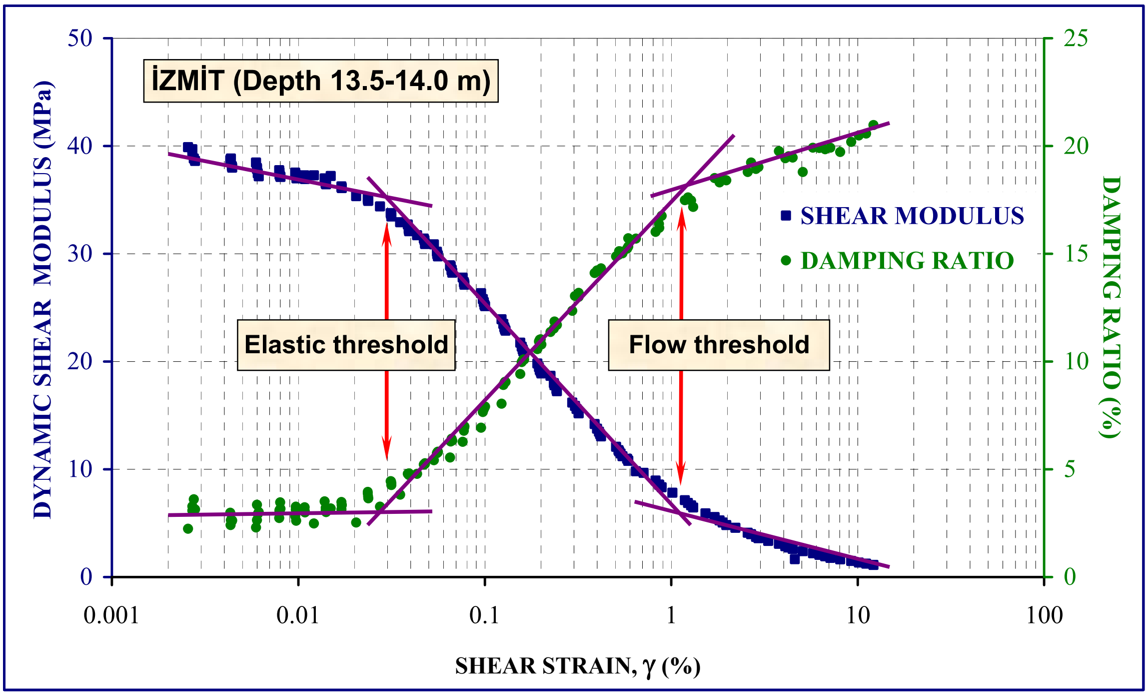

Figure 5.1. Variation of shear modulus and damping ratio with shear strain for a soil sample (Okur and Ansal, 2004)

It appears suitable to treat the cyclic stress-strain behavior of soils in three consecutive stages. In the first stage, the soil sample will respond elastically without any significant reduction in its stress-strain and shear strength properties. The imposed cyclic stresses are small thus induced cyclic strain amplitudes are insignificant. If the imposed cyclic stress levels were lower than the elastic threshold, the reduction of the dynamic shear modulus as well as the post cyclic shear strength would be negligible. Once the elastic threshold is exceeded, the soil sample will respond in elasto-plastic manner. This can be considered as the second stage in the cyclic behavior of soils. During this stage the induced cyclic shear strains would lead to strain softening, particle structure breakdown, and pore pressure accumulation leading to rapid deterioration of stress-strain and shear strength characteristics up to the flow threshold. If the flow threshold is exceeded, the soil sample would experience large strain amplitudes due to the significant reduction of the dynamic shear modulus. This third stage can be considered as the transition to the steady state in the cyclic behavior of soils.

5.3. Nonlinear Site Response Analysis and Codes

There are two main groups of soil models to account for the soil nonlinearity: equivalent linear models, and nonlinear models. A number of studies have been conducted to compare the response of soil deposits using both equivalent linear and direct nonlinear methods and the common observation is that while both methods give similar response spectra, the equivalent linear method underestimates displacements and overestimates accelerations (Constantopoulos *et al*., 1973; Finn *et al*., 1977, 1978; Yu *et al*., 1993).

The response of nonlinear models is determined through direct numerical integration of the equation of motion in small time steps (*e.g.,* explicit finite difference technique). Nonlinear models can account for the nonlinear behavior of soil using various constitutive soil models. The constitutive models implemented in various nonlinear model programs have different features that can include using updated stress-strain relationships, pore-pressure generation, and/or cyclic modulus degradation. These features, unavailable in the equivalent linear model, allow more accurate calculations of soil behavior. Because they may be formulated in terms of effective stresses, unlike equivalent linear models, nonlinear models can account for the build up of porewater pressure that can cause the soil to soften. An important application of nonlinear soil models is in liquefaction hazard analysis. The wave equation solution can be combined with the numerical solution of the diffusion equation to compute the redistribution and dissipation of excess porewater pressures. Nonlinear models can also predict permanent deformations since the strain does not return to zero following cyclic loading. The accuracy of a nonlinear site response model depends on the constitutive model it uses; good constitutive models require numerous parameters which must be determined through lab tests and/or field tests. This amount of effort required to develop the required parameters for accurate models often limits their frequency of use. Nonlinear models tend to be necessary for analyses where large strains or displacements are expected (Kramer and Paulsen, 2004).

Nonlinear one-dimensional ground response analysis characterize the stress-strain behavior of the soil by cyclic stress-strain models such as the hyperbolic model, modified hyperbolic model, Ramberg-Osgood model, Hardin-Drnevich-Cundall-Pyke (HDCP) model, Martin-Davidenkov model, and Iwan-type model. Others have been based on advanced constitutive models such as the nested yield surface model (Kramer, 1996). The Cam-Clay and the modified Cam-Clay models are of this type (Roscoe and Schofield, 1963; Roscoe and Burland, 1968). In all these models, the nonlinear shear behavior is commonly described by a shear stress-strain backbone curve.

The models that represent the nonlinear behavior of soils more accurately are based on advanced constitutive models that use basic principles of mechanics. These models generally require a yield surface that describes the limiting stress conditions for which elastic behavior is observed, a hardening law that describes changes in the size and shape of the yield surface as plastic deformation occurs, and a flow rule that relates plastic strain increments to stress increments (Kramer, 1996).

In order to implement these models and solve the governing equations in a computer code, finite elements (FE), finite differences, or direct time integration methods can be used.

5.3.1. Cyclic1D

To study the dynamic response of saturated soil systems as an initial boundary value problem, a two-dimensional plane-strain FE code was developed (Parra, 1996; Yang, 2000; Elgamal *et al*., 2002). Saturated soil is modeled as a two-phase material based on the Biot theory of porous media (Biot, 1962). The formulation is defined by the equation of motion for solid-fluid mixture and the equation of mass conservation for the fluid phase and Darcy's law. There two governing equations are given in the finite element matrix form as follows:

$$\begin{aligned} M\ddot{U} + \int_{\Omega} B^{T} \sigma' d\Omega + Q_{p} - f^{S} = 0 \\ Q^{T}\dot{U} + S\dot{p} + Hp - f^{P} = 0 \end{aligned} \tag{5.1}$$

where **M** is the mass matrix, U is the displacement vector, **B** is the strain-displacement matrix, σ' the effective stress vector, Q the discrete gradient operator, p the pore-pressure vector, **H** the permeability matrix, **S** the compressibility matrix. A superscript T denotes matrix transpose and a superposed dot denotes time derivative. The vectors f^s and f^p include the effects of body forces and prescribed boundary conditions for the solid-fluid mixture and the fluid phase respectively.

A plasticity-based constitutive model with emphasis on simulating the cyclic mobility response mechanism and associated pattern of shear strain accumulation is used in this code. They incorporated this constitutive model into a two-phase (solid-fluid), fully coupled finite element code and implemented this model in a one-dimensional computer program called Cyclic1D (Yang and Elgamal, 2001; Yang *et al*., 2004). Calibration of the model has been done based on a unique set of laboratory monotonic and cyclic triaxial tests and dynamic centrifuge experiments (Lai *et al*., 2004). The calibration focused on reproducing the prominent characteristics of dynamic soil response as dictated by the cyclic mobility mechanism. The program is still being improved, and it has been chosen in this study because of its uncomplicated use and because it incorporated many physical properties of soils.

This model's constitutive model is based on the framework of multi-surface plasticity (Prevost, 1985; Parra, 1996). According to classical convention of plasticity, it is assumed that nonlinearity and anisotropy result from plasticity and the material elasticity is linear and isotropic (Hill, 1950). The yield function is a conical surface in principal stress space (Figure 5.2). In this figure, the hardening zone is defined by a number of similar yield surfaces with a common apex at $-p_0'$ along the hydrostatic axis. The outermost surface is designated as the failure surface.

The Cyclic1D web site was developed aiming to greatly simplify user interfaces, without undue compromise on modeling flexibility. At the input interface, soil materials are classified into 15 categories, each with a set of pre-defined material constants. Thus, the typical user is relieved from an otherwise much involved calibration process. Moreover, the user may define an input base excitation either from a built-in library or by uploading his/her own file. To assist the user in processing the results, the output interface features online graphical data rendering, animation, and automated report generation. Implemented user interfaces are as follows: *Input* interface, *Simulation*, *Output* interface and *Report* generator.

The input interface is implemented as an interactive web page using HTML language. The user defines and submits a FE model using a web browser such as Internet Explorer or Netscape. A FE model is defined by specifying: (1) the soil profile of interest; (2) material composition of the profile; (3) Rayleigh viscous damping coefficients; and (4) base seismic excitation.

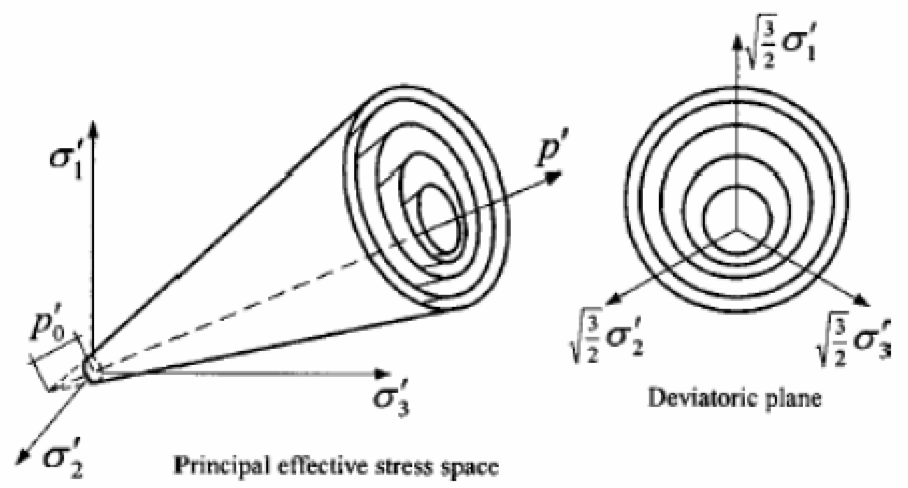

Figure 5.2. Conical yield surface in principal stress space and deviatoric plane (Prevost 1985; Parra, 1996 and Elgamal *et al.,* 2002)

5.3.2. DEEPSOIL - Nonlinear

DEEPSOIL graphical user interface is composed of 6 stages/windows for nonlinear analysis and intuitively guides the user from the beginning to the end of the site response analysis.

- *Analysis type selection:* First step is selection of analysis type. The user selects either Frequency domain analysis which is further divided into Linear/Non-linear. User should also choose the bedrock type and how the stiffness of soil layers will be defined (either in shear wave velocity or as shear modulus).
- *Define soil profile/properties:* This stage defines the soil profile and soil properties. In addition, the units of the input data will be selected. Another input is the water table location.

- *Analysis control:* Analysis control stage allows selection of step control scheme for time domain analysis
- *Motion control:* Input motion and layers for output display will be selected.
- *Viscous damping formulation / optimum modes selection:* The type of viscous damping formulation and optimum modes/frequencies for each stage is selected. This window is unique to DEEPSOIL. This window will help control the introduction of numerical damping through frequency dependent nature of the viscous damping formulation.
- *Output:* Various outputs can be visually displayed / printed / exported to a text file. The outputs of DEEPSOIL are acceleration / strain / stress time histories, response spectrum, Fourier amplitude spectrum, Fourier amplification ratio spectrum. In addition, PGA profile can be displayed. The column displacement time history can be animated after performing the time domain analysis.

DEEPSOIL incorporates extended hyperbolic model. Modified hyperbolic model, developed by (Matasovic 1993), is based on the hyperbolic model by Konder and Zelasko (1963), but adds two additional parameters Beta and s that adjust the shape of the backbone curve ξ. There is no coupling between the confining pressure and shear stress. DEEPSOIL extends the model to allow coupling by making γ_r (reference strain) confining pressure dependent (Hashash and Park 2001). This model is termed extended hyperbolic model.

5.3.3. NERA

In 1998, the computer program EERA (Equivalent-linear Earthquake Response Analysis) was developed in FORTRAN 90. In 2001, the implementation principles used for EERA were applied to NERA, a nonlinear site response analysis program based on the material model developed by Iwan (1967) and Mroz (1967). NERA stands for Nonlinear Earthquake Response Analysis. EERA and NERA's implementations take full advantages of FORTRAN 90 and spreadsheet program Excel.

There are four basic commands in the NERA pull-down menu:

1. *Process Earthquake Data* - Read and process earthquake input motion (input/output in worksheet *Earthquake*)

2. *Calculate step-by-step* - Read profile, material curves, and execute the main iterative calculation (input/output in worksheet Iteration)

3. *Calculate Output*

- *Acceleration/Velocity/Displacement* - Calculate time history of acceleration, relative velocity and displacement at the top of selected sub-layers (input/output in worksheet *Acceleration*)
- *Stress/Strain* - Calculate stress and strain at the middle of selected sublayers (input/output in worksheets *Strain*)
- *Amplification* - Calculate amplification factors between two sub-layers (input/output in worksheets *Ampli*)
- *Fourier Spectrum* - Calculate Fourier amplitude spectrum of acceleration at the top of selected sub-layer. (input/output in worksheet *Fourier*)
- *Response Spectrum* - Calculate all response spectra at the top of selected sub-layers (input/output in worksheet *Spectra*)
- *All of the above* - Calculate all the output

4. *Duplicate Worksheet* - Duplicate selected worksheet for defining new material curves, and adding new output (*e.g.*, response spectra for several sub-layers)

A NERA workbook is made of nine types of worksheets, which have predefined names that should not be changed. As indicated in Table 5.1, six of nine types of worksheet can be duplicated and modified using *Duplicate Worksheet* in the NERA pull-down menu. This feature is useful for obtaining output at several sub-layers and defining additional material curves. Table 5.1 also indicates the number of input required in each worksheet.

Table 5.1. Types of worksheets in NERA and their contents

Worksheet	Contents	Duplication	Number of input
Earthquake	Earthquake input time history	No	7
Mat I	Material curves (G/G_{max} and Damping versus strain for material type i)	Yes	Dependent on number of soil layers
Profile	Vertical profile of layers	No	Dependent on number of data points per material curve
Iteration	Results of main calculation	No	2
Acceleration	Time history of acceleration/velocity/displ acement	Yes	1
Strain	Time history of stress and strain	Yes	1
Ampli	Amplification between two sub-layers	Yes	3
Fourier	Fourier amplitude spectrum of acceleration	Yes	2
Spectra	Response spectra	Yes	2

In general, a NERA site response analysis is performed in three successive steps.

Step 1

- Define all earthquake data in worksheet *Earthquake*
- Use *Process Earthquake Data*

Step 2

- Define the soil profile in worksheet *Profile*
- Define all the material stress-strain response curves in worksheets *Mat*...
- Define the main calculation parameters in worksheet *Iteration*
- Use *Calculate step-by-step*

Step 3

- Define the input parameters in worksheets *Acceleration*
- Use *Calculate Output and Acceleration/...*
- Define the input parameters in worksheets *Strain*
- Use *Calculate Output and Stress-Strain*
- Repeat the same process for *Ampli*, *Fourier*, and *Spectra*

5.3.4. YUSAYUSA

The original version of YUSAYUSA, one-dimensional effective stress dynamic response analysis code, was developed at the University of Tokyo by Professors Towhata and Ishihara (Ishihara and Towhata, 1980). Ishihara and Dr. Yoshida improved the code by adding various features such as Ramberg-Osgood model and dynamic allocation system. YUSAYUSA-2 (Yoshida and Towhata, 2003) has the following characteristics.

- Both total and effective stress analyses are possible.
- Strain dependent nonlinear characteristics are taken into account.
- Excess pore water pressure generation under cyclic shear (dilatancy) is considered.
- Dissipation of the excess pore water pressure and transient state during it can be considered.
- Elastic base, *i.e.*, damping due to energy dissipation into semi-infinite region can be considered.

YUSAYUSA-2 analyzes horizontally layered ground composed of soil particle or mixture of soil particle and water by one-dimensional finite element method based on the Biot's equation, which was improved later by Towhata, especially on the treatment of seepage. In the one-dimensional analysis, Biot's governing equation in the horizontal direction and that in the vertical direction can be separated. Although YUSAYUSA-2 solves these equations separately, the result of each analysis is necessary for solving the other equation, therefore, result of both analyses are interacted to each other. Figure 5.3 shows flow of the analysis in YUSAYUSA-2.

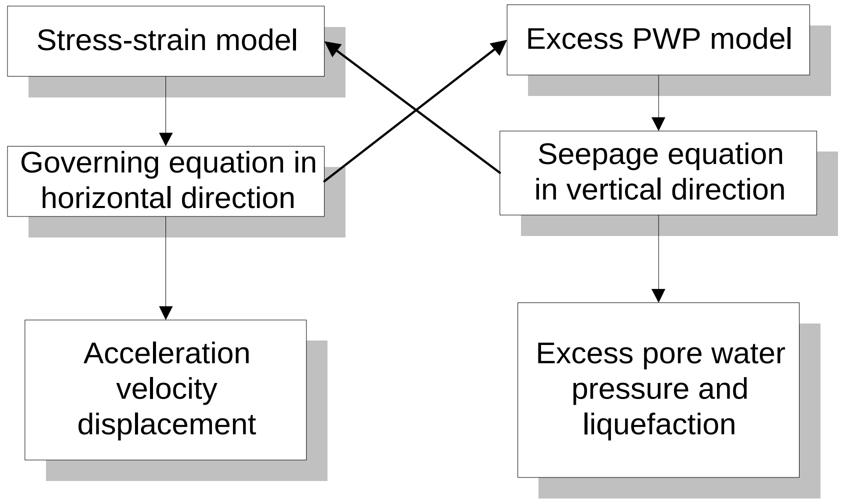

Figure 5.3. Flow of analysis in YUSAYUSA-2 (Yoshida and Towhata, 2003)

YUSAYUSA-2 employs hyperbolic model and Ramberg-Osgood model and uses Masing's rule to compute hysteresis curve. Numerical integration is conducted using the Newmark's β method. Stress-path method is used to compute excess pore water pressure generation due to dilatancy (Figure 5.4).

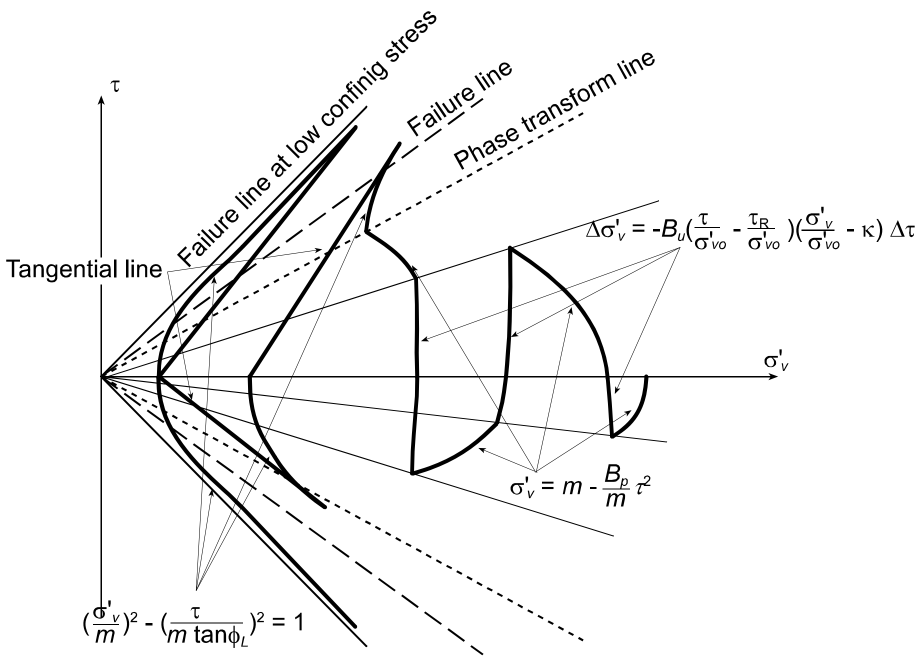

Figure 5.4. Schematic figure showing the stress path model (Yoshida and Towhata, 2003)

5.4. Identification of Nonlinear Behavior Based on Ground Motion Records

In geotechnical engineering field, it is well established by laboratory and field tests that stress – strain relationships of soils is strain dependent, nonlinear and hysteretic, especially for large shear strain levels. However, evidence of nonlinear site response in seismological observations has been observed more recently with increasing number of good quality strong motion data.

Due to the nonlinear behavior of soils, amplification factors are dependent on the intensity of shaking. This can be demonstrated by comparing the amplification factors for a soil site with respect to a reference rock site using acceleration time history data of different magnitudes representing weak and strong motions. Reference station is selected as a nearby site of outcropping rock. The amplification factors are reduced with increasing shaking intensity, resulting from reduced shear modulus and increased damping. The relationship between peak accelerations on soil sites with respect to reference rock sites is also an indicator of nonlinearity in site response. The increased nonlinearity of soft soil response at higher accelerations reduces the amplification factors.

When a suitable reference rock site could not be found in an acceptable vicinity of the soil site of interest, another technique not depending on reference site named as horizontal to vertical spectral ratio method (HVSR) can be used to assess site amplifications. Recent search results imply that the HVSR technique is sensitive to ground-motion intensity and can be used to detect and study nonlinear site response (Dimitriu *et al.*, 2000; Wen *et al.*, 2006).

Prior to studying nonlinear site response analysis, it was intended to evaluate the site response nonlinearity based on the recorded strong-motion data obtained at some recording stations during the recent major earthquakes in Turkey based on available geotechnical and strong motion data. The acceleration time histories recorded during major earthquakes (Dinar 1995 and Kocaeli 1999) in recent years at Dinar and Istanbul (Fatih, Zeytinburnu and Atakoy) strong motion stations were evaluated for estimating site response nonlinearity. The peak horizontal accelerations and spectral amplitudes recorded on soil and on nearby rock outcrop sites were compared during main shock and aftershocks and when appropriate reference rock site was not available the spectral ratio of horizontal to vertical ground motion were used to assess site response nonlinearity. The results obtained are discussed with respect to soil nonlinearity and the level of ground shaking intensity that would induce nonlinearity.

5.4.1. Dinar Case Study

The earthquake sequence that affected Dinar was composed of small to medium size foreshocks, main shock, and aftershocks. The foreshocks started on September 26, 1995 and the main shock (Ms=6.1) took place on October 1, 1995 followed by large number of aftershocks. Table 5.2 lists the data for the selected events recorded in Dinar station. The fault plane solutions indicate a normal faulting with a strike of N130E and a dip of 41°. The hypocenter of the earthquake was located right under Dinar with a focal depth of 24 km (Eyidogan and Barka, 1996; Durukal *et al.*, 1998).

A detailed geotechnical investigation composed of in-situ penetration tests; seismic wave velocity measurements by suspension PS Logging technique were carried out to determine the soil stratification and soil properties by the Dinar strong motion station (Ansal *et al.,* 1997). The ground water table is almost at the ground surface. As shown in Figure 5.5, the soil profile consisted mostly of sandy, silty clay layers with shear wave velocities ranging between 150-250 m/sec in the top 42 m. Very stiff and dense sandy clayey gravel layer with shear wave velocities around 600 m/sec was encountered below this depth (Ansal, 1999).

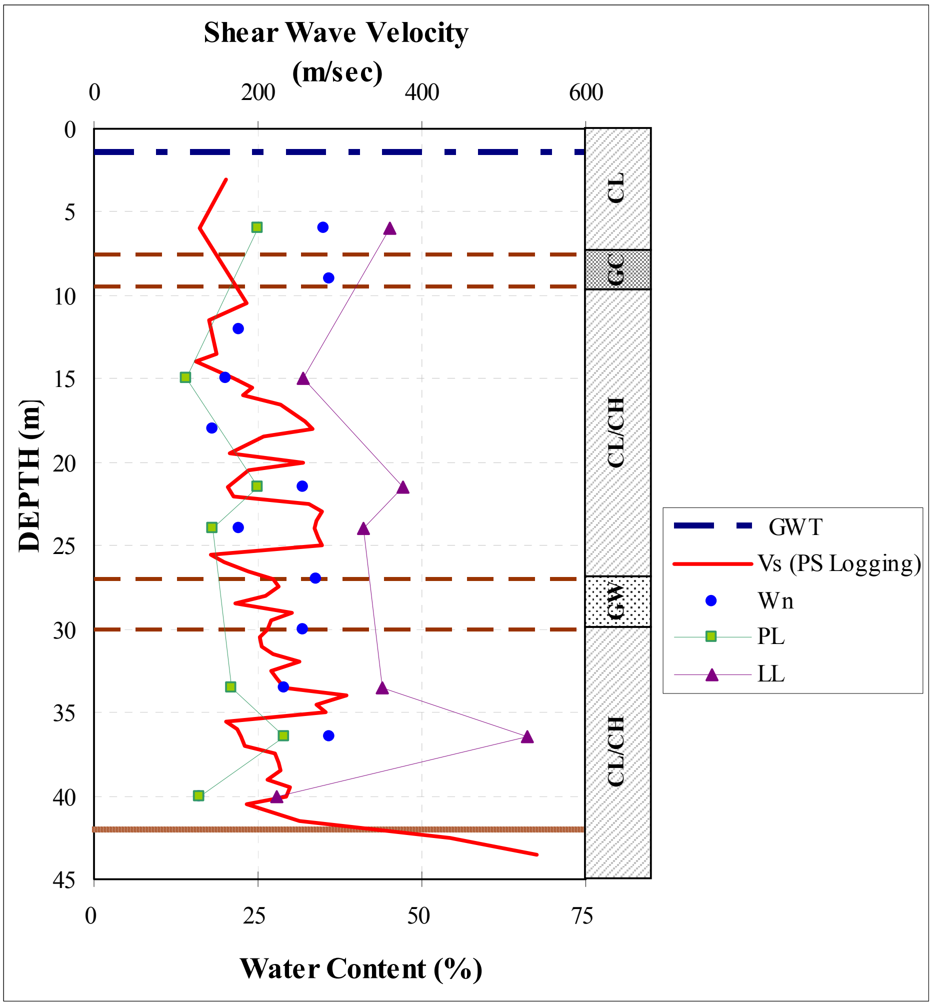

Figure 5.5. Soil profile at Dinar strong motion station

Table 5.2. Selected events recorded at Dinar station

TIME		M_L	PGA (g)	
			NS	EW
"Strong"	26/9/14:58	4.6	0.100	0.182
	27/9/14:15	4.7	0.089	0.188
	1/10/15:57	6.0	0.279	0.356
	1/10/18:02	4.9	0.214	0.116
	1/10/21:14	4.2	0.084	0.174
	3/10/7:38	4.3	0.070	0.146
	5/10/16:15	4.6	0.092	0.137
	6/10/16:15	4.4	0.090	0.170
	4/4/98/16:17	4.6	0.137	0.135
	26/9/15:18	4.6	0.100	0.182
"Weak"	26/9/15:18	4.1	0.056	0.085
	28/9/13:26	4.0	0.037	0.036

Fourier Amplitude Spectra of some events selected from Table 5.2 with magnitude range of M=4.0 to M=6.0 are shown in Figure 5.6. Shift of the fundamental frequencies to lower values can be observed with increasing magnitudes.

Typical nonlinear effects are known as deamplification of strong motion and the decrease of the fundamental frequencies of soil deposits. Deamplification of strong motion was evaluated in Dinar strong motion station data by applying the horizontal-to-vertical spectral ratio (HVSR) technique. Smoothed average spectrum of the two horizontal motions was divided by the vertical motion spectrum (Figure 5.7). This ratio only reflects site effects in the ground motion, independent of source and path. The recordings given in Table 5.2 represent 12 earthquakes (ML=4.0-6.0); PGA varies between 0.036-0.356g. In order to assess nonlinearity, selected recordings for this station were divided into two groups to represent weak and strong motions. Mean H/V spectra curves are calculated for weak (PGA<0.1g) and strong motion (PGA>0.1g). The weak (linear) and strong (nonlinear) motion responses show some differences. Between 1.45 and 4.4 Hz, the nonlinear response exceeds the linear one. Above this frequency, the average strong motion ratio stays below the average of weak motion ratio except for a very short frequency range (8-8.5 Hz). For frequencies larger than 9.5 Hz, nonlinear response drops below unity (deamplification) which may also indicate nonlinearity. As also shown in Figure 5.7, H over V ratio of events with magnitude range of M=4.0 to 6.0, shift of the fundamental frequencies to lower values can be observed with increasing excitation strength.

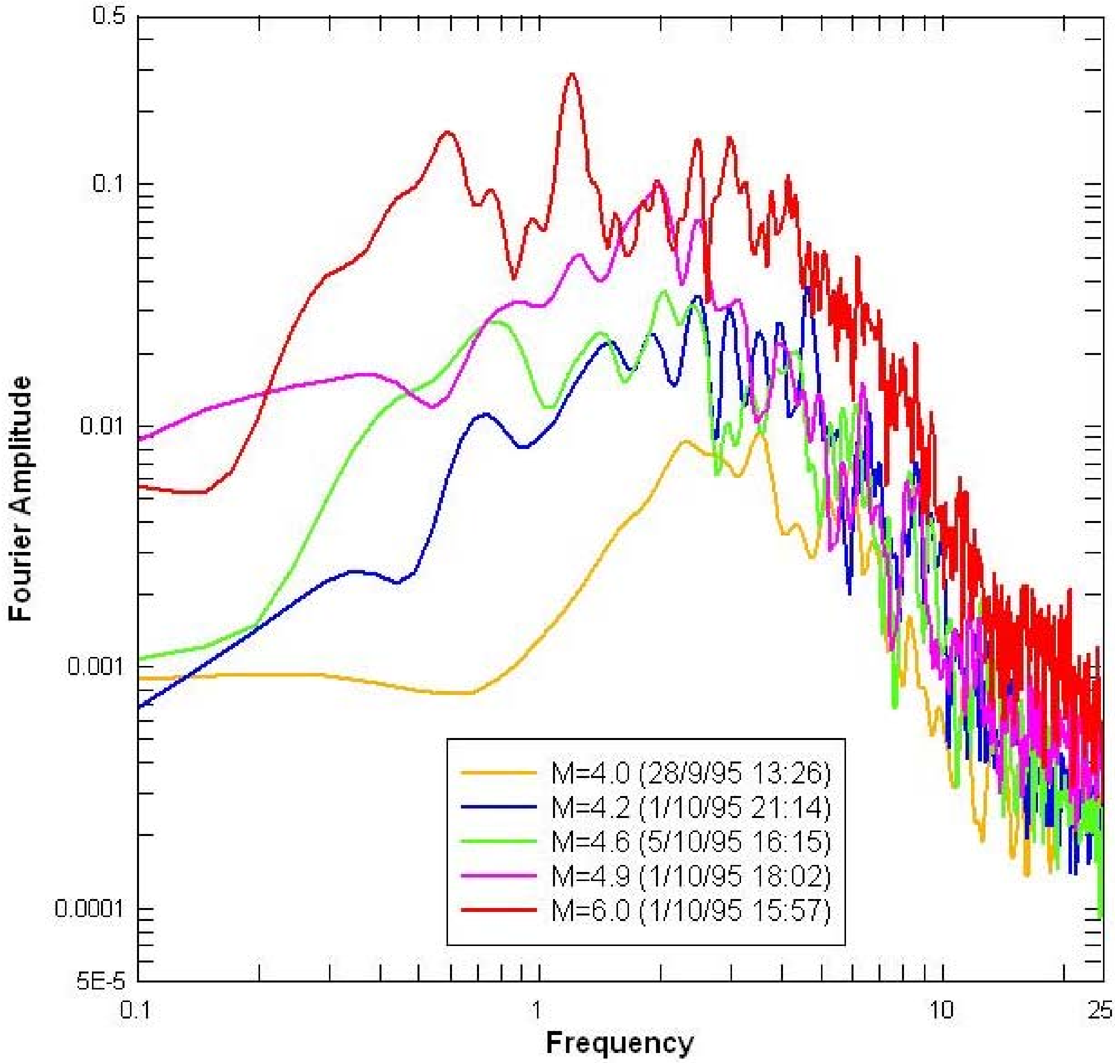

Figure 5.6. Fourier amplitude spectra at Dinar strong motion station for the main event-selected foreshock and aftershocks

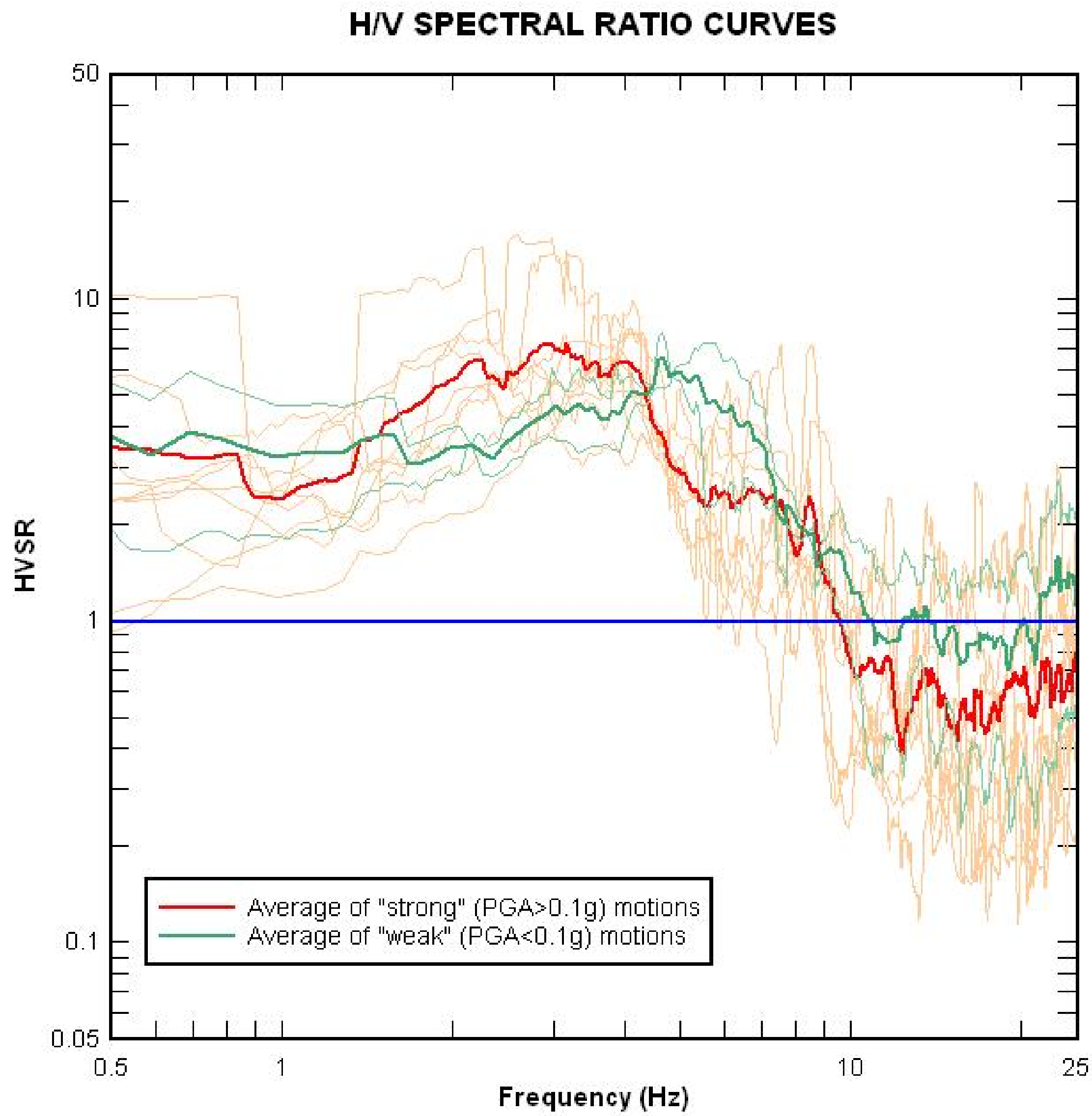

Figure 5.7. Mean HVSR curves for the strong and weak motions recorded at Dinar station listed in Table 5.2

5.4.2. Istanbul Case Study

Acceleration time histories were recorded at strong motion stations located in different parts of Istanbul during the 1999 Kocaeli Earthquake. Even though the epicenter and related fault rupture were approximately 100km away, peak ground accelerations were in the range that may induce nonlinear soil behavior at three soil stations namely Zeytinburnu (0.12g), Ataköy (0.16g), and Fatih (0.19g). The spectral ratios and peak ground acceleration ratios with respect to the reference rock site at Maslak (MSK) for these three stations for the Kocaeli Earthquake main shock (Mw=7.4) and for two aftershocks (ML=5.8 and 4.4) were calculated to determine if nonlinear site behavior can be observed.

In terms of PGA ratios only Fatih station records follow the expected decreasing trend with the increase in the magnitude (Figure 5.8). However, strong motion amplification ratios for three soil sites are below the average value of weak motions. This can be regarded as one indication of soil response nonlinearity (Higashi and Sasatani, 2000). In terms of spectral ratios, the same trend is also visible for the records obtained in Fatih station.

In terms of PGA amplification ratios as given in Table 5.3, there was no nonlinearity in the site response in Zeytinburnu and Ataköy stations however nonlinearity was observed at Fatih during the 1999 Kocaeli Earthquake main shock of 17 August 1999.

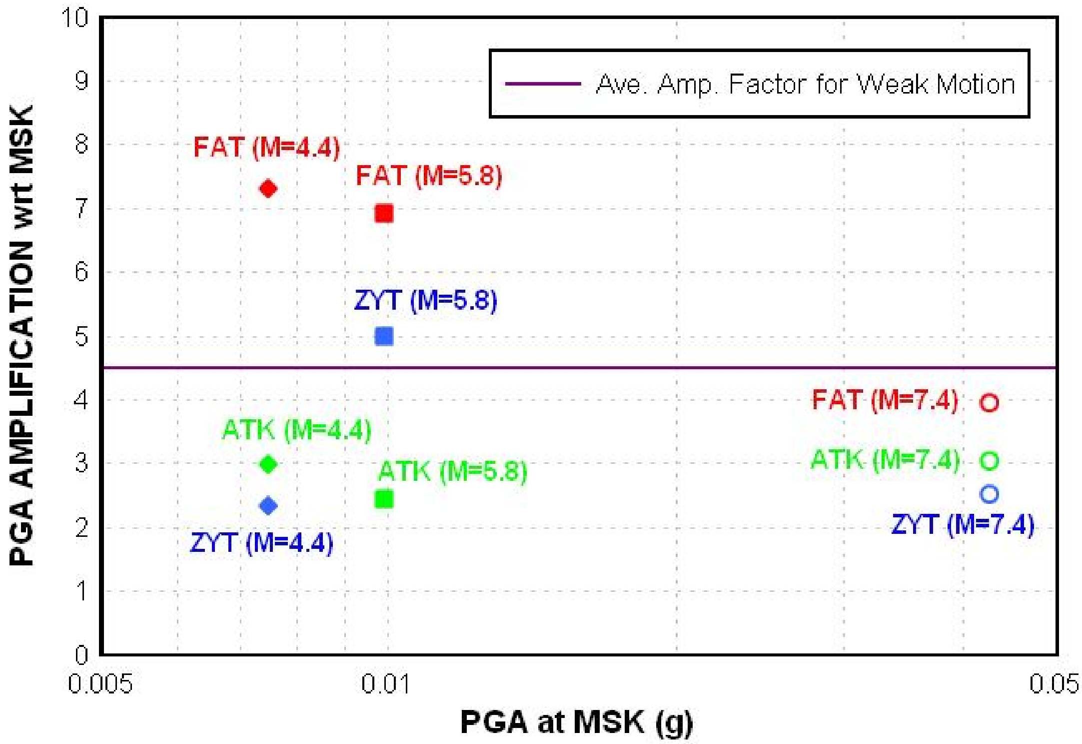

Figure 5.8. PGA amplification ratios for the Istanbul strong motion soil stations (FAT, ATK, ZYT) with respect to PGA at rock station (MSK) during main event (transparent symbols) and weak ground motion (solid symbols) records

Table 5.3. Amplification ratios (AR) in terms of PGA with respect to MSK

Station	Direction	PGA (g)	AR (M4.4)	Ratio of [AR (M7.4)/AR (M4.4)]
Zeytinburnu	NS	0.104	1.7	1.349
	EW	0.111	3.3	0.825
Ataköy	NS	0.099	2.8	0.798
	EW	0.157	3.3	1.184
Fatih	NS	0.183	7.5	0.552
	EW	0.151	7.0	0.530

Figure 5.9 shows the spectral amplification ratios for main event (strong motion) to average of the aftershocks (weak motions). Especially, at Zeytinburnu and Fatih stations in EW direction, the amplification factor for strong motion become smaller than those for weak motions. This nonlinear site response evidence cannot be observed clearly in the amplification ratio curves for Ataköy.

Even though the difference in the level of peak accelerations recorded at Ataköy (0.157g) compared to Fatih (0.183g) is not significant most likely due to the differences of site conditions nonlinear response was observed at Fatih site. The average shear wave velocities, $V_{s,30}$ for strong motion sites FAT, ATK and ZYT are computed as 287, 369 and 336 m/sec, respectively. The ATK station with the highest average shear wave velocity can be considered as the site among the others which may behave more linearly under similar shaking intensities.

5.4.3. Results of Study

The earthquake strong motion characteristics on the ground surface are affected by the local site conditions especially in the case of softer alluvial deposits. Soil layers depending on their properties could demonstrate nonlinear response even under relatively low acceleration levels thus modifying the strong ground motion on the ground surface.

Typical nonlinear effects are deamplification of strong motion and the decrease of the fundamental frequencies of soil deposits. It is possible to observe the nonlinear site response in terms of amplification ratios with respect to peak ground accelerations or spectral amplitudes calculated for weak and strong ground motion records. The spectral ratio technique can be selected as SSR or HVSR according to the absence of reference rock site.

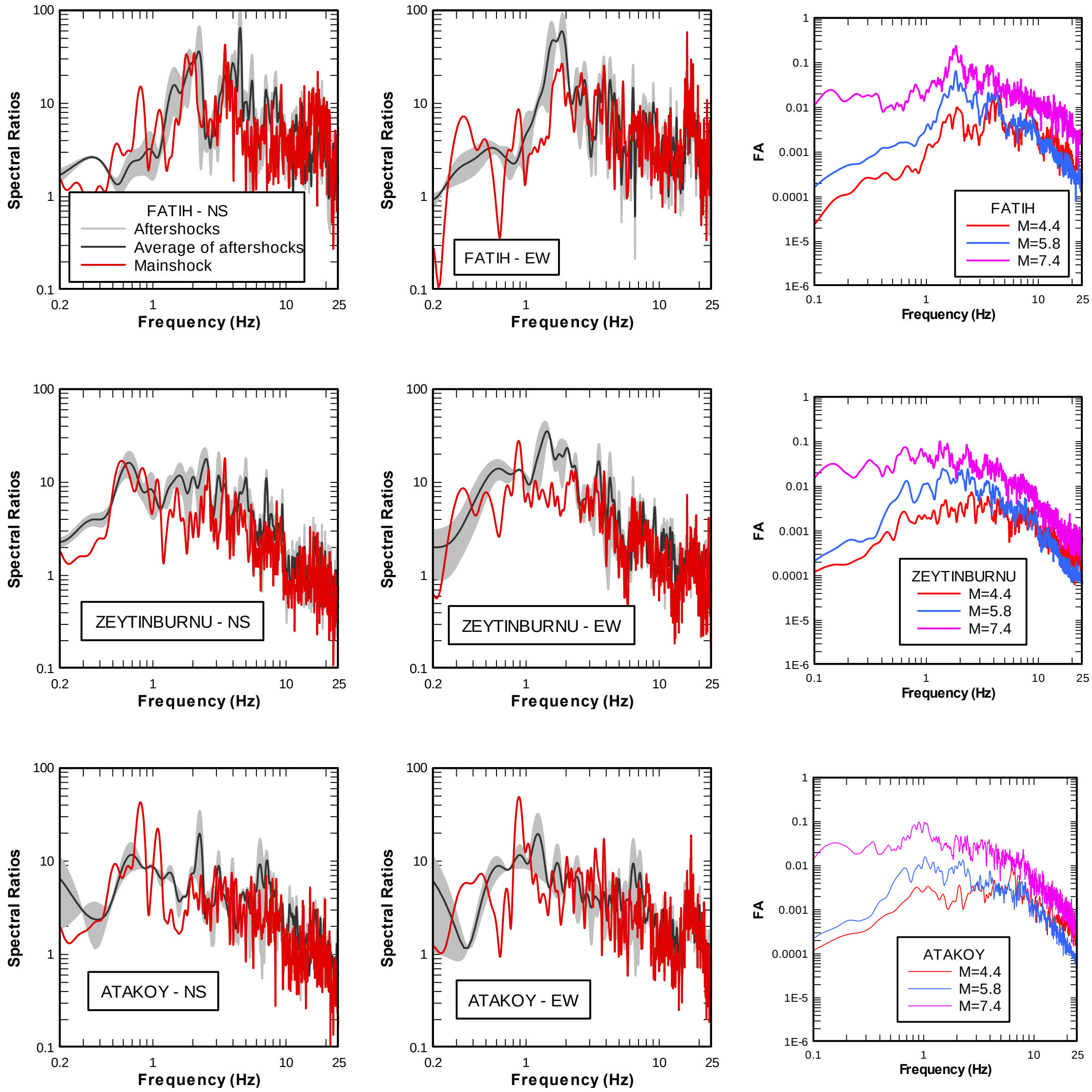

Figure 5.9. Spectral ratios for the Istanbul strong motion stations (FAT, ATK, ZYT) for strong and average of weak ground motion records with respect to Maslak reference rock site, and Fourier amplitude spectra at these stations

5.5. Identification of Nonlinear Behavior Based on Vertical Array Data

Examination of the vertical array record is one of the best methods to identify the nonlinear behavior of ground and to evaluate the accuracy of the analytical method. In this section, Ataköy vertical array where only weak – moderate ground motion were recorded, yet, and researches based on these records are reviewed.

Ataköy vertical array site consists of four downhole triaxial accelerometers located at the depths of 25, 50, 75, 140 m and one accelerometer located on the ground surface. The nonlinearity studies for this site are limited to the recorded small magnitude earthquakes. Figure 5.10 is a map showing the location of Ataköy vertical array site and the epicenter locations of selected events.

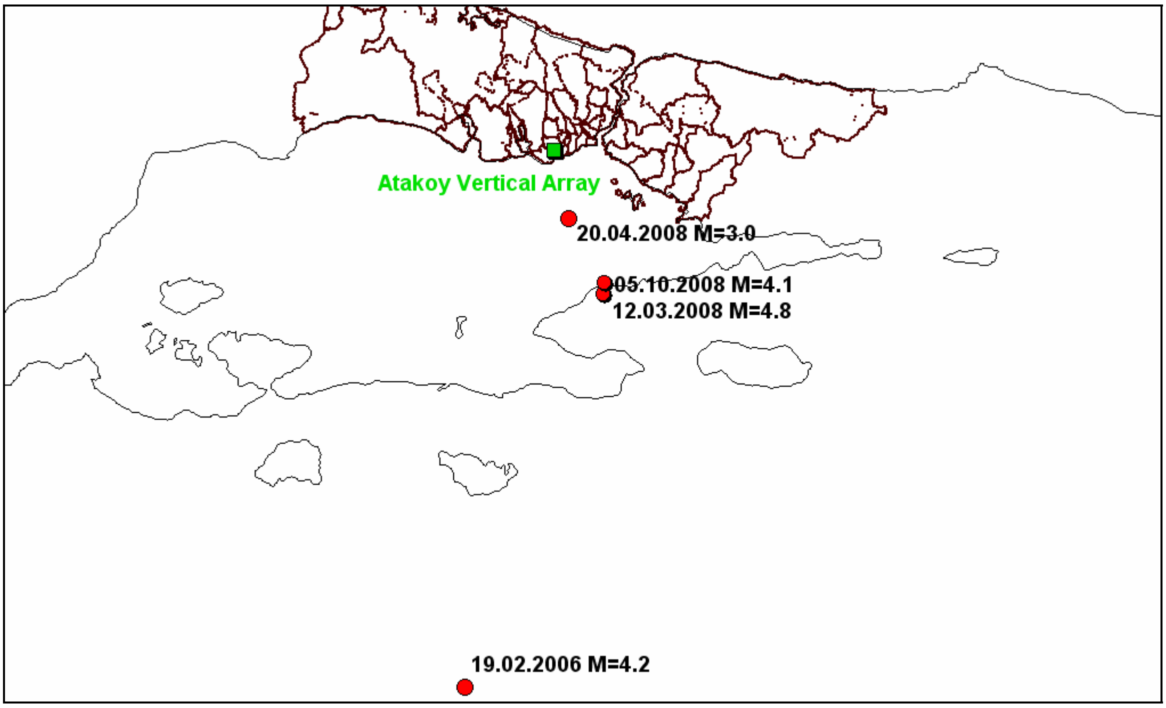

Figure 5.10. Location of Ataköy vertical array site and the epicenter locations of selected events

The recorded time histories and the response spectra of these records are given in the following figures in the order of events 19.12.2006 M= 4.2, Balikesir; 12.03.2008 M = 4.8, Yalova, PGA= 8.03 mg; 05.10.2008 M = 4.1, Yalova, PGA= 1.98 mg; and 20.04.2008 M = 3.0, Marmara Sea, PGA= 1.36 mg.

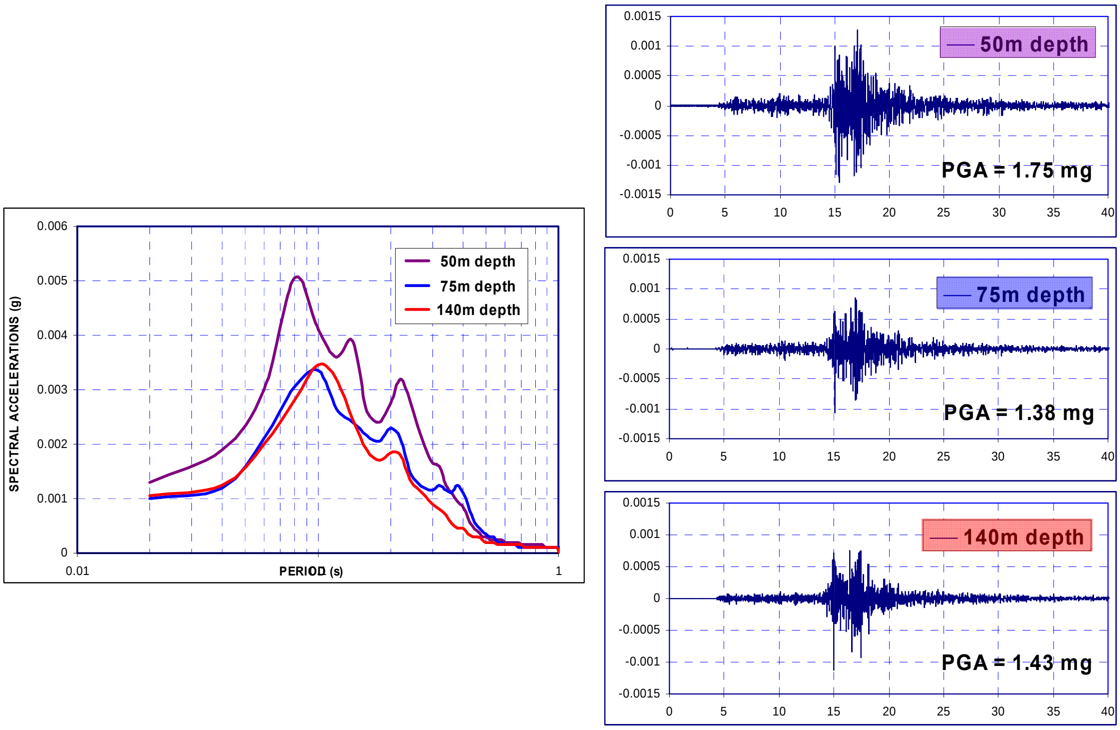

Figure 5.11. The time histories recorded at different depths and the response spectra of these records during the event: 19.12.2006 M= 4.2, Balikesir

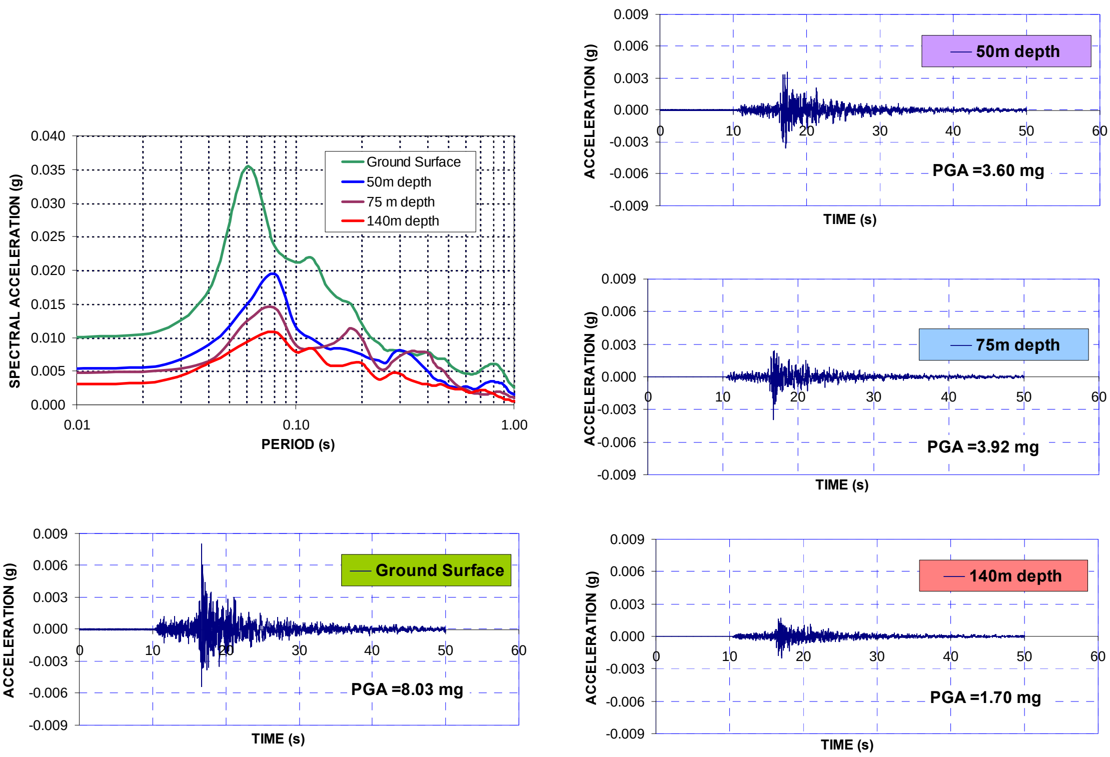

Figure 5.12. The time histories recorded at different depths and the response spectra of these records during the event: 12.03.2008 M = 4.8, Yalova, PGA= 8.03 mg

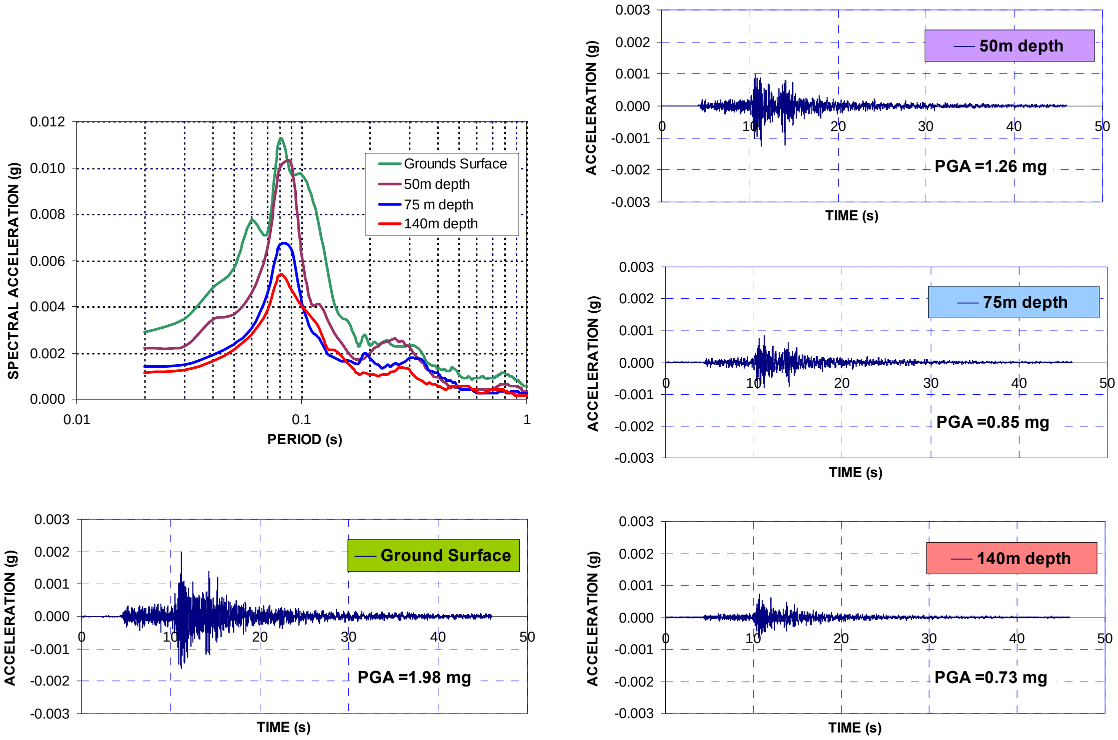

Figure 5.13. The time histories recorded at different depths and the response spectra of these records during the event: 05.10.2008 M = 4.1, Yalova, PGA= 1.98 mg

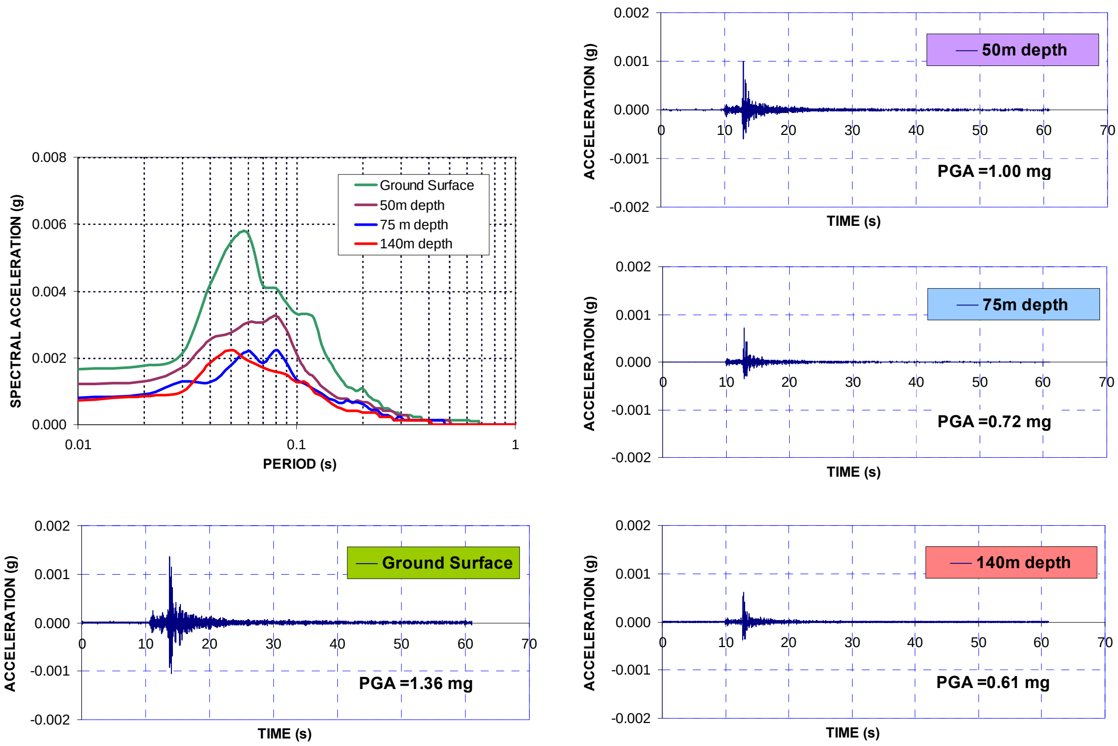

Figure 5.14. The time histories recorded at different depths and the response spectra of these records during the event: 20.04.2008 M = 3.0, Marmara Sea, PGA= 1.36 mg

Since, the recorded earthquakes are small magnitude earthquakes, amplification was observed at the record on the ground surface with respect to the downhole records, as the records get closer to the surface. No observation of deamplifying in high-frequency amplitudes was experienced, however, very slight shifts to lower frequencies of the spectral resonant peaks of the soil deposit were observed. It should be noted that although the behavior is in elastic range, the amplifications are not linear by depth. From the Figures, it is observed that the amplification is higher at the 50 m depth with respect to 75m when compared with the deepest record.

6. SITE RESPONSE ANALYSIS AND MICROZONATION METHODOLOGY

6.1. Introduction

Seismic microzonation can be considered as the process for estimating the response of soil layers under earthquake excitations and the variation of earthquake ground motion characteristics on the ground surface. The purpose of microzonation is to provide input for urban planning and for the assessment of the vulnerability of the building stock for different hazard (performance) levels (ISSMGE/TC4, 1999).

Site specific free field earthquake characteristics on the ground surface are the essential components for microzonation with respect to ground shaking intensity, liquefaction susceptibility and for the assessment of the seismic vulnerability of the urban environment. The adopted microzonation methodology is based on a grid system and is composed of three stages. In the first stage, regional seismic hazard analyses need to be conducted to estimate earthquake characteristics on rock outcrop for each cell. In the second stage, the representative site profiles should be modeled based on the available borings and in-situ tests. The third stage involves site response analyses for estimating the earthquake characteristics on the ground surface and the interpretation of the results for microzonation (Ansal *et al.*, 2004a, 2004b, 2005b, 2005c, 2007b and 2007c). In addition to the generation of base maps for urban planning, microzonation maps with respect to spectral accelerations, peak acceleration and peak velocity on the ground surface can be estimated to assess the vulnerability of the building stock (Ansal and Tönük, 2007a; Ansal *et al.,* 2004c, 2005a, 2006a, 2007a, 2009) and lifeline systems (Ansal *et al.,* 2008).

Recently, a very comprehensive site investigation study was carried out on the European side of Istanbul as part of the large-scale microzonation project for the Istanbul Metropolitan Municipality (OYO, 2007). 2912 borings (mostly down to 30m depth with approximately 250m spacing) were conducted within an area of about 182 km^2 to investigate local soil conditions. Standard Penetration Test (SPT), Cone Penetration Test (CPT), PS-Logging, Refraction Microtremor (ReMi), seismic reflection and refraction measurements were carried out at each borehole location. Samples collected in the field were tested in the laboratory to determine index and engineering properties of local soils within the investigated area. A detailed microzonation study with respect to earthquake ground shaking parameters is carried out for Zeytinburnu using part of these recently complied soil data and based on probabilistic seismic hazard scenario by Erdik *et al.* (2004) to demonstrate the applicability the methodology proposed to generate microzonation maps for urban areas and to show the effects of detailed site investigations and more comprehensive microzonation procedure.

6.2. Microzonation Methodology

6.2.1. Seismic Hazard and Earthquake Motion

The regional earthquake hazard may be based on probabilistic or deterministic approach. In the case of microzonation for urban planning it is preferable to adopt a probabilistic earthquake hazard assessment but in the case of earthquake scenarios for estimating possible earthquake damage, depending on the seismicity of the investigated region, deterministic approach can be preferable (Ansal *et al.*, 2009; Erdik *et al.,* 2004). Independent of the methodology adopted for the earthquake hazard evaluation, whether it is probabilistic or deterministic, realistic recorded or simulated acceleration time histories are needed to conduct site response analyses for the investigated area.

The results of the earthquake hazard analysis corresponding to 475 year return period are calculated in terms of peak ground (PGA) and spectral accelerations (SA) at T=0.2s and T=1.0s periods to be used for microzonation for each cell in Zeytinburnu.

Hazard compatible acceleration time histories (in terms of expected fault type, fault distance, and earthquake magnitude) are compiled (PEER, 2009) and site response analyses are performed using as many acceleration time histories as possible. It was demonstrated by Ansal and Tönük (2007b) and it will be shown in this study again that if limited number of input acceleration time histories (*e.g.,* 3 records as specified in some earthquake codes) are used even with scaling to the same PGA amplitudes for site response analysis, the results in terms of PGA and ground shaking intensity can be different for different sets of input acceleration time histories. The time histories can be real earthquake acceleration records, or alternatively can be calculated using simulation models. In case of using real acceleration time histories PGA scaling approach is adopted. It is preferable to conduct large number of site response analyses using different input acceleration time histories to eliminate the differences that are observed between different sets (Ansal and Tönük, 2007a, 2007b) and also to take into account the variability due to the earthquake characteristics.

In Zeytinburnu case, all available previously recorded acceleration time histories compatible with the earthquake hazard assessment in terms of probable magnitude, distance and fault mechanism are selected as input outcrop motion. Ground motion sets are downloaded from PEER website. The criteria used in the selection included earthquakes with a magnitude range of Mw = 7.0-7.4 and strike slip mechanism, and site conditions with NEHRP (BSSC, 2001) site classification of B/C boundary and source distance of 20-30km.

The input acceleration time histories are scaled with respect to the peak accelerations determined from regional seismic hazard study since this approach is observed to be practical and give consistent results as shown by Ansal *et al.* (2006b). For Zeytinburnu case, 24 scaled acceleration time histories are used as input motion for site response analyses by Shake91 (Idriss and Sun, 1992) and the average of the acceleration response spectra on the ground surface are determined to obtain the necessary parameters for microzonation. Selected time histories scaled with acceleration values at engineering bedrock level are shown in Figure 6.1.

6.2.2. Site Characterization

The investigated region was divided into cells by a grid system of 250m×250m and site characterization was performed for each cell based on available borings and other relevant information by defining representative soil profiles. Shear wave velocity profiles were established down to the engineering bedrock with estimated shear wave velocity of 750m/s.

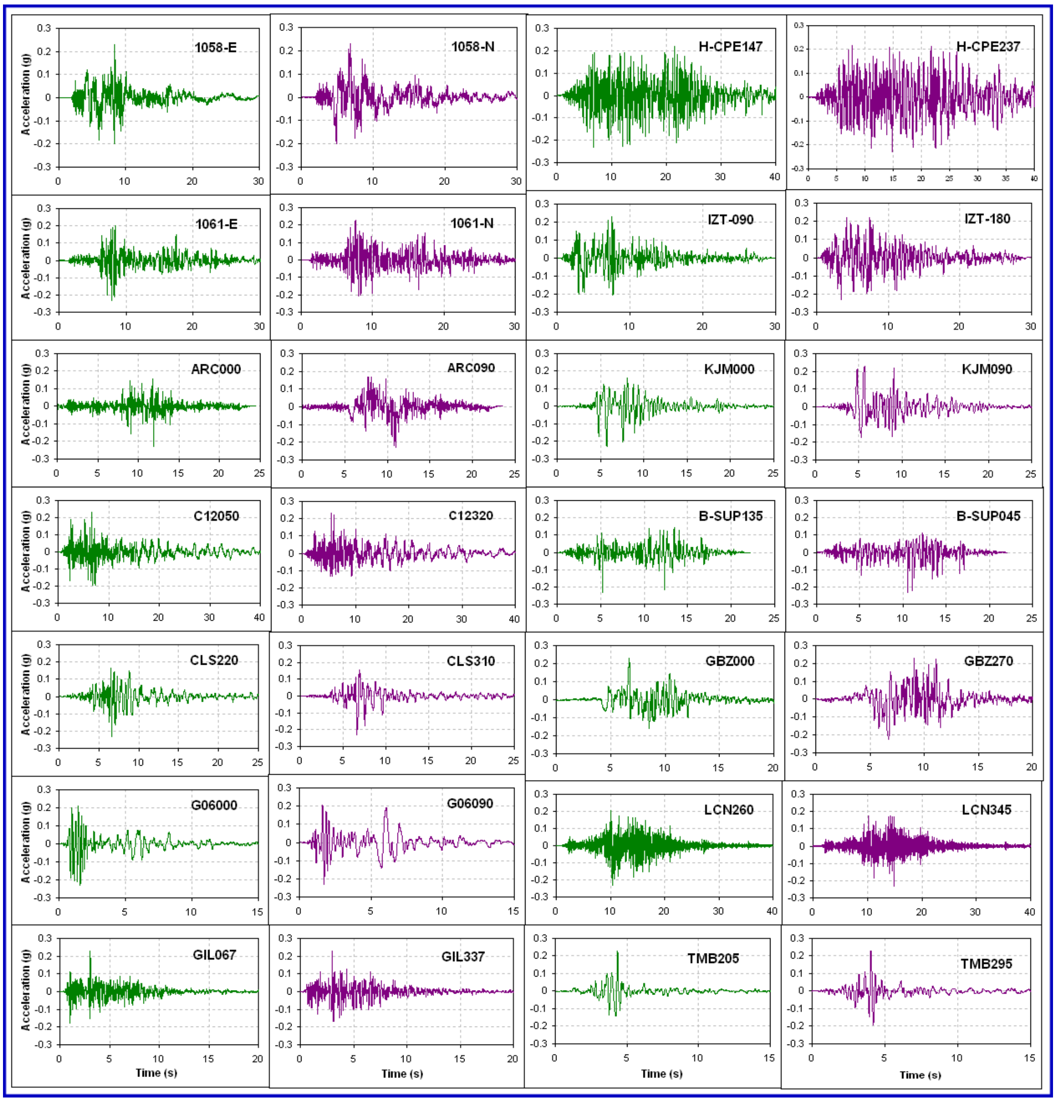

Figure 6.1. PGA scaled acceleration time histories used as input motion in site response analysis

Typically, representative soil profiles for each cell where one or more borehole data are available are generated by considering the most suitable borehole, and for the cells with no available borehole information, representative soil profiles are selected from the neighboring cells by utilizing the available data. Interpolations between neighboring boreholes may be performed taking into consideration the surface geology.

For the Zeytinburnu case there was at least one boring for each cell. Geotechnical data included a borehole with a depth of at least 30m for each cell where SPT, ReMi and/or PS Logging measurements and laboratory index test results are available. Geological data together with seismic measurements provided engineering bedrock (Vs > 750m/s) depths for all the cells. Variations of shear wave velocities with depth for the top 30m of soil profiles are determined from SPT blow counts using empirical relationships proposed in the literature (*e.g.* Iyisan, 1996). Shear wave velocity profiles down to the engineering bedrock are estimated based on seismic wave velocity measurements. If applicable, the calculated shear wave velocity profiles are compared with respect to shear wave velocity data obtained from in-situ borehole seismic wave velocity measurements and are modified when necessary.

Typical soil profiles for Zeytinburnu are illustrated in Figure 6.2. The variation of site classification according to NEHRP yielded only C and D site classes in Zeytinburnu as shown in Figure 6.3. This is partly due to the fact that NEHRP site classification is based on relatively large ranges of average shear wave velocities.

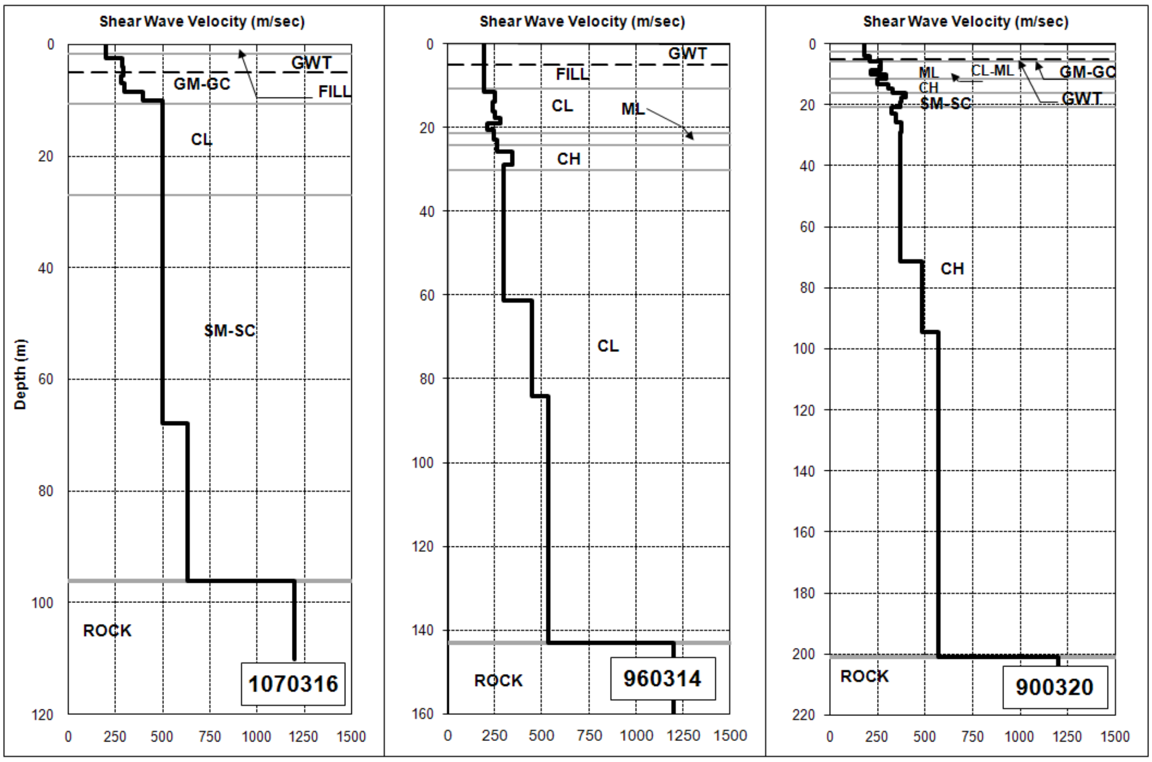

Figure 6.2. Typical soil profiles and variation of shear wave velocity with depth in Zeytinburnu

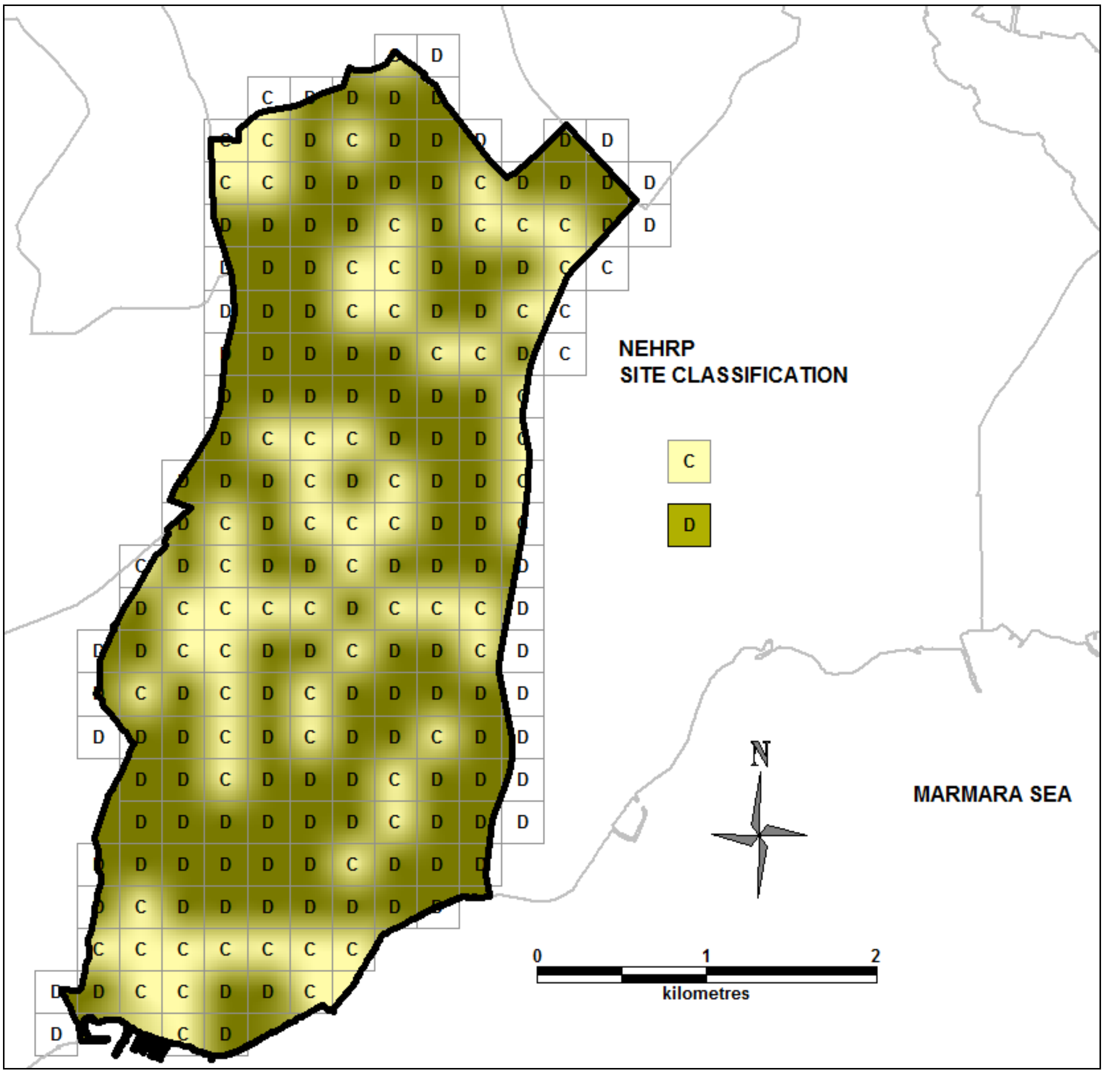

Figure 6.3. Variation of site classes in Zeytinburnu according to NEHRP (BSSC, 2001)

6.2.3. Site Response Analysis

For all soil layers in a soil profile; soil type, thickness, total unit weight, shear wave velocity, and G/G_{MAX} and damping relationships need to be provided as input to be used in site response analysis. For site response analysis, selection of strain dependent shear modulus and damping ratio relationships appropriate for that particular soil type affects results as much as soil stratification and thickness of the layers.

Earthquake characteristics (peak ground accelerations and elastic acceleration response spectra) on the ground surface are determined by conducting one dimensional site response analysis on soil profiles of each cell for all selected input motion records. All previously recorded strong ground motion time histories compatible with the earthquake hazard assessment in terms of possible magnitude; distance and fault mechanism selected as the input rock outcrop motion are scaled for each cell with respect to the peak accelerations obtained from earthquake hazard study. The average acceleration response spectra calculated on the ground surface using all scaled input acceleration time histories as input in site response analyses can be used as the response spectra corresponding to earthquake hazard scenario spectrum for each cell.

Studies on microzonation with respect to peak spectral accelerations using two different sets of three real (compatible with the earthquake hazard for Zeytinburnu that were scaled with respect to the identical peak accelerations and one set of three simulated (compatible with the time dependent earthquake hazard spectra) acceleration time histories reveal that independent than the scenario selected, acceleration time histories used in site response analysis, in other words source characteristics are very important. Acceleration time histories recorded during same or different earthquakes on different site conditions may be very different and can introduce significant variability in engineering applications and to estimations of different earthquake characteristics. One approach is to adopt a probabilistic interpretation of the calculated elastic acceleration response spectra from all site response analyses using as much as possible number of real input acceleration records obtained on compatible tectonic, seismic and site conditions (Ansal and Tönük, 2007b). This approach has the advantage of defining the hazard level in accordance with the purpose of the microzonation.

6.3. Seismic Microzonation with respect to Ground Motion

In assessing the ground shaking intensity the purpose is to estimate the relative effects of local site conditions on the level of ground motion characteristics. Therefore all available data from site characterization such as equivalent shear wave velocity (V_{s30}) as well as results of site response analyses conducted for each cell should be evaluated together to achieve realistic and consistent results. The empirical amplification relationships such as the one proposed by Borcherdt (1994) enables the estimation of site-specific peak spectral accelerations based on equivalent (average) shear wave velocities (V_{s30}) measured or estimated for the top 30m of soil profile. Site response analyses using

Shake91 (Idriss and Sun, 1992) yields acceleration time histories on the ground surface to estimate peak ground acceleration as well as elastic acceleration response spectrum on the ground surface. Peak ground velocities on the ground surface were determined by integration of acceleration time histories. The results obtained were mapped using GIS techniques by applying linear interpolation among the grid points, thus enabling a smooth transition of the selected parameters. Soft transition boundaries are preferred to show the variation of the mapped parameters. More defined clear boundaries were not used due to the accuracy of the study. This allows some flexibility to the urban planners and avoids misinterpretation by the end users that may consider the clear boundaries as accurate estimations for the different zones.

Site response analysis, whether it is conducted by Shake91 (Idriss and Sun, 1992) or using similar programs can sometimes yield relatively high spectral amplifications or low peak ground acceleration values depending on the thickness of the deposit, estimated initial shear moduli, and on the characteristics of the input acceleration time histories. Even though the amplification relationships by Borcherdt (1994) are more empirical, the spectral accelerations calculated using equivalent shear wave velocities can be more consistent compared with the selected soil profiles.

The ground shaking intensity microzonation map that should reflect the estimated relative shaking intensity levels is based on the combination of two parameters: The peak spectral acceleration at short period range calculated from Borcherdt (1994) using V_{s30} is adopted as one microzonation parameter and average spectral acceleration calculated between the 0.1s and 1.0s periods using the average acceleration spectrum determined from the results of all site response analyses conducted for each cell is adopted as the second microzonation parameter.

The peak spectral acceleration for the short period (T=0.2 sec) were determined based on average (equivalent) shear wave velocity using the empirical relationship proposed by Borcherdt (1994);

$$S_a = F_a S_s \tag{6.1}$$

where S_S is the spectral acceleration at T=0.2s on the rock outcrop obtained from the seismic hazard analysis. The spectral amplification factor, F_a was defined based on the average shear wave velocity V_{s30}.

$$F_a = \left(760/V_{s30}\right)^{m_a} \tag{6.2}$$

where;

$$m_a = \begin{cases} -PGA + 0.45 & : 0.1g < PGA \le 0.2g \\ -1.5PGA + 0.55 & : 0.2g < PGA \le 0.4g \\ -0.05 & : PGA > 0.4g \end{cases} \tag{6.3}$$

where PGA is the peak ground acceleration at the rock outcrop estimated based on the seismic hazard analysis.

The second approach adopted was to conduct one dimensional site response analysis using Shake91 (Idriss and Sun, 1992) to determine peak ground accelerations and elastic acceleration response spectra on the ground surface. For each soil layer in the soil profiles, total unit weight, thickness, shear wave velocity, and G/G_{max} and damping relationships are provided as input. The strain dependent relationships used for in the site response analysis are summarized in Table 6.1.

The microzonation map with respect to ground shaking intensity is calculated by the superimposition of these maps with respect to these two parameters. Superposition of empirically and analytically calculated spectral accelerations is assumed to provide a realistic assessment of the variation of site effects. The approach was developed and used for most of the seismic microzonation studies conducted in Turkey during the last decade (Ansal *et al.,* 2007c, 2007b, 2006a, 2005c, 2005b, 2005a, 2004c, 2004b; 2004a, Kılıç *et al.,* 2006).

Table 6.1. G/G_{max} and damping ratio - shear strain relationships used in site response analysis

Material No	Soil Type	Reference
1	Clay (CH) PI=60%	Vucetic ve Dobry (1991)
2	Clay (CL) PI=45%	Vucetic ve Dobry (1991)
3	Clay (CH) PI=30%	Vucetic ve Dobry (1991)
4	Clay (CL) PI=15%	Vucetic ve Dobry (1991)
5	Silt	Darendeli (2001)
6	Sand (SC-SM)	Darendeli (2001)
7	Sand	Seed and Idriss (1970)
8	Gravel	Seed and Idriss (1970)
9	Gravel	Menq (2003)
10	Rock 0-6 m	EPRI (1993)
11	Rock 6-16 m	EPRI (1993)
12	Rock 16-37 m	EPRI (1993)
13	Rock 37-76 m	EPRI (1993)

The proposed methodology for microzonation maps is based on the division of the investigated urban area into three zones (as A, B, and C) with respect to frequency distribution of the selected ground shaking parameters (Ansal *et al.,* 2004a, 2004b). The site characterizations, as well as all the analyses performed, require various approximations and assumptions and therefore, the absolute numerical values for the selected ground shaking parameters may not be very accurate and besides may not be needed for urban planning purposes. Their relative values are more important then their absolute values. In this approach, variations of the calculated parameters are considered separately and their frequency distributions are determined to calculate the 33 and 67 percentiles to define the boundaries between the three zones as illustrated in Figure 6.4. The zone A shows the most favorable 33 per cent (*e.g.,* low spectral accelerations, high average shear wave velocities), zone B shows the medium 34 per cent and zone C shows the most unsuitable 33 per cent (*e.g.,* high spectral accelerations, low average shear wave velocities). However, if the difference between 33 percentile and 67 percentile values is less than 20 per cent, the area is divided only into two zones using 50 percentile because division of the area into three zones based on relatively small differences may not be practically justifiable (Ansal *et al.*, 2004a, Studer and Ansal, 2004).

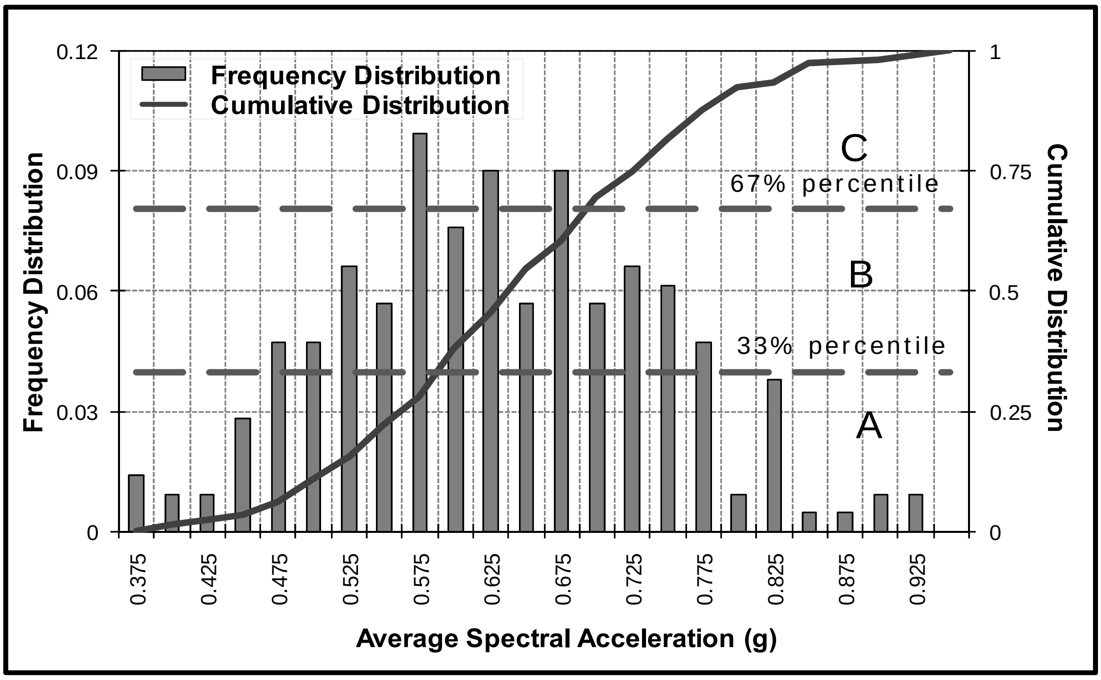

Figure 6.4. Relative microzonation approach adopted with respect to the statistical distribution

The microzonation map for Zeytinburnu with respect to average shear wave velocity generated using the relative zonation approach is presented in Figure 6.5 where V_{s30} values determined from detailed soil profiles vary in a relatively narrow range (with 33 percentile as 309m/s and 67 percentile as 362m/s) within Zeytinburnu and the distribution of V_{s30} can be represented with two zones with respect to median (50 percentile) value of 333m/s.

The microzonation with respect to equivalent shear wave velocity given in Figure 6.5 is useful in evaluating the effects of site conditions. However, it only reflects the characteristics of the existing site conditions. It is obvious that in developing microzonation maps to assess earthquake hazard scenarios consideration of probable earthquake characteristics is an essential input to achieve reliable results since the site response as well as the building vulnerability is directly related to the characteristics of the earthquake input.

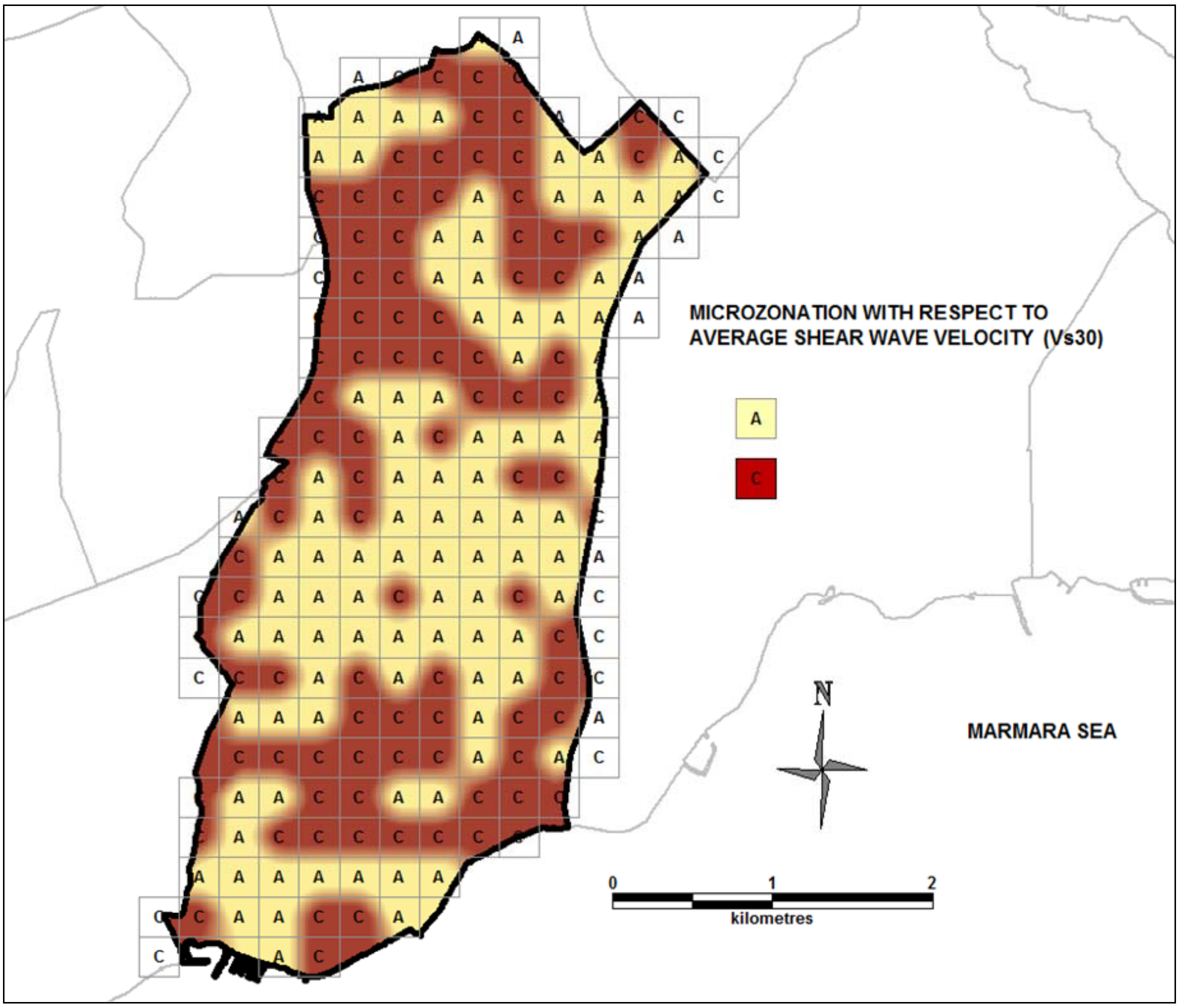

Figure 6.5. Microzonation with respect to average shear wave velocity

In the adopted methodology the first one of the microzonation parameters is the peak spectral accelerations (at T=0.2s) calculated from the empirical relationship (Equation (6.1)) proposed by Borcherdt (1994) using equivalent shear wave velocities.

Microzonation map was produced in accordance with the relative mapping in terms of three zones. For Zeytinburnu case, however, since the difference between peak spectral accelerations (at T=0.2s) calculated from Borcherdt (1994) relationships corresponding to 33 and 67 percentiles of the distribution (0.658g and 0.706g) was smaller than 20 per cent, the area was divided into two zones using 50 percentile (median) value of 0.678g as recommended by Studer and Ansal (2004).

In Figure 6.6, A_{Borch} shows the more favorable regions for lower 50 per cent where spectral accelerations are less than 0.678g and C_{Borch} shows the more unsuitable regions with higher 50 per cent with respect to peak spectral accelerations where the spectral accelerations are higher than 0.678g.

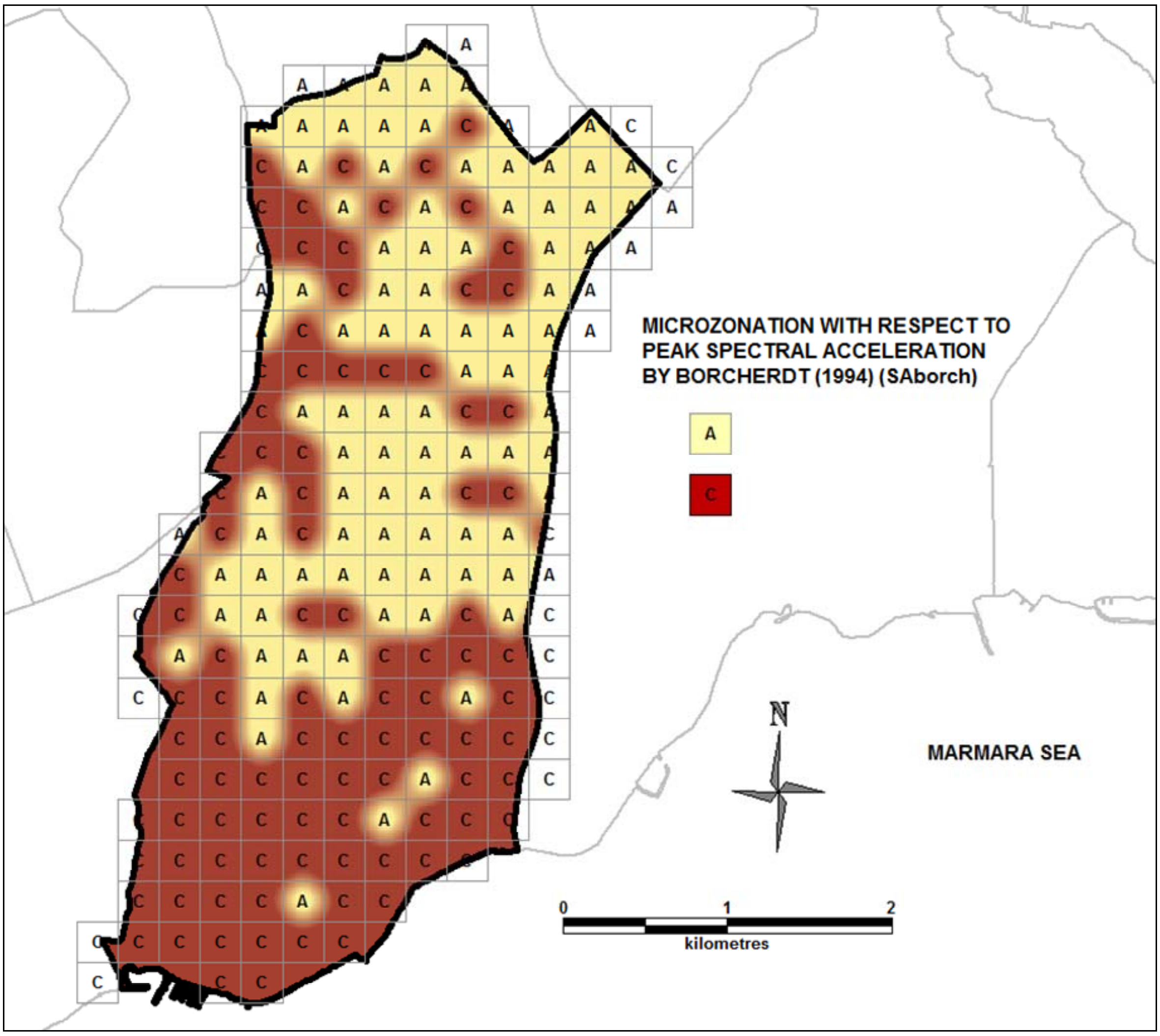

Figure 6.6. Microzonation with respect to peak spectral accelerations based on Borcherdt (1994) formulations

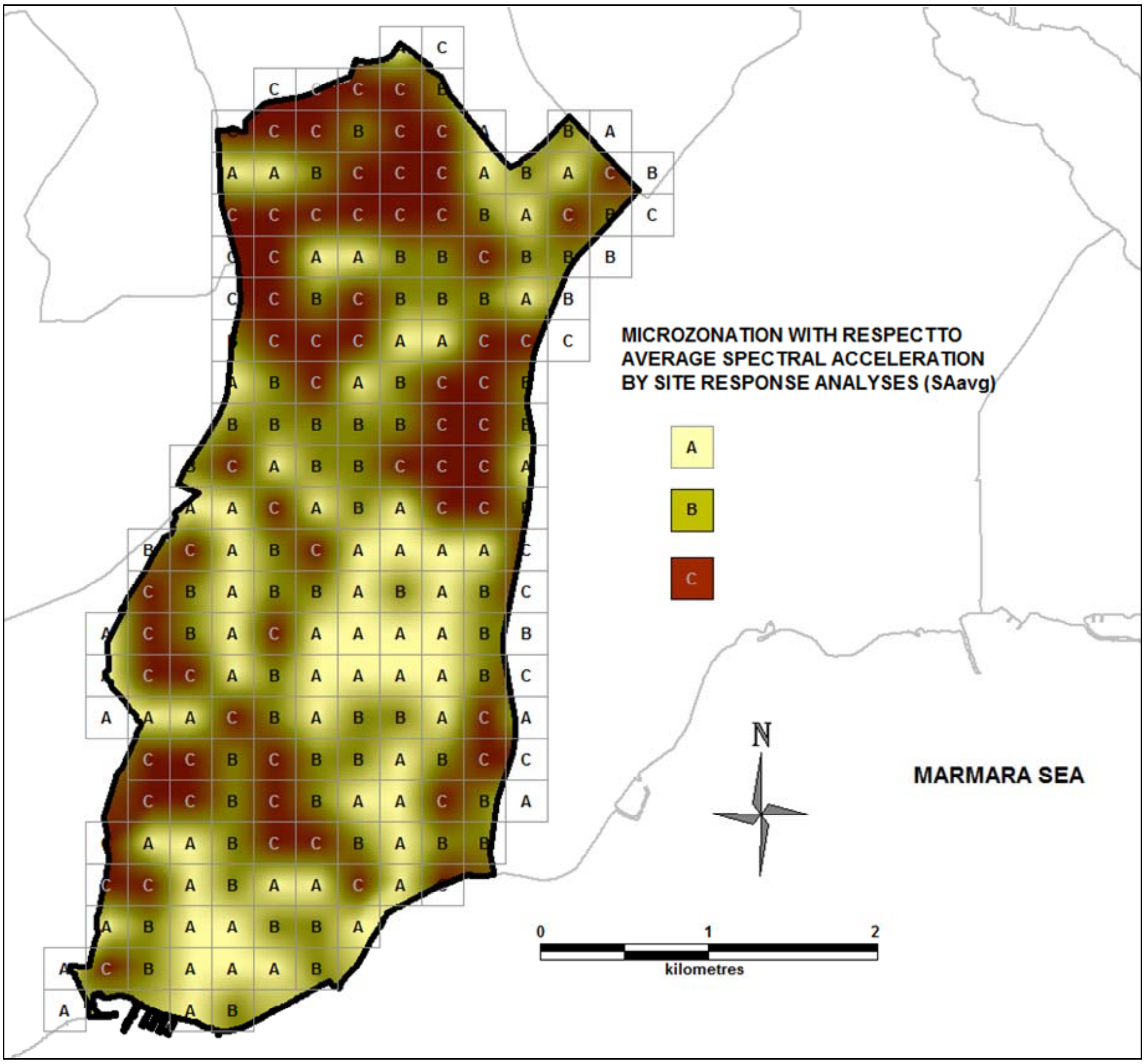

Figure 6.7. Microzonation map with respect to average spectral accelerations calculated by site response analyses

For microzonation with respect to ground shaking intensity, the second microzonation parameter adopted is the average spectral accelerations calculated between the 0.1s and 1.0s periods using the average acceleration spectra determined from the results of the all site response analyses conducted for each cell. The range of average spectral accelerations computed for the period interval of 0.1-1.0s was between 0.885g and 1.283g for Zeytinburnu case and since the difference between 33 and 67 percentiles was in the order of 45 per cent, the area was divided into three zones with respect to spectral accelerations corresponding to 33 and 67 percentiles. In Figure 6.7, A_{avg} shows the most favorable regions with lower 33 percentile and C_{avg} shows the most unsuitable regions with higher 33 percentile with respect to average spectral accelerations.

As can be seen from these maps (Figure 6.6 and Figure 6.7), there are similarities and differences between the average spectral accelerations obtained by site response analyses and the spectral accelerations calculated using Borcherdt (1994) based on equivalent shear wave velocity. The most important difference is in the range of values for both parameters. In the case of site response analysis the range of average spectral accelerations was much larger allowing microzonation with respect to three zones.

The final microzonation map is a superimposed map of microzonation map showing microzonation for average spectral accelerations obtained from site response analyses (A_{avg}, B_{avg}, C_{avg}) and microzonation map showing microzonation for short period spectral accelerations calculated according to Borcherdt (1994) (A_{Borch}, B_{Borch}, C_{Borch}) and is independent of the absolute value of the ground shaking intensity. The superimposition of zones is achieved by applying following conditions:

A_{GS} if A_{avg} and A_{Borch} or A_{avg} and B_{Borch} or B_{avg} and A_{Borch},

B_{GS} if B_{avg} and B_{Borch} or A_{avg} and C_{Borch} or C_{avg} and A_{Borch},

C_{GS} if C_{avg} and C_{Borch} or C_{avg} and B_{Borch} or B_{avg} and C_{Borch}.

Hence, the superimposed map is composed of three relative zones (A_{GS}, B_{GS}, C_{GS}) where A_{GS} shows the areas with lower ground shaking and C_{GS} shows the areas with higher ground shaking potential as shown in Figure 6.8.

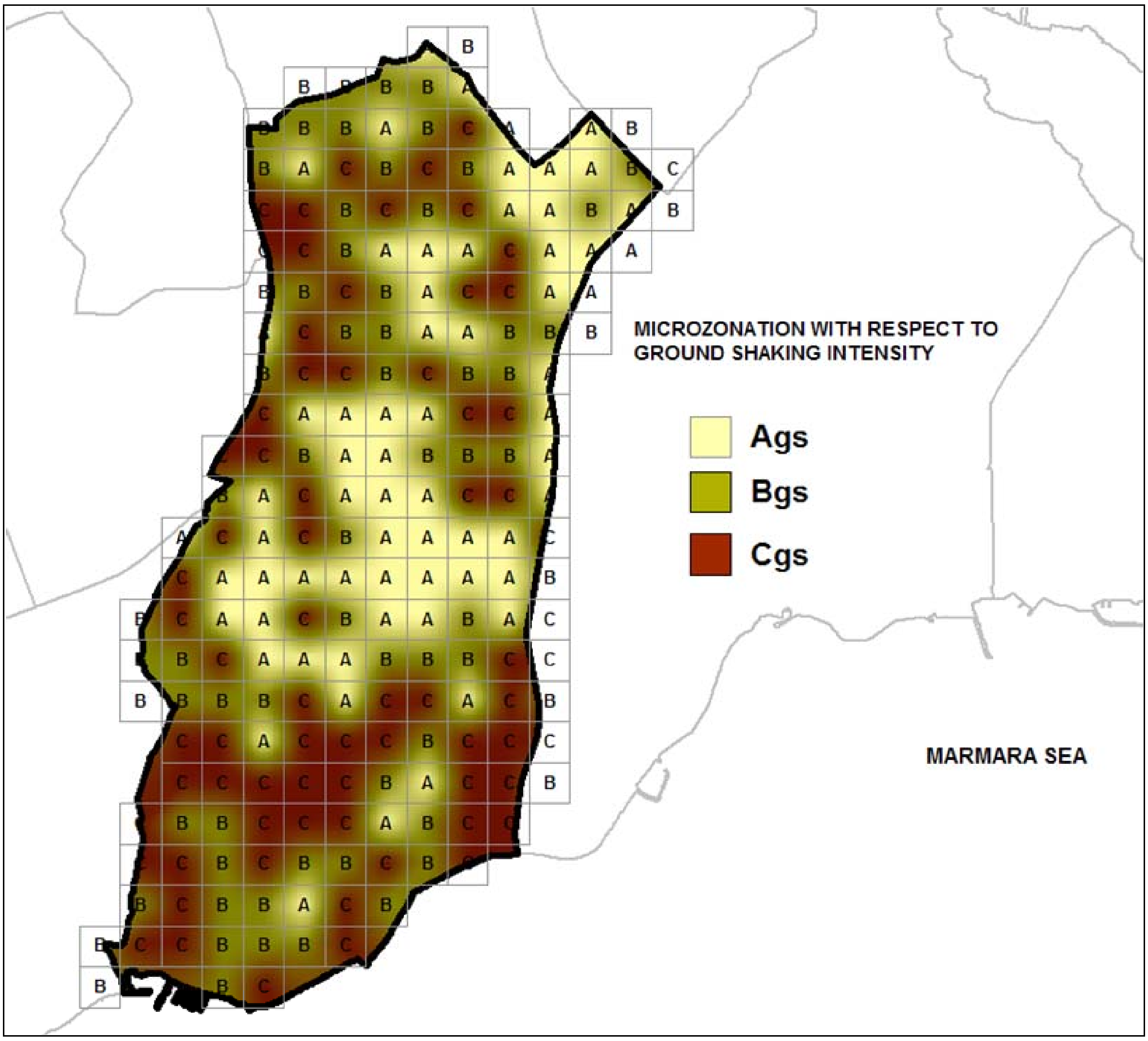

Figure 6.8. Microzonation for ground shaking intensity based on detailed site characterization and site response analysis using PGA scales 24 seismic hazard compatible acceleration time histories

6.4. Comparisons with Previous Microzonation Studies

Microzonation with respect to ground shaking intensity as given in Figure 6.8 is compared with two previous microzonation studies conducted for Zeytinburnu. The first one was the pilot study conducted within the framework of Istanbul Earthquake Master Plan (Ansal *et al.*, 2005a, Kilic *et al.*, 2005). This study was of preliminary nature and was carried out to demonstrate the applicability of the previously developed microzonation methodology (Ansal *et al.*, 2004c, Studer and Ansal, 2004) utilizing all the available boring data in the area from previous investigations. The grid size adopted was

250m×250m however, the numbers of borings were relatively limited and there were borings only in 100 cells out of 230. Representative soil profiles for each cell with no available borehole information are estimated based on the borings in the neighboring cells by utilizing the available data. Interpolations between neighboring cells were performed taking into consideration the surface geology.

In this earlier version of the microzonation procedure for ground shaking intensity (Studer and Ansal, 2004), the first approach adopted was the estimation of the peak spectral amplifications based on equivalent shear wave velocity using the empirical relationship proposed by Midorikawa (1987).

$$A_K = 68 \cdot V_{Seq}^{-0.6} \tag{6.4}$$

where A_K is the spectral amplification and V_{Seq} is the equivalent shear wave velocity, in m/sec.

The second approach adopted was to conduct one dimensional site response analysis using the Excel Subroutine EERA (Bardet *et al.*, 2000) to determine elastic acceleration response spectra on the ground surface (Ansal *et al.,* 2005a). Site response analyses were conducted using three earthquake hazard spectra compatible simulated acceleration time histories (Papageorgiou *et al.*, 1998). Microzonation with respect to ground shaking intensity from this first study is shown in Figure 6.9.

The microzonation maps shown in Figure 6.8 and in Figure 6.9 are significantly different from each other. Since the microzonation given in Figure 6.8 is based on very detailed site investigation and based on large number of site response analyses it can be considered more reliable. However, the microzonation as given in Figure 6.9 which was based on limited soil borings and mostly based on surface geology in addition the use of a slightly different and more simplified approach yielded results that can be considered to be on the unsafe side in comparison to Figure 6.8.

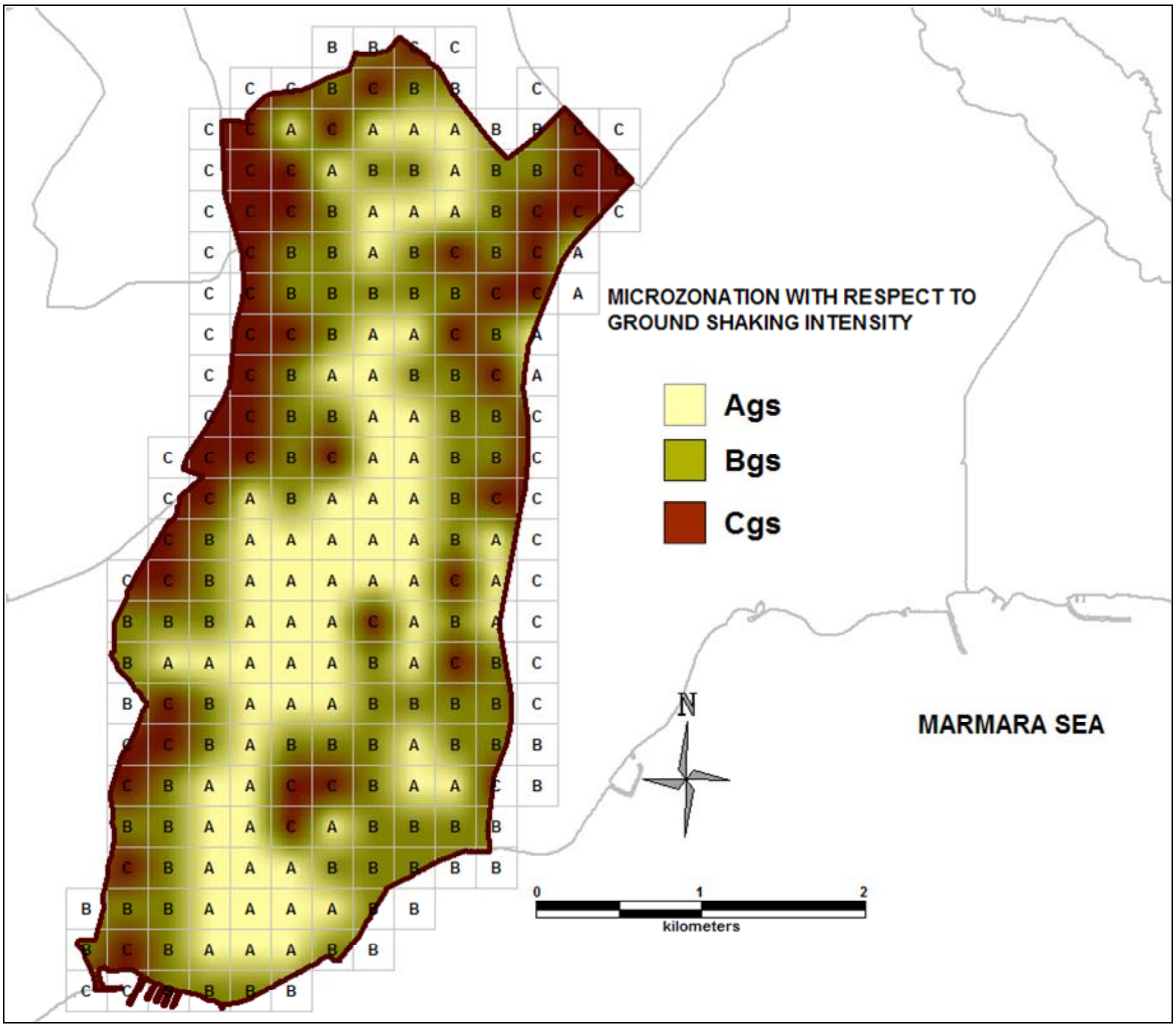

Figure 6.9. Microzonation for ground shaking intensity based on limited site investigations and limited site response analysis (Ansal *et al.*, 2005a)

The second study conducted was a part of the EU FP6 Project “LessLoss - Risk Mitigation for Earthquakes and Landslides” (Ansal *et al.*, 2006a). In this study, site characterization was identical to first study but this time site response analysis was performed for different sets of input acceleration time histories as well for large number of earthquake hazard compatible real acceleration time histories that were scaled with respect to peak round acceleration calculated for each cell at the bedrock outcrop again based on the earthquake hazard study (Erdik *et al.*, 2004). Microzonation for ground shaking intensity was estimated based on the same approach as explained in detail in the previous section (Chapter 6.3) and presented in Figure 6.10.

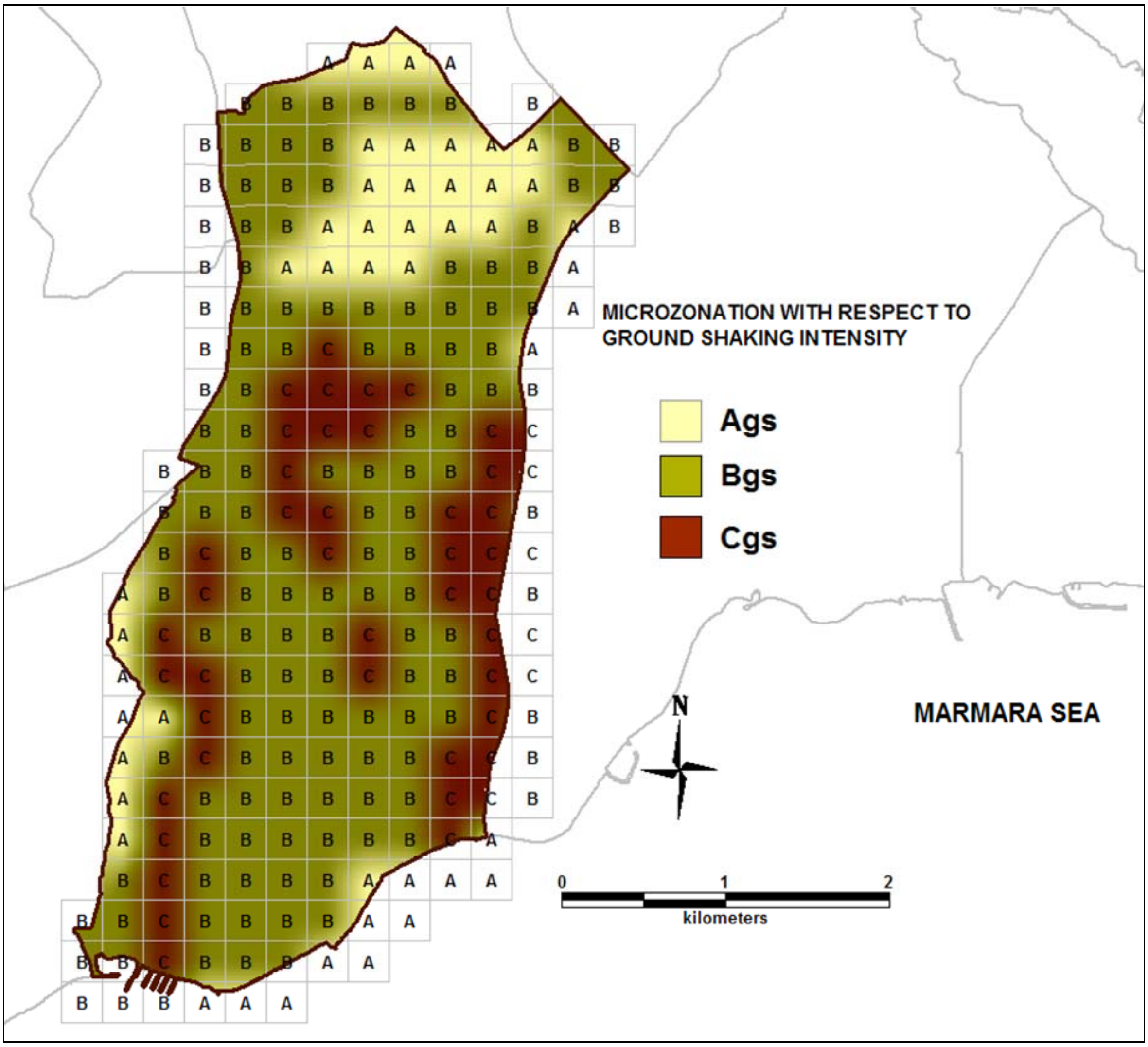

Figure 6.10. Microzonation for ground shaking intensity based on limited site investigations and site response analyses using large number of PGA scaled hazard compatible acceleration time histories (Ansal *et al.,* 2007b)

As can be observed from the comparison of Figure 6.8 and Figure 6.10, there are again significant differences between the ground shaking intensity microzonation maps and as in the previous case the results are on the unsafe side in comparison to the detailed microzonation. In this case since the methodology was almost identical and the only difference was the site characterization data set, it is clearly evident that quantity and quality of site investigations and site characterization are the main controlling factors in seismic microzonation.

6.5. Microzonation with respect to Peak Ground Acceleration

Even though microzonation with respect to ground shaking intensity can be considered as a suitable criterion for land use and urban planning, it represents only the relative level of shaking intensity. Since detailed site characterization and large number of site response analyses are performed, the results obtained in terms of average peak ground acceleration can also be used as additional microzonation maps with respect to ground shaking intensity that are relevant with respect to liquefaction susceptibility and building vulnerabilities.

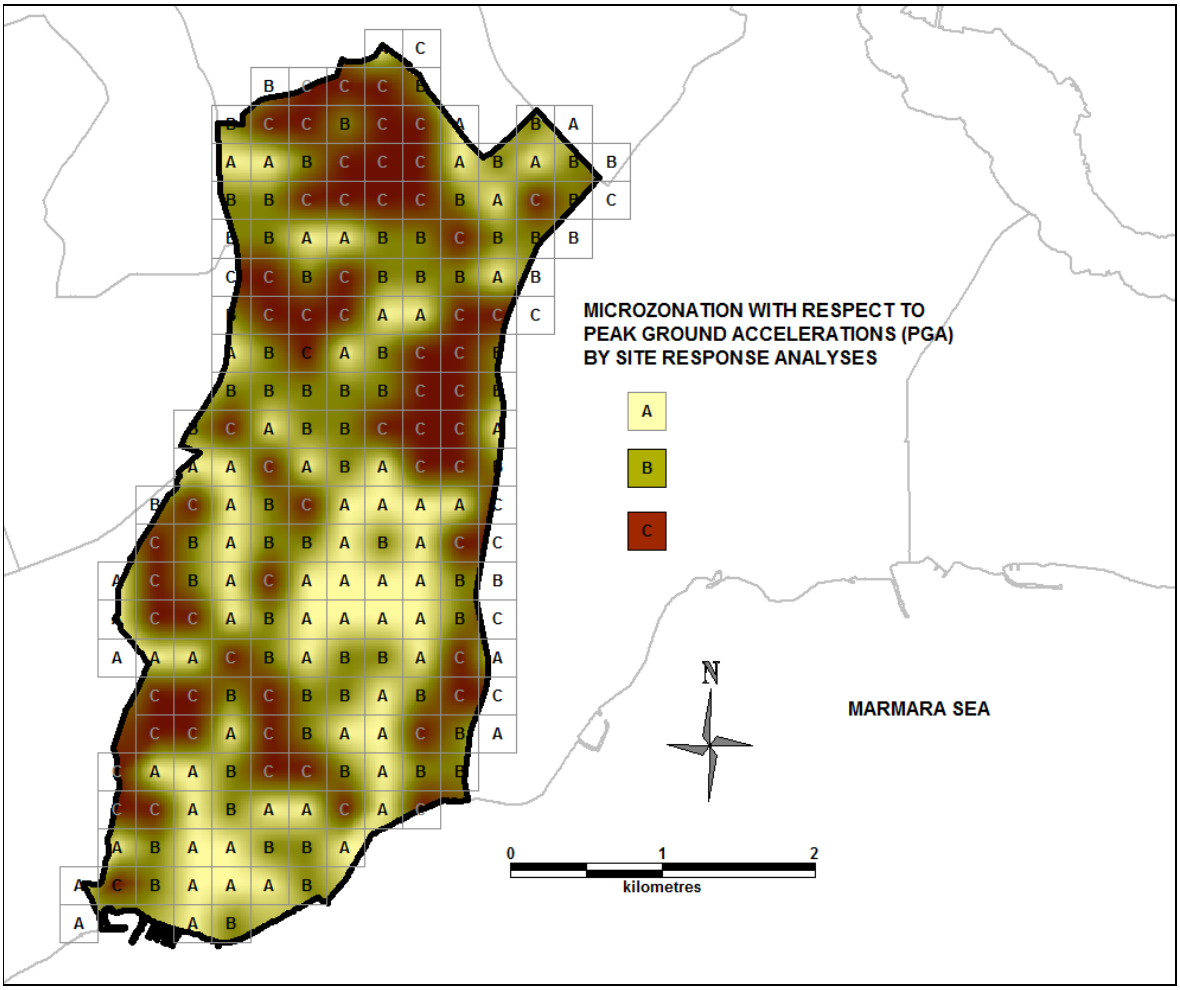

Figure 6.11. Microzonation map with respect to peak ground acceleration (PGA) based on detailed site characterization and site response analysis using PGA scales 24 seismic hazard compatible acceleration time histories

The microzonation with respect to PGA based on detailed site investigation and large number of site response analyses as shown in Figure 6.11 can be compared with the PGA microzonation maps obtained from the previous studies based on limited number of site investigations and using different sets of input acceleration time histories.

In Figure 6.12, three sets of PGA microzonation maps are given to demonstrate the importance of the input motion characteristics in the site response analysis with respect to earthquake ground motion characteristics calculated on the ground surface. The difference in the microzonation maps even though was not very significant between the two PGA microzonations calculated using different sets of real acceleration time histories, is still important as pointed out by Ansal and Tönük (2007b). The other issue is the difference in all three PGA microzonation with respect to the PGA microzonation based on detailed site characterization as given in Figure 6.11. This difference again indicates the importance of the detailed site investigations.

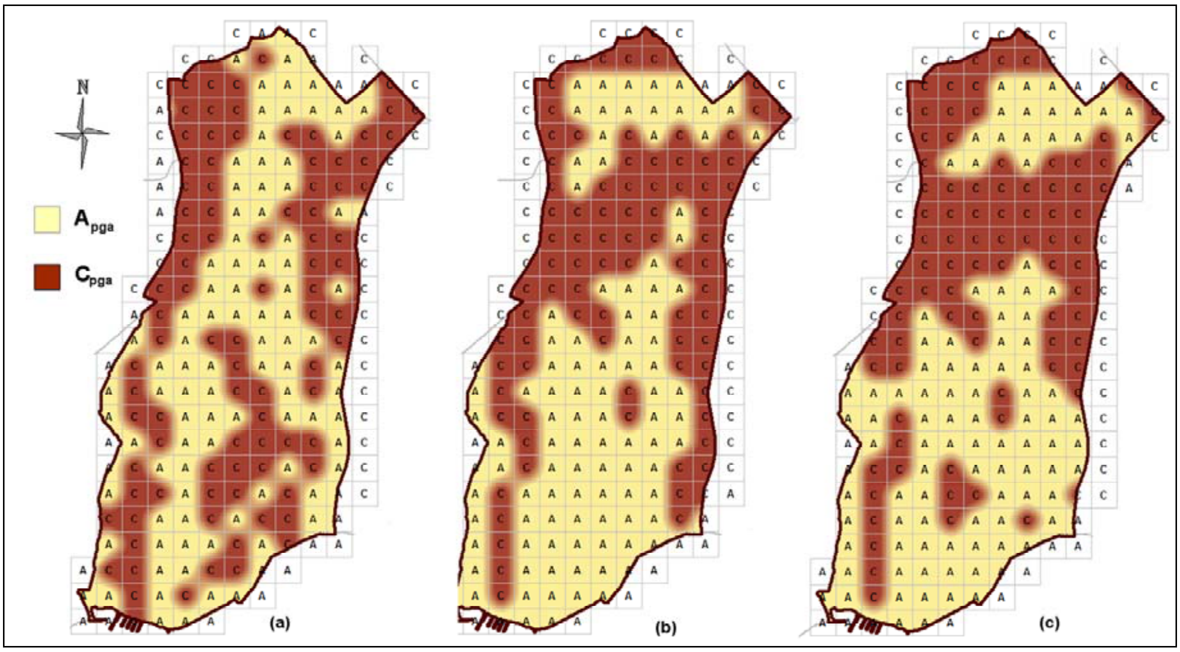

Figure 6.12. Microzonation map with respect to with respect to peak ground acceleration calculated using (a) three earthquake hazard spectrum compatible simulated acceleration time histories; (b) first set of three real acceleration time histories (c) second set of three real acceleration time histories scaled to the same PGAs estimated by the earthquake hazard study

6.6. Microzonation with respect to Peak Ground Velocity

In addition to microzonation with respect to peak ground acceleration microzonation maps can be calculated with respect to peak ground velocity calculated by the integration of acceleration time histories calculated by site response analyses. The results obtained in terms of average peak ground velocity can also be used as additional microzonation maps with respect to ground shaking intensity that are relevant with respect to building and lifeline vulnerabilities.

The peak ground velocity microzonation map as shown in Figure 6.13 is determined by the integration of the acceleration time histories calculated on the ground surface using 24 PGA scaled real acceleration time histories for the detailed site characterization as in the case of PGA microzonation given in Figure 6.11. The comparison of PGA and PGV microzonation maps is significantly different indicating the importance of the selected microzonation parameter and the resulting earthquake damage scenario estimations.

6.7. Summary and Results

Microzonation with respect to ground shaking intensity was based on two parameters: (1) average spectral accelerations calculated between the 0.1 and 1.0 s periods using the average acceleration spectrum calculated for each boring from the results of the 24 site response analysis conducted for each location, (2) the peak spectral accelerations calculated from Borcherdt (1994) using equivalent shear wave velocities. The zonation with respect to ground shaking intensity is produced with respect to three regions where zone A_{GS} shows the areas with very low ground shaking intensity, zone B_{GS} shows the areas with low to medium ground shaking intensity, and zone C_{GS} shows the areas with high ground shaking intensity.

Based on the microzonation studies conducted during the recent years, two conclusions may be drawn: 1) the detailed site investigation and related detailed site characterization is very important and essential when performing site response analyses to have reliable and more accurate information on ground shaking characteristics for microzonation, and 2) the methodology followed and the type and number of acceleration time histories used for site response analysis to generate microzonation maps can have significant effect on the final microzonation.

The last issue is the selection of microzonation parameters. It was shown that microzonation with respect to different parameters such as PGA and PGV can give significantly different microzonation maps. Therefore the selections of the microzonation parameter need to be compatible with the main purpose of the microzonation project.

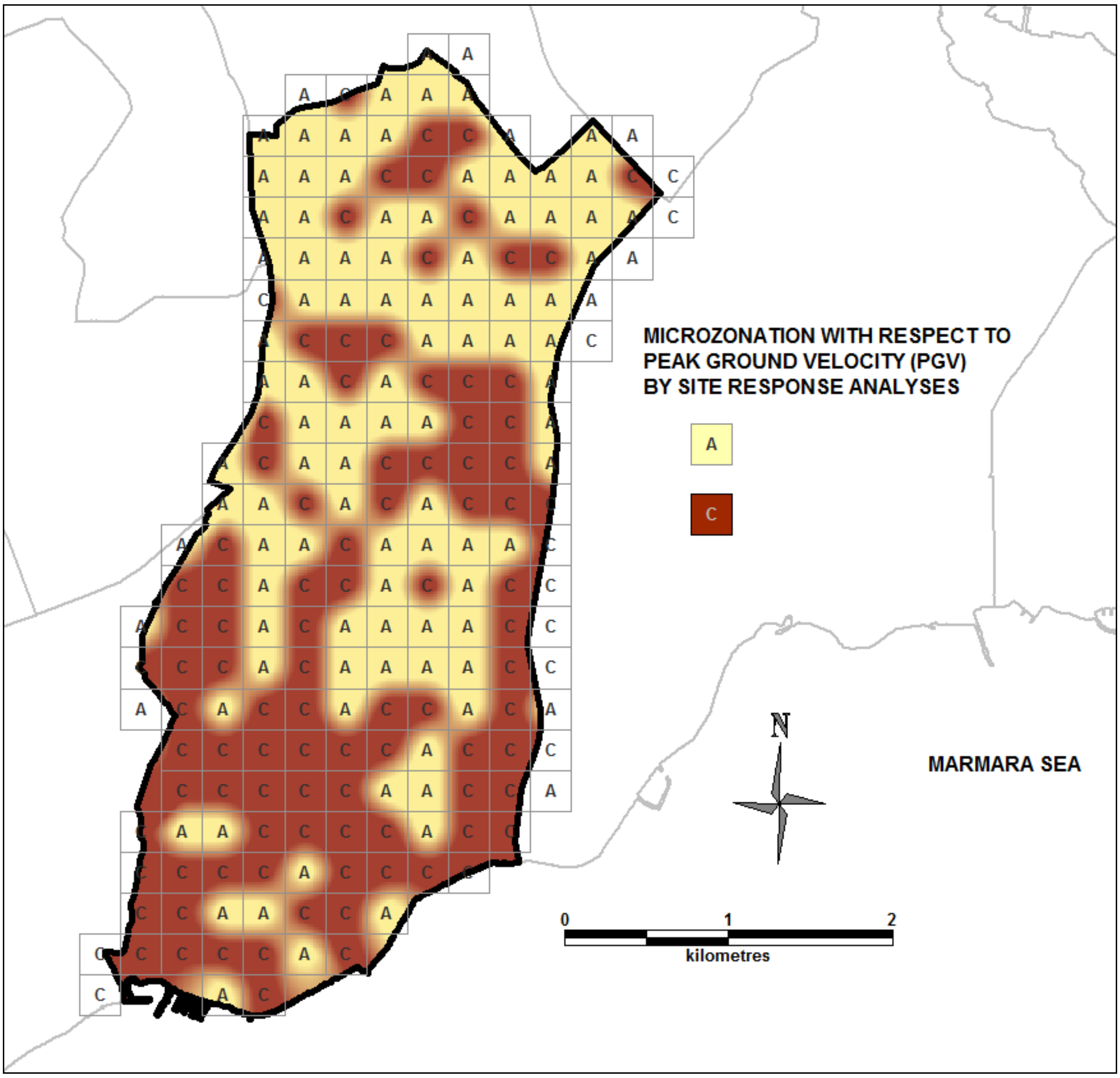

Figure 6.13. Microzonation map with respect to peak ground velocity (PGV) based on detailed site characterization and site response analysis using PGA scales 24 seismic hazard compatible acceleration time histories

7. CONCLUSIONS AND FUTURE RECOMMENDATIONS

7.1. Conclusions

Estimation of earthquake characteristics on the ground surface at the selected site to be used for the engineering analysis is the first step for any structural or geotechnical earthquake analysis. The objectives of this study were to review and improve different components of site response analyses in order to achieve a robust methodology for more comprehensive and realistic assessment. The conclusions derived from different parts of the thesis are as follows:

7.1.1. Attenuation Relations

New empirical attenuation relations have been developed for eight ground motion parameters which are PGA, PGV, root mean square of acceleration, Arias intensity, cumulative absolute velocity, maximum spectral acceleration, spectrum intensity and acceleration spectrum intensity. These engineering ground motion parameters have the advantage of describing ground-motion damage potential. These parameters were selected to be used as scaling parameters to assess how different scaling parameters affect the calculated ground motion characteristics. The need for developing new predictive relations was due to the lack of existing relations for some of the parameters selected.

These new empirical attenuation relationships proposed for the prediction of the engineering ground motion parameters on rock outcrop are based on Next Generation Attenuation (NGA) database. They are valid for magnitudes in the range of M=5.0 – 8.0 and Joyner and Boore distance with the range R_{JB}= 1.0 – 150 km. The validity of the model is demonstrated by comparison with previous studies. However, existing relationships are limited to some of the selected parameters. In general, for the parameters compared, the proposed relationships are in good agreement with previously proposed attenuation relationships. The shapes of the present equations follow a trend similar to the proposed equations.

The differences observed in the comparison of the proposed relations with other studies can be attributed to the different amounts of data that these relationships have been based on, various options to take the horizontal components, different distance definitions, soil categories, and fault-type definitions. Also in some studies alternative definitions of ground motion parameters are used as in the case of Arias intensity such as largest of the two horizontal peaks, arithmetic average, or their geometric mean, which can also explain the observed discrepancies.

7.1.2. Scaling of Input Motion

Although selected in accordance with the site-specific hazard parameters the ground motions may have different characteristics in time and frequency domain and thus play an important role in model behavior by introducing a significant scatter in non-linear dynamic response. Scaling the records for time-domain analysis to values chosen consistent with site-specific hazard parameters is a way to handle this situation. Scaling the input motion according to the most appropriate parameters so that the scatter of the model response is reduced is also important when design is required for different performance levels such as limit, serviceability *etc.* and also for displacement and acceleration sensitive structures and components (Heuze *et al.,* 2004).

Using scaling parameters determined from proposed empirical attenuation relationships, it is investigated to understand how ground motion selection and scaling affects the site response. Using 1D equivalent-linear model at selected soil profiles with pre-determined levels of earthquake hazard, first the resulting response variability was investigated when analyzed under a series of ground motion records selected as compatible with the site-specific earthquake hazard. Site specific earthquake hazard is considered as dependent on the fault type, magnitude range, and epicenter distance. Then using the same family of records, this time scaled with respect to different intensity measures such as PGA, PGV, I_a, *etc.* the analysis were repeated and the variability introduced by scaling and the effectiveness of scaling parameters was evaluated including the selection of records from different distance – magnitude ranges.

It is observed that site response analyses should be performed using a bin of input motions. The number of time histories in the bin should be large enough to provide a stable estimate of the median and to provide a smaller variation.

Presented results for two case studies are for the 10-40km distance and 6.5-7.5 magnitude ranges. The analyses were carried out using Shake91 computer code thus the obtained results directly depend on the formulation adopted in this code. In the first case study conducted, it was observed that scaling with respect to Arias intensity especially in the case of spectral accelerations at T=0.2s, yielded the most suitable scaling option among the three scaling procedures studied for conducting site response analyses if the damage parameter is selected as spectral accelerations. However, in the cases where damage parameter can be taken as peak ground accelerations (*i.e.,* liquefaction susceptibility or landslide hazard) than scaling with respect to peak acceleration should be preferred as suggested in EC8.

In the second case study, it appears that distance to the fault is one of the earthquake hazard parameters that may affect the outcome both with respect to peak ground or spectral accelerations, thus in selecting real time histories, the records need to be selected compatible with the regional hazard in terms of fault type, magnitude and fault distance.

The general parametric study on scaling with eight different scaling parameters for three damage parameters (PGA. PGV, SA_{max}) based on nine bins of magnitude and distance pairs for three soil profiles reveal that: (1) when there are enough large number of input motions, the variation of average damage parameter is not sensitive to selected magnitude – distance bin, (2) the soil profile depth is a dominating factor on the results, as the profile gets deeper the selection of scaling parameter is not important, (3) the selection of scaling parameter is closely related with the damage parameter, the variance in the PGA and SA_{max} is smaller when the input motions are scaled with respect to acceleration based parameters like PGA, Arias intensity, acceleration spectrum intensity, and the variance in the PGV is smaller when the input motions are scaled with respect to velocity based parameters like PGV, cumulative absolute velocity, (4) SD/mean is a preferable comparison parameter, for which the minimum value may indicate the best scaling parameter.

7.1.3. Site Response Analysis: Equivalent Linear Approach

Site response analysis models solve wave propagation problem for a layered, nonlinear medium. The principal characteristic distinguishing various analysis routines is that the methods differ in the simplifying assumptions that are made, in the representation of stress–strain relations of soil and in the methods used to integrate the equation of motion. There are two general categories of models for representing nonlinear soil behavior in site response analyses: equivalent-linear and fully-nonlinear models.

The equivalent-linear method models the nonlinear variation of soil shear moduli and damping ratio as a function of shear strain. The hysteretic stress-strain behavior of soils under symmetrical loading is represented by an equivalent modulus, G, and an equivalent damping ratio, ξ. An iterative procedure, based on linear dynamic analysis, is performed to find the G and ξ corresponding to the computed shear strains.

Two equivalent linear site response analysis programs, SHAKE and DEEPSOIL were compared to search the impact of different schemes on the predicted ground motion parameters. Average of DEEPSOIL analysis gives slightly higher values as compared with the average spectrum obtained from SHAKE analysis for all of three soil profiles and three complex shear modulus options of DEEPSOIL. The difference is observed to increase as the profile gets shallower.

SHAKE analysis were repeated for the three soil profiles adopting family of effective stress depending modulus degradation and material damping curves to modify SHAKE to take into account effective stress dependency of dynamic properties. The curves are developed from the proposed soil model by Darendeli (2001) for each sublayer of the soil profiles. Site response analysis carried out to evaluate the effect of confining pressure dependency on predicted ground motions show that using confining pressure dependent curves results in larger intensity ground motions than those predicted with average generic curves because of the fact that modulus degradation and material damping curves become increasingly linear as confining pressure increases.

Analyses based on stress dependent dynamic properties were rerun adopting frequency dependent characteristics into Shake91. This modification by taking frequency dependent behavior into account improved lower amplification in high frequency range disadvantage of the equivalent linear analysis. The improvement was more pronounced as the soil profile gets deeper.

7.1.4. Site Response Analysis: Nonlinear Approach

Nonlinearity of the sites has significant importance on the ground motion characteristics. Nonlinear effects on seismic waves would be an increase in damping and a decrease in propagation velocity, with consequent reduction in high-frequency amplitudes and shifts to lower frequencies of the spectral resonant peaks of the soil deposit. Nonlinear soil response may be typically defined as the decrease in near-surface amplification of seismic waves as the amplitude of the input wave increases. It is believed that as strain increases, an increasingly hysteretic character of the stress-strain relationship in soils causes this phenomenon.

It is possible to observe the nonlinear site response in terms of amplification ratios with respect to peak ground accelerations or spectral amplitudes calculated for weak and strong ground motion records. The spectral ratio technique can be selected as SSR or HVSR according to the absence of reference rock site.

Examination of the vertical array record is one of the best methods to identify the nonlinear behavior of ground and to evaluate the accuracy of the analytical method.

7.1.5. Site Response Analysis and Microzonation

Microzonation with respect to ground shaking intensity was based on two parameters: (1) average spectral accelerations calculated between the 0.1 and 1.0 s periods using the average acceleration spectrum calculated for each boring from the results of the all site response analysis conducted for each location, (2) the peak spectral accelerations calculated from Borcherdt (1994) using equivalent shear wave velocities. The zonation with respect to ground shaking intensity is produced with respect to three regions where zone A_{GS} shows the areas with very low ground shaking intensity, zone B_{GS} shows the areas with low to medium ground shaking intensity, and zone C_{GS} shows the areas with high ground shaking intensity.

Based on the microzonation studies conducted during the recent years, two conclusions may be drawn: 1) the detailed site investigation and related detailed site characterization is very important and essential when performing site response analyses to have reliable and more accurate information on ground shaking characteristics for microzonation, and 2) the methodology followed and the type and number of acceleration time histories used for site response analysis to generate microzonation maps can have significant effect on the final microzonation.

The last issue is the selection of microzonation parameters. It was shown that microzonation with respect to different parameters such as PGA and PGV can give significantly different microzonation maps. Therefore the selections of the microzonation parameter need to be compatible with the main purpose of the microzonation project.

7.2. Future Recommentations

Within the scope of this thesis attempts were made to give critical overview of the different components of site response analyses. The following issues that this study has identified are recommended to be considered for further studies:

(1) As a part of this thesis, Shake91 code was modified such as the equivalent linear scheme takes into account both frequency and confining pressure dependency of dynamic soil parameters. Modified Shake91 program can be attempted to be unified with the proposed methodology as a package: Records compatible with site-specific hazard parameters would be selected from the database and scaled to values evaluated from the proposed attenuation relations in accordance with the hazard parameters. For a given damage parameter, the results would be given for the site response analysis that used the records scaled to the most appropriate parameter so that the scatter of the model response is minimum.

(2) The site response analyses performed in this study should be repeated with alternative nonlinear soil models and fully nonlinear computational routines to investigate the effects of these models and analysis routines.

(3) The sites considered in this study were selected on the basis of available geotechnical and geophysical data. New sites, preferably the vertical array sites with defined soil profiles that have recorded strong motion at different depths would be very helpful to verify the results obtained by modified equivalent linear scheme and proposed methodology.

(4) The results of microzonation studies based on modified Shake91 should be compared with those from previously conducted microzonation studies. This method may be enhanced further.

APPENDIX A: OUTPUT FOR SCALING STUDIES

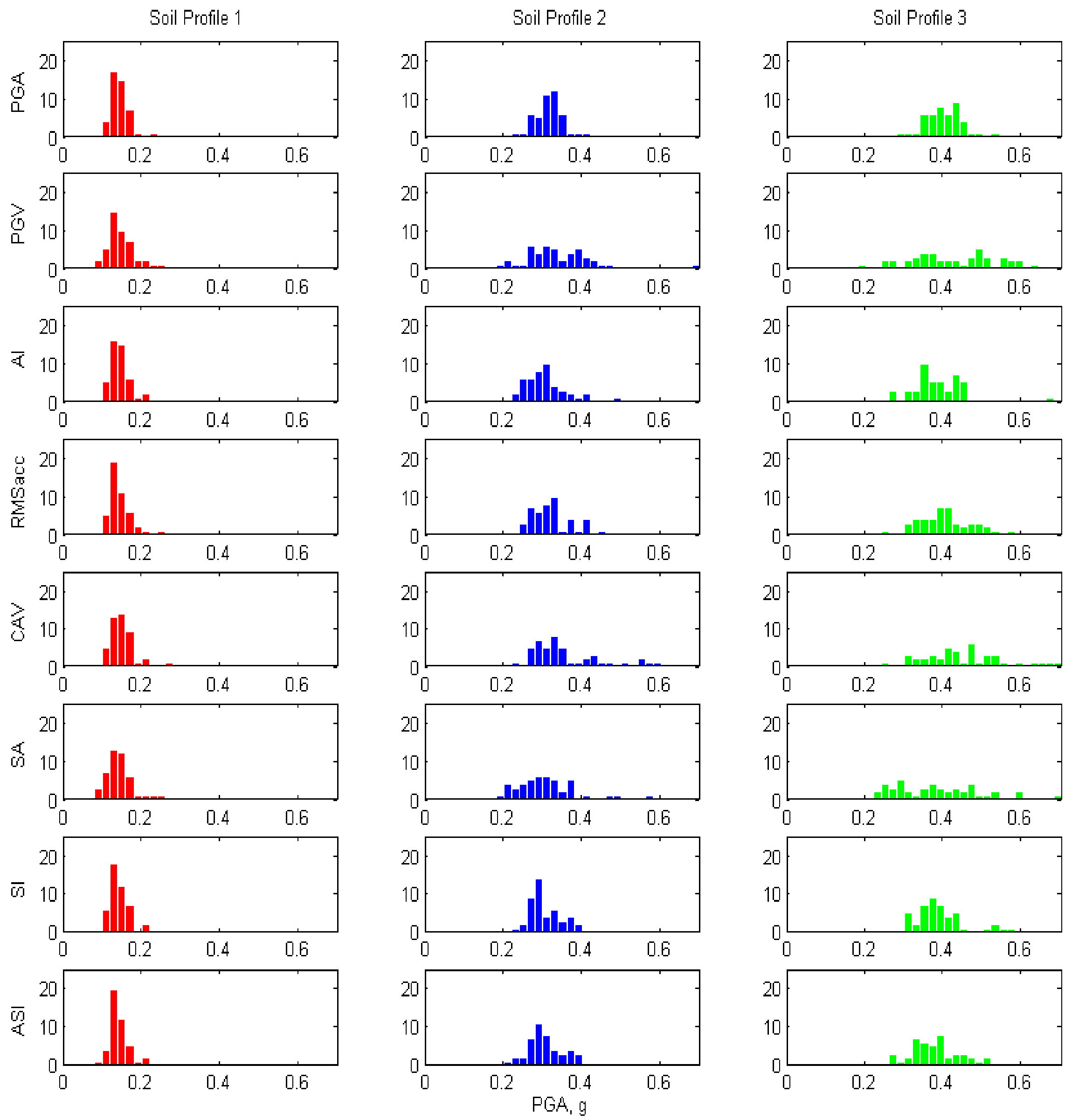

(a)

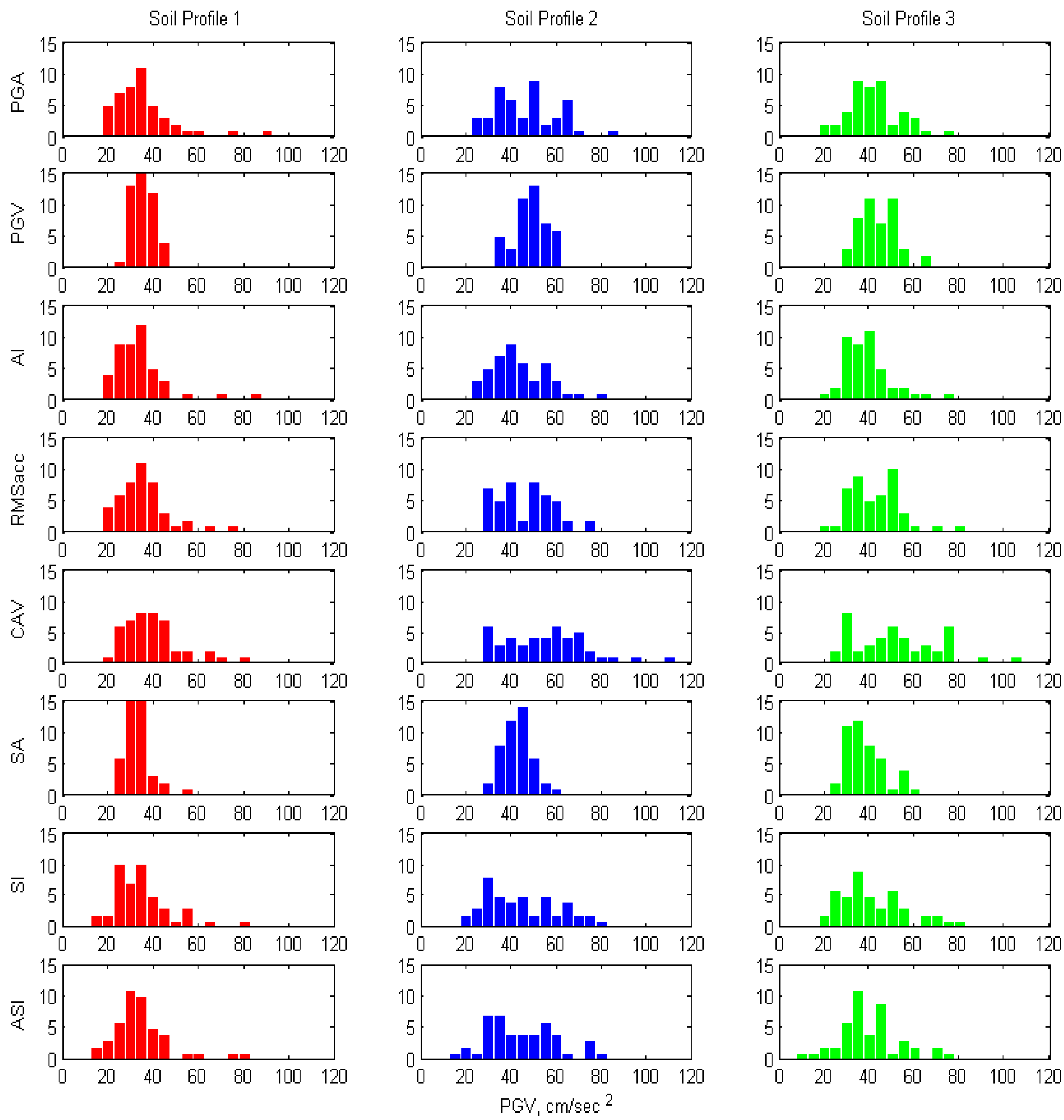
Soil Profile 1
Soil Profile 2
Soil Profile 3
PGA
PGV
AI
RMSacc
CAV
SA
SI
ASI
PGV, cm/sec 2

(b)

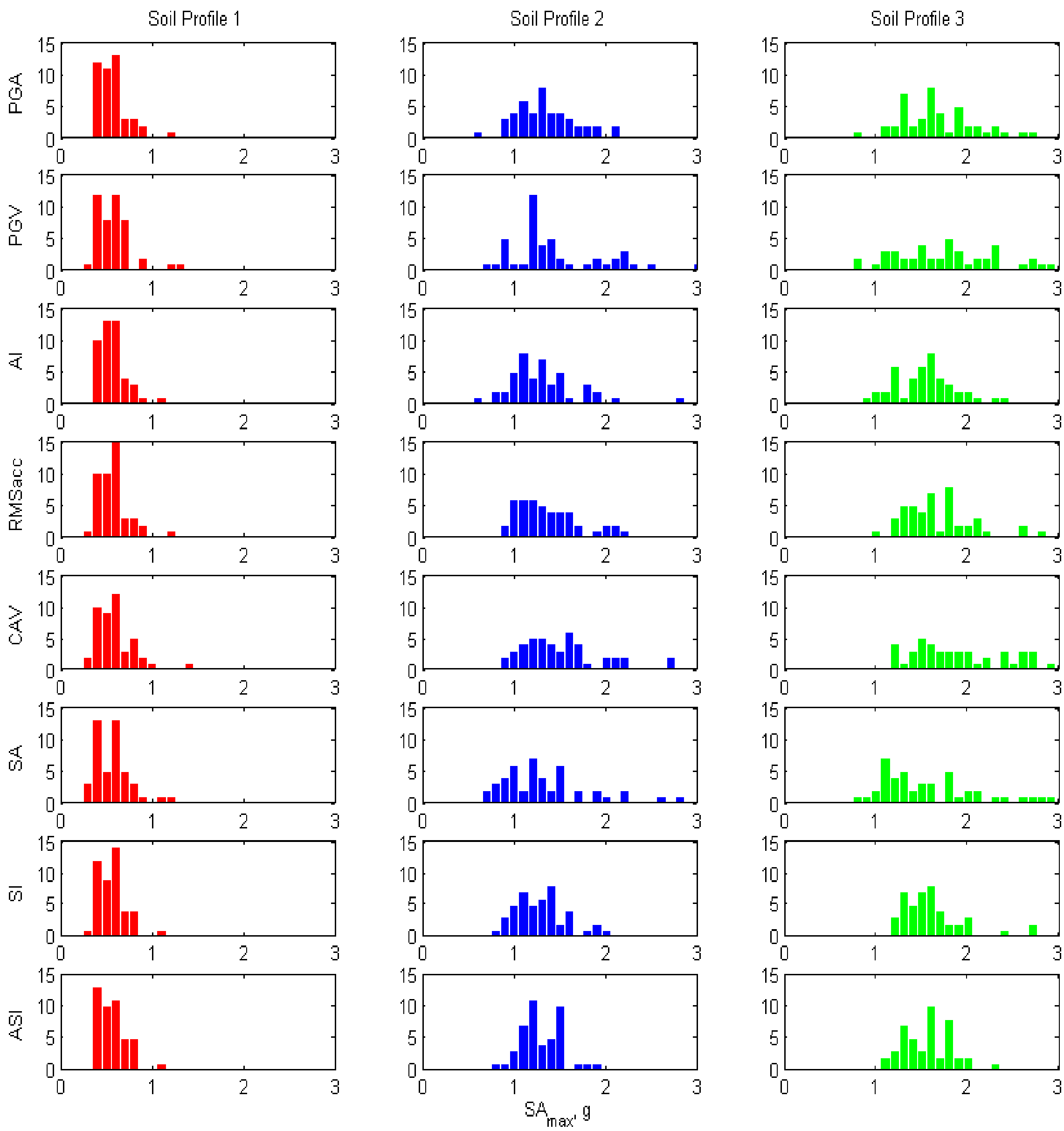

(c)

Figure A.1. Histograms of (a) peak ground acceleration, PGA; (b) peak ground velocity, PGV; (c) maximum spectral accelerations, SA_{max} for three soil profiles calculated on the ground surface from the site response analysis that used input time histories (magnitude bin: 6.0≤M<6.5, distance bin: 0≤R<30km) scaled with respect to eight scaling parameters

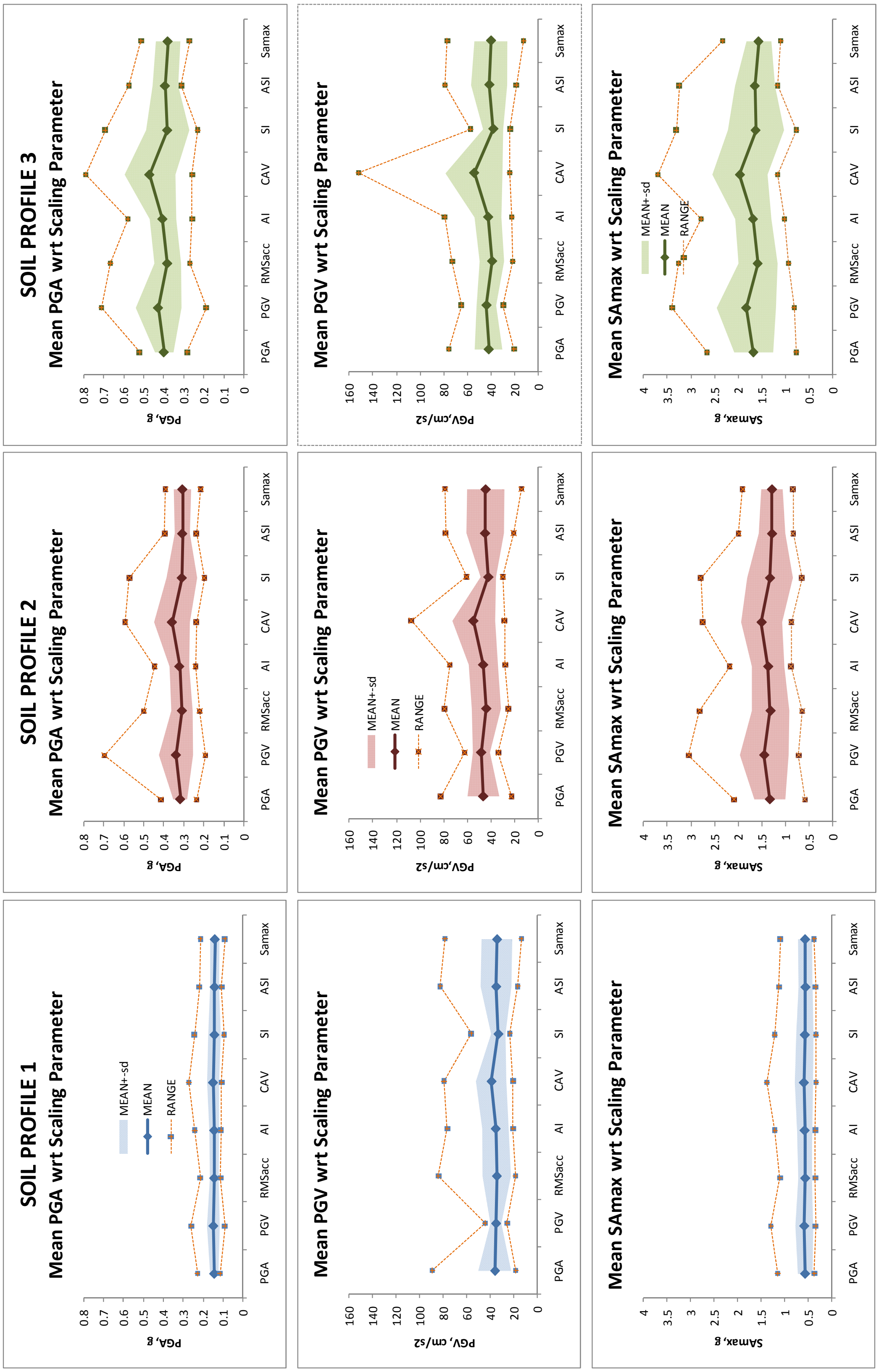

Figure A.2. Variation of mean, mean±sd and range of PGA, PGV and SA_{max} for three soil profiles with respect to scaling parameters (magnitude bin: 6.0≤M<6.5, distance bin: 0≤R<30km)

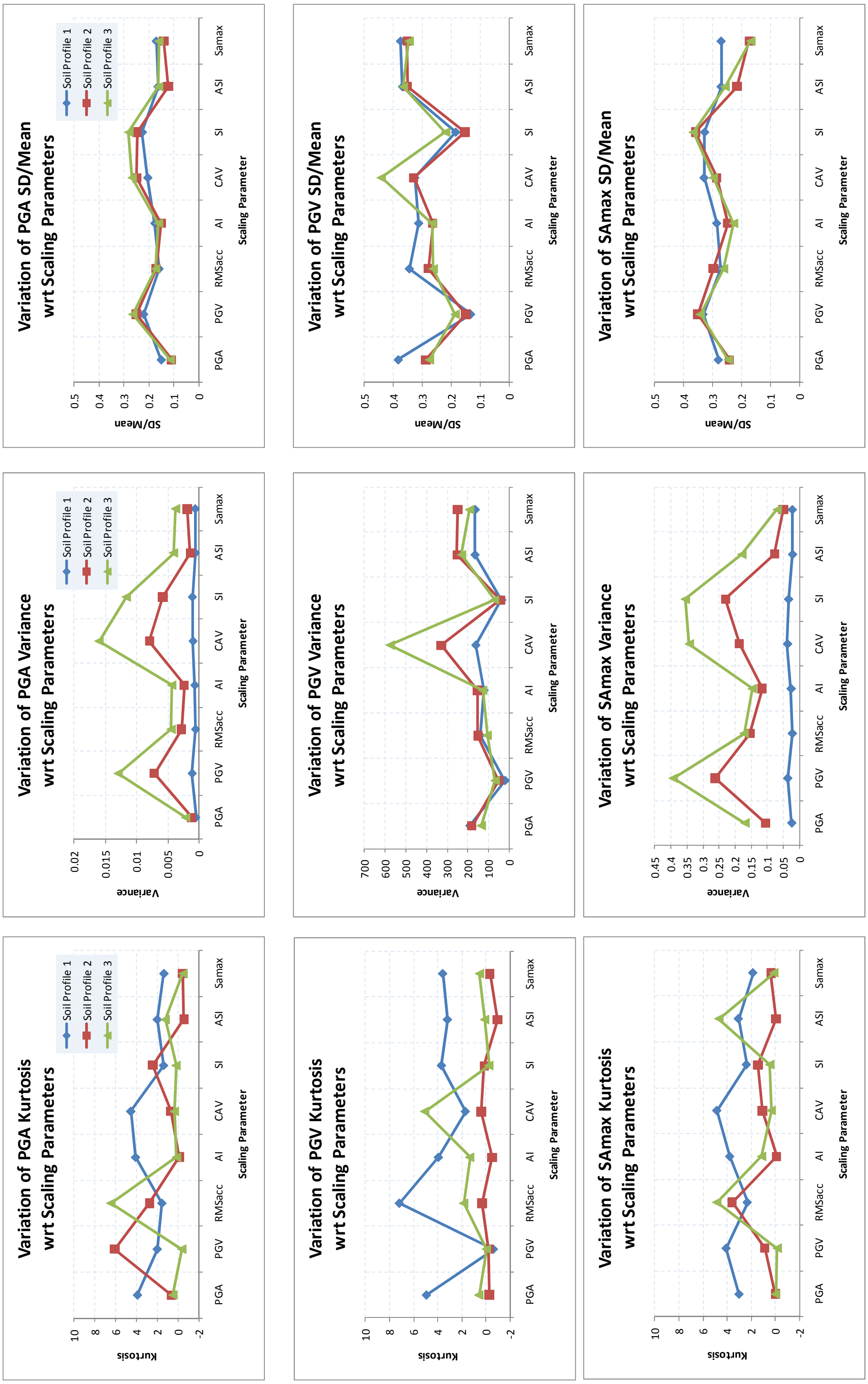

Figure A.3. Variation of kurtosis, variance and SD/mean of PGA, PGV and SA_{max} for three soil profiles with respect to scaling parameters (magnitude bin: 6.0≤M<6.5, distance bin: 0≤R<30km)

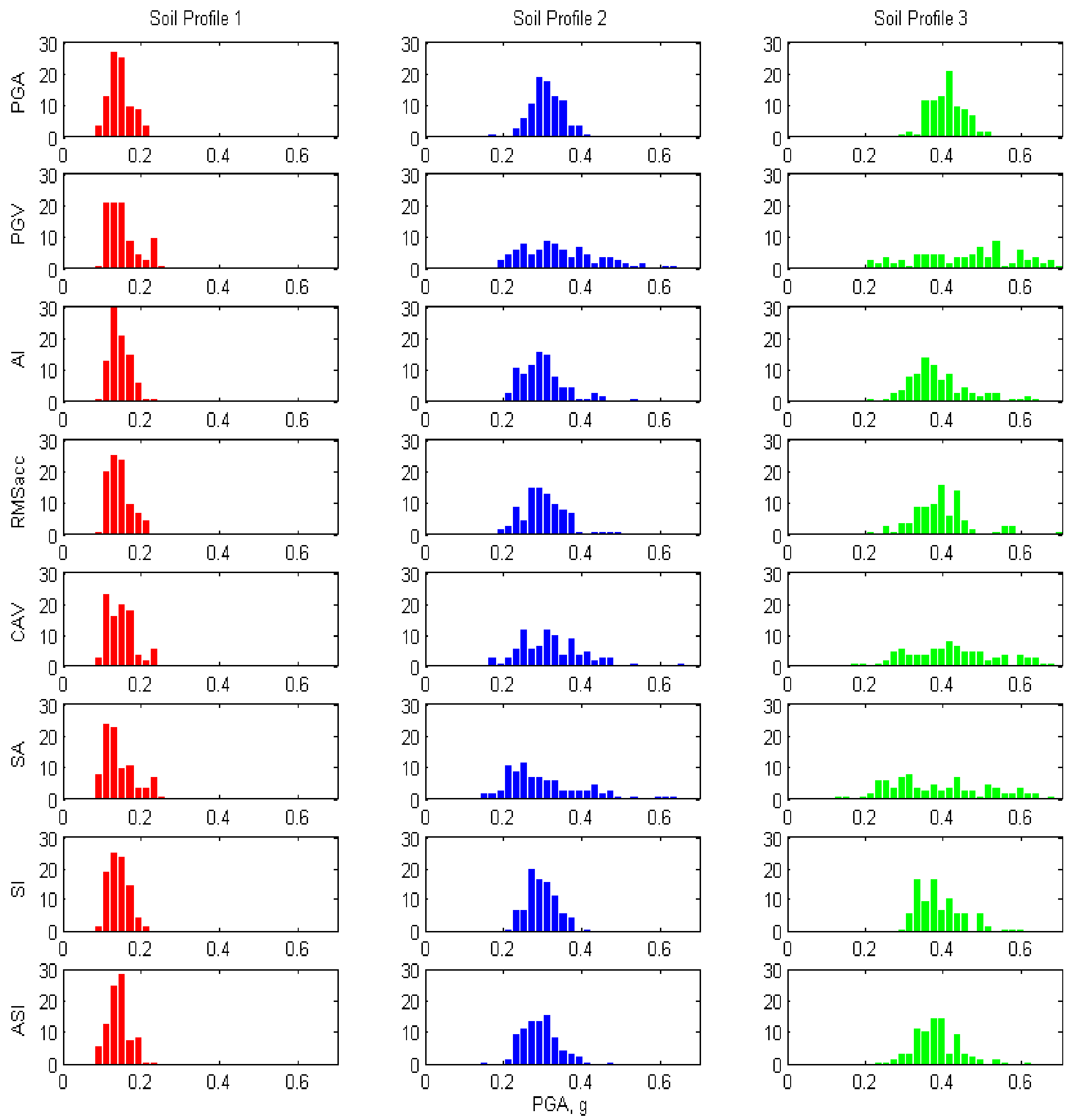

Soil Profile 1
Soil Profile 2
Soil Profile 3
PGA
PGV
AI
RMSacc
CAV
SA
SI
ASI
PGA, g

(a)

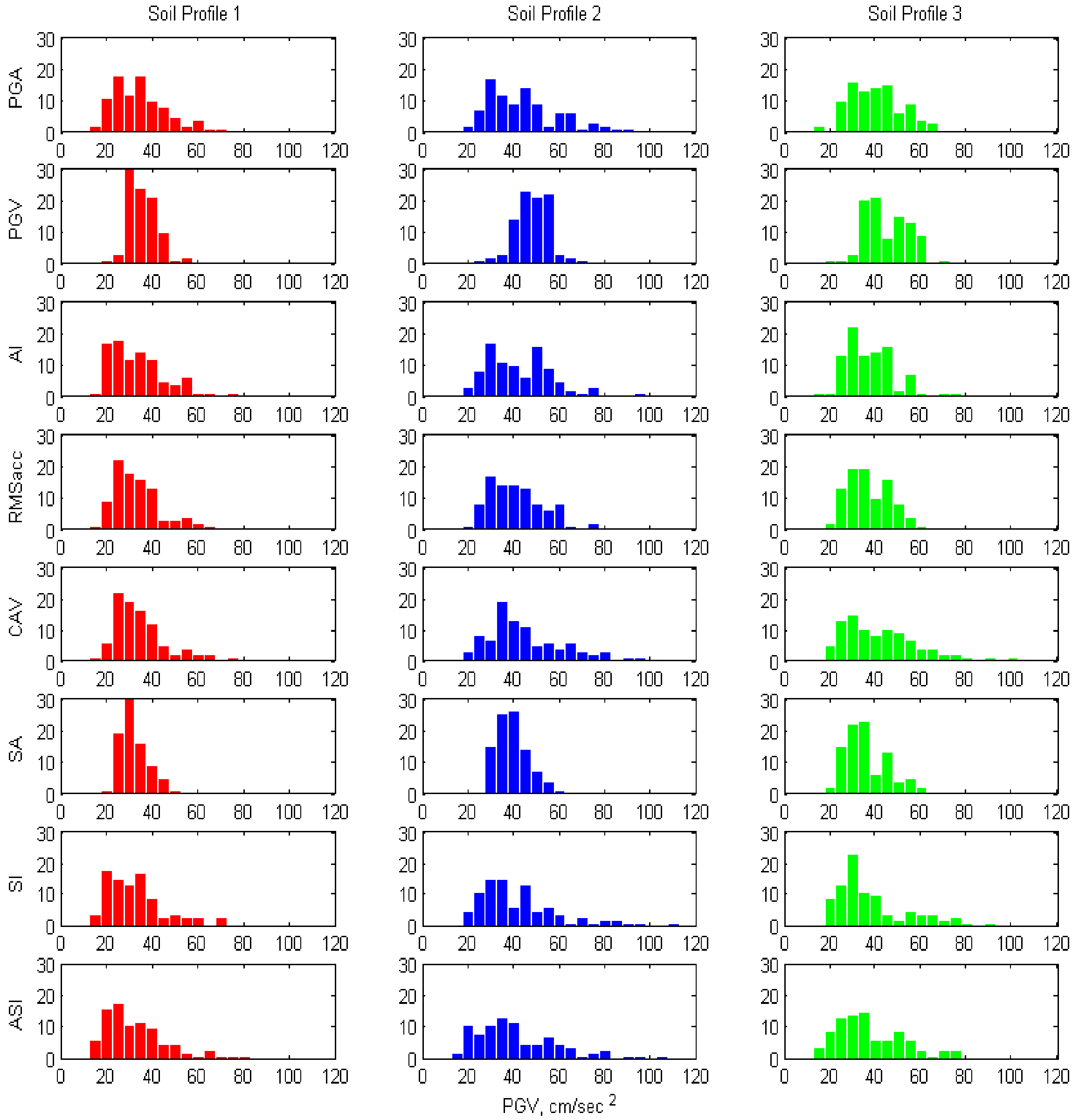

Soil Profile 1
Soil Profile 2
Soil Profile 3
PGA
PGV
AI
RMSacc
CAV
SA
SI
ASI
PGV, cm/sec 2

(b)

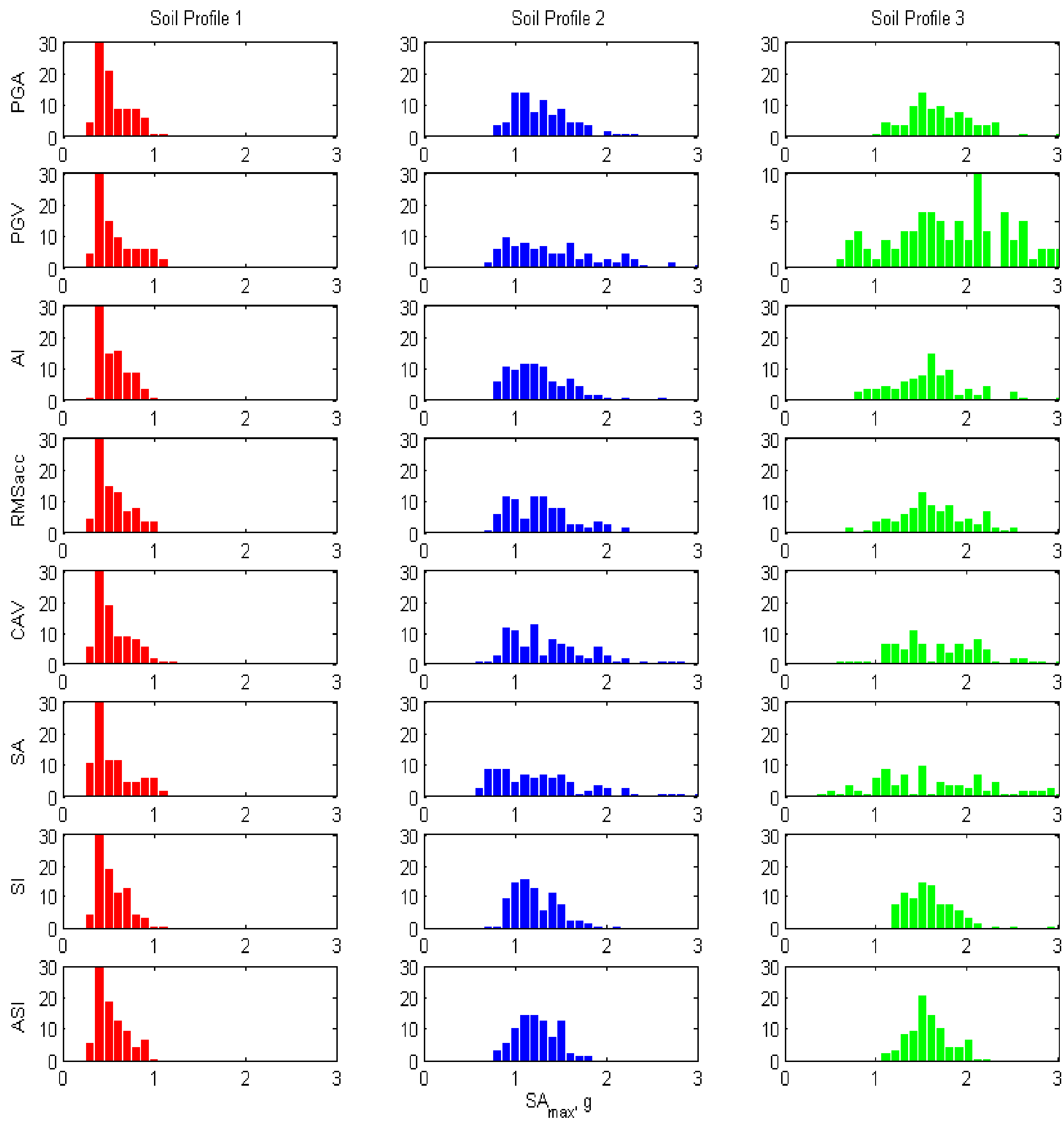

(c)

Figure A.4. Histograms of (a) peak ground acceleration, PGA; (b) peak ground velocity, PGV; (c) maximum spectral accelerations, SA_{max} for three soil profiles calculated on the ground surface from the site response analysis that used input time histories (magnitude bin: 6.0≤M<6.5, distance bin: 30≤R<60km) scaled with respect to eight scaling parameters

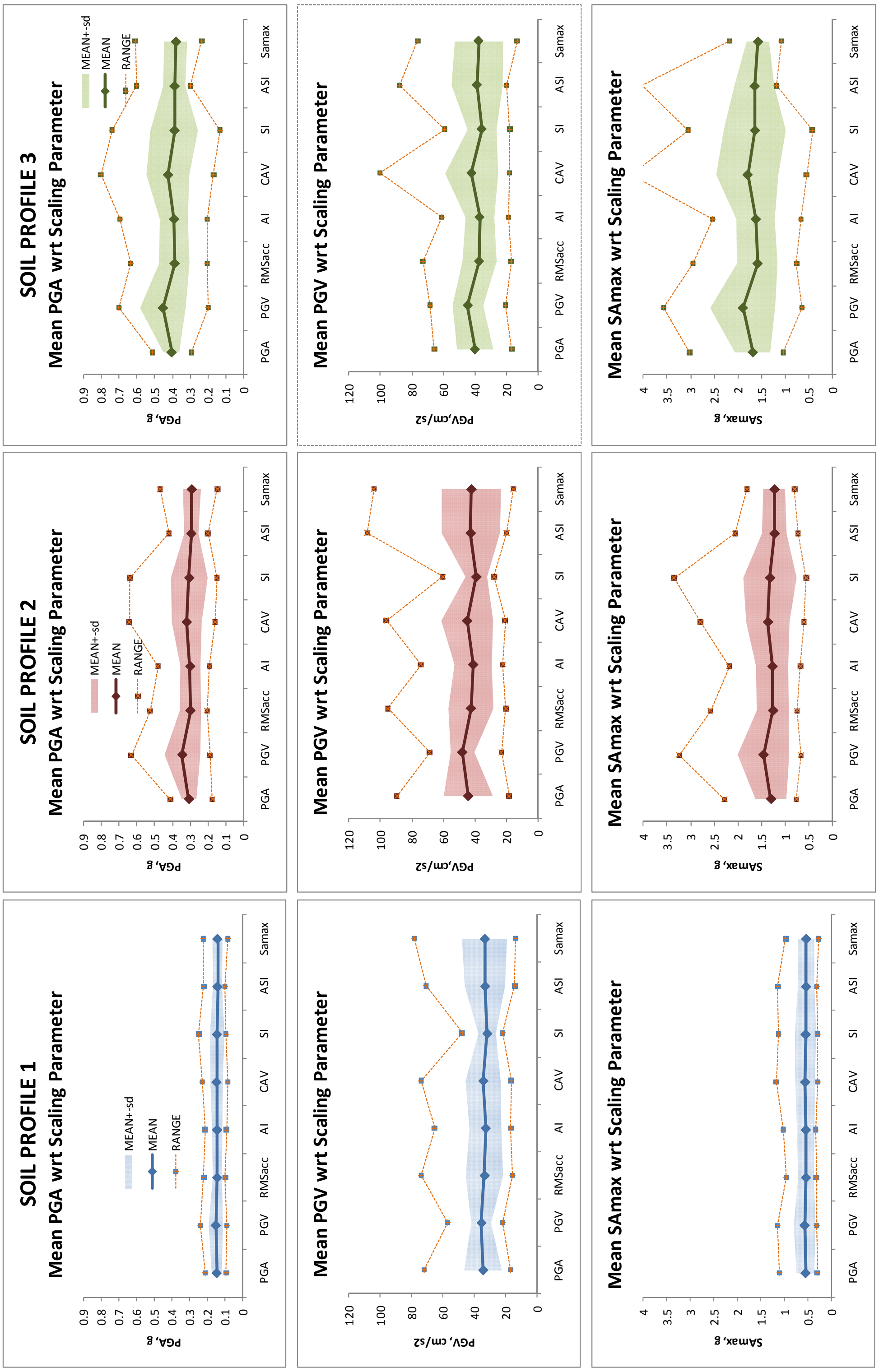

Figure A.5. Variation of mean, mean±sd and range of PGA, PGV and SA_{max} for three soil profiles with respect to scaling parameters (magnitude bin: 6.0≤M<6.5, distance bin: 30≤R<60km)

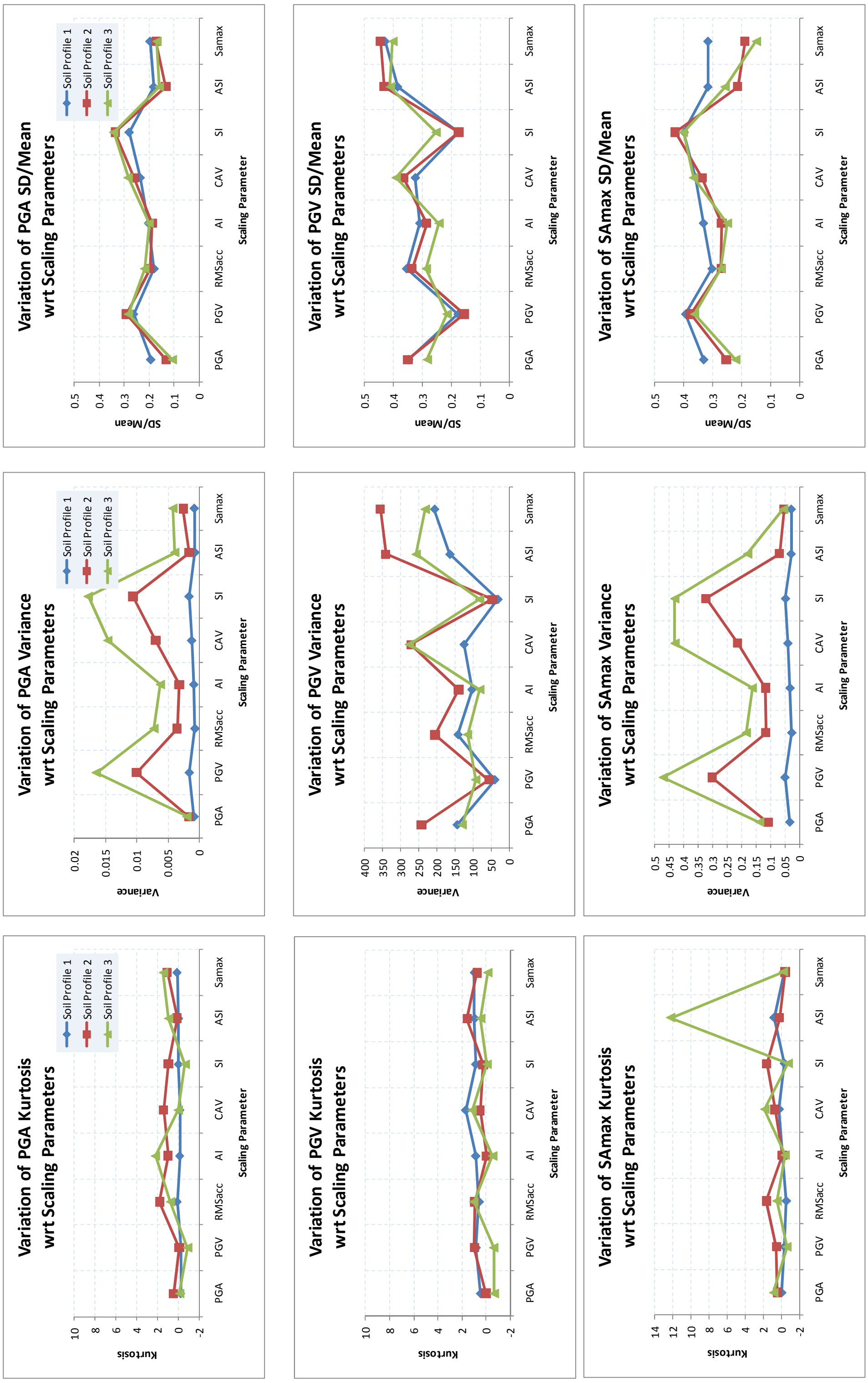

Figure A.6. Variation of kurtosis, variance and SD/mean of PGA, PGV and SA_{max} for three soil profiles with respect to scaling parameters (magnitude bin: 6.0≤M<6.5, distance bin: 30≤R<60km)

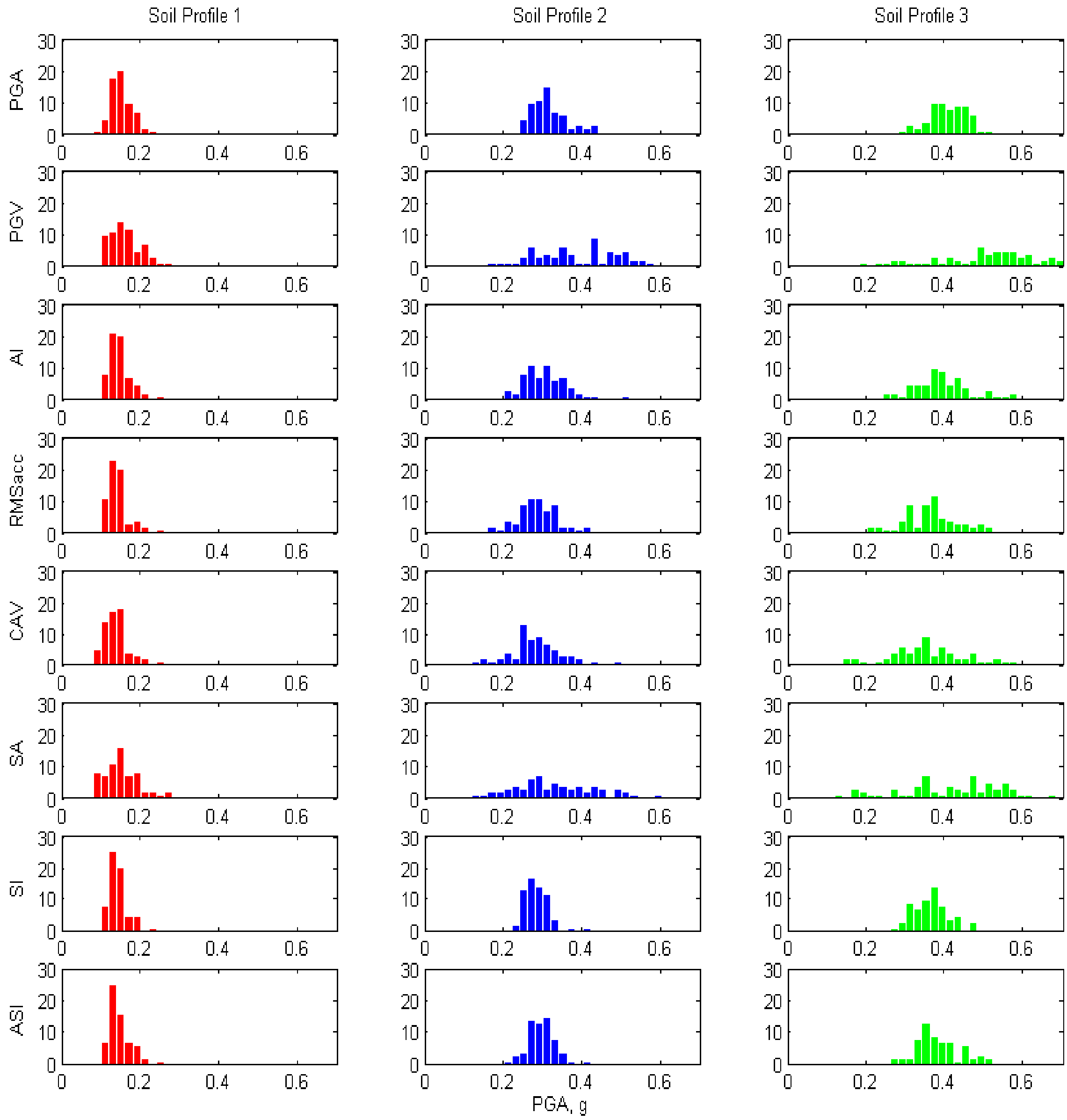
Soil Profile 1
Soil Profile 2
Soil Profile 3
PGA
PGV
AI
RMSacc
CAV
SA
SI
ASI
PGA, g

(a)

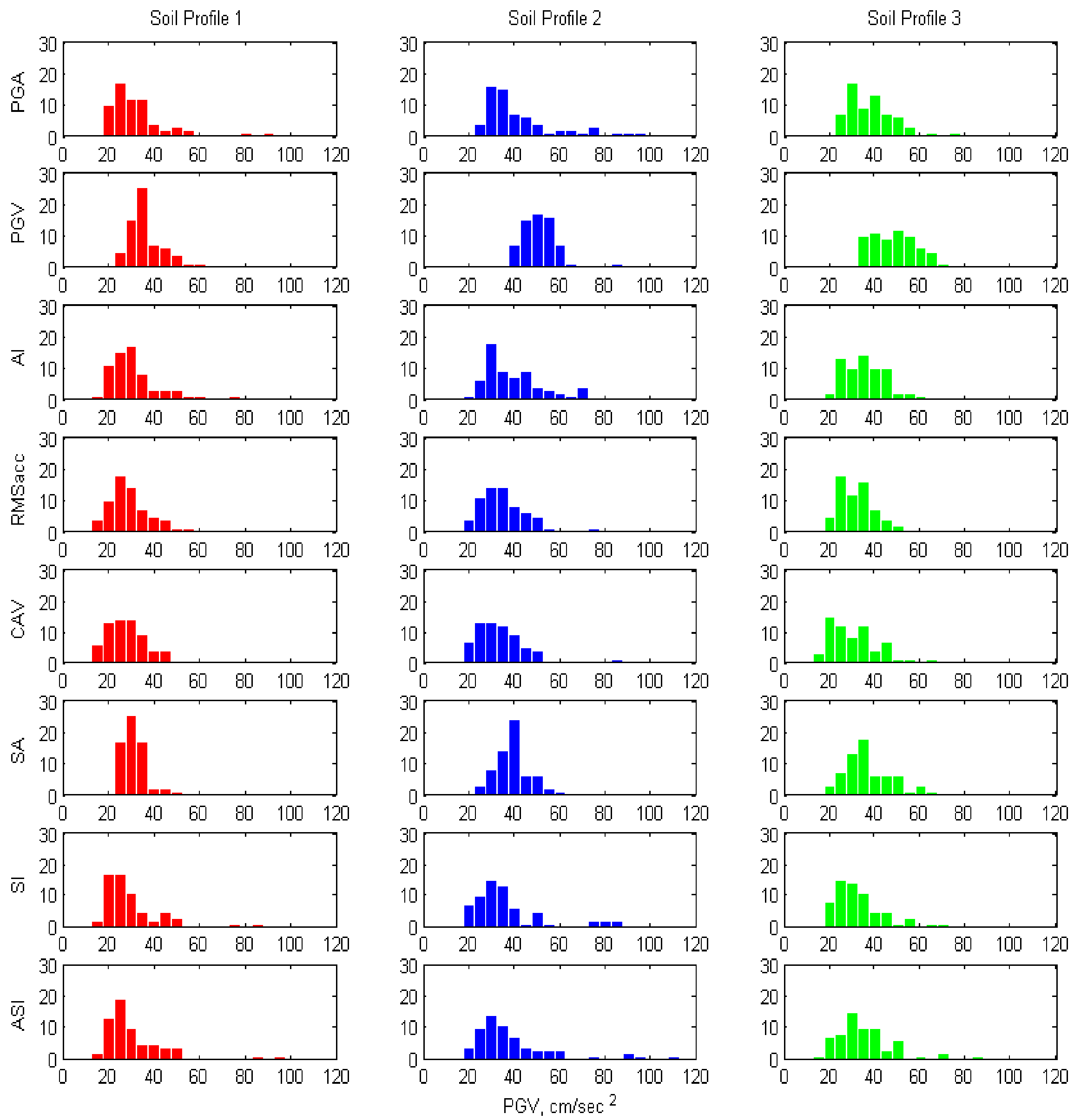
Soil Profile 1
Soil Profile 2
Soil Profile 3
PGA
PGV
AI
RMSacc
CAV
SA
SI
ASI
PGV, cm/sec 2

(b)

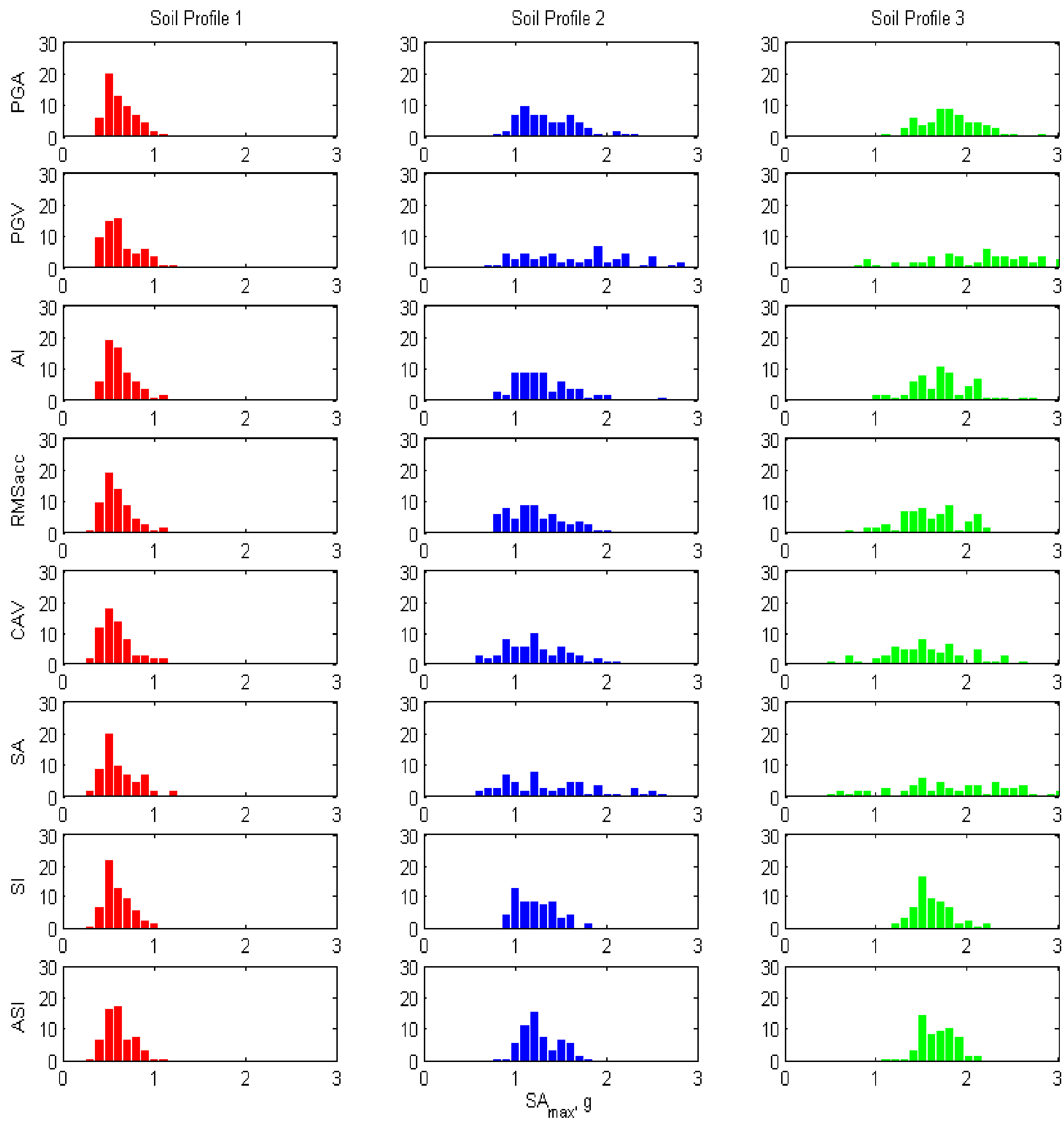

(c)

Figure A.7. Histograms of (a) peak ground acceleration, PGA; (b) peak ground velocity, PGV; (c) maximum spectral accelerations, SA_{max} for three soil profiles calculated on the ground surface from the site response analysis that used input time histories (magnitude bin: 6.0≤M<6.5, distance bin: 60≤R<90km) scaled with respect to eight scaling parameters

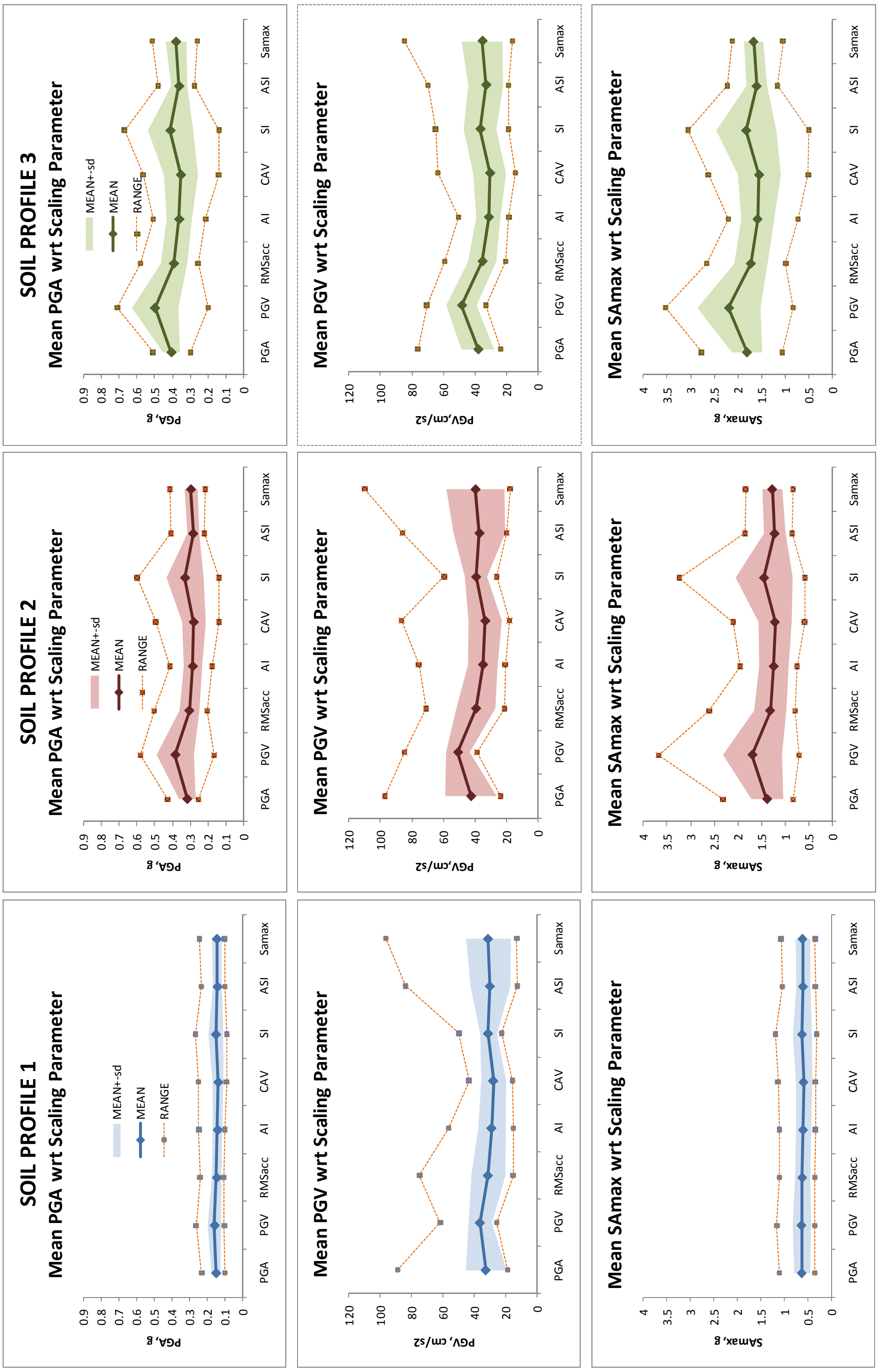

Figure A.8. Variation of mean, mean±sd and range of PGA, PGV and SA_{max} for three soil profiles with respect to scaling parameters (magnitude bin: 6.0≤M<6.5, distance bin: 60≤R<90km)

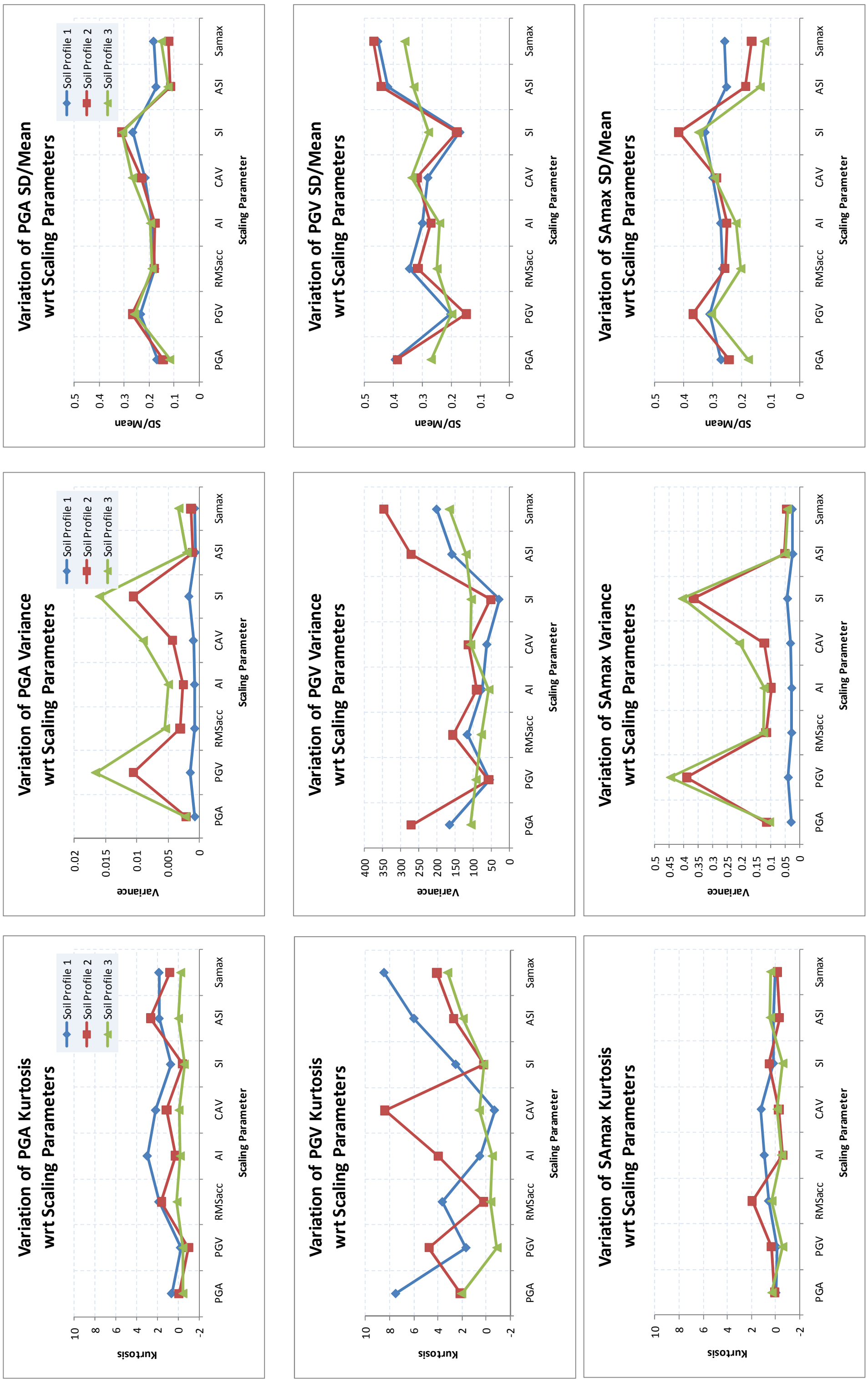

Figure A.9. Variation of kurtosis, variance and SD/mean of PGA, PGV and SA_{max} for three soil profiles with respect to scaling parameters (magnitude bin: $6.0 \leq M < 6.5$, distance bin: $60 \leq R < 90$km)

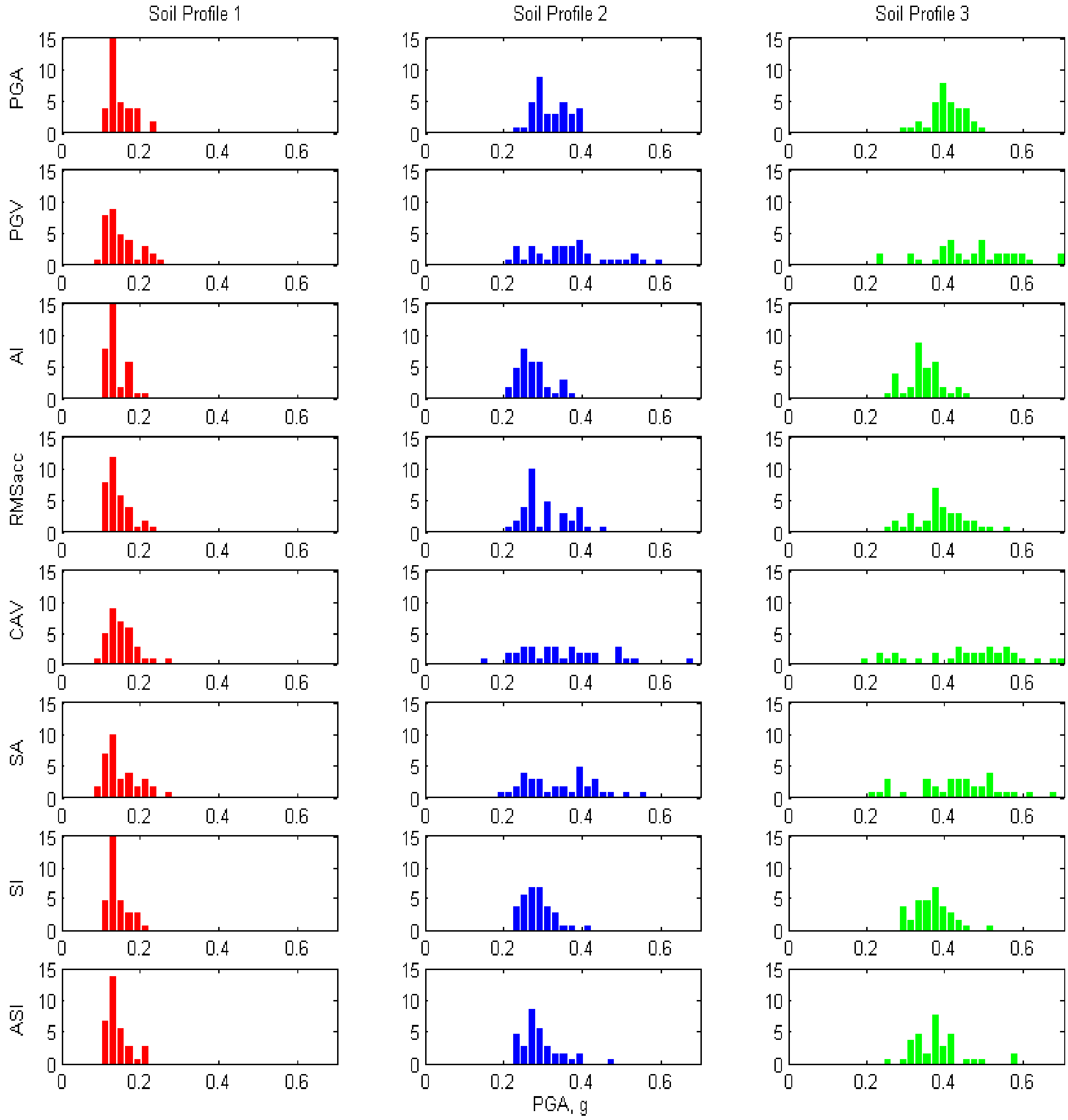
Soil Profile 1
Soil Profile 2
Soil Profile 3
PGA
PGV
AI
RMSacc
CAV
SA
SI
ASI
PGA, g

(a)

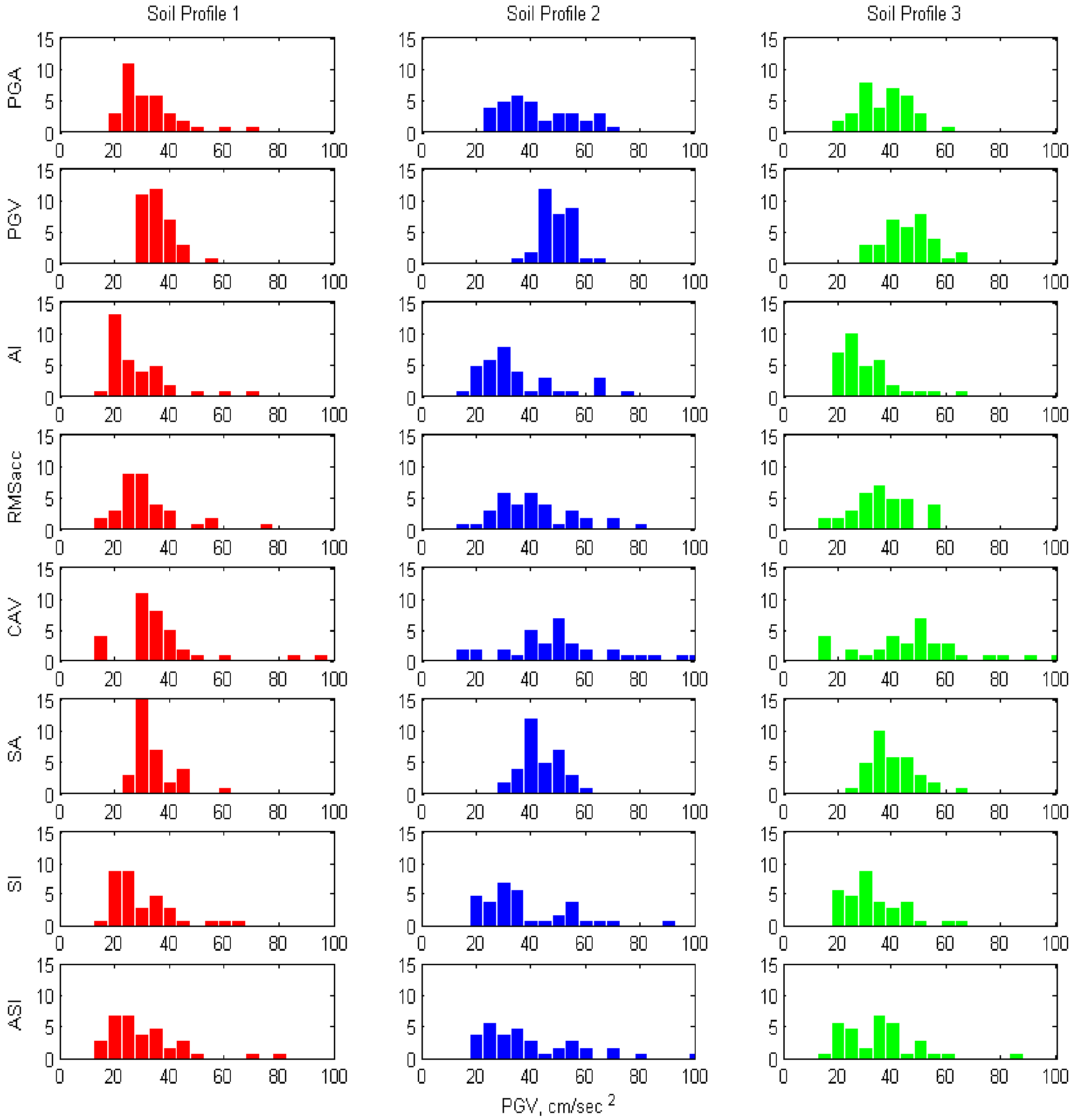
Soil Profile 1
Soil Profile 2
Soil Profile 3
PGA
PGV
AI
RMSacc
CAV
SA
SI
ASI
PGV, cm/sec 2

(b)

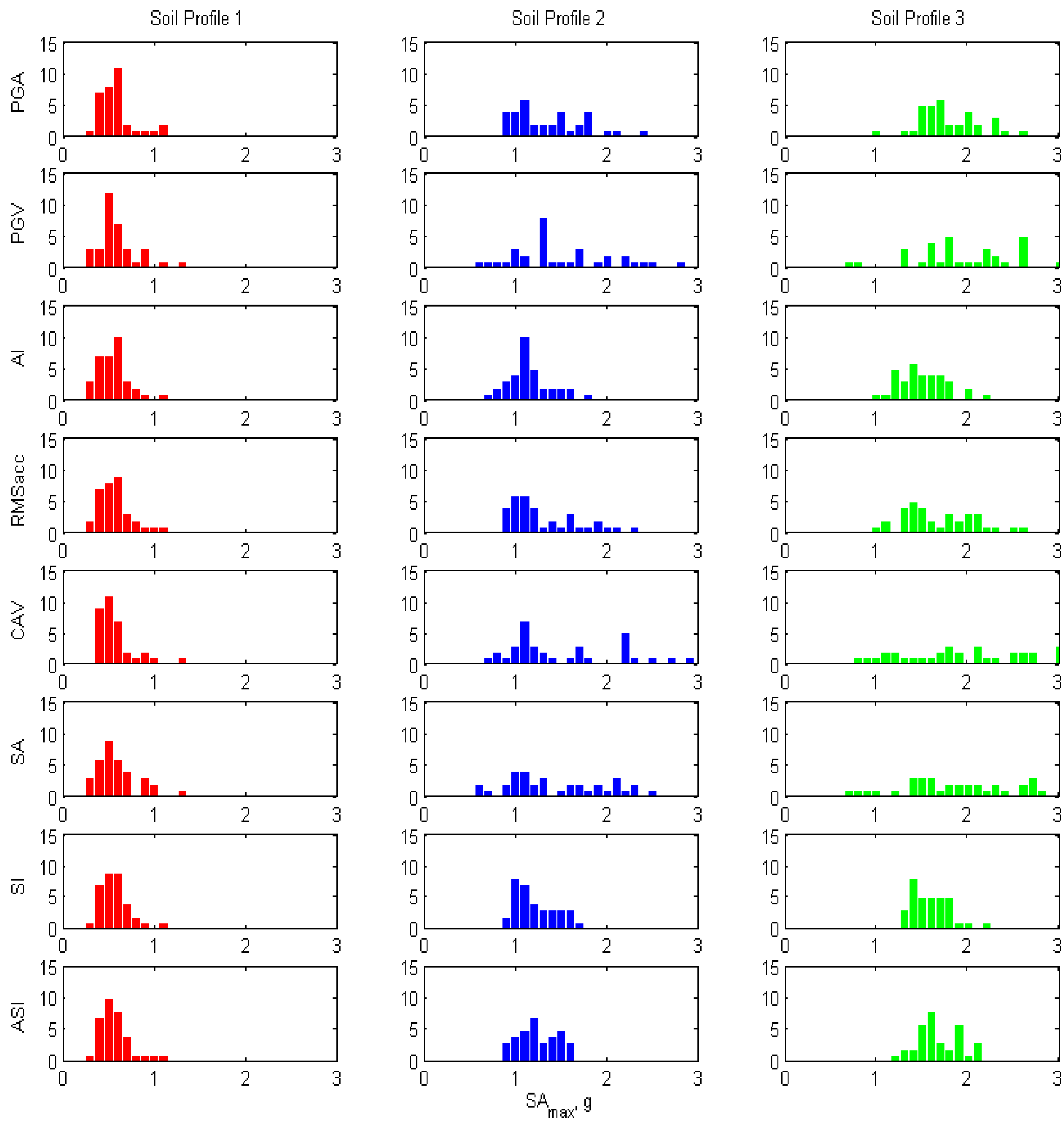

(c)

Figure A.10. Histograms of (a) peak ground acceleration, PGA; (b) peak ground velocity, PGV; (c) maximum spectral accelerations, SA_{max} for three soil profiles calculated on the ground surface from the site response analysis that used input time histories (magnitude bin: 6.5≤M<7.0, distance bin: 0≤R<30km) scaled with respect to eight scaling parameters

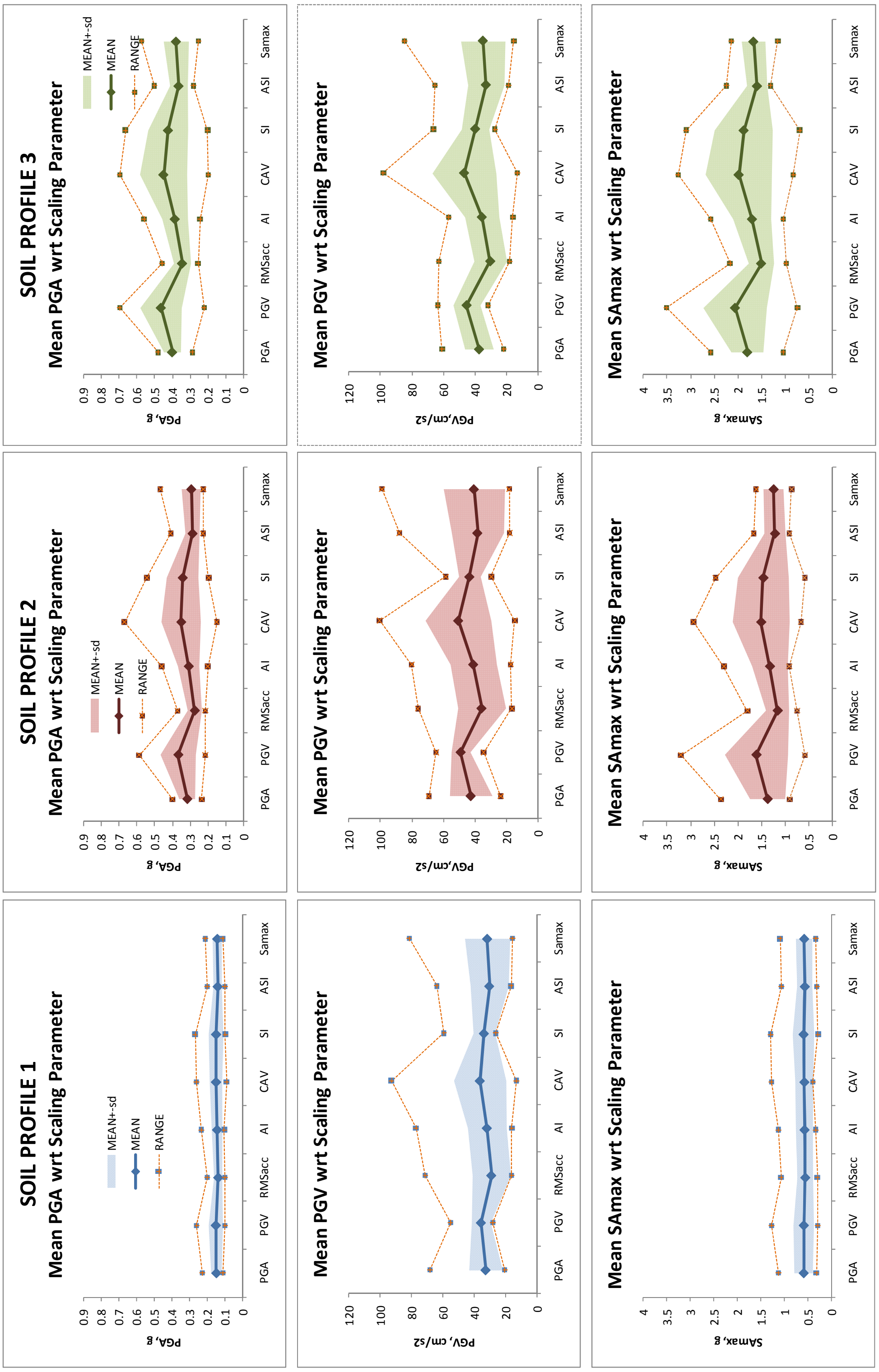

Figure A.11. Variation of mean, mean±sd and range of PGA, PGV and SA_{max} for three soil profiles with respect to scaling parameters (magnitude bin: 6.5≤M<7.0, distance bin: 0≤R<30km)

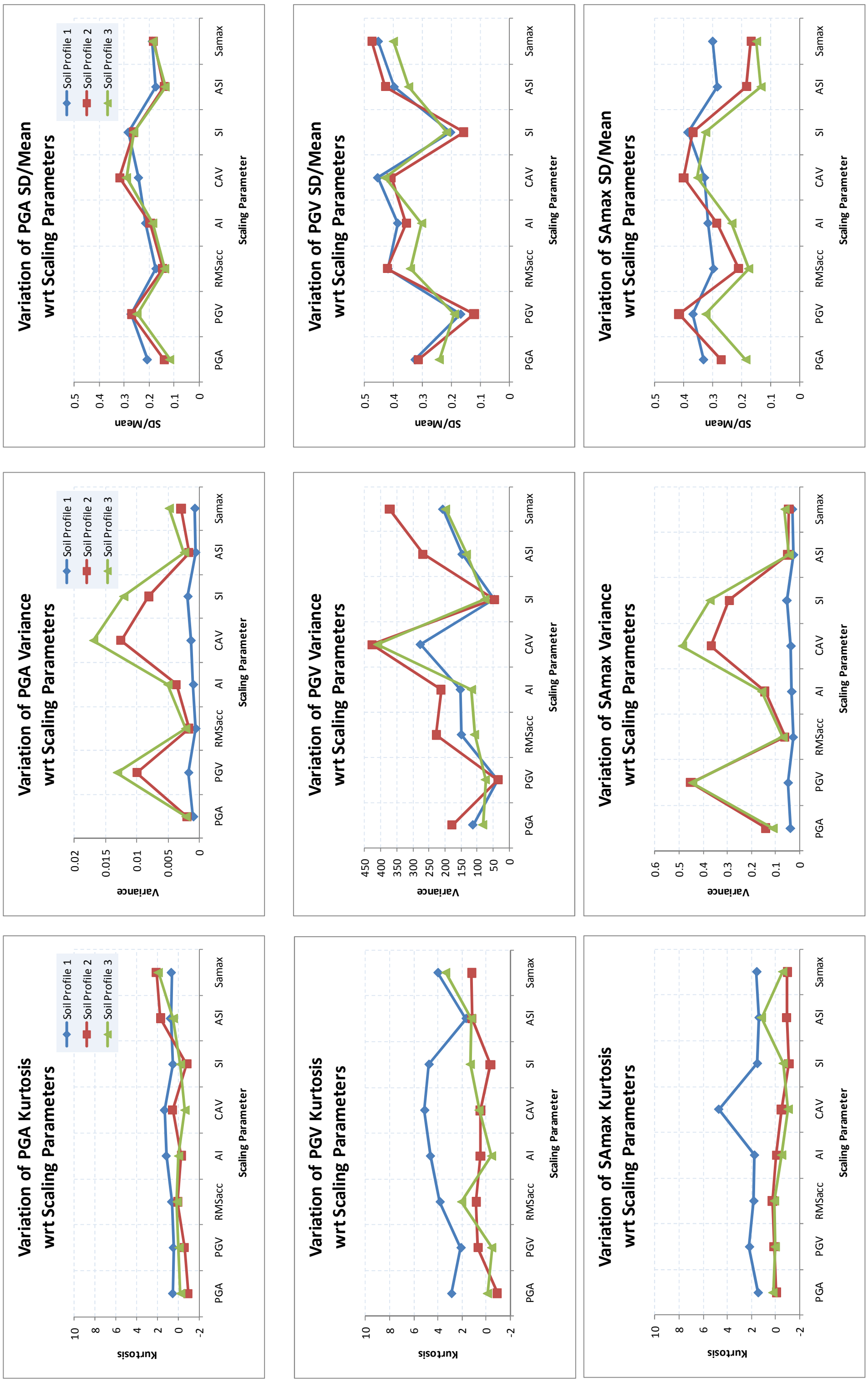

Figure A.12. Variation of kurtosis, variance and SD/mean of PGA, PGV and SA_{max} for three soil profiles with respect to scaling parameters (magnitude bin: $6.5 \leq M < 7.0$, distance bin: $0 \leq R < 30$km)

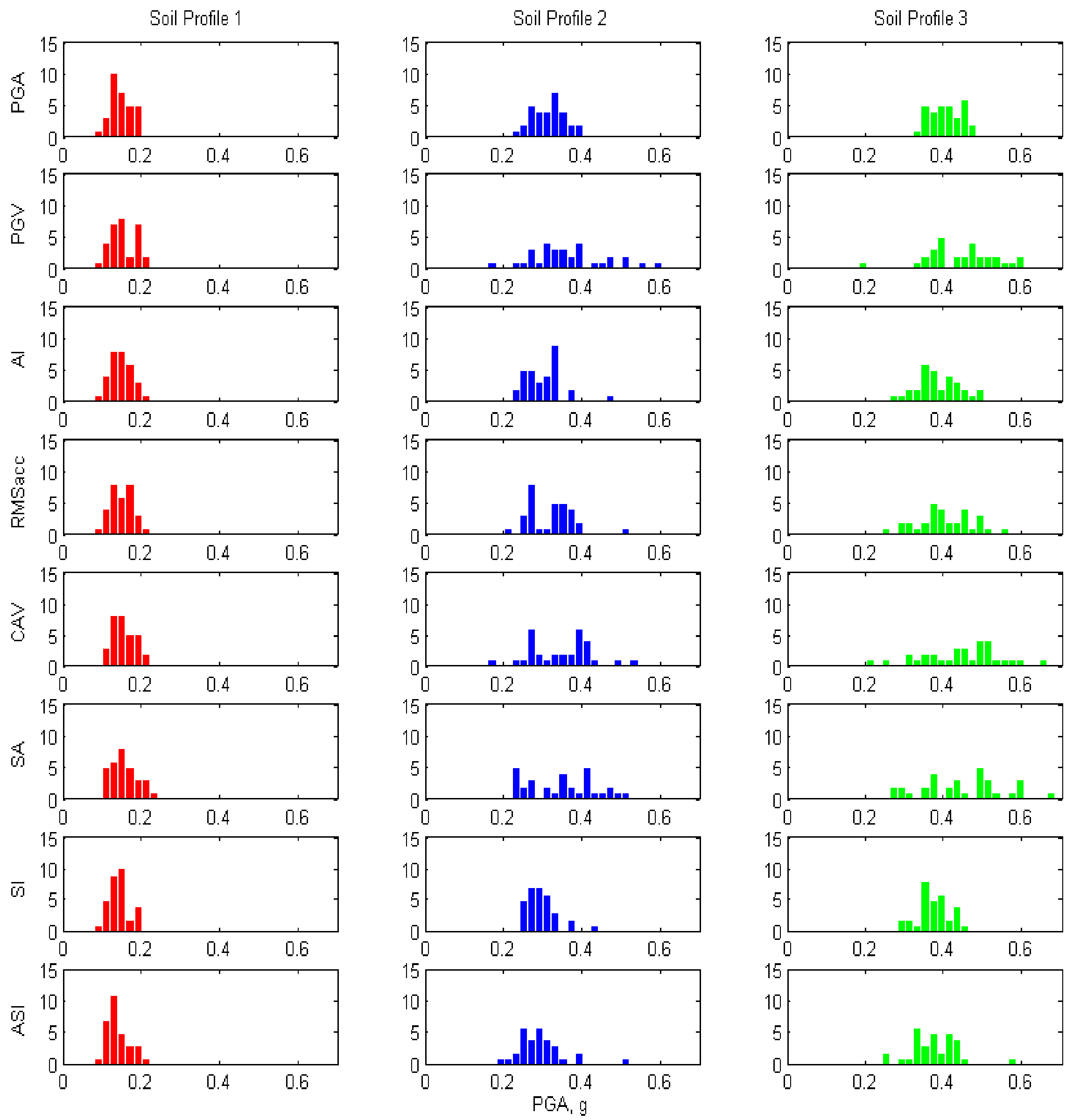
Soil Profile 1
Soil Profile 2
Soil Profile 3
PGA
PGV
AI
RMSacc
CAV
SA
SI
ASI
PGA, g

(a)

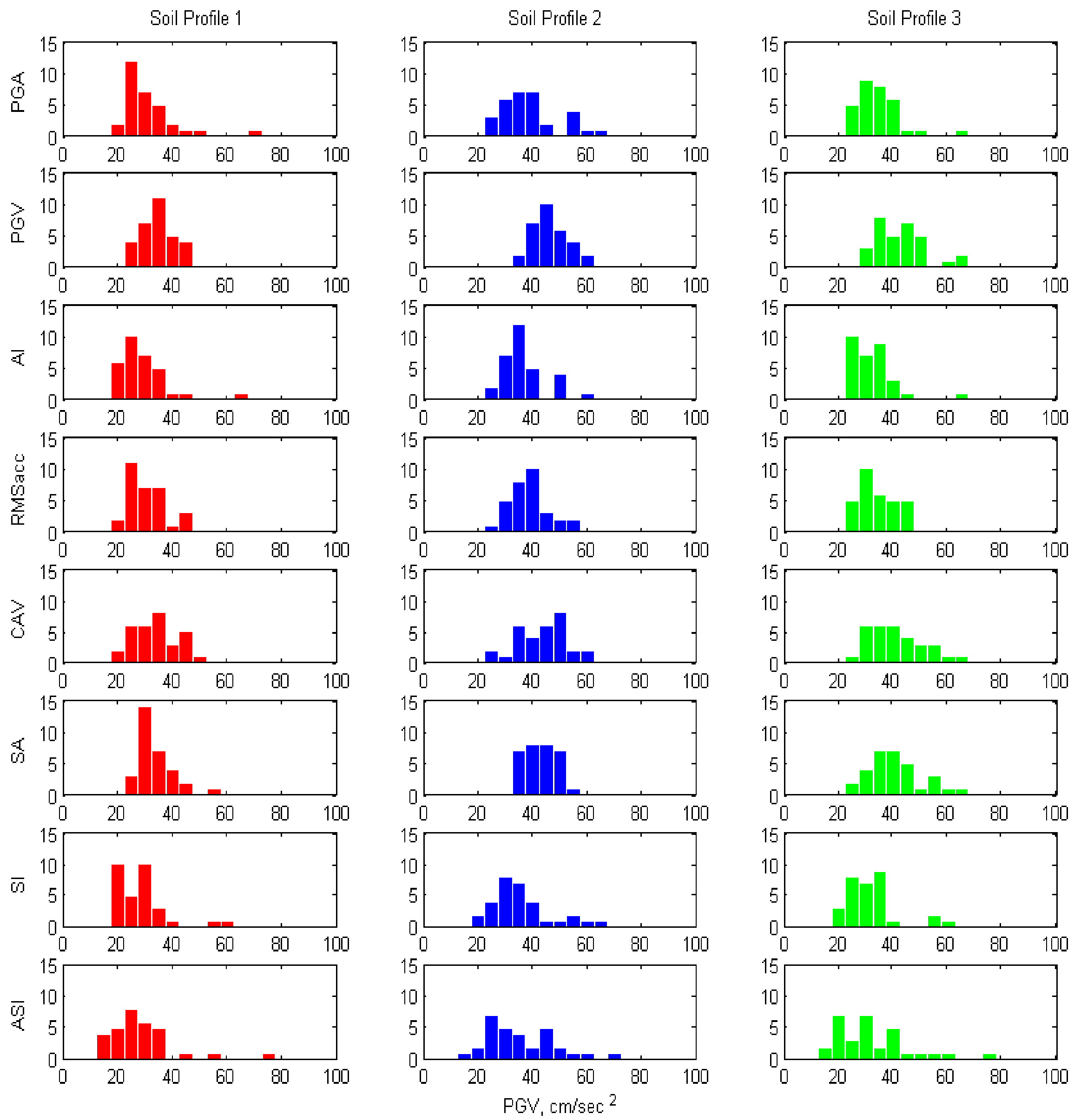
Soil Profile 1
Soil Profile 2
Soil Profile 3
PGA
PGV
AI
RMSacc
CAV
SA
SI
ASI
PGV, cm/sec 2

(b)

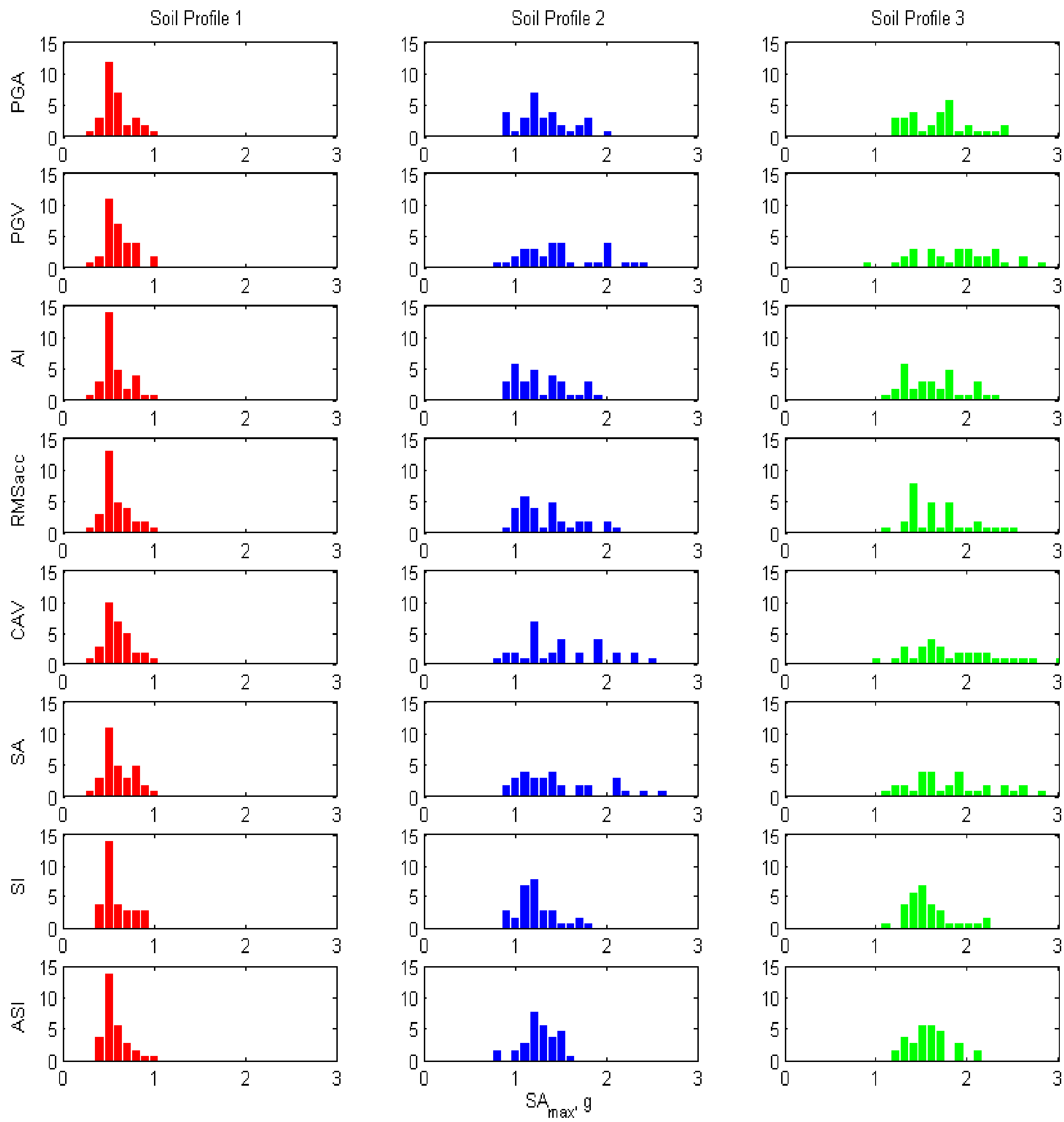

(c)

Figure A.13. Histograms of (a) peak ground acceleration, PGA; (b) peak ground velocity, PGV; (c) maximum spectral accelerations, SA_{max} for three soil profiles calculated on the ground surface from the site response analysis that used input time histories (magnitude bin: 6.5≤M<7.0, distance bin: 30≤R<60km) scaled with respect to eight scaling parameters

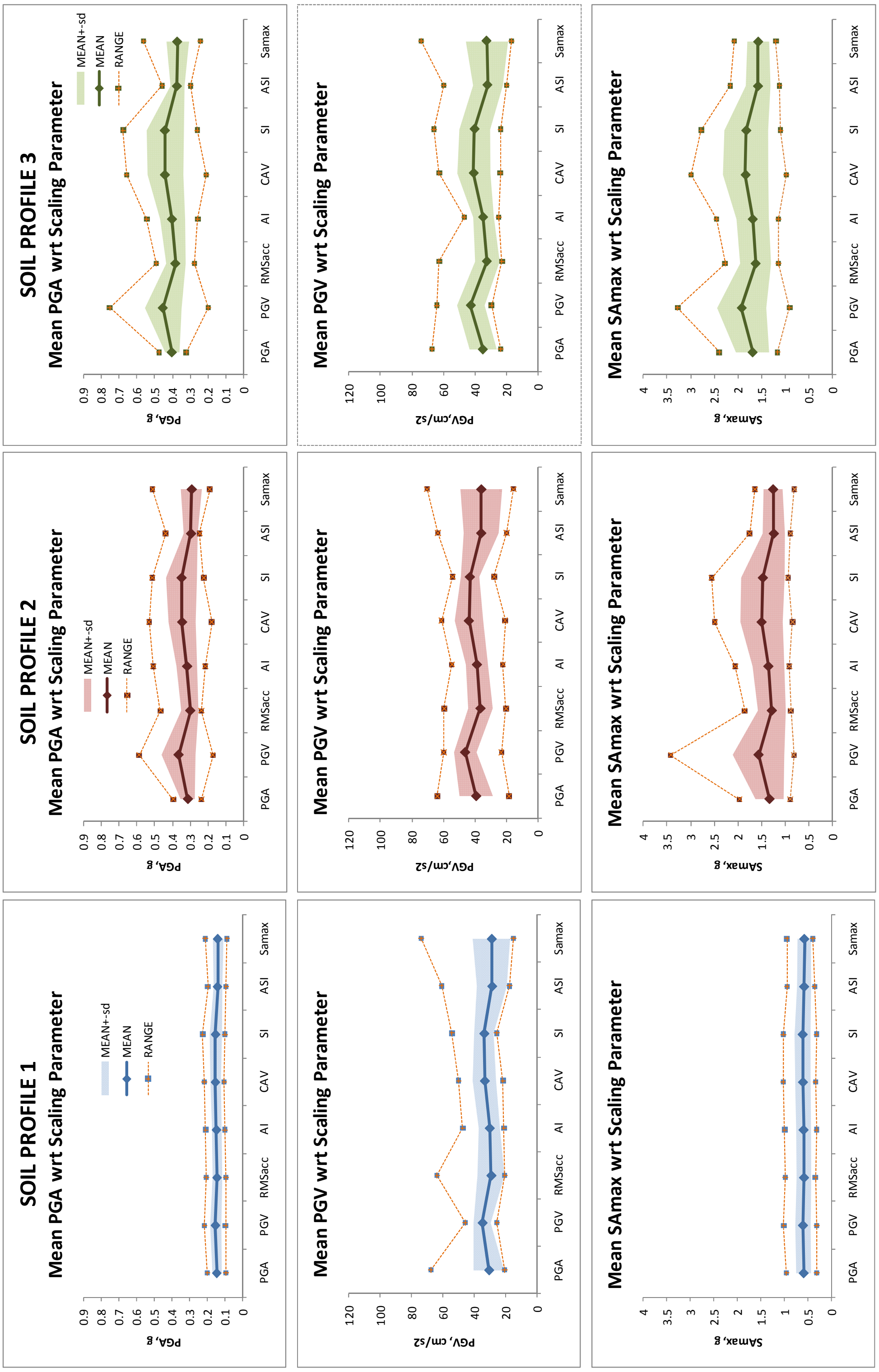

Figure A.14. Variation of mean, mean±sd and range of PGA, PGV and SA_{max} for three soil profiles with respect to scaling parameters (magnitude bin: 6.5≤M<7.0, distance bin: 30≤R<60km)

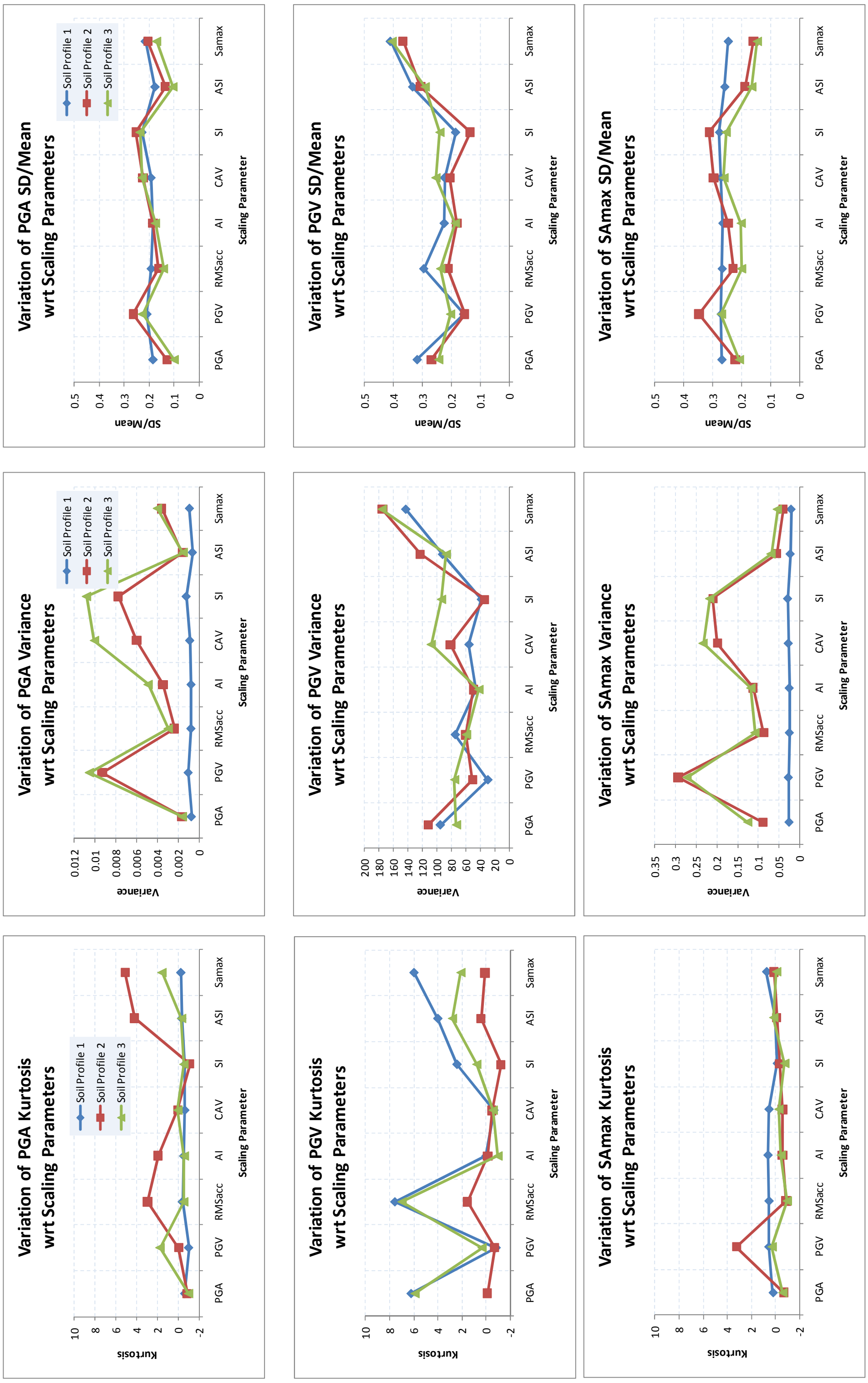

Figure A.15. Variation of kurtosis, variance and SD/mean of PGA, PGV and SA_{max} for three soil profiles with respect to scaling parameters (magnitude bin: 6.5≤M<7.0, distance bin: 30≤R<60km)

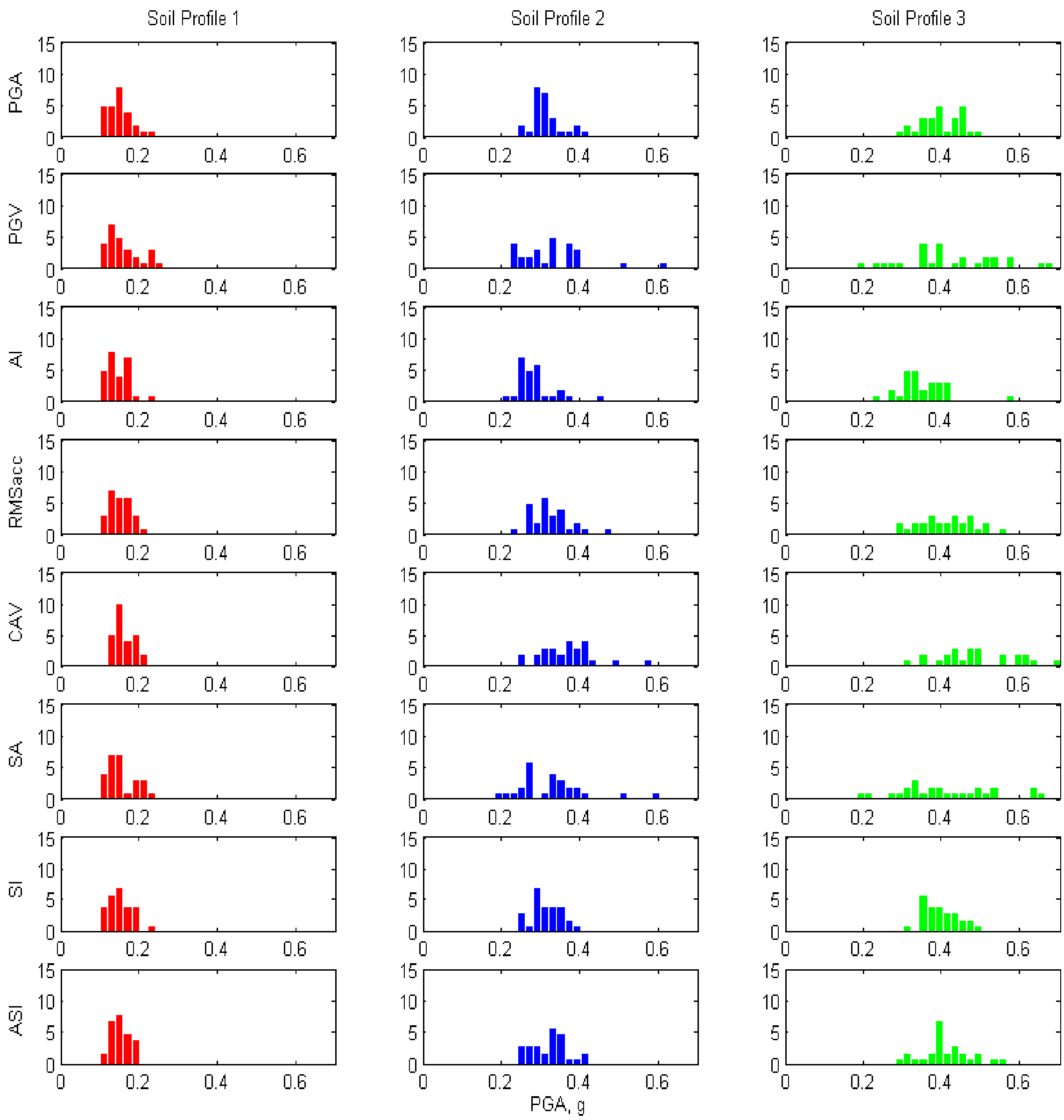
Soil Profile 1
Soil Profile 2
Soil Profile 3
PGA
PGV
AI
RMSacc
CAV
SA
SI
ASI
PGA, g

(a)

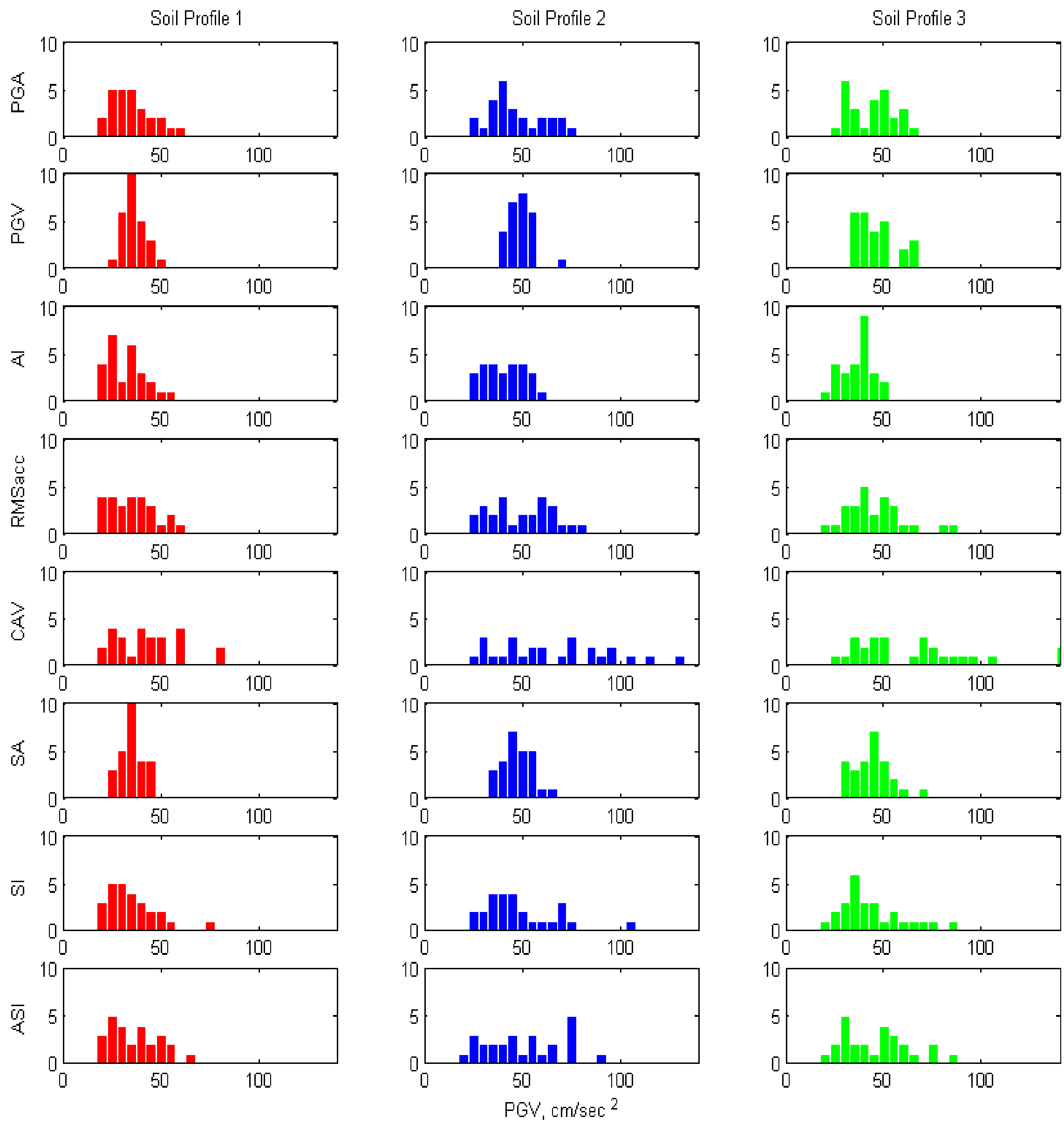
Soil Profile 1
Soil Profile 2
Soil Profile 3
PGA
PGV
AI
RMSacc
CAV
SA
SI
ASI
PGV, cm/sec 2

(b)

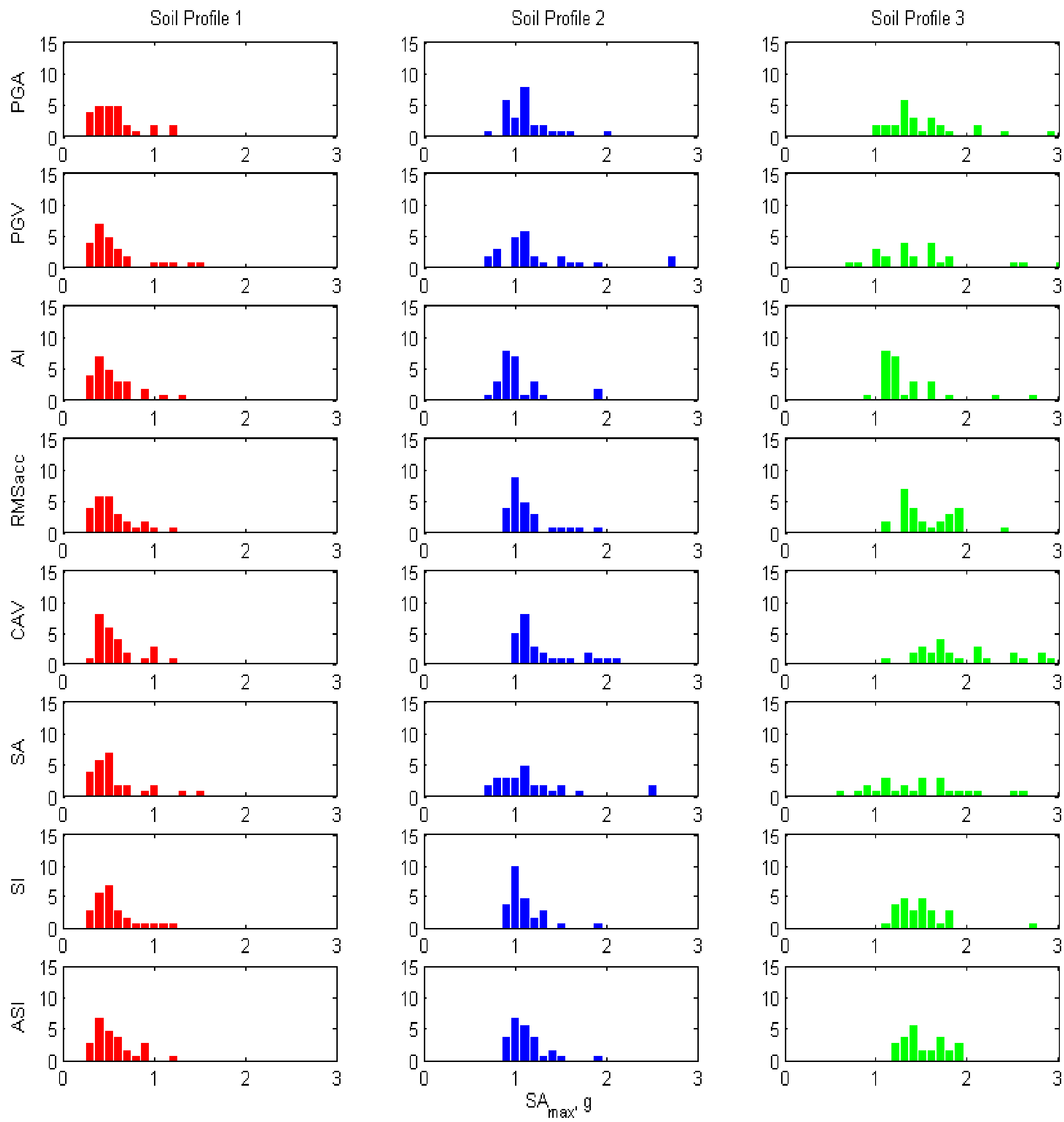

(c)

Figure A.16. Histograms of (a) peak ground acceleration, PGA; (b) peak ground velocity, PGV; (c) maximum spectral accelerations, SA_{max} for three soil profiles calculated on the ground surface from the site response analysis that used input time histories (magnitude bin: 6.5≤M<7.0, distance bin: 60≤R<90km) scaled with respect to eight scaling parameters

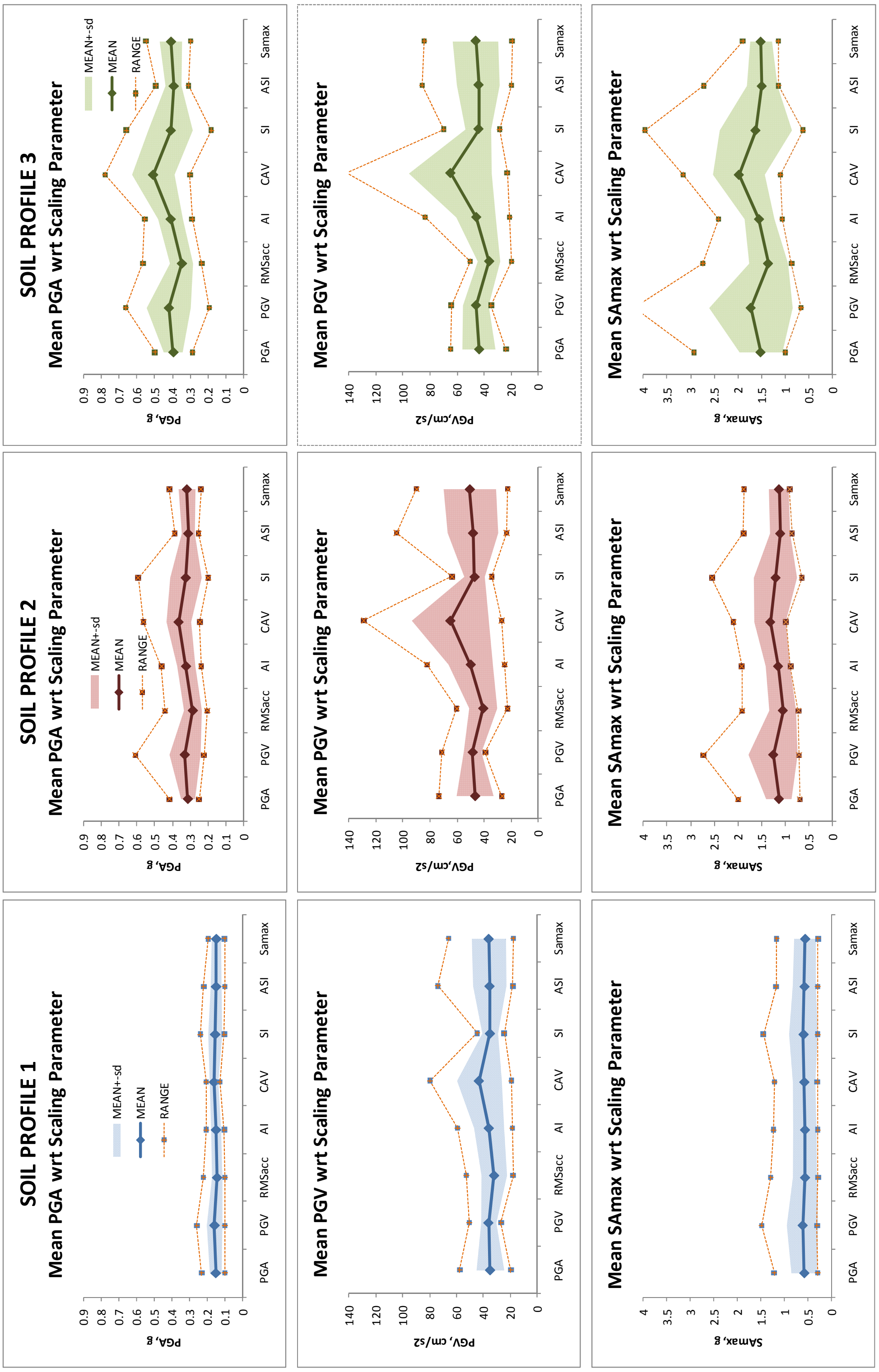

Figure A.17. Variation of mean, mean±sd and range of PGA, PGV and SA_{max} for three soil profiles with respect to scaling parameters (magnitude bin: 6.5≤M<7.0, distance bin: 60≤R<90km)

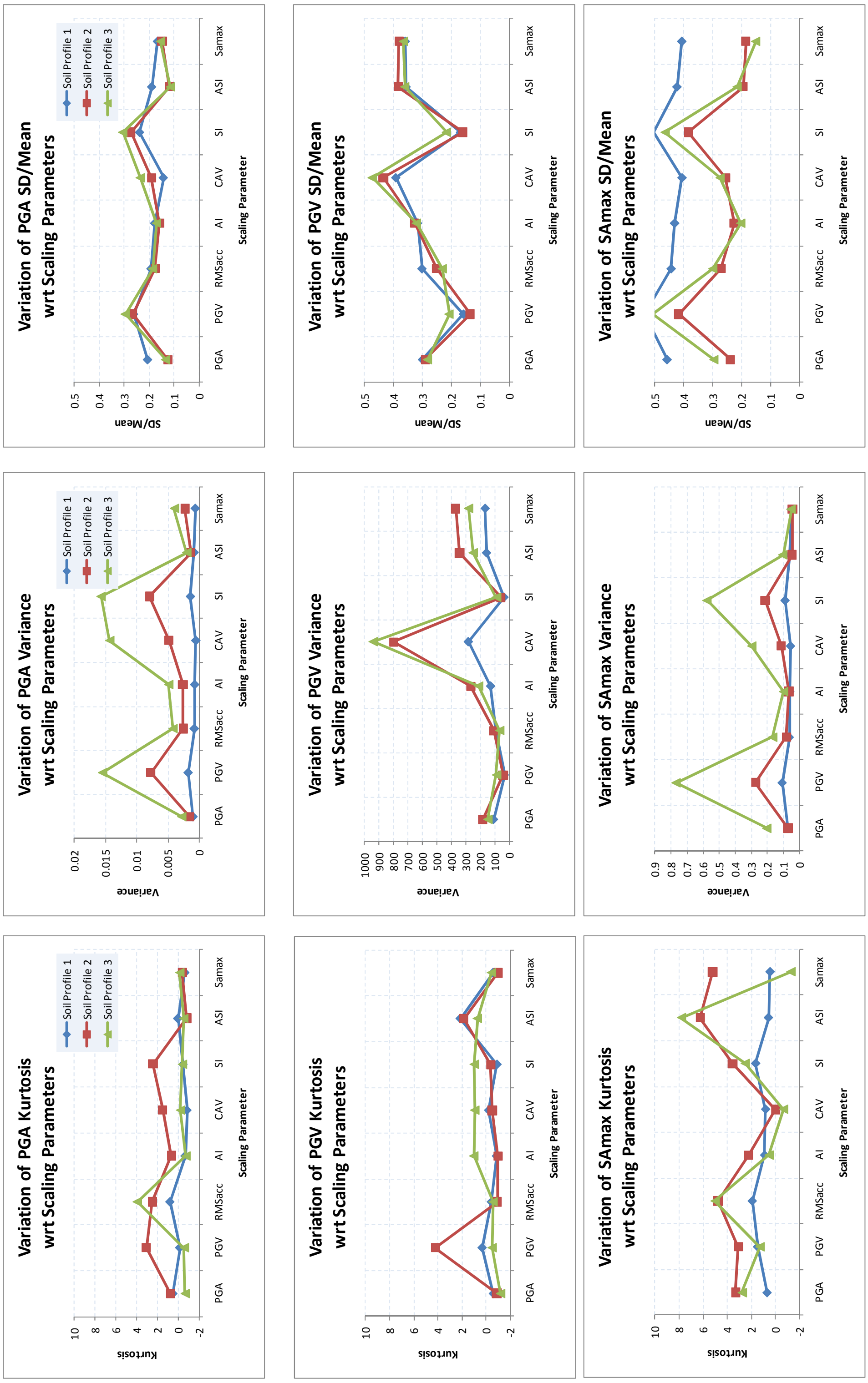

Figure A.18. Variation of kurtosis, variance and SD/mean of PGA, PGV and SA_{max} for three soil profiles with respect to scaling parameters (magnitude bin: 6.5≤M<7.0, distance bin: 60≤R<90km)

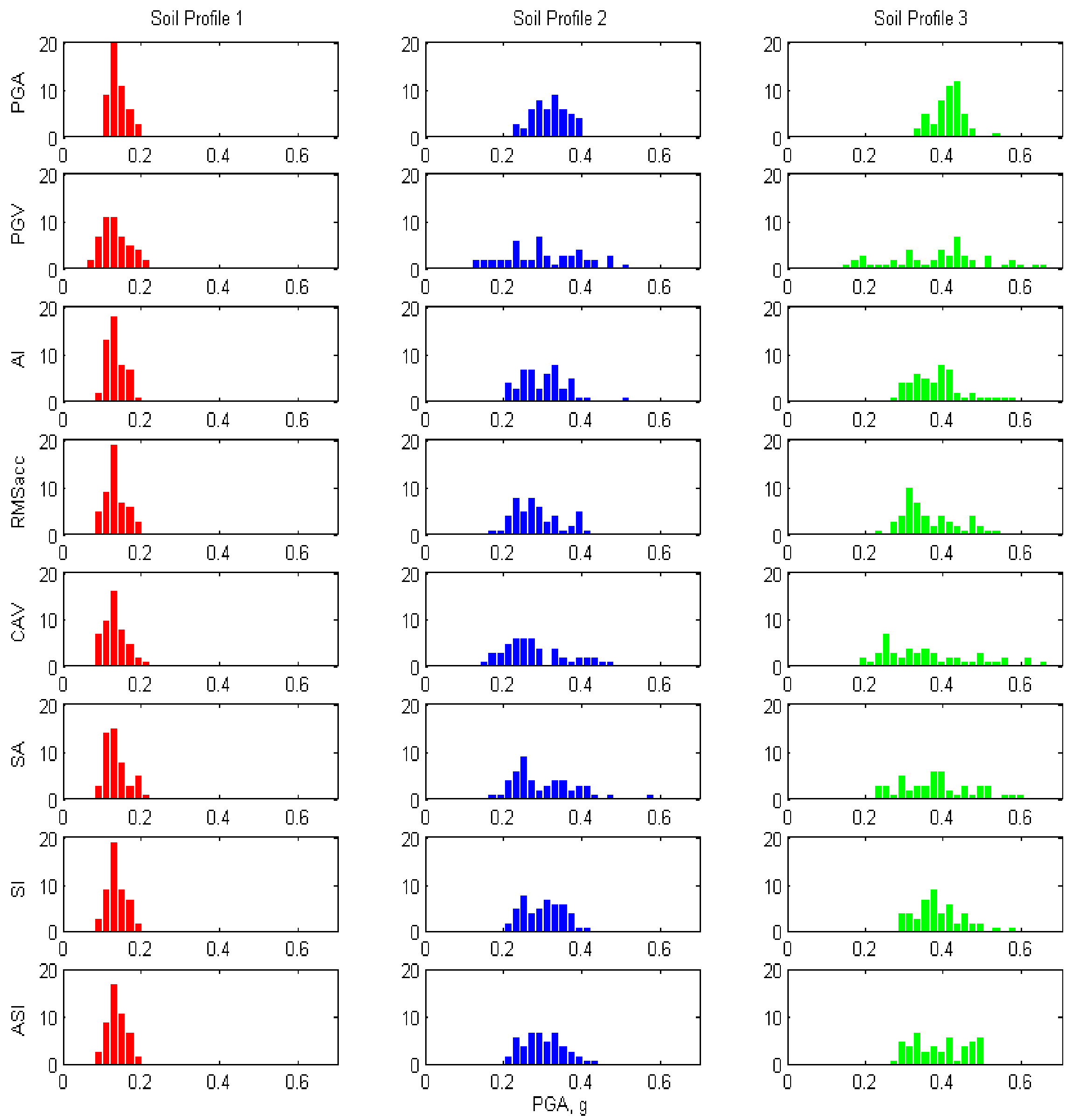
Soil Profile 1
Soil Profile 2
Soil Profile 3
PGA
PGV
AI
RMSacc
CAV
SA
SI
ASI
0
10
20
0
0.2
0.4
0.6
PGA, g

(a)

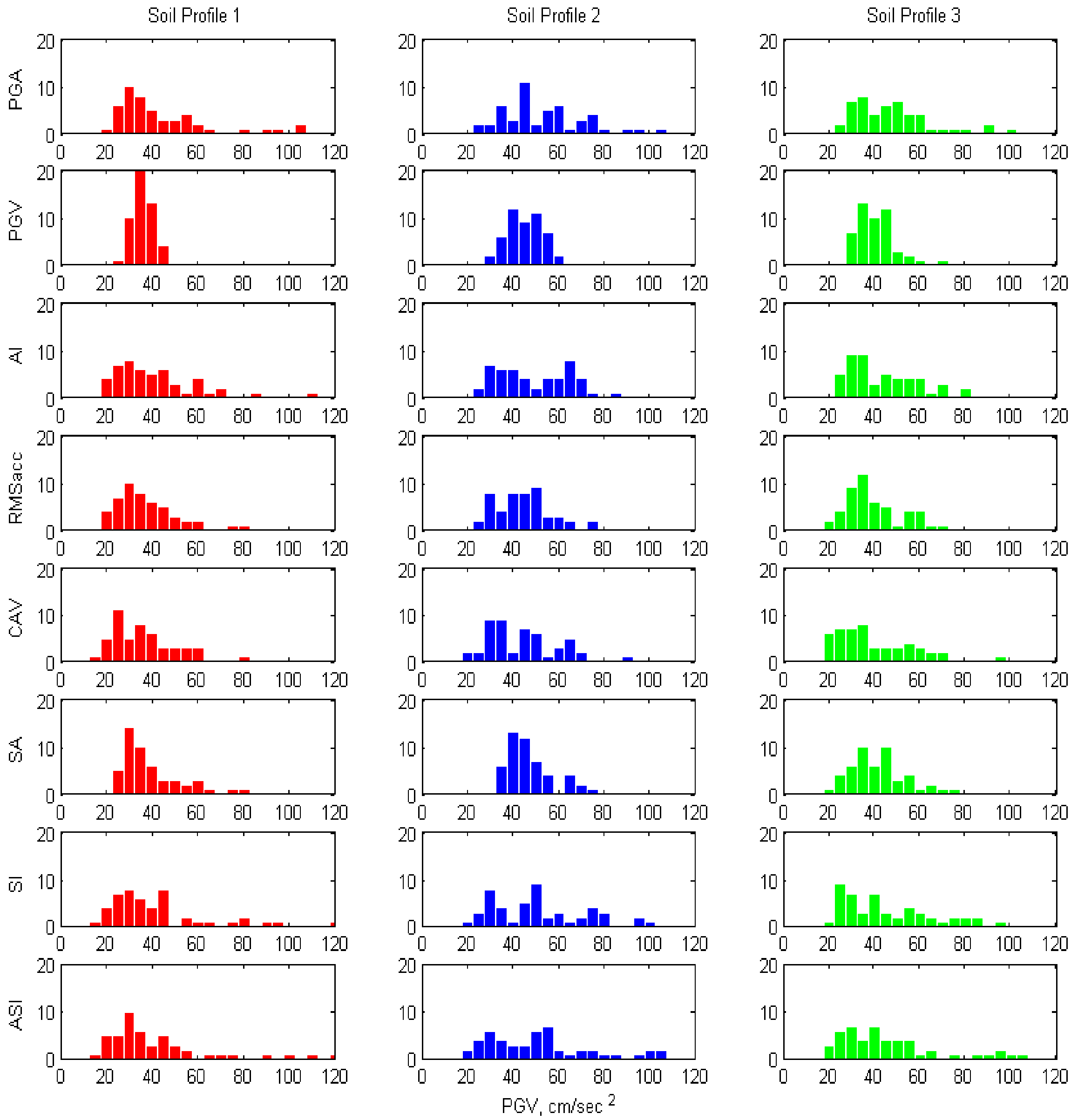
Soil Profile 1
Soil Profile 2
Soil Profile 3
PGA
PGV
AI
RMSacc
CAV
SA
SI
ASI
PGV, cm/sec 2

(b)

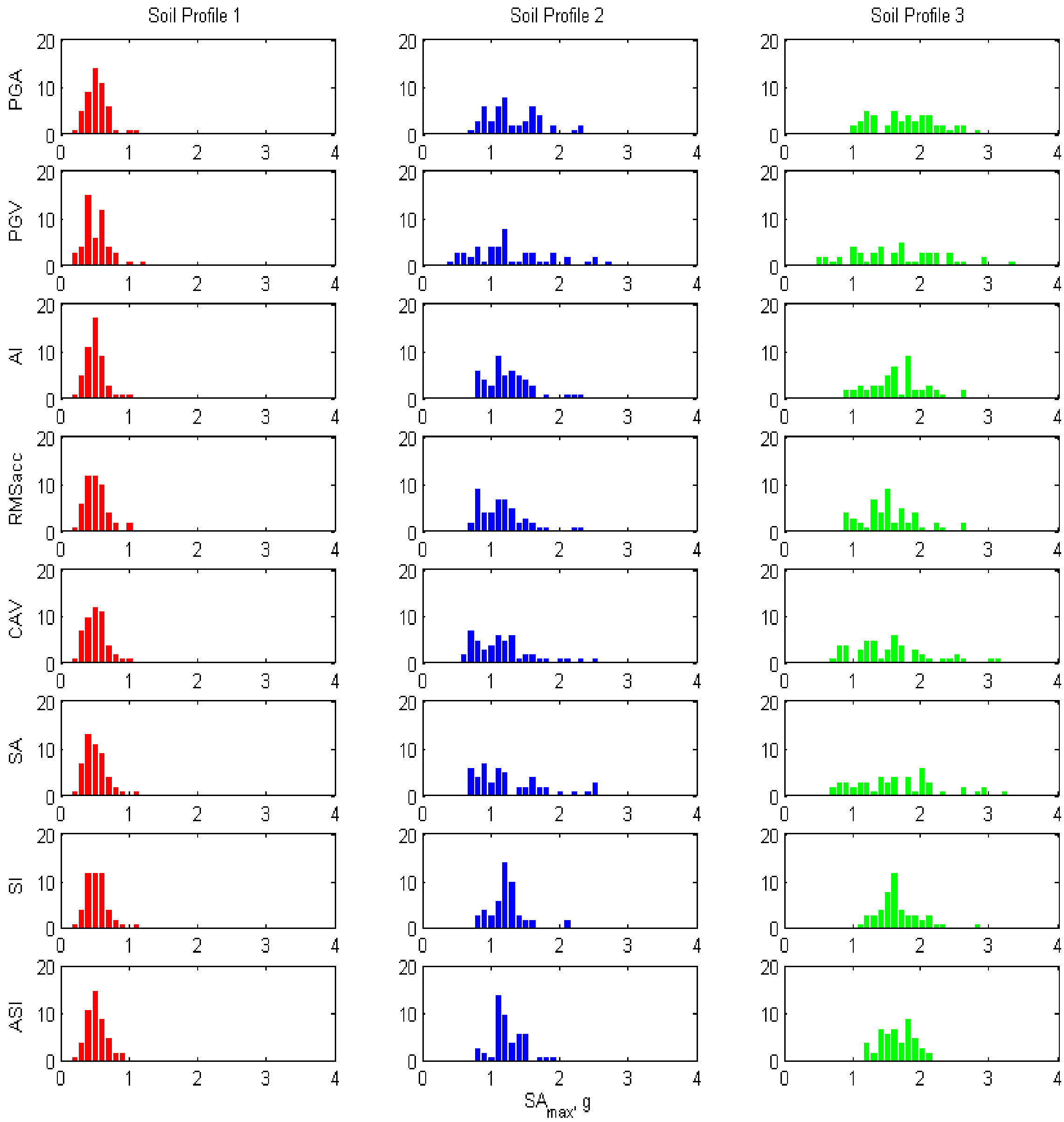

(c)

Figure A.19. Histograms of (a) peak ground acceleration, PGA; (b) peak ground velocity, PGV; (c) maximum spectral accelerations, SA_{max} for three soil profiles calculated on the ground surface from the site response analysis that used input time histories (magnitude bin: 7.0≤M<7.7, distance bin: 0≤R<30km) scaled with respect to eight scaling parameters

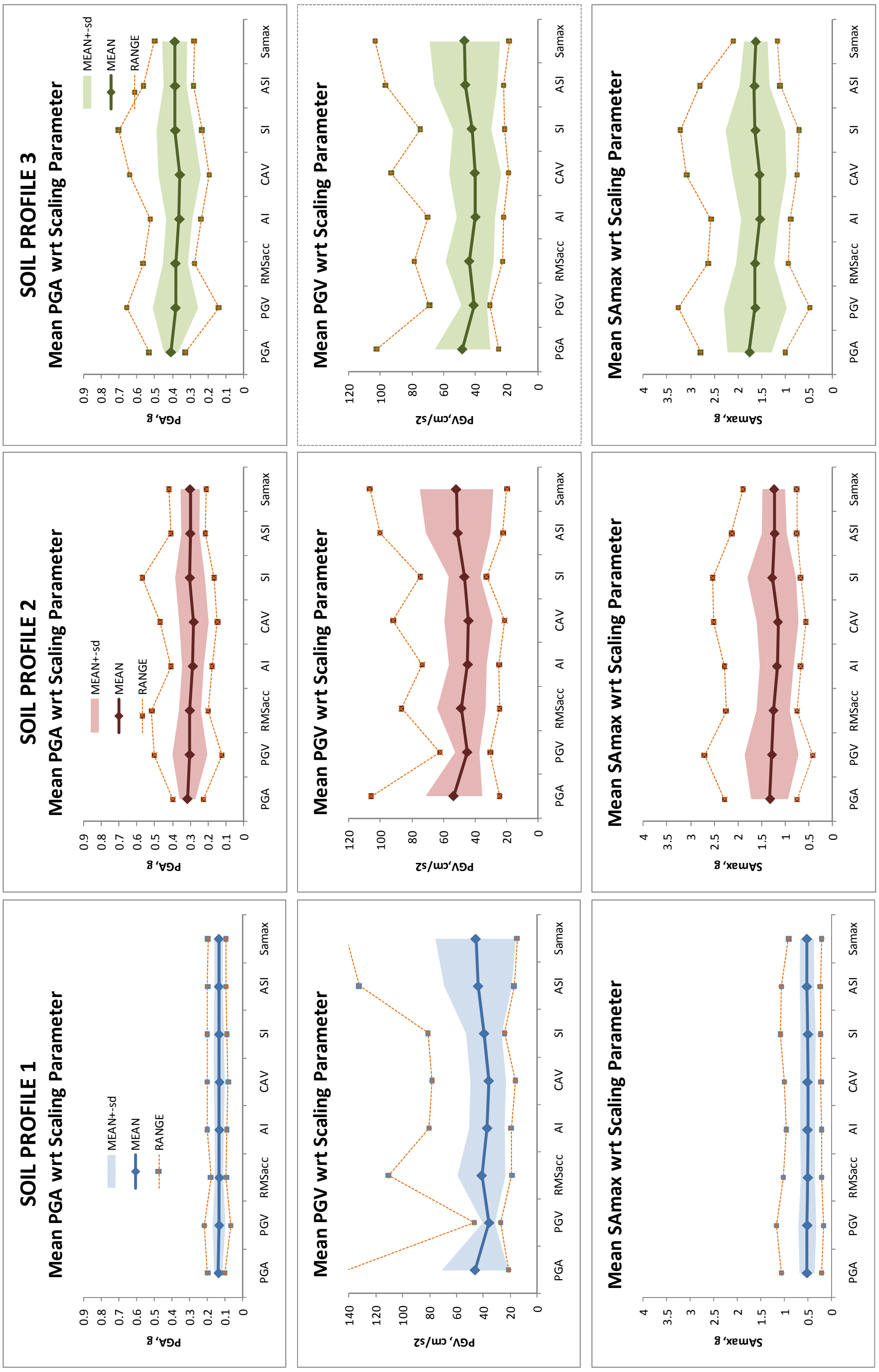

Figure A.20. Variation of mean, mean±sd and range of PGA, PGV and SA_{max} for three soil profiles with respect to scaling parameters (magnitude bin: 7.0≤M<7.7, distance bin: 0≤R<30km)

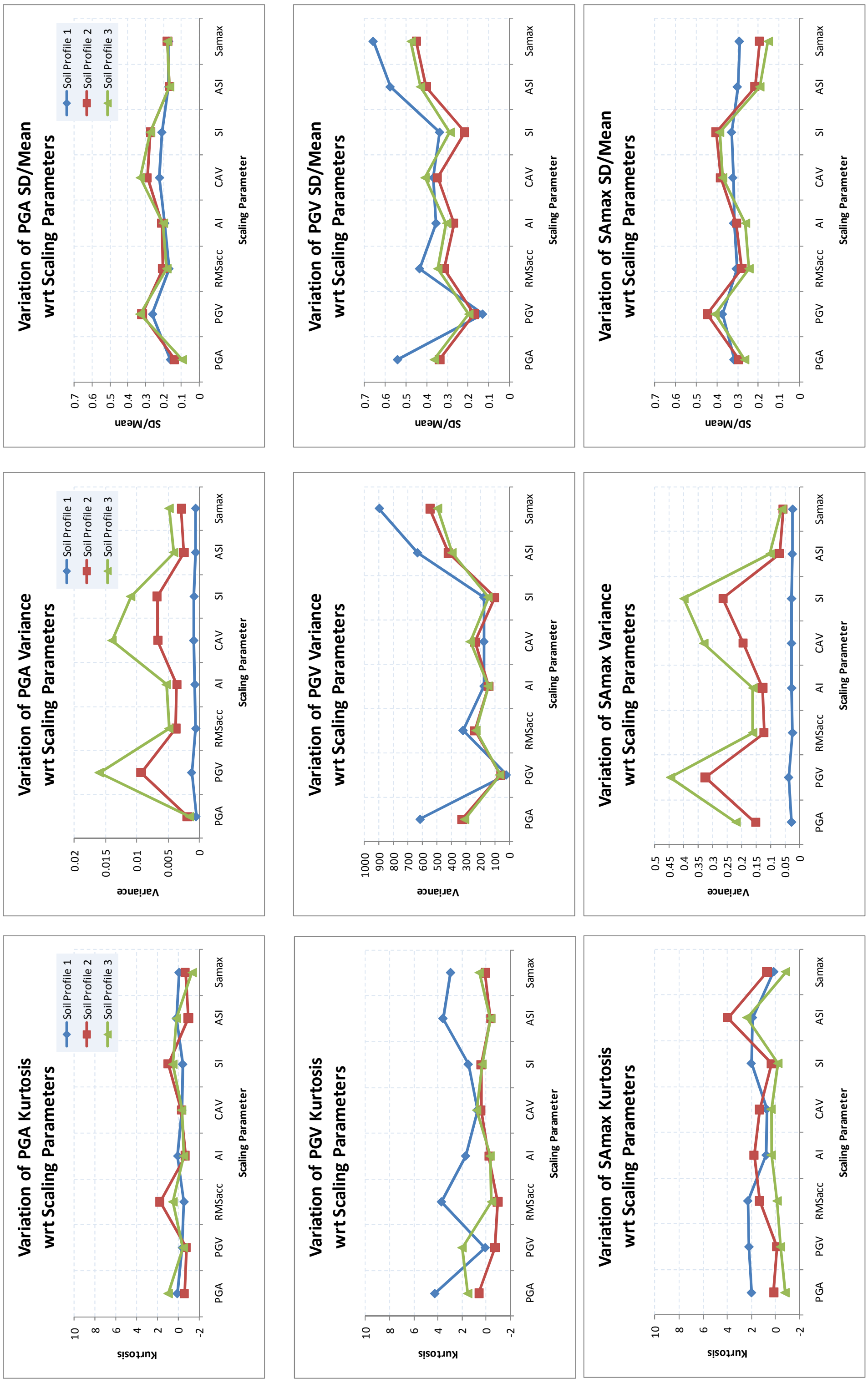

Figure A.21. Variation of kurtosis, variance and SD/mean of PGA, PGV and SA_{max} for three soil profiles with respect to scaling parameters (magnitude bin: 7.0≤M<7.7, distance bin: 0≤R<30km)

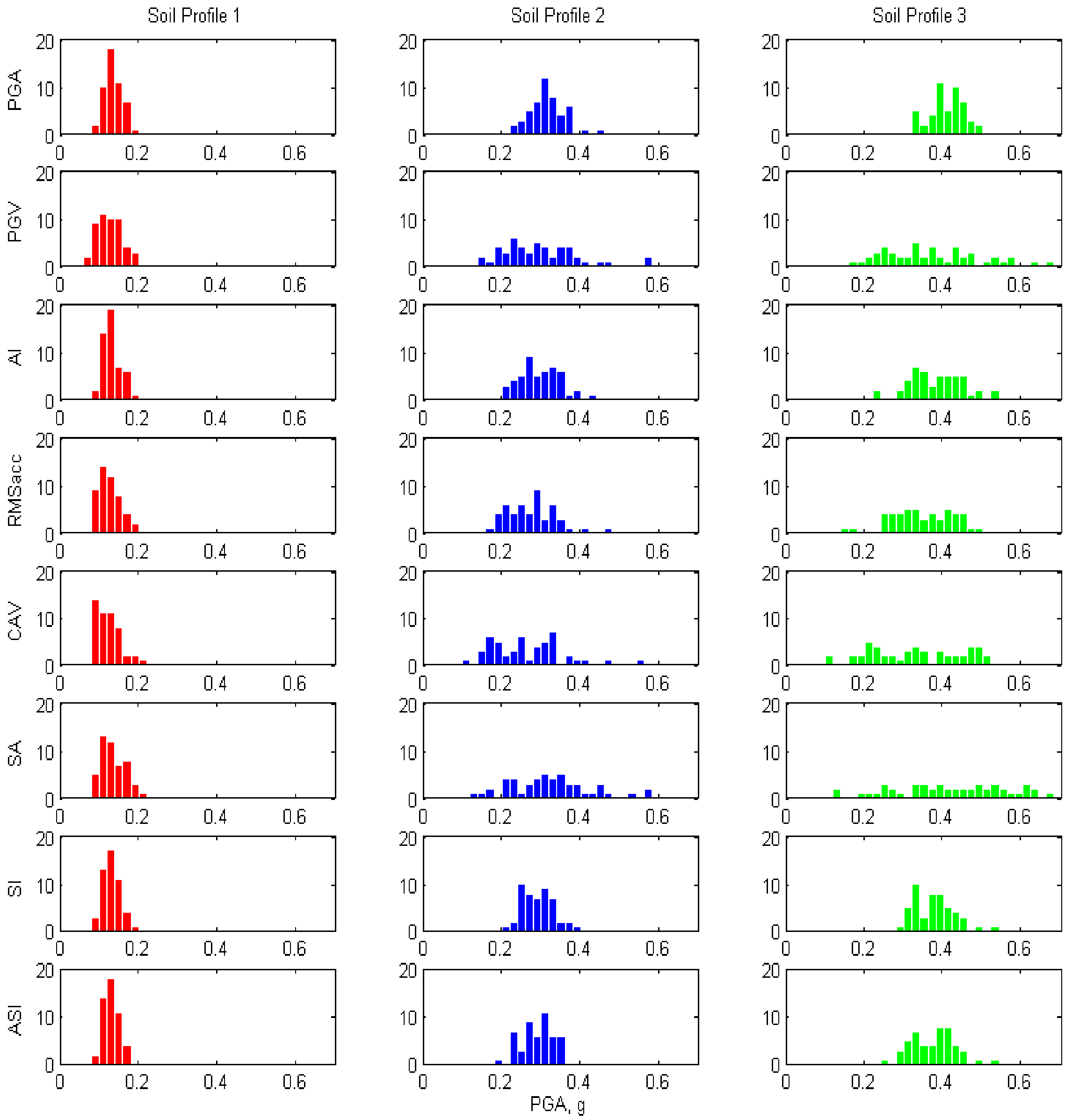
Soil Profile 1
Soil Profile 2
Soil Profile 3
PGA
PGV
AI
RMSacc
CAV
SA
SI
ASI
PGA, g

(a)

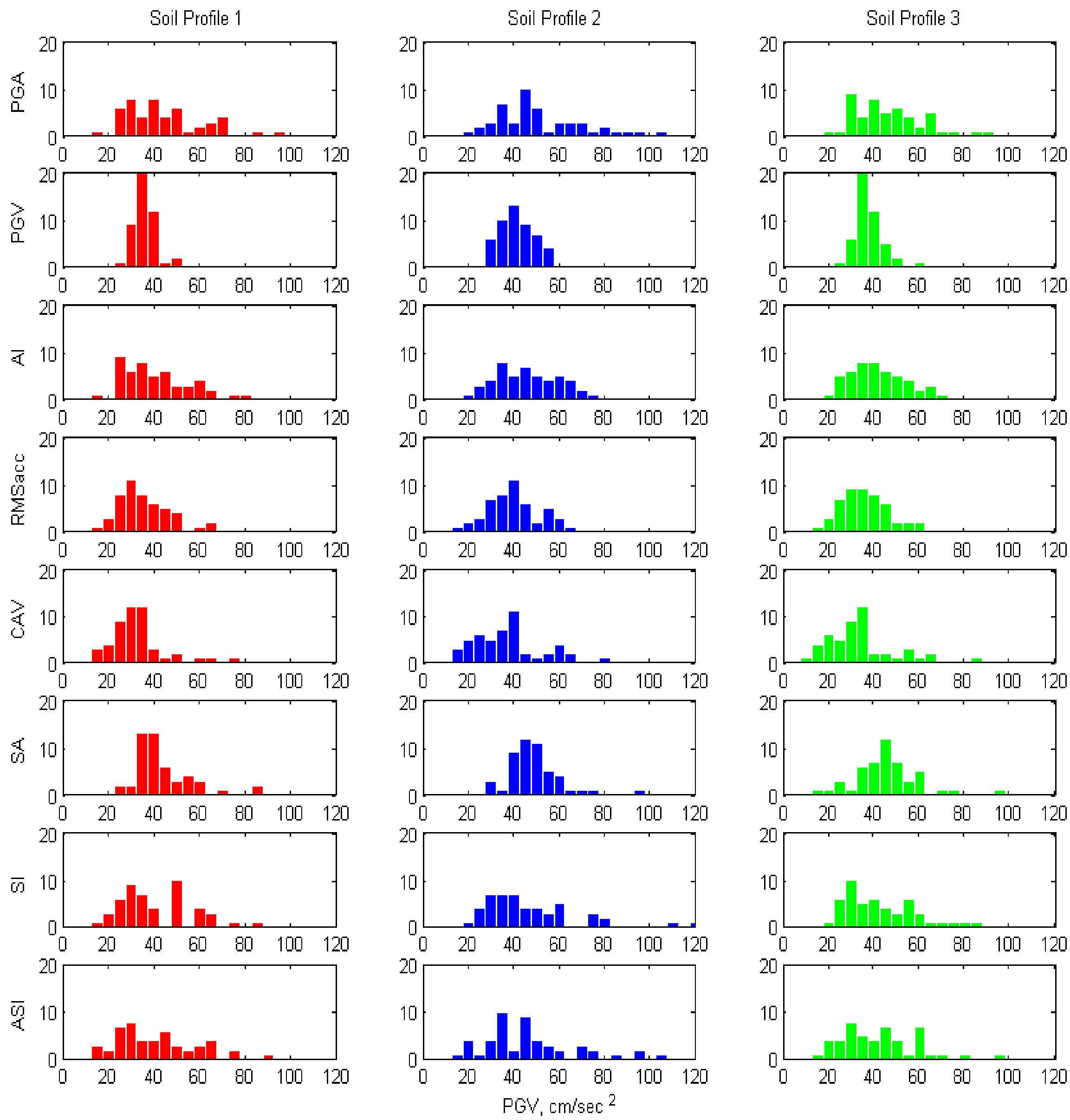

Soil Profile 1
Soil Profile 2
Soil Profile 3
PGA
PGV
AI
RMSacc
CAV
SA
SI
ASI
PGV, cm/sec 2

(b)

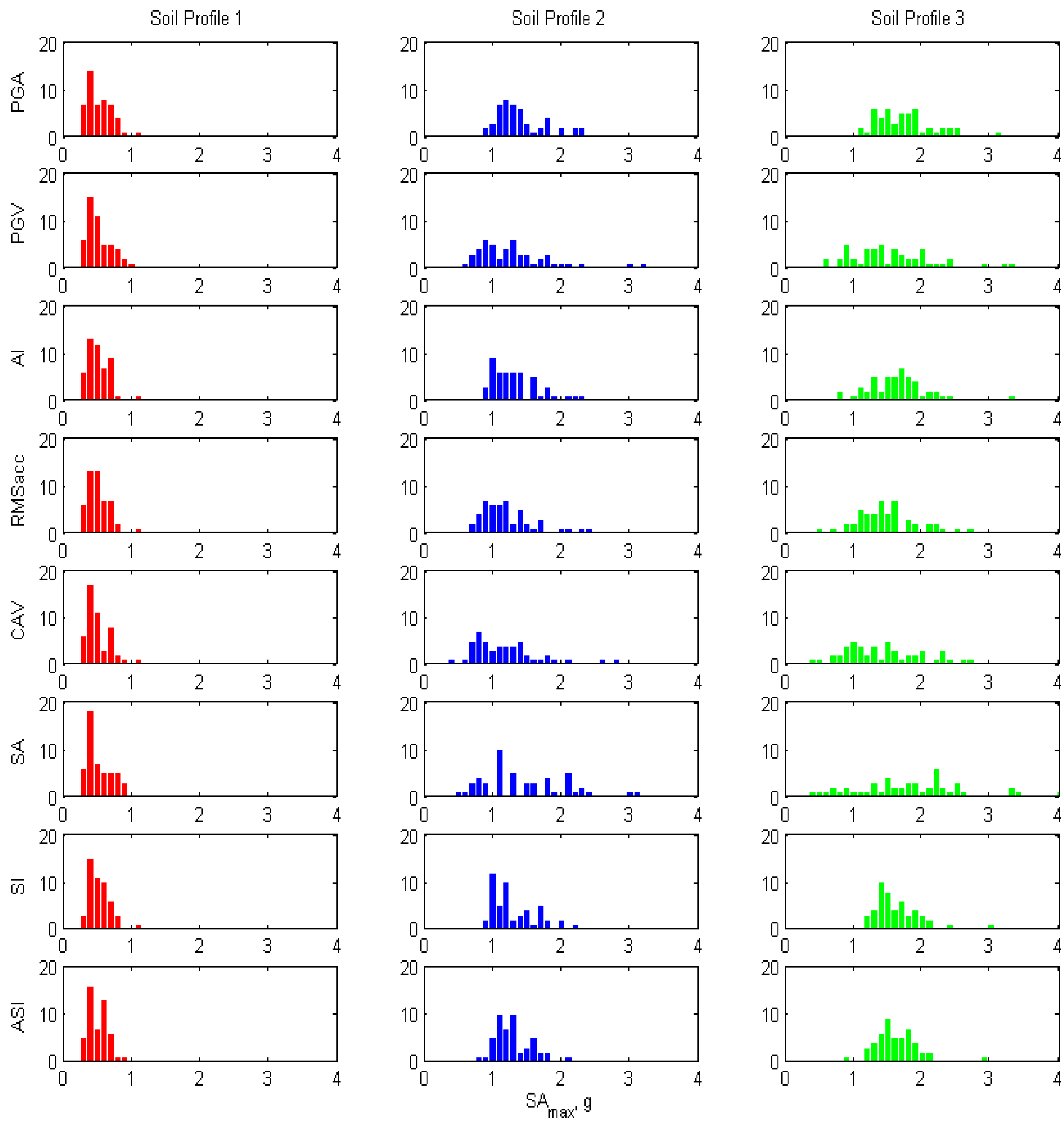

(c)

Figure A.22. Histograms of (a) peak ground acceleration, PGA; (b) peak ground velocity, PGV; (c) maximum spectral accelerations, SA_{max} for three soil profiles calculated on the ground surface from the site response analysis that used input time histories (magnitude bin: 7.0≤M<7.7, distance bin: 30≤R<60km) scaled with respect to eight scaling parameters

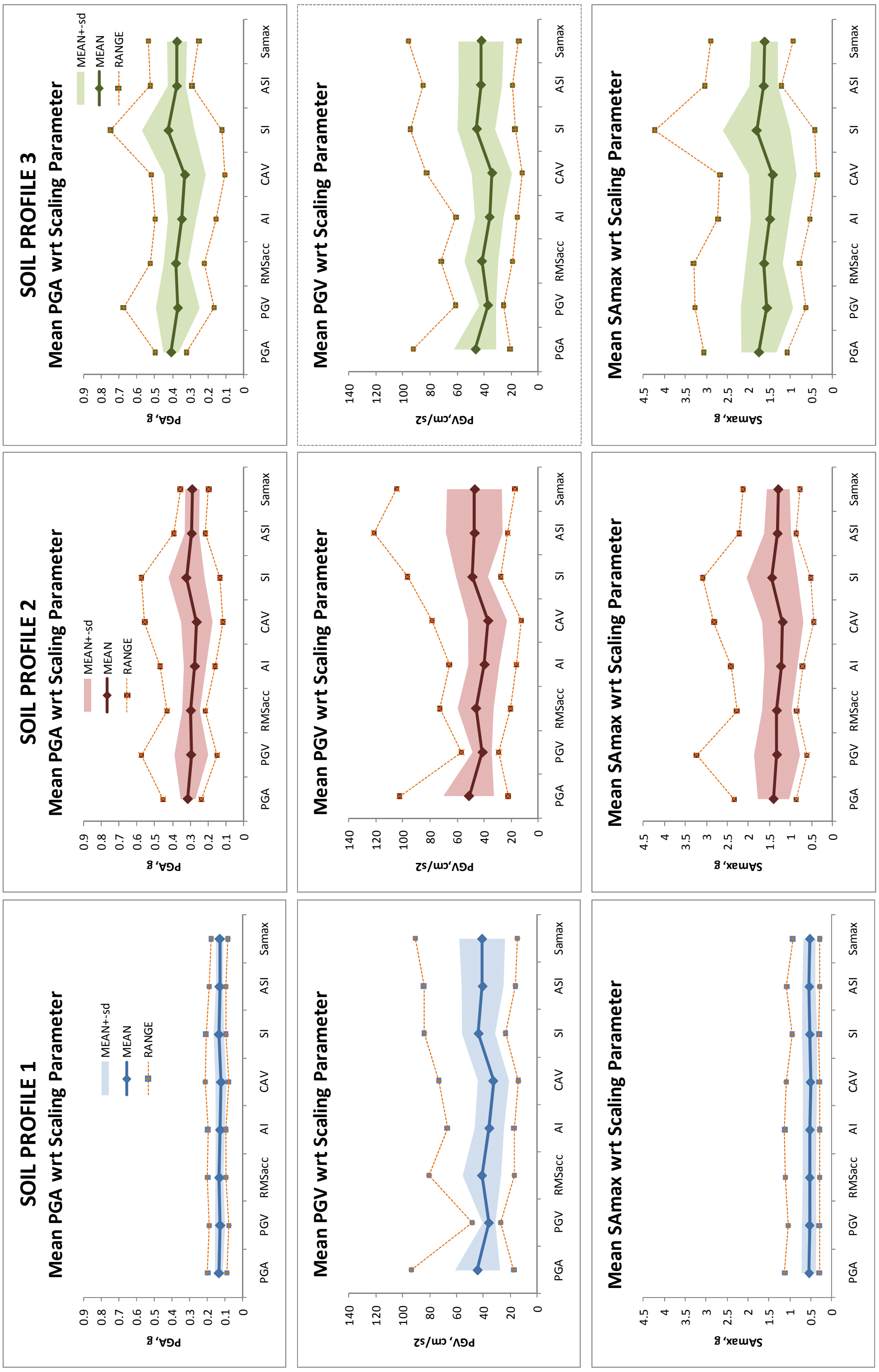

Figure A.23. Variation of mean, mean±sd and range of PGA, PGV and SA_{max} for three soil profiles with respect to scaling parameters (magnitude bin: 7.0≤M<7.7, distance bin: 30≤R<60km)

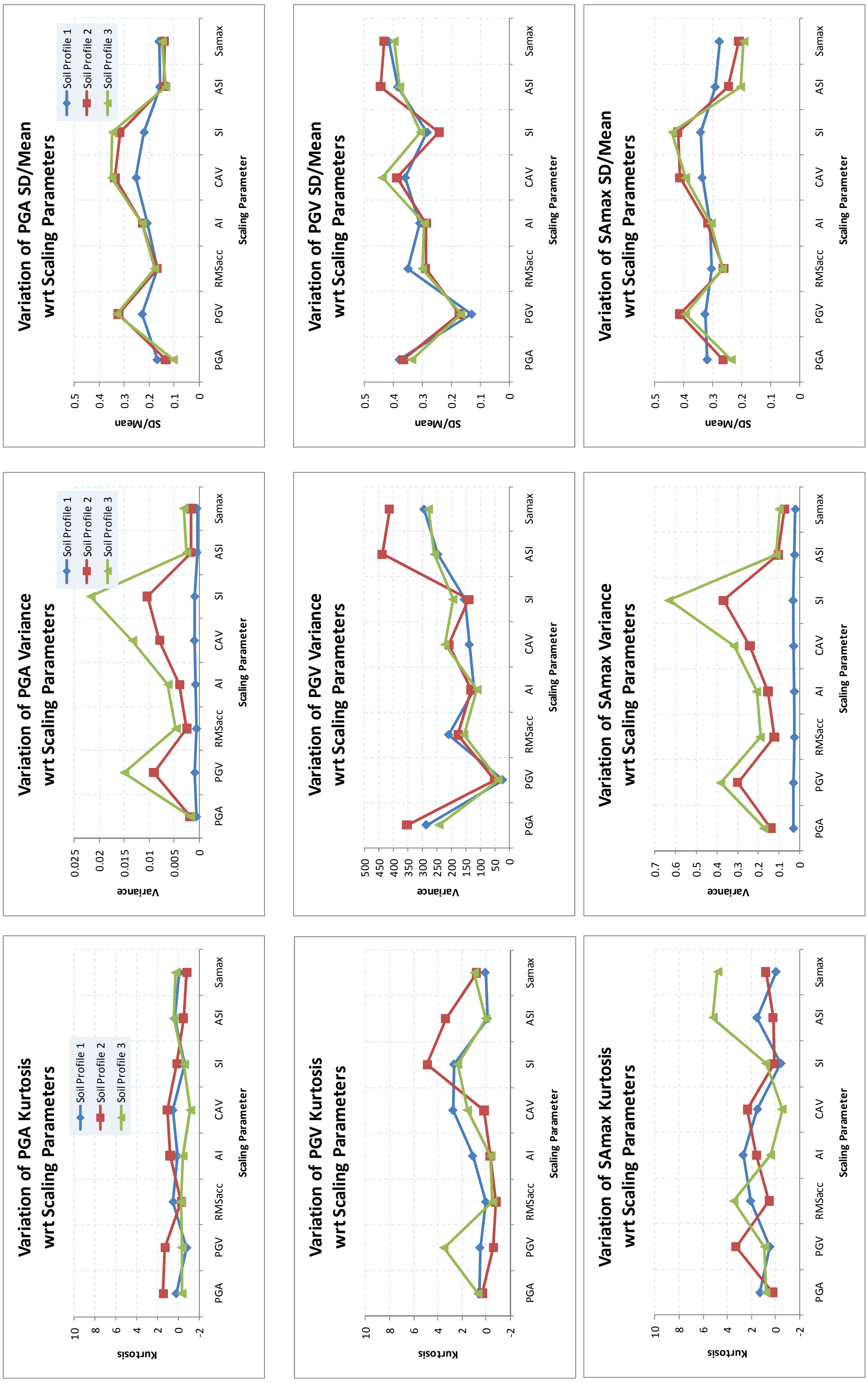

Figure A.24. Variation of kurtosis, variance and SD/mean of PGA, PGV and SA_{max} for three soil profiles with respect to scaling parameters (magnitude bin: 7.0≤M<7.7, distance bin: 30≤R<60km)

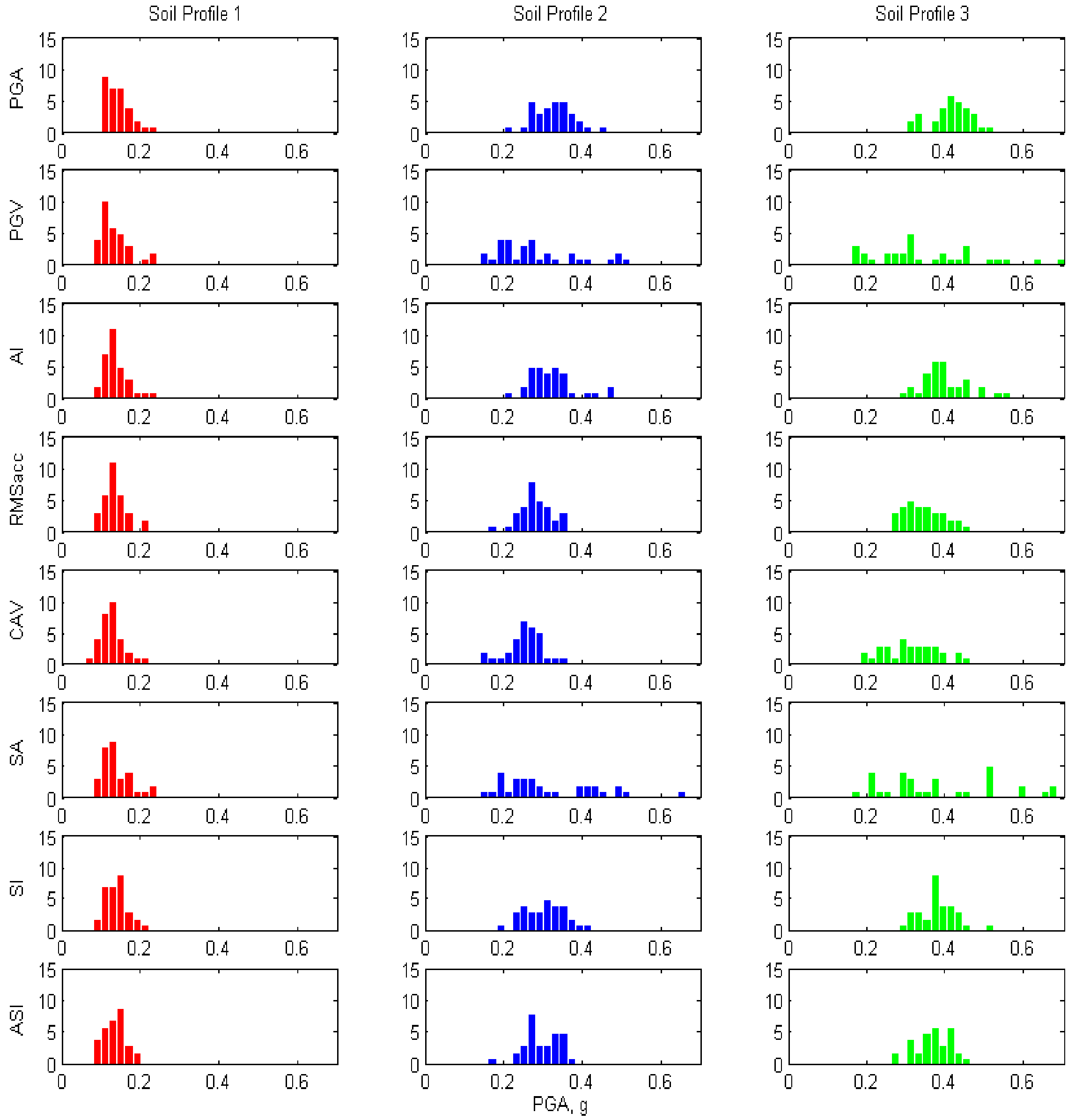

Soil Profile 1
Soil Profile 2
Soil Profile 3
PGA
PGV
AI
RMSacc
CAV
SA
SI
ASI
PGA, g

(a)

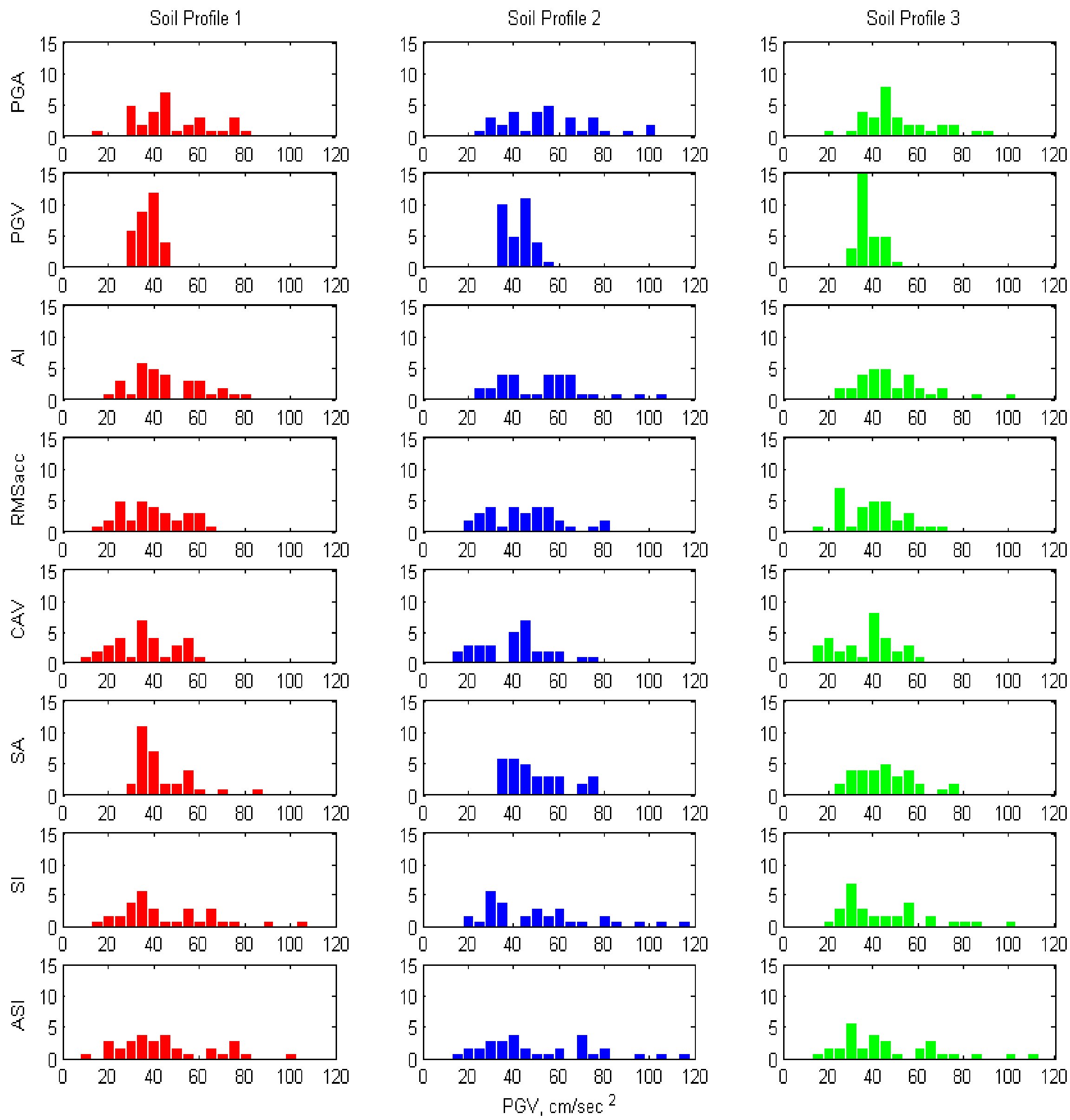
Soil Profile 1
Soil Profile 2
Soil Profile 3
PGA
PGV
AI
RMSacc
CAV
SA
SI
ASI
PGV, cm/sec 2

(b)

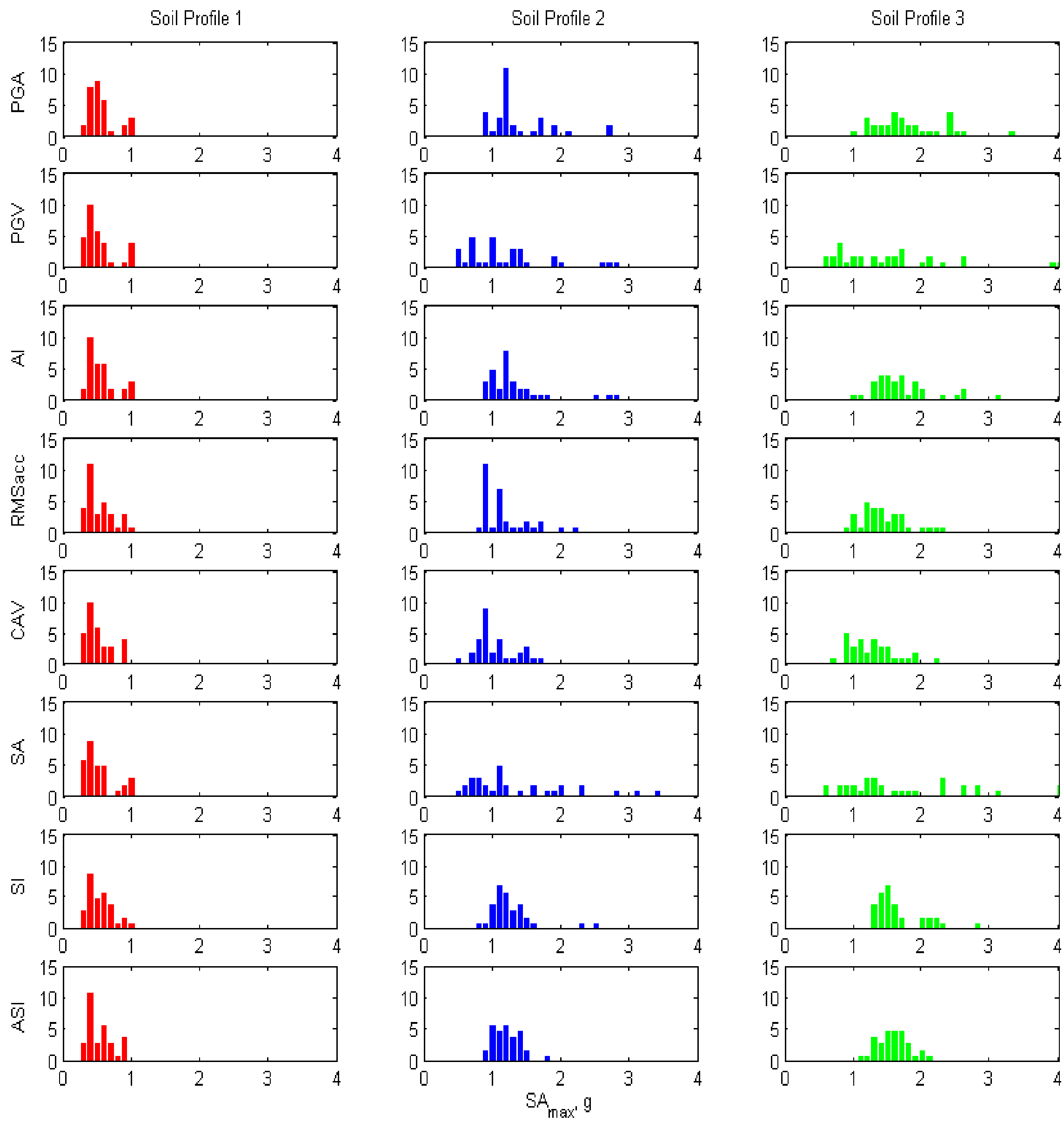

(c)

Figure A.25. Histograms of (a) peak ground acceleration, PGA; (b) peak ground velocity, PGV; (c) maximum spectral accelerations, SA_{max} for three soil profiles calculated on the ground surface from the site response analysis that used input time histories (magnitude bin: 7.0≤M<7.7, distance bin: 60≤R<90km) scaled with respect to eight scaling parameters

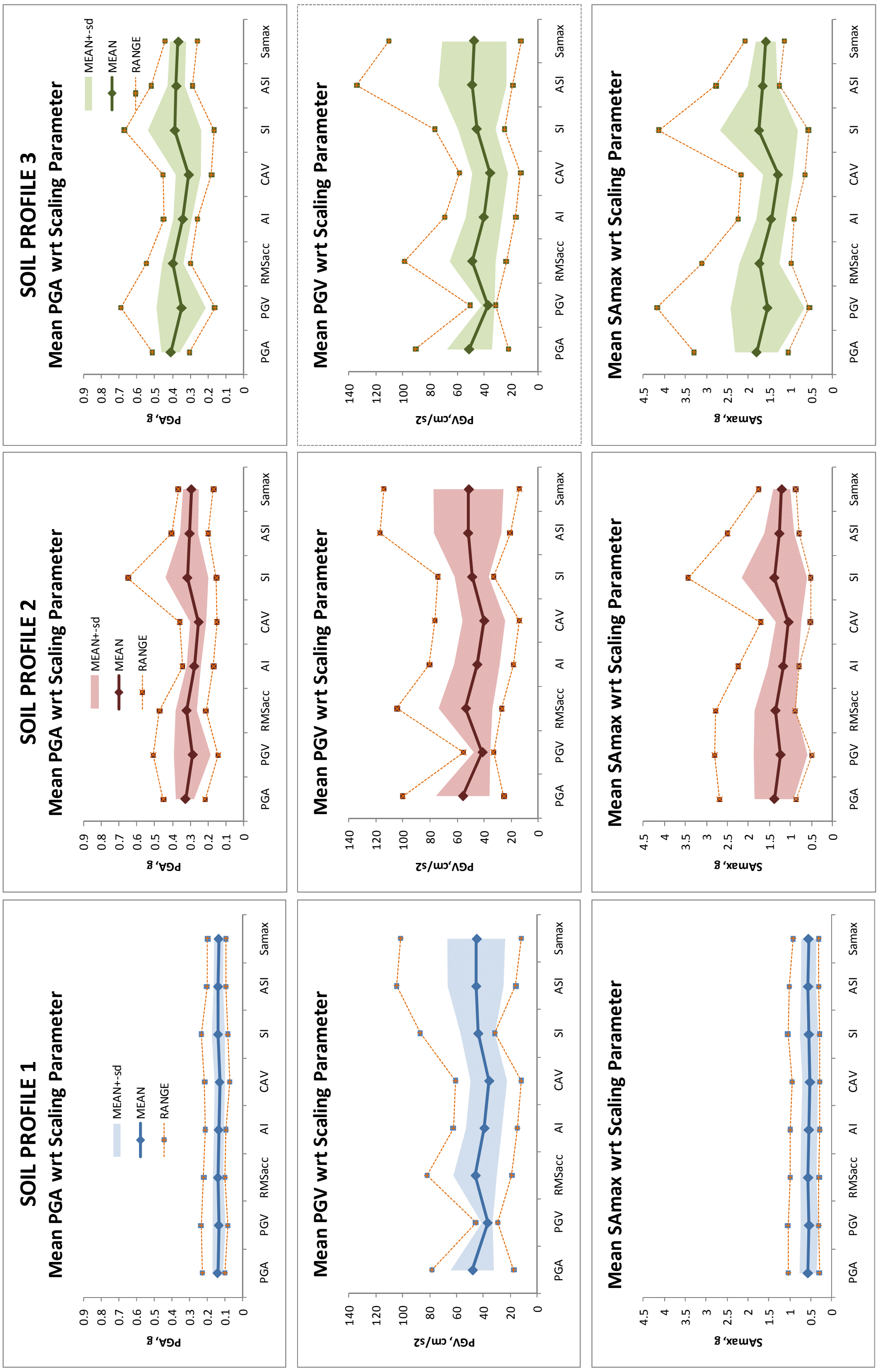

Figure A.26. Variation of mean, mean±sd and range of PGA, PGV and SA_{max} for three soil profiles with respect to scaling parameters (magnitude bin: 7.0≤M<7.7, distance bin: 60≤R<90km)

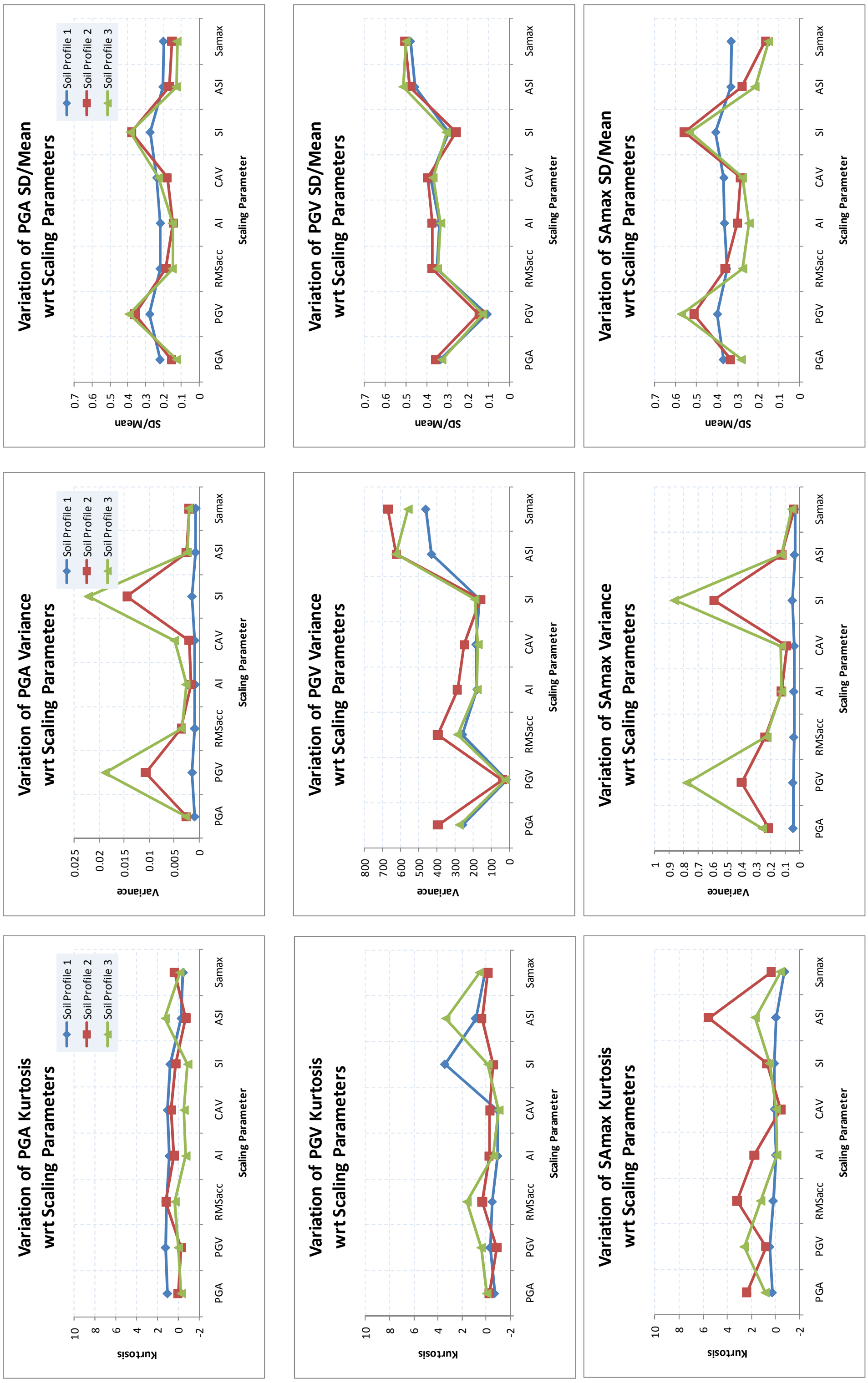

Figure A.27. Variation of kurtosis, variance and SD/mean of PGA, PGV and SA_{max} for three soil profiles with respect to scaling parameters (magnitude bin: 7.0≤M<7.7, distance bin: 60≤R<90km)

REFERENCES

Abrahamson N., G. Atkinson, D. Boore, Y. Bozorgnia, K. Campbell, B. Chiou, I. M. Idriss, W. Silva and R. Youngs, 2008, “Comparisons of the NGA Ground-Motion Relations”, *Earthquake Spectra*, Vol. 24, No. 1, pp. 45-66.

Abrahamson, N. and W. Silva, 2008, “Summary of the Abrahamson & Silva NGA Ground-Motion Relations”, *Earthquake Spectra*, Vol. 24, No. 1, pp. 67-97.

Abrahamson, N. A. and K. M. Shedlock, 1997, “Overview”, *Seismological Research Letters*, Vol. 68, No. 1, pp. 9–23.

Abrahamson, N. A. and P. C. Somerville, 1996, “Effects of the Hanging Wall and Footwall on Ground Motions Recorded during the Northridge Earthquake”, *Bulletin of the Seismological Society of America*, Vol. 86, No. 1B, pp. S93–S99.

Abrahamson, N. A. and R. R. Youngs, 1992, “A Stable Algorithm for Regression Analyses Using the Random Effects Model”, *Bulletin of the Seismological Society of America*, Vol. 82, No. 1, pp. 505–510.

Aguirre, J. and K. Irikura, 1997, “Nonlinearity, Liquefaction, and Velocity Variation of Soft Soil Layers in Port Island, Kobe, during the Hyogo-ken Nanbu Earthquake”, *Bulletin of the Seismological Society of America*, Vol. 87, pp. 1244-1258.

Akaike, H., 1974, “A New Look at the Statistical Model Identification”, *I.E.E.E. Transactions on Automatic Control*, Vo1. 19, pp. 716-72.

Aki, K., 1993, “Local Site Effects on Weak and Strong Ground Motion”, *Tectonophysics*, Vol. 218, pp. 93-111.

Akkar, S. and J. J. Bommer, 2007, “Empirical Prediction Equations for Peak Ground Velocity Derived from Strong-Motion Records from Europe and the Middle East”, *Bulletin of the Seismological Society of America*, Vol. 97, No. 2, pp. 511-530.

Ambraseys, N. N. , J. Douglas, S. K. Sarma and P. M. Smit, 2005, “Equations for the Estimation of Strong Ground Motions from Shallow Crustal Earthquakes Using Data from Europe and the Middle East: Horizontal Peak Ground Acceleration and Spectral Acceleration”, *Bulletin of Earthquake Engineering*, Vol. 3, No. 1, pp. 1-53.

Ambraseys, N. N. and J. J. Bommer, 1995, “Attenuation Relations for Use in Europe: An Overview”, in *Proceedings of Fifth SECED Conference on European Seismic Design Practice* , E.A. Elnashai (ed.), Chester, United Kingdom, pp. 67–74, A.A. Balkema, Rotterdam.

Ansal, A., A. Akinci, G. Cultrera, M. Erdik, V. Pessina, G. Tönük and G. Ameri, 2009, “Loss Estimation in Istanbul Based on Deterministic Earthquake Scenarios of the Marmara Sea Region (Turkey)”, *Soil Dynamics and Earthquake Engineering*, Vol. 29.

Ansal A., A. Kurtuluş and G.Tönük, 2008, “Damage to Water and Sewage Pipelines in Adapazari during 1999 Kocaeli, Turkey Earthquake”, *Proceedings of Sixth International Conference on Case histories in Geotechnical Engineering*, Arlington, Virginia, ABD, Paper No:3.17.

Ansal, A., A. Kurtuluş and G. Tönük, 2007a, “Earthquake Damage Scenario Software for Urban Areas”, Keynote Lecture, *International Conference on Computational Methods in Structural Dynamics and Earthquake Engineering*, M. Papadrakakis, D. C. Charmpis, N. D. Lagaros, Y. Tsompanakis (eds.), Rethymno, Crete, Greece.

Ansal, A., G. Tönük and Y. Bayraklı, 2007b, “Microzonation with respect to Ground Shaking Intensity Based on 1D Site Response Analysis”, *XIV European Conference on Soil Mechanics and Geotechnical Engineering*, Madrid, Spain.

Ansal, A., G. Tönük and A. Kurtuluş, 2007c, "Microzonation with Respect to Ground Shaking Intensity and Seismic Hazard Scenarios", Invited Lecture, *Sixth National Conference on Earthquake Engineering*, Istanbul, Turkey, Vol. 3, pp. 133-151 (in Turkish).

Ansal, A., G. Tönük, M. Demircioğlu, Y. Bayraklı, K. Şeşetyan and M. Erdik, 2006a, "Ground Motion Parameters for Vulnerability Assessment", *Proceedings of the First European Conference on Earthquake Engineering and Seismology*, Geneva, Switzerland, Paper Number: 1790.

Ansal, A., E. Durukal and G. Tönük, 2006b, "Selection and Scaling of Real Acceleration Time Histories for Site Response Analyses", *Proceedings of ETC12 Workshop*, Athens, Greece.

Ansal, A., K. Özaydın, M. Erdik, Y. Yıldırım, H. Kılıç, Ş. Adatepe, P. T. Özener, M. Tonaroğlu, K. Şeşetyan and M. Demircioğlu, 2005a, "Seismic Microzonation for Urban Planning and Vulnerability Assessment", *Proceedings of the International Symposium of Earthquake Engineering (ISEE2005)*, Awaji Island, Kobe, Japan.

Ansal, A., M. Erdik, H. Eyidoğan, K. Özaydın, M. Yıldırım, and B. Siyahi, 2005b, *Special Technical Requirements for Microzonation Maps*, Istanbul Metropolitan Municipality (in Turkish).

Ansal, A., G. Tönük and Y. Bayrakli, 2005c, *Microzonation for Site Conditions for Bakirköy, Gemlik, Bandırma, Tekirdağ, Eskisehir and Körfez, Microzonation and Hazard Vulnerability Studies for Disaster Mitigation in Pilot Municipalities*, Project Report, Bogazici University Kandilli Observatory and Earthquake Engineering Research Institute, Turkey.

Ansal, A., Y. Biro, A. Erken, and U. Gulerce, 2004a, "Seismic Microzonation: A Case Study", in A. Ansal (edt.), *Recent Advances in Earthquake Geotechnical Engineering and Microzonation*, Chapter 8, pp. 253-266, Kluwer Academic Publications, Dordrecht.

Ansal, A., J. Laue, J. Buchheister, M. Erdik, S M. Springman, J. Studer and D. Koksal, 2004b, "Site Characterization and Site Amplification for a Seismic Microzonation Study in Turkey", *Proceedings of 11th International Conference on Soil Dynamics and Earthquake Engineering and 3rd Earthquake Geotechnical Engineering*, San Francisco, USA.

Ansal, A., M. Erdik, J. Studer, S. Springman, J. Laue, J. Buchheister, D. Giardini, D. Faeh and D. Koksal, 2004c, "Seismic Microzonation for Earthquake Risk Mitigation in Turkey", *Proceedings of 13th World Conference of Earthquake Engineering*, CD Paper No. 1428, Canada.

Ansal, A., R. İyisan and M. Özkan, 1997, "A Preliminary Microzonation Study for the Town of Dinar", *Proceedings of Special Technical Session on Earthquake Geotechnical Engineering: Seismic Behavior of Ground and Geotechnical Structures, 14th ICSMFE*, Hamburg, pp. 3-9.

Ansal, A. and G. Tönük, 2007a, "Ground Motion Parameters for Loss Estimation", Keynote Lecture, *Fourth International Conference on Urban Earthquake Engineering*, Tokyo Institute of Technology, Tokyo, Japan, pp.7-14.

Ansal, A. and G. Tönük, 2007b, "Source and Site Effects for Microzonation", Theme Lecture, *Fourth International Conference on Earthquake Geotechnical Engineering*, K.Pitilakis (ed.), Chapter 4, pp.73-92, Springer.

Ansal, A., 1999, "Strong Ground Motions and Site Amplification", Theme Lecture, in P.S.Pinto (edt.), *Second International Conference on Earthquake Geotechnical Engineering*, Vol.3, pp. 879-894.

Arias, A., 1970, "A Measure of Earthquake Intensity", in R. J. Hansen (edt.), *Seismic Design for Nuclear Power-Plants*, pp. 438–483, MIT Press, Cambridge, Massachusetts.

Assimaki, D. and E. Kausel, 2002, "An Equivalent Linear Algorithm with Frequency- and Pressure-Dependent Moduli and Damping for the Seismic Analysis of Deep Sites", *Soil Dynamics and Earthquake Engineering*, Vol. 22, No. 9-12, pp. 959-965.

Bardet, J. P., K. Ichii and C. H. Lin, 1998, *EERA, A computer program for equivalent linear earthquake site response analysis of layered soils deposits*, University of Southern California, Los Angeles.

Beresnev, I. A. and K. L. Wen, 1996, "Nonlinear Soil Response-A Reality?", *Bulletin of the Seismological Society of America*, Vol. 86, pp. 1964-1978.

Beresnev, I. A., G. M. Atkinson, P. A. Johnson and E. H. Field, 1998, "Stochastic Finite-Fault Modeling of Ground Motions From the 1994 Northridge, California Earthquake. II. Widespread Nonlinear Response at Soil Sites", *Bulletin of the Seismological Society of America*, Vol. 88, No. 6, pp. 1402-1410.

Biot, M. A., 1962, "The Mechanics of Deformation and Acoustic Propagation in Porous Media", *Journal of Applied Physics*, Vol. 33, No.4, pp.1482–1498.

Bommer, J. J. and A. B. Acevedo, 2004, "The Use of Real Earthquake Accelerograms as Input to Dynamic Analysis", *Journal of Earthquake Engineering*, Vol. 8, No. 1, pp. 43-91.

Bonilla, L. F., R. J. Archuleta and D. Lavallee, 2005, "Hysteretic and Dilatant Behavior of Cohesionless Soils and Their Effects on Nonlinear Site Response: Field Data Observations and Modeling", *Bulletin of the Seismological Society of America*, Vol. 95, No. 6, pp. 2373-2395.

Boore, D. M. and G. M. Atkinson, 2008, "Ground-Motion Prediction Equations for the Average Horizontal Component of PGA, PGV, and 5% Damped PSA at Spectral Periods between 0.01 s and 10.0 s", *Earthquake Spectra*, Vol. 24, No. 1, pp. 99-138.

Boore, D. M. and W. B. Joyner, 1991, “Estimation of Ground Motion at Deep-soil Sites in Eastern North America”, *Bulletin of the Seismological Society of America*, Vol. 81, pp. 2167–2185.

Borcherdt, R. D., 2002a, “Empirical Evidence for Site Coefficients in Building Code Provisions”, *Earthquake Spectra*, Vol. 18, No. 2, pp. 189-217.

Borcherdt, R. D., 2002b, “Empirical Evidence for Acceleration-Dependent Amplification Factors”, *Bulletin of the Seismological Society of America*, Vol. 92, No. 2, pp. 761-782.

Borcherdt, R. D., 1994, “Estimates of Site Dependent Response Spectra for Design (Methodology and Justification)”, *Earthquake Spectra*, Vol. 10, No. 4, pp. 617-654.

Brillinger, D. R. and H. K. Preisler, 1984, “An Exploratory Analysis of the Joyner-Boore Attenuation Data”, *Bulletin of the Seismological Society of America*, Vol. 74, No. 4, pp. 1441–1450.

BSSC, 1997, *NEHRP Recommended Provisions for Seismic Regulations for New Buildings, Part 1 — Provisions*, 1997 Edition, Building Seismic Safety Council, Washington, D.C., 337 pp.

BSSC, 2001, *NEHRP Recommended Provisions for Seismic Regulations for New Buildings and Other Structures, (FEMA 368 and 369), 2000 Edition*, Prepared by the Building Seismic Safety Council for the Federal Emergency Management Agency, Washington, DC.

Campbell, K. W. and Y. Bozorgnia, 2008, “NGA Ground Motion Model for the Geometric Mean Horizontal Component of PGA, PGV, PGD and 5% Damped Linear Elastic Response Spectra for Periods Ranging from 0.01 to 10 s”, *Earthquake Spectra*, Vol. 24, No. 1, pp. 139-171.

Campbell, K. W. and Y. Bozorgnia, 2003, "Updated Near-Source Ground Motion (Attenuation) Relations for the Horizontal and Vertical Components of Peak Ground Acceleration and Acceleration Response Spectra", *Bulletin of the Seismological Society of America*, Vol. 93, No. 1, pp. 314–331.

Campbell, K. W., 2003, "Engineering Models of Strong Ground Motion", in W. F. Chen and C. Scawthorn (eds.), *Earthquake Engineering Handbook*, pp. 5.1 – 5.76, CRC Press LLC, Boca Raton.

Campbell, K.W., 1981, "Near-Source Attenuation of Peak Horizontal Acceleration", *Bulletin of the Seismological Society of America*, Vol. 71, pp. 2039–2070.

CEN, 2006, *Eurocode EC8 – Design of Structures for Earthquake Resistance*, European Standard, European Committee for Standardisation, Brussels.

Chin, B. and K. Aki, 1991, "Simultaneous Study of the Source, Path, and Site Effects on Strong Ground Motion during the 1989 Loma Prieta Earthquake: A Preliminary Result on Pervasive Nonlinear Site Effects", *Bulletin of the Seismological Society of America*, Vol. 81, pp. 1859-1884.

Chiou, B. S.J. and R. R. Youngs, 2008, "An NGA Model for the Average Horizontal Component of Peak Ground Motion and Response Spectra", *Earthquake Spectra*, Vol. 24, No. 1, pp. 173-215.

Constantopoulos, I. V., J. M. Roesset and J. T. Christian, 1973, "A Comparison of Linear and Exact Nonlinear Analyses of Soil Amplification", *Fifth World Conference on Earthquake Engineering*, Rome, Session 5B, pp. 225.

Cooley, J. W. and J. W. Tukey, 1965, "An Algorithm for the Machine Calculation of Complex Fourier Series", *Mathematics of Computation*, Vol. 19, No. 90, pp. 297-301.

Crouse, C. B. and J. W. McGuire, 1996, “Site Response Studies for Purpose of Revising NEHRP Seismic Provisions”, *Earthquake Spectra*, Vol. 12, No. 3, pp. 407-439.

Cultrera, G., D. M. Boore, W. B. Joyner and C. M. Dietel, ,1999, “Nonlinear Soil Response in the Vicinity of the Van Norman Complex Following the 1994 Northridge, California, Earthquake”, *Bulletin of the Seismological Society of America*, Vol. 89, pp. 1214–1231.

Danciu, L. and G-A. Tselentis, 2007, “Engineering Ground-Motion Parameters Attenuation Relationships for Greece”, *Bulletin of the Seismological Society of America*, Vol. 97, No. 1B, pp. 162–183.

Darendeli, M. B., 2001, *Development of a New Family of Normalized Modulus Reduction and Material Damping Curves*, Ph. D. Dissertation, The University of Texas at Austin.

Darendeli, M. B., K. H. Stokoe, II, E. M. Rathje and C. J. Roblee, 2001, “Importance of Confining Pressure on Nonlinear Soil Behavior and Its Impact on Earthquake Response Predictions of Deep Sites”, *15th International Conference on Soil Mechanics and Geotechnical Engineering*, Istanbul, Turkey.

Davidian M. and D. M. Giltinan, 1995, *Nonlinear Models for Repeated Measurement Data*, Chapman and Hall / CRC, New York.

Dimitriu, P., N. Theodulidis and P.-Y. Bard, 2000, “Evidence of Nonlinear Site Response in HVSR from SMART1 (Taiwan) Data”, *Soil Dynamics and Earthquake Engineering*, Vol. 20, pp. 155-165.

Douglas, J., 2003, “Earthquake Ground Motion Estimation Using Strong-Motion Records: A Review of Equations for the Estimation of Peak Ground Acceleration and Response Spectral Ordinates”, *Earth-Science Reviews*, Vol. 61, No. 1-2, pp. 43-104.

Draper, N.R. and H. Smith, 1981, *Applied Regression Analysis*, John Wiley, New York.

Durukal, E., M. Erdik, J. Avcı, Ö. Yüzügüllü, C. Zülfikar, T. Biro and A. Mert, 1998, "Analysis of the Strong Motion Data of the 1995 Dinar, Turkey Earthquake", *Soil Dynamics and Earthquake Engineering*, Vol. 17, pp. 557-578.

Elgamal, A., Z. Yang and E. Parra, 2002, "Computational Modeling of Cyclic Mobility and Post-Liquefaction Site Response", *Soil Dynamics and Earthquake Engineering*, Vol. 22, No. 4, pp. 259-271.

Elgamal, A.-W., M. Zeghal and E. Parr, 1995, "Identification and Modeling of Earthquake Ground Response", *First International Conference on Earthquake Geotechnical Engineering*, Tokyo, Japan, Vol. 3, pp. 1369-1406.

EPRI, Electrical Power Research Institute, 1988, *A Criterion for Determining Exceedance of the Operating Basis Earthquake*, EPRI NP-5930, Electrical Power Research Institute, Palo Alto, California.

EPRI, Electrical Power Research Institute, 1993, *Guidelines for Determining Design Basis Ground Motions*, EPRI TR-102293, Vol. 1, Electrical Power Research Institute, Palo Alto, California.

Erdik, M., M. Demircioglu, K. Sesetyan, E. Durukal and B. Siyahi, 2004, "Earthquake Hazard in Marmara Region", *Soil Dynamics and Earthquake Engineering*, Vol. 24, pp.605-631.

Eyidogan, H. and A. Barka, 1996, "The October 1995 Dinar Earthquake, SW Turkey", *Terra Nova*, Vol. 8, pp. 179-185.

Field, E. H. and S. E. Hough, 1997, "The Variability of PSV Response Spectra across a Dense Array Deployed during the Northridge Aftershock Sequence", *Earthquake Spectra*, Vol. 13, No. 2, pp. 243-257.

Finn, W. D. L., K. W. L. Michael and G. R. Martin, 1978, "Comparison of Dynamic Analysis of Saturated Sand", *Proceedings of the ASCE Geotechnical Engineering*

Division, Specialty Conference on Earthquake Engineering and Soil Dynamics, Pasadena, CA, June 19-21, 1978, pp. 472-491.

Finn, W. D. L., K. W. Lee and G. R. Martin, 1977, “An Effective Stress Model for Liquefaction”, *Journal of the Geotechnical Engineering Division*, Vol. 103, No. 6, pp. 517-533.

Goulet, C. A., 2008, "Ground Motion Parameters That Control Ground Response Analysis Results", *Presentation in 2008 COSMOS Technical Session*, Oakland, CA.

Hardin, B. O. and V. P. Drnevich, 1972, “Shear Modulus and Damping in Soils: Design Equations and Curves”, *Journal of the Soil Mechanics and Foundations Division*, Vol. 98, No. 6, pp. 603-624.

Hartzell, S., E. Cranswick, A. Frankel, D. Carver and M. Meremonte, 1997, “Variability of Site Response in the Los Angeles Urban Area”, *Bulletin of the Seismological Society of America*, Vol. 87, No. 6, pp. 1377-1400.

Hashash, Y. M. A. and D. Park, 2001, “Non-linear One-dimensional Seismic Ground Motion Propagation in the Mississippi Embayment”, *Engineering Geology*, Vol. 62, No. 1-3, pp. 185-206.

Hashash, Y. M. A., D. R. Groholski, C. A. Phillips and D. Park, 2009, *DEEPSOIL V3.5beta, User Manual and Tutorial*.

Heaton, T. H., F. Tajima and A.W. Mori, 1986, “Estimating Ground Motions Using Recorded Accelerograms”, *Surveys in Geophysics*, Vol. 8, No. 1, pp. 25–83.

Heuze, F., R. Archuleta, F. Bonilla, S. Day, M. Doroudian, A. Elgamal, S. Gonzales, M. Hoehler, T. Lai, D. Lavallee, B. Lawrence, P. -C. Liu, A. Martin, L. Matesic, B. Minster, R. Mellors, D. Oglesby, S. Park, M. Riemer, J. Steidl, F. Vernon, M. Vucetic, J. Wagoner and Z. Yang, 2004, “Estimating Site-Specific Strong

Earthquake Motions”, *Soil Dynamics and Earthquake Engineering*, Vol. 24, No. 3, pp. 199-223.

Higashi, S. and T. Sasatani, 2000, “Nonlinear Site Response in Kushiro during the 1994 Hokkaido Toho-oki Earthquake”, *Bulletin of the Seismological Society of America*, Vol. 90, No. 4, pp. 1082-1095.

Hill, R., 1950, *The Mathematical Theory of Plasticity*, Clarendon Press, Oxford.

Housner, G. W., 1952, *Intensity of Ground Motion during Strong Earthquake*, California Institute of Technology, Pasadena, California.

Idriss, I. M. and H. B. Seed, 1968, “Seismic Response of Horizontal Soil Layers”, *Journal of the Soil Mechanics and Foundation Division*, Vol. 94, No. SM4, pp. 1003-1031.

Idriss, I. M. and J. I. Sun, 1992, *Shake91, A Computer Program for Conducting Equivalent Linear Seismic Response Analysis of Horizontally Layered Soil Deposits*, Modified based on the original SHAKE program by Schnabel, Lysmer and Seed, 1972.

Idriss, I. M., 2008, “An NGA Empirical Model for Estimating the Horizontal Spectral Values Generated by Shallow Crustal Earthquakes”, *Earthquake Spectra*, Vol. 24, No. 1, pp. 217-242.

Idriss, I. M., 1991a, “Earthquake Ground Motions at Soft Soil Sites”, Special Session in Honor of H. B. Seed, *Proceedings of Second International Conference on Recent Advances in Geotechnical Earthquake Engineering and Soil Dynamics*, St. Louis.

Idriss, I.M., 1991b, *Procedures for Selecting Earthquake Ground Motions at Rock Sites*, Report to U.S. Department of Commerce, revised 1993.

Ishihara, K. and I. Towhata, 1980, “One-Dimensional Soil Response Analysis during Earthquakes Based on Effective Stress Method”, *Journal of Faculty of Engineering, University of Tokyo*, Vol. 135, No. 4.

ISSMGE/TC4, 1999, *Manual for Zonation on Seismic Geotechnical Hazards*, Technical Committee for Earthquake Geotechnical Engineering TC4, ISSMGE, Japanese Society of Soil Mechanics.

Iwan, W. D., 1967, "On a Class of Models for the Yielding Behavior of Continuous and Composite Systems", *Journal of Applied Mechanics, ASME*, Vol. 34, pp.612-617.

Iyisan, R., 1996, "Correlations between Shear Wave Velocity and In-Situ Penetration Test Results", *Technical Journal of Turkish Chamber of Civil Engineers*, Vol. 7, No. 2, pp. 1187-1199 (in Turkish).

Joyner, W.B. and D.M. Boore, 1994, "Errata: Methods for Regression Analysis of Strong-Motion Data", *Bulletin of the Seismological Society of America*, Vol. 84, No. 3, pp. 955–956.

Joyner, W.B. and D.M. Boore, 1993, "Methods for Regression Analysis of Strong-Motion Data", *Bulletin of the Seismological Society of America*, Vol. 83, No. 2, pp. 469–487.

Joyner, W.B. and D.M. Boore, 1981, "Peak Horizontal Acceleration and Velocity from Strong-Motion Records Including Records from the 1979 Imperial Valley, California, Earthquake", *Bulletin of the Seismological Society of America*, Vol. 71, No. 6, pp. 2011–2038.

Kanai, K., 1951, "Relation between the Nature of Surface Layer and the Amplitude of Earthquake Motions", *Bulletin of Tokyo Earthquake Research Institute*.

Kappos, A. J. and P. Kyriakakis, 2000, "A Re-Evaluation of Scaling Techniques for Natural Records", *Soil Dynamics and Earthquake Engineering*, Vol. 20, No. 1-4, pp. 111-123.

Kayen, R. E. and J. K. Mitchell, 1997, "Assessment of Liquefaction Potential during Earthquakes by Arias Intensity", *Journal of Geotechnical and Geoenvironmental Engineering*, Vol. 123, No. 12, pp. 1162-1174.

Kazama, M., 1996, “Nonlinear Dynamic Behavior of the Ground Inferred from Strong Motion Array Records at Kobe Port Island during the 1995 Hyogo-Ken Nanbu Earthquake”, *Proceedings of International Workshop on Site Response Subjected to Strong Earthquake Motion*, Yokusaka, Japan, Vol. 2, pp. 185-200.

Kılıç H., P. T. Özener, A. Ansal, M. Yıldırım, K. Özaydın, S. Adatepe, 2006, “Microzonation of Zeytinburnu Region with respect to Soil Amplification: A Case Study”, *Journal of Engineering Geology*, Vol. 86, pp. 238-255.

Kokusho, T., 1980, “Cyclic Triaxial Test of Dynamic Soil Properties for Wide Strain Range”, *Soils and Foundations*, Vol. 20, pp. 45-60.

Konder, R. L. and J. S. Zelasko, 1963, “Hyperbolic Stress-Strain Formulation of Sands”, *Second Pan American Conference on Soil Mechanics and Foundation Engineering*, Sao Paulo, Brazil, pp. 289-324.

Kramer, S. L. and R. A. Mitchell, 2005, “Ground Motion Intensity Measures for Liquefaction Hazard Evaluation”, *Earthquake Spectra*, Vol. 22, No. 2, pp. 413–438.

Kramer, S. L. and S. B. Paulsen, 2004, “Practical Use of Geotechnical Site Response Models”, *Proceedings of International Workshop on Uncertainties in Nonlinear Soil Properties and their Impact on Modeling Dynamic Soil Response*, PEER Center Headquarters, Richmond, California.

Kramer, S. L., 1996, *Geotechnical Earthquake Engineering*, Prentice-Hall, New Jersey.

Lai, T., A. Elgamal, Z. Yang, D. W. Wilson and B. L. Kutter, 2004, “Numerical Modeling of Dynamic Centrifuge Experiments on a Saturated Dense Sand Stratum”, *11th International Conference on Soil Dynamics and Earthquake Engineering and 3rd International Conference on Earthquake Geotechnical Engineering*, 7-9 January 2004, University of California, Berkeley.

Lay, T. and T.C. Wallace, 1995, *Modern Global Seismology*, Academic Press, San Diego.

Marek, A. R., J. D. Bray and N. Abrahamson, 1999, *Task 3: Characterization of Site Response General Site Categories*, PEER-1999/03, Pacific Earthquake Engineering Research Center, University of California, Berkeley, 1999-02, 139 pp.

Martinez-Rueda, J. E., 1998, "Scaling Procedure for Natural Accelerograms Based on a System of Spectrum Intensity Scales", *Earthquake Spectra*, Vol. 14, No. 1, pp. 135-152.

Matasovic, N., 1993, *Seismic Response of Composite Horizontally–Layered Soil deposits*, University of California, Los Angeles.

Menq, F. Y., K. H. Stokoe and E. Kavazanjian, 2003, "Linear Dynamic Properties of Sandy and Gravelly Soils from Largescale Resonant Tests", *International Symposium IS Lyon 03, Deformation Characteristics of Geomaterials*, Lyon, France.

Mróz, Z., 1967, "On the Description of Anisotropic Workhardening", *Journal of Mechanics and Physics of Solids*, Vol.15, pp. 163-175.

Naeim F., A. Alimoradi and S. Pezeshk, 2004, "Selection and Scaling of Ground Motion Time Histories for Structural Design Using Genetic Algorithms", *Earthquake Spectra*, Vol. 20, No. 2, pp. 413-426.

Okur, D. V. and A. Ansal, 2007, "Stiffness Degradation of Natural Fine Grained Soils during Cyclic Loading", *Soil Dynamics and Earthquake Engineering*, Vol. 27, No. 9, pp. 843-854.

Okur, V. and A. Ansal, 2004, "Stress-Strain Characteristics of Fine Grained Soils under Cyclic Loading", *International Conference on Cyclic Behaviour of Soils and Liquefaction Phenomena,* Bochum, Germany.

OYO Inc., Japan, 2007, *Production of Microzonation Report and Maps on European Side (South)*, Final Report to Istanbul Metropolitan Municipality.

Paciello, A., D. Rinaldis and R. Romeo, 2000, "Incorporating Ground Motion Parameters Related to Earthquake Damage into Seismic Hazard Analysis", *Proceedings of the Sixth International Conference on Seismic Zonation: Managing Earthquake Risk in the 21st Century*, Earthquake Engineering Research Institute, Oakland, CA.

Parra, E., 1996, *Numerical Modeling of Liquefaction and Lateral Ground Deformation Including Cyclic Mobility and Dilative Behavior in Soil Systems*, Ph. D. Dissertation, Department of Civil Engineering, Rensselaer Polytechnic Institute, Try, NY.

PEER, *Pacific Earthquake Engineering Research Center: Ground Motion Selection and Modification Program*, http://peer.berkeley.edu/gmsm/

PEER, *Pacific Earthquake Engineering Research Center: NGA Database*, http://peer.berkeley.edu/nga/

Power, M., B. Chiou, N. Abrahamson, Y. Bozorgnia, T. Shantz and C. Roblee, 2008, "An Overview of the NGA Project", *Earthquake Spectra*, Vol. 24, No. 1, pp. 3-21.

Prevost, J.-H., 1985, "A Simple Plasticity Theory for Frictional Cohesionless Soils", *Soil Dynamics and Earthquake Engineering*, Vol. 4, No. 1, pp. 9-17.

Priestley, M. J. N., 2000, "Performance Based Seismic Design", Keynote Address, *12th World Conference on Earthquake Engineering*, Auckland, New Zealand.

Roscoe, K. H. and A. N. Schofield, 1963, "Mechanical Behaviour of an Idealized 'Wet' Clay", *Proceedings of 2nd European Conference on Soil Mechanics*, Wiesbaden, Germany, Vol.1, pp.47-54.

Roscoe, K. H. and J. B. Burland, 1968, "On the Generalized Stress-Strain Behaviour of 'Wet' Clay", in J. Heyman and F.A. Leckie (eds.), *Engineering Plasticity*, University Press, Cambridge, pp.535-609.

Schnabel, P. B., J. Lysmer and H. B. Seed, 1972, *SHAKE: A Computer Program for Earthquake Response Analysis of Horizontally Layered Sites*, Report No. EERC 72/12, Earthquake Engineering Research Center, University of California, Berkeley.

Seed, H. B. and I. M. Idriss, 1970, *Soil Moduli and Damping Factors for Dynamic Response Analyses*, Report EERC 70-10, Earthquake Engineering Research Center, University of California, Berkeley.

Seed, H. B. and I. M. Idriss, 1982, "Ground Motions and Soil Liquefaction during Earthquakes", *Engineering Monographs on Earthquake Criteria, Structural Design, and Strong Motion Records*, Vol. 5, Earthquake Engineering Research Institute.

Seed, H. B., R. T. Wong, I. M. Idriss and K. Tokimatsu, 1986, "Moduli and Damping Factors for Dynamic Analyses of Cohesionless Soils", *Journal of Geotechnical Engineering*, Vol. 112, No. 11, pp. 1016-1032.

Siyahi B., E. Durukal and Z. Altaç, 2001, "Evaluation of Strong Motion Data from the Kocaeli and Düzce, Turkey Earthquakes in view of Arias Intensity", *Proceedings 15ICSMGE Earthquake Geotechnical Engineering Satellite Conference on Lessons Learned from Recent Strong Earthquakes*, Istanbul, pp. 189-194.

Spence, R. (editor), 2007, *Earthquake Disaster Scenario Prediction and Loss Modelling for Urban Areas*, EU LessLoss Report No.7, EU FP7 Project.

S-Plus Software, Professional Release 1, 1988–1999, MathSoft, Inc; 2000.

Spudich, P., W.B. Joyner, A.G. Lindh, D.M. Boore, B.M. Margaris, and J.B. Fletcher, 1999, "SEA99: A Revised Ground Motion Prediction Relation for Use in Extensional Tectonic Regimes", *Bulletin of the Seismological Society of America*, Vol. 89, No. 5, pp. 1156–1170.

Stewart J. P., S. J. Chiou, J. D. Bray, R. W. Graves, P. G. Somerville and N. A. Abrahamson, 2001, *Ground Motion Evaluation Procedures for Performance-Based*

Design, PEER Report 2001/09, Pacific Earthquake Engineering Research Center, Berkeley, September.

Stewart J. P., S.-J. Chiou, J. D. Bray, R. W. Graves, P. G. Somerville and N. A. Abrahamson, 2002, “Ground Motion Evaluation Procedures for Performance Based Design”, *Soil Dynamics and Earthquake Engineering*, Vol. 22, No. 9-12, pp. 765-772.

Studer, J., A. Ansal, 2004, *Seismic Microzonation for Municipalities, Manual*, Research Report for Republic of Turkey, Ministry of Public Works and Settlement, General Directorate of Disaster Affairs, World Institute for Disaster Risk Management, Inc.

Su, F., J.G. Anderson, and Y. Zeng, 1998, “Study of Weak and Strong Ground Motion Including Nonlinearity from the Northridge, California Earthquake Sequence”, *Bulletin of the Seismological Society of America*, Vol. 88, No. 6, pp. 1411-1425.

Sugito, M., N. Aida and T. Masuda, 1994, “Frequency Dependent Equilinearized Technique for Seismic Response Analysis of Multi-Layered Ground”, *Journal of Geotechnical Engineering, Proceedings of of JSCE*, Vol. 493, pp. 49-58 (in Japanese).

Travasarou, T., J. B. Bray and A. Abrahamson, 2003, “Empirical Attenuation Relationship for Arias Intensity”, *Earthquake Engineering and Structural Dynamics*, Vol. 32, No. 7, pp. 1133–1155.

Turkish Earthquake Code (TEC), 2007, *Specification for Buildings to be Built in Earthquake Areas*, Ministry of Public Works and Settlement, Government of Republic Turkey.

Udaka, T., 1975, *Analysis of Response of Large Embankments to Traveling Base Motions*, Department of Civil and Environmental Engineering Berkeley, University of California.

Ueshima, T. and N. Nakazono, 1996, "Application of Equivalent Linear Method Considering Frequency Dependent Characteristics on Earthquake Record at Lotung", *Proceedings of the 51st Annual Conference of the Japanese Society of Civil Engineers*, Vol. 1, pp. 408-409 (in Japanese).

Uniform Building Code (UBC), 1997, International Conference of Building Officials, Whittier, California.

Von Thun, J. L., L. H. Rochim, G. A. Scott and J. A. Wilson, 1988, "Earthquake Ground Motions for Design and Analysis of Dams", *Earthquake Engineering and Soil Dynamics II – Recent Advance in Ground Motion Evaluation*, pp. 122-141, Geotechnical Special Publication 20, ASCE, New York.

Vucetic M., 1994, "Cyclic Threshold Shear Strains in Soils", *Journal of Geotechnical Engineering*, Vol. 120, No. 12, pp. 2208-2228.

Vucetic, M and R. Dobry, 1991, "Effect of Soil Plasticity on Cyclic Response", *Journal of Geotechnical Engineering*, Vol. 117, No. 1, pp.89-107.

Wald, D. J., V. Quitoriano, T. H. Heaton, and H. Kanamori, 1999, "Relationships between Peak Ground Acceleration, Peak Ground Velocity, and Modified Mercalli Intensity in California", *Earthquake Spectra*, Vol. 15, No. 3, pp. 557–564.

Wen, K. L., I. A. Beresnev and Y. T. Yeh, 1994, "Nonlinear Soil Amplification Inferred from Downhole Strong Seismic Motion Data", *Geophysical Research Letters*, Vol. 21, pp. 2625-2628.

Wen, K. L., T. M. Chang, C. M. Lin and H. J. Chiang, 2006, "Identification of Nonlinear Site Response Using the H/V Spectral Ratio Method", *Terrestrial Atmospheric and Oceanic Sciences*, Vol. 17, No. 3, pp. 533-546.

Yang, Z. and A. Elgamal, 2001, *Cyclic1D Pre-release Beta Version (November 2001)*, http://cyclic.ucsd.edu

Yang, Z., 2000, *Numerical Modeling of Earthquake Site Response Including Dilation and Liquefaction*, Ph. D. Dissertation, Dept. of Civil Engineering and Engineering Mechanics, Columbia University, New York, NY.

Yang, Z., J. Lu and A. Elgamal, 2004, "A Web-based Platform for Live Internet Computation of Seismic Ground Response", *Advances in Engineering Software*, Vol. 35, pp. 249-259.

Yasuda, S., S. Negishi, Y. Yoshikawa and I. Moromoto, 1995, "Microzonation for Liquefaction to Detect Liquefaction Sites Immediately after an Earthquake", *Proceedings of the Fifth International Conference on Seismic Zonation*, Nice, France.

Yoshida, N. and I. Suetomi, 1996, *DYNEQ: A Computer Program for Dynamic Analysis of Level Ground Based on Equivalent Linear Method*, Reports of Engineering Research Institute, Sato Kogyo Co. Ltd, pp.61-70.

Yoshida, N. and I. Towhata, 2003, *YUSAYUSA – 2 and SIMMDL – 2 Theory and Practice – Revised Version (ver. 2.10)*.

Yoshida, N. and S. Iai, 1998, "Nonlinear Site Response and Its Evaluation and Prediction", in K. Irikura, K. Kudo, H. Okada, and T. Sasatani (eds), *Proceedings of Second International Symposium on the Effects of Surface Geology on Seismic Motion*, Vol. 1, pp. 71-90.

Yoshida, N., 1994, "Applicability of Conventional Computer Code SHAKE to Nonlinear Problem", *Proceedings of Symposium on Amplification of Ground Shaking in Soft Ground*, Japanese Society on Soil Mechanics and Foundation Engineering, pp. 14-31 (in Japanese).

Yoshida, N., S. Kobayashia, I. Suetomia and K. Miura, 2002, "Equivalent Linear Method Considering Frequency Dependent Characteristics of Stiffness and Damping", *Soil Dynamics and Earthquake Engineering*, Vol. 22, No. 3, pp. 205-222.

Yu, G., J. G. Anderson and R. Siddharthan, 1993, "On the Characteristics of Nonlinear Soil Response", *Bulletin of the Seismological Society of America*, Vol. 83, No. 1, pp. 218-244.